Mechatronic design for repeatability of a single-camera alignment system in pick-and-place machines

Verstegen, Paul

DOI
10.4233/uuid:d0423cf6-90b8-4a2a-b4cd-a1cff0f84c96

Publication date
2019

Document Version
Final published version

Citation (APA)
Verstegen, P. (2019). *Mechatronic design for repeatability of a single-camera alignment system in pick-and-place machines*. [Dissertation (TU Delft), Delft University of Technology].
https://doi.org/10.4233/uuid:d0423cf6-90b8-4a2a-b4cd-a1cff0f84c96

Important note
To cite this publication, please use the final published version (if applicable).
Please check the document version above.

Mechatronic design for repeatability of a single-camera alignment system in pick-and-place machines

Paul Verstegen

Mechatronic design for repeatability of a single-camera alignment system in pick-and-place machines

Proefschrift

ter verkrijging van de graad van doctor
aan de Technische Universiteit Delft,
op gezag van de Rector Magnificus prof.dr.ir. T.H.J.J. van der Hagen,
voorzitter van het College voor Promoties,
in het openbaar te verdedigen op donderdag 4 april 2019 om 15:00 uur
door

Paulus Petrus Hendricus VERSTEGEN

HBO-ingenieur in de elektrotechniek, Hogeschool Eindhoven, Nederland
geboren te Zeeland, Nederland

Dit proefschrift is goedgekeurd door de promotoren.

Samenstelling promotiecommissie bestaat uit:

Rector Magnificus	voorzitter
Prof.dr.ir. J.L. Herder	Technische Universiteit Delft, promotor
Ir. J.W. Spronck	Technische Universiteit Delft, copromotor

Onafhankelijke leden:

Prof.dr.ir. P.P. Jonker	Technische Universiteit Delft
Prof.ir. R.H. Munnig Schmidt	Technische Universiteit Delft
Prof.dr. E.A. Lomonova	Technische Universiteit Eindhoven
Prof.dr.ir. M. Steinbuch	Technische Universiteit Eindhoven
Ir. J.M.M. van Gastel	Fontys Hogeschool Eindhoven

ISBN 978-90-9024624-6

The research described in this thesis has been financially supported by the Dutch government programme IOP precision engineering as part of the project IPT02313 Advanced assembling systems for miniature components.

Cover design by Ester Selten, Essential Design

Voor Eefke

Contents

Nomenclature

Abbreviations

ADC	Analog to digital converter
BA	Board Alignment
BGA	Ball Grid Array
BM	Board Move
CA	Component Alignment
CCD	Charge Coupled Device
CMOS	Complementary Metal Oxide Semiconductor
COM	Center of mass
cph	Components Per Hour
CPLD	Complex Programmable Logic Device
CPU	Central Processing Unit
DOF(s)	Degree(s) Of Freedom
FEM	Finite Element Method
FET	Field Effect Transistor
FOV	Field Of View
FPGA	Field programmable gate array
fps	frames per second
IC(s)	Integrated Circuit(s)
LED	Light Emitting Diode
PCB	Printed Circuit Board
P&P	Pick and Place
SMD	Surface Mounted Device
SMT	Surface Mount Technology
VGA	Video Graphics Array (600×480 pixels)
SVGA	Super Video Graphics Array (800×600 pixels)
XGA	Extended Graphics Array (1024×768 pixels)
WD	Working Distance

Terms and definitions

Accuracy	Determined by random errors and calibration residue
Board alignment system	System used to determine the position (x, y and ϕ-direction) of a PCB
Board handling	Board Run In, Board Move, Board Run Out
Component alignment system	System used to determine the position (x, y and ϕ-direction) of a component
Land (pad)	Position on PCB where the components termination must be placed.
Mirror box	Robot holding the shuttle and mirrors
PCB features	Fiducials or artwork on a PCB
P&P	Pick-and-place; term used to indicate that a component is picked and placed
P&P machine	Machine used to place components on a PCB; a machine contains one or more P&P robots
P&P process	Processes in the P&P cycle (Pick, Move, Component Alignment, Place)
P&P machine processes	All processes that take place in a pick-and-place machine
P&P robot	Robot able to pick and place components on the PCB;
Repeatability	1σ value
Throughput	Number of components placed per hour
Terminations	End caps, leads or pins of a component

Chapter 1

Introduction

The demand for smart electronic devices like telephones, tablets, smart sensor based systems and automotive is still growing and will grow further in the future [54, 97]. Not only the amount of devices but also the functionality of these devices is still increasing. Inside electronic devices printed circuits boards (PCBs) are applied, which consist of electrical printed wires on a non conductive carrier. On top of a PCB up to hundreds of electronic components can be placed [33]. To contain all these components the dimensions have decreased over the years and surface-mount-technology (SMT) has been introduced, where components are mounted onto the surface of a printed circuit board (PCB) in-stead of through the PCB (through-hole-components) [13, 56]. The production or assembly of a PCB is done using a production line. To be able to produce the numerous electronic devices in the future the production capacity of these lines needs to be increased.

This chapter is divided in sections where Section 1.1 introduces the processes that take place in a production line to assemble PCBs. Analysing this production line shows that the pick-and-place machine (P&P machine) is often the machine that limits the throughput. Therefore, the P&P machine is described in more detail.

Section 1.2 will give a brief overview of the research that has been taken place to increase the throughput of production lines. The conclusion of this section will be that increasing the throughput of a production line by designing a new layout of a P&P machine can increase the throughput by a factor 3 or more. Therefore a new layout is proposed for this research.

Section 1.3 will give an introduction to the required component's placement accuracy followed by Section 1.4 where the research goal is determined.

This chapter ends with Section 1.5 presenting the structure of this thesis.

1.1 Introducing printed circuit board assembly

Figure 1.1 shows the process flow of a typical SMT assembly line [102] to assemble PCBs. The assembly line starts with a machine that dispenses

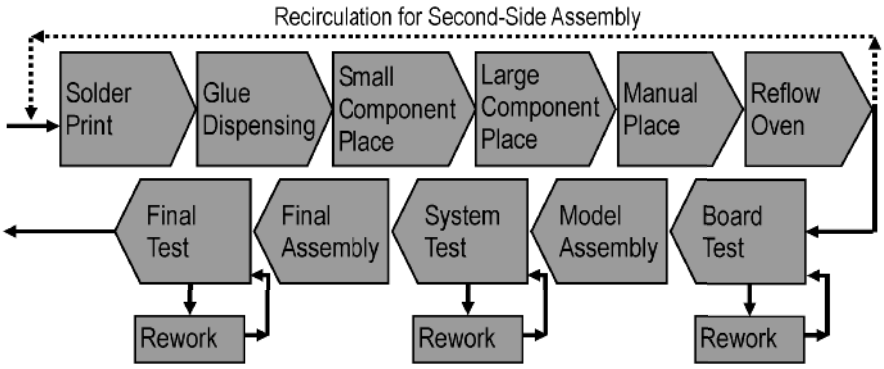

Figure 1.1: *Standard surface-mount-technology line process flow [102]*

solder paste, followed by a machine that applies glue onto the PCB. Small components are placed onto the PCB by the first P&P machine. In series with the first P&P machine, a second P&P machine is added to the line to place the larger components. Components that cannot be placed by a P&P machine are manually inserted. In the reflow oven the components are soldered or glued onto the PCB. If components must be placed on the other side of the PCB, the board is reversed and the previous process steps are repeated. Then the board is tested and if necessary reworked. Depending on the product, steps can be added to come from a single board to an electronic device.

To improve the throughput of a SMT production line it is required to determine the throughput limitations. Several studies state that the high cost of P&P machines, with respect to the other machines in a SMT production line, results often in a line setup where the P&P machine is the limiting resource [17, 27, 77, 99, 103]. To be able to understand the limitations of a P&P machine, the processes that takes place in a P&P machine will be analysed.

A commercial P&P machine is presented in Fig. 1.2. This machine consists of twelve narrow and four wider P&P robots. Depending on the properties of the components to be placed, a type of P&P robot is chosen. The design of this machine allows the sixteen P&P robots to be active concurrently. In front of the machine the feeder systems are visible. Each feeder system can carry several reels with components. Assembling the PCB means that the P&P robot picks a component from a reel, the component is moved to the desired position above the PCB where the component is accurately placed in the solder paste or glue. Figure 1.3 is taken from the IPC-9850 standard [53] and shows the sequence of the processes that are executed by a P&P machine and the explanation of the presented processes is in the next list:

- **Board Run In**: the PCB is fed into the P&P machine with limited

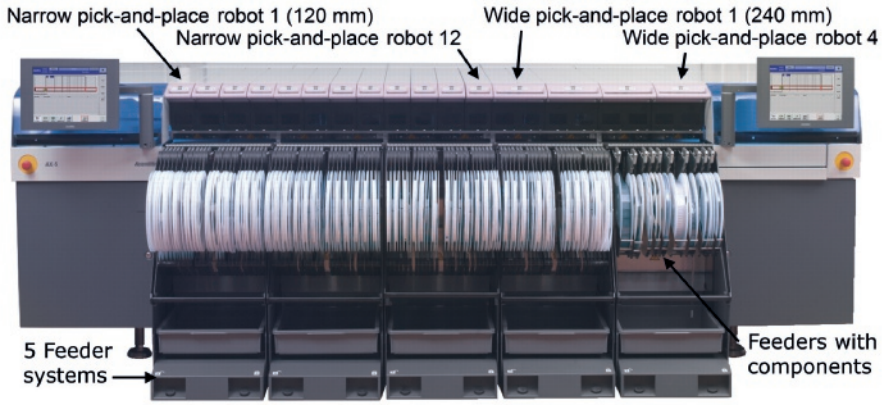

Figure 1.2: *Front view of an Assembléon B.V. AX-5. This pick-and-place machine is equipped with twelve narrow pick-and-place robots (width 120 mm) and four wider pick-and-place robots(width 240 mm). In front five feeder systems each holding multiple feeder reels with components*

accuracy

- **B(oard) Move**: the PCB is transported to the area where the P&P robot can place the components onto the PCB
- **BA (Board Alignment)**: the position of the PCB is determined and is mostly realised using a vision system
- **Nozzle exchange**: depending on the component to be handled the required nozzle is picked from the nozzle storage position
- **Pick**: the P&P robot picks a component from one of the feeders; the pick process consists of moving downward to the component, build up vacuum, pick a component and then move upward; this is the process where the P&P cycle starts
- **Move**: the P&P robot moves to the component alignment position
- **CA (Component Alignment)**: the position of the component is determined and is mostly realised using a vision system
- **Move**: the P&P robot moves to the place position above the PCB
- **Place**: the P&P robot places the component on the required position on the PCB
- **Move**: the P&P robot moves to one of the feeders to pick a new component; this is the process where the P&P cycle stops
- **B(oard) Move**: the PCB is transported to the area to unload the PCB
- **Board Run Out**: all components are placed by the P&P robot(s) so the PCB runs out

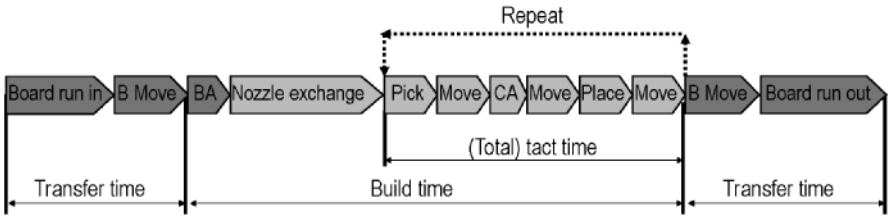

Figure 1.3: *Overview of pick-and-place processes performed by a pick-and-place machine [53]*

The time required for the processes board run in, board move and board run out is called the transfer time; the time required for the processes pick, move, component alignment and place is the (total) tact time; adding the time required for board alignment and nozzle exchange to the (total) tact time gives the build time.

To assemble a complete PCB several processes are repeated multiple times. The loops that are required to assemble a PCB depends on the layout of the P&P machine and the design of the PCB. The design of the PCB is determined by the function it has to perform and these layouts result in other capacities.

1.2 Throughput

Several studies can be found on increasing the throughput of a complete SMT production line. Crama et al.[15] divide the PCB assembly problem in eight different subproblems starting at the assembly shop level and ending at machine level, where Laakso et al. [68] divide the assembly problem in four different subproblems from machine level to assembly shop level. Ho et al.[43, 44, 45] divide the optimisation of the assembly problem into two main groups of decision problems: setup management and process optimisation. Setup management uses optimisation techniques to optimise the line setup and/or the choices that can be made with respect to the handling of PCBs or the grouping of PCBs into families; process optimisation makes choices on component allocation, component sequencing and feeder arrangement. Component allocation is allocating components to different types of P&P machines available in a plant or assembly line. Component sequencing determines the sequence of component placement and feeder arrangement determines the position of a feeder in a P&P machine. These three optimisation subjects are influencing directly the throughput of a P&P machine.

Using setup management, Crama et al.[14] optimise a factory by first decomposing the total planning problem of a production plant, whereafter the throughput is improved by using simple local search methods for sub-

problems. Where Feo et al.[29] have realised, tested and successfully used a software tool to plan PCB assembling facilities. Ellis et al.[26] use grouping of PCBs into families to improve the throughput of a production line.

Wang et al.[105] present an optimisation approach for the throughput of a machine concept using a moving feeder rack, moving PCB and a cartesian robot. Through optimisation of the scheduling of the movements of these three systems, the efficiency is improved. Csaszar et al.[16, 17, 18] present in their papers optimisation strategies for multi-station P&P machines equipped with a walking-beam PCB transport system and multiple nozzles on the P&P robot. The optimisation concerns the feeder slot assignment and the placement sequence for all P&P robots of the machine. Dikos et al.[20] and Grunow et al.[41] show in their papers that optimisation, by feeder position combined with component sequence planning, can be used to increase the throughput for multi-head machines too. In their paper the nozzles are attached to a turret. Klomp et al.[61] and Ellis et al.[25] present both a case study to optimise the feeder slot assignment for a turret-type machine (Fuji CP IV/3). Ayob et al.[2, 4, 5, 3] present in their work several optimisation approaches to increase the performance of a multi-head P&P machine.

From these studies it can be concluded that there are several different types of P&P machines. Wischoffer[107] divides P&P machines in four categories depending on the throughput of a machine where throughput can be defined as components placed per hour. The throughput is an important performance indicator of a P&P machine. The first category is called the entry-level (low volume); machines in this category typically have a throughput of 3,000 to 5,000 components per hour (*cph*). The second category contains the mid-range machines with a throughput of 8,000 to 14,000 *cph*. High-end machines have a throughput of 20,000-30,000 *cph* and are placed in the third category. Finally, the fourth category is called the ultra high speed machines; these machines have a throughput of 40,000 and more components per hour. With help of these categories it can already be concluded that the request to increase the throughput is depending on the P&P machines in the production line.

Although the presented optimisation techniques increase the throughput the maximum achieved improvement is determined by the capabilities of the machine. Increasing the throughput beyond the capabilities of a P&P machine requires a new layout of a P&P machine.

A solution to increase the throughput of assembly lines can be to replace the P&P machines by a machine of a higher category. So an entry-level machine can be replaced by a mid-range machine. But for the ultra high speed machines this is not feasible. Appendix A shows the study that has been performed to design a P&P machine layout that is able to increase the throughput of an ultra high speed machine.

From the study presented in Appendix A it is concluded that: adding a shuttle, able to bring components close to the placement position, will increases the throughput by at least a factor two. To achieve this throughput the maximum allowed pick-and-place cycle time is 225 ms.

1.3 Placement accuracy

Fig. 1.1 shows a SMT production line containing two P&P machines each having its own required placement accuracy, where the first P&P machine is used to place the small components and the second P&P machine to place the larger components. Due to the fact that small components can cover up to 85% of the components on a PCB [33, 49] the first P&P machine is often an ultra high speed P&P machine. Small components are fed into the P&P machine using 8 mm tapes. In this thesis small components are defined as components with a size from approximately 0.254 $mm \times 0.508$ mm (0201 components) to 6 $mm \times 6$ mm.

There are two types of placement errors of a component on a PCB: systematic and random. Systematic errors can be compensated by calibration where random errors are unpredictably and cannot be compensated for. After the required P&P machine calibration [96] the placement accuracy is determined by the random errors (repeatability) and a calibration residue (offset).

The required accuracy for component placement is determined by their dimensions. Gastel et al. [33, pg.10] and Gerits et al. [35] state that after calibration components with terminations down to 300 μm can be placed with a repeatability of 17 μm (1σ). Kalen[58] shows that the placement accuracy to handle 0201 components must be in the range of 15 to 20 $\mu m\,(1\sigma)$. In this research not the 17 $\mu m\,(1\sigma)$ but the lower 15 $\mu m\,(1\sigma)$ value is adapted and defined as the P&P machines' repeatability requirement.

1.4 Research objective

In Section 1.2 it was stated that a shuttle concept pick-and-place machine will have an increased throughput of a factor two. To achieve this throughput an additional shuttle is required. Meanwhile, it is required to maintain the component's placement repeatability on the PCB. Combining high throughput and micrometer repeatability is the design challenge of this mechatronic system.

> *The goal and main design challenge in this research is the design and validation of a fast and accurate alignment system for integration in a shuttle concept pick-and-place machine. The validation has to be executed using a demonstrator.*

To achieve this goal the V-model [91] mechatronic approach is used during the design of the alignment system for 15 μm (1σ) repeatability. The competitive engineering method [38] is adopted to specify the requirements.

1.5 Structure of the thesis

In this chapter the addition of a shuttle to a P&P robot, which will decrease the time available for the alignment processes, was introduced. This leads to the research question to design an alignment concept for the shuttle concept P&P robot.
In Chapter 2 the methods used to design, build and test the alignment systems are presented.
In Chapter 3 the accuracy requirements for the alignment system that will be added to the shuttle concept machine layout are discussed. The influence of the various P&P processes is determined and solutions are selected.
In Chapter 4 the integration of the alignment systems with a shuttle concept P&P machine is presented. Using an iterative method four designs are created and presented. One design is selected to be built and validated.
Chapter 5 shows the selection and the realisation of the board and component alignment system. The realisation is achieved with help of specially designed parts combined with commercially available parts.
Chapter 6 describes the layout of the P&P machine shuttle concept demonstrator. This demonstrator is used to validate the repeatability of the alignment systems.
In Chapter 7 the repeatability results of the experiments with the demonstrator are presented and discussed.
Finally, in Chapter 8 the conclusions and recommendations are presented.

Chapter 2

Method

In [94] mechatronics is defined as a synergistic combination of precision mechanical engineering, electronic control, systems thinking, in the design of products and processes. By this definition the design of integrated alignment systems for a pick-and-place machine is a mechatronic design assignment.

To structure software and system design the V-model approach is often used [91, 34, 104, 94]. The V-model starts with requirements of the overall design and splits up the design in subsystems and modules followed by validations performed on modules, subsystems and the overall design. This results in early validation of parts of the design, which can be used to alter the design if required. In this thesis the chapters are organised to fit in the V-model.

This chapter starts with the introduction of the V-model and explaining how the chapters that will follow fit in the V-model. Each of the following sections will be used to explain the preconditions and methods of the next chapters of this thesis.

2.1 V-model for mechatronic system design

The V-model used in this thesis is shown in Fig. 2.1. The V-model method starts in the left top with the requirements. While lowering into the V, the complete system is split up in subsystems, which are split up in modules. The module designs are validated. Then tests are performed on the subsystems and finally the complete system is validated with respect to the requirements.

The V-model shows the approach of a design where the product is split-up into subsystems that are also tested as subsystems. How to design the subsystems is not discussed. Gilb [38] states that all steps taken during a subsystem design are cyclic processes, which can influence other subsystem designs. Therefore requirements that are used inside the V-model to specify subsystems or modules will change during the design phases. The requirements at the left top of the V-model should not change because then the

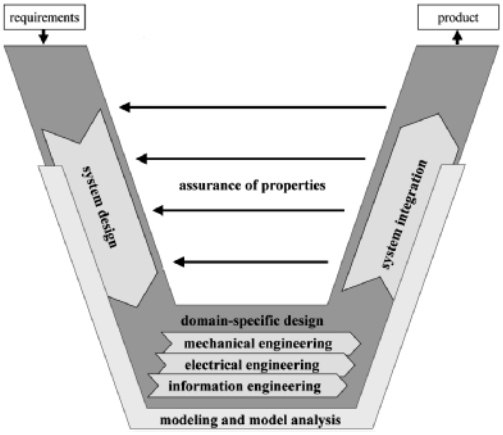

Figure 2.1: *V-model used for mechatronic design processes as described by VDI [104]*

performance of the overall product will change. In this thesis, the method to specify requirements is used for product and system requirements.

In Fig. 2.2 a V-model is shown that is adapted to this thesis including the chapter numbers. The V-model starts (left top) with the requirements of the complete system. These requirements will not change during the design process, because they are not part of the iterative cycles that are used in the design process. The first step in system design is the integration of the alignment systems with the shuttle concept P&P machine. The design of the alignment systems that fits the integration requirements is the next step. Subsequent the different modules of the alignment systems are designed and validated using tests. A demonstrator is realised to validate the integration of the alignment systems.

To be able to achieve the final goal a general decision is taken in this research that commercial available modules are used if possible. The advantage of commercial available modules is that these modules can be used easily if they match the requirements. The disadvantage is that the specifications of these modules are fixed and can not be altered for this research. So in general the design cycle has been started with a brief investigation on commercial modules that can be used. If no modules can be found to match the requirements, these modules will be designed and build in this project.

The next sections will discuss the research approach in the same order as the V-model shows. This means it starts with the choices made for the requirements; then a section will follow on the choices made for the alignment concept. Followed by the modules chosen. Finally, choices made for the demonstrator that is used to test the alignment concept are described.

The requirements of a subsystem will change because they are part of the iterative process where the requirements for the product will not change.

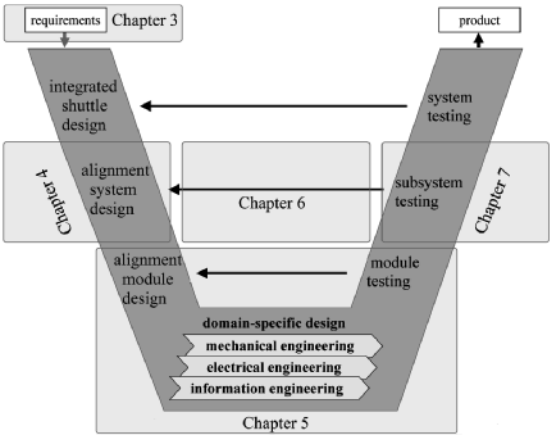

Figure 2.2: *V-model used for mechatronic design processes as described by VDI [104] adapted to alignment system design including the chapters of this thesis*

This means that it is not possible to determine the requirements for each subsystem on forehand. The requirements for the subsystems will be determined during the design phase. The system requirements will be determined in the next chapter.

2.2 Requirement specification

The left top corner of the V-model starts with the requirements, but it is not defined how requirements must be specified. Requirements must be defined in such a way that these are clear and measurable. Gilb proposes in the competitive engineering method [37, 38] to define requirements using multiple attributes to specify a requirement. In this thesis eight attributes are selected, which are presented in Table 2.1.

The use of multiple attributes for the specification of a requirement is used to ensure clearly definition of the specification. The tag is the name of the requirement used in this thesis followed by the gist, which describes in an informal way the requirement. Rationale is added to be able to discuss the why the tag is used as a specification. The scale and meter are used to describe the measure including a general description how the requirement can be measured. The attributes past, must and plan are numerical values that can be measured as described in meter.

Gilb indicates more attributes that can be used. But for this thesis the eight selected attributes will describe the requirements sufficiently unambiguously.

In this chapter the requirements are prescribed by the first five attributes: tag, gist, rationale, scale and meter. The numerical values past,

Requirement attributes	
Tag	name of the requirement
Gist	a rough informal description
Rationale	reasons that support the choice of this requirement
Scale	definition of the scale of measure
Meter	definition of how we are going to measure or test the attribute in practice
Past	a known benchmark of a value in the past
Must	a future requirement target, which is necessary for system survival; this is the minimum requirement to be met will the system be usable in the future
Plan	a future requirement target, which is necessary for system success and satisfaction

Table 2.1: *Requirements are specified using eight attributes*

must and plan will be determined in the next chapter where the specifications are discussed more deliberated. The next step is to determine the requirements to be used as input for the V-model.

IPC standardisation

IPC, the Association Connecting Electronics Industries, is a trade association whose aim is to standardise the assembly and production requirements of electronic equipment by releasing standards. One of these standards is IPC-9850 standard [53] "surface mount placement equipment characterization". In this standard it is proposed to specify or determine three major performance indicators to characterise a P&P machine: accuracy, throughput and reliability. Two performance indicators have already been presented in the previous chapter being accuracy (Section 1.2)and throughput (Section 1.3). These two performance indicators are translated in requirements in the next subsections.

In the standard it is also proposed to use reliability as a performance indicator. This performance can be evaluated and expressed in several different indicators. The standard proposes methods to determine the indicators and these methods assumes the ability to assemble PCBs. During the assembling tasks failures will occur and these failures can be used to determine numbers for the performance indicator reliability. This research will not end with a fully operational P&P machine that can be used to prove the reliability. Although reliability is an important performance indicator for P&P machines, throughput and accuracy will be the two main performance indicators. The requirements for throughput and accuracy will be discussed in the next sections.

Requirement attributes	
Tag	process time
Gist	average time required for a process part of the (total) time tact loop
Rationale	adding extra process time will have a negative impact on the throughput; thereby this requirement must be taken into account during the designs
Scale	ms
Meter	determine the time required for each process multiple times; enabling the determination of an average

Table 2.2: *The requirement specification for throughput*

2.2.1 Throughput

Throughput is an accepted performance indicator of a P&P machine indicating the number of components placed and expressed in components per hour (cph). Figure 1.3 showed all processes that occur in P&P cycle as well the definition of the transfer time, build time and (total) tact time. The time needed to place one component can be calculated by adding the time required for each individual processes within the (total) tact time. The transfer time and build time will also influence the throughput. Depending on the PCB layout the transfer time, build time and (total) tact time will change. So calculating the throughput is depending on the PCB, and as stated before this research will not end with a complete P&P machine but with an integrated alignment system.

To be able to set requirements that will influence the throughput, the average required process time for the processes that take place in the (total) tact time loop are used to determine the throughput requirement. Therefore the process time expressed in milliseconds [ms] is used for the throughput requirement. The attributes for this requirement are defined in Table 2.2.

The addition of a shuttle to a P&P machine decreases the time required for the move processes. In Appendix A it is concluded that the benefits on throughput of the shuttle concept P&P machine means that the alignment systems must be integrated without adding additional time to the P&P cycle or distances to the move process. Therefore, while integrating the alignment systems, the distances introduced should be minimised. In Appendix A it is shown that the shuttle must follow the P&P robot within an average range of 50 mm. The time required for the alignment process must be minimised.

2.2.2 Accuracy

In this section the goal is to determine the requirement attributes for placement accuracy. The IPC-9850 standard defines three accuracy indicators to describe the P&P machine accuracy performance [53, pg.5] where only

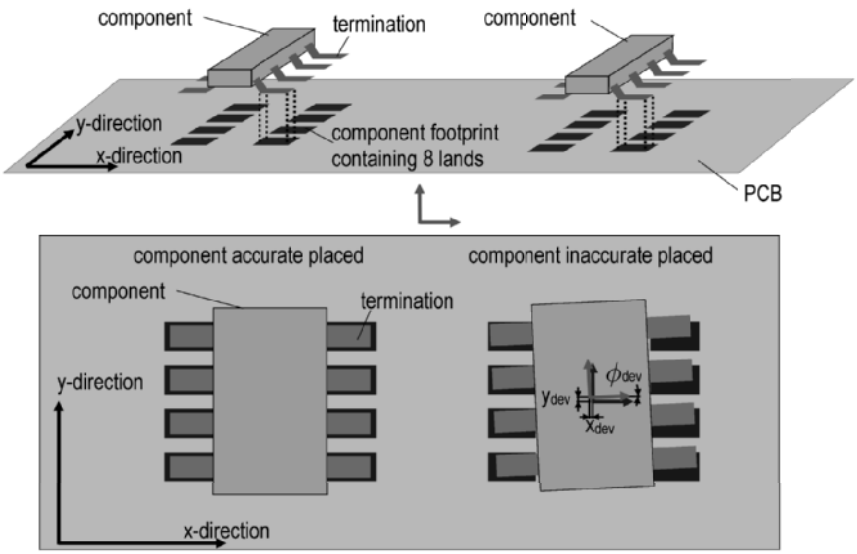

Figure 2.3: *Top: Alignment of the component's terminations with respect to the footprint of the component present on the PCB. The terminations of the component must be aligned with the lands of the footprint. Bottom: Top view of two components and the PCB. The left component is aligned with the footprint. The right component is misaligned with the footprint, resulting in a overall deviation of the component in x-, y- and ϕ-direction (x_{dev}, y_{dev}, ϕ_{dev})*

repeatability can be calculated without a full operational P&P machine. Repeatability is defined using the one standard deviation (1σ) as a measure for accuracy.

In order to understand placement accuracy, the placement of two components is presented in Fig. 2.3. The top graph of this figure shows two components, each containing eight terminations. The terminations must be placed on the footprints present on the PCB. The footprint of these specific components is a pattern of 2 rows of 4 lands (rectangular shapes). Ideally, for a perfect placed component, the center of the terminations is placed on the center of the lands. The bottom graph of Fig. 2.3 shows the top view of the two components placed on the PCB. The left component is placed onto the footprint, because the center of every termination is in the center of its land of the footprint this component is perfect placed with no deviation. The right component is placed having a deviation in x-, y- and ϕ-direction (x_{dev}, y_{dev} and ϕ_{dev}).

The deviation in x-, y- and ϕ-direction in a P&P process will have a normal/gaussian distribution, which can be characterised by the average value ($\bar{X}$) and the standard deviation (σ). The average can be calculated with (Equation 2.1) and the standard deviation can be calculated with (Equation 2.2).

$$Average\ of\ X_{dev}, \quad \bar{X} = \frac{1}{n}\sum_{i=1}^{n} X_i \tag{2.1}$$

$$Standard\ Deviation\ of\ X_{dev}, \quad \sigma_x = \sqrt{\frac{1}{n-1}\sum_{i=1}^{n}(X_i - \bar{X})^2} \tag{2.2}$$

In Section 1.3 it is stated that there are two types of placement errors after placing a component on a PCB: systematic and random errors. When the constant systematic errors are measured it is possible to compensate for these errors using calibration. A calibration residue will remain, which will contribute to the average value.

The repeatability is calculated separately for the x-, y- and ϕ-direction. During the design of the P&P robot the ϕ-rotation will be implemented as the last axis of the P&P robot. Therefore the deviation in ϕ-rotation can be corrected separately from the x-, y-deviation. It is therefore that the repeatability in the ϕ-direction will not be shown in this thesis.

In this thesis the repeatability and the calibration residue are used to determine the accuracy of the new integrated alignment concept. During the analysis of the concept, the repeatability will be determined and the feasibility of calibration will be shown.

Requirement attributes	
Tag	repeatability in x- and y-direction
Gist	measure for placement accuracy
Rationale	the x-, y- and ϕ-repeatability are measures used for placement accuracy; while the alignment of a component in ϕ-direction is independent controllable by the final component rotation, the ϕ-repeatability will not be taken into account during the tests
Scale	μm (1σ)
Meter	if possible multiple tests are performed to determine the average value and the repeatability (1σ)

Table 2.3: *The requirement specification for accuracy*

Estimation of repeatability

During the design of the integrated alignment systems, the repeatability must be estimated. Therefore the metrology loop concept is introduced. A metrology loop is the loop that describes the machine parts that contribute to the repeatability.

As example the metrology loop during board alignment is shown as a dotted line in Fig. 2.4. A frame is holding a robot, which contains the board alignment vision system. An actuated PCB transport system holds the PCB. Each actuated system is equipped with a position measurement device. For the determination of the position of the PCB the metrology loop is used. The metrology loop for this measurement contains: the mechanical dimensions of the PCB transport system with its position measurement system, the frame, the position measurement system of the board alignment robot, mechanical dimensions of the robot and finally the board alignment vision system where the loop will be closed at the PCB.

During the board alignment an image of a PCB's fiducial (special marker) is acquired by the board alignment vision system; the image is transferred and then processed by software to determine the fiducial's position within the image. The position of the fiducial is known with respect to the sensor inside the board alignment system. Since the board alignment system is attached to the P&P robot, the measured position of the P&P robot with respect to the frame can be used to determine the position of the board alignment system's sensor. Additionally, the position of the PCB during alignment can be determined using the PCB transport system position sensor. Now the loop is closed and the position of the fiducial mark is known. The position of a second fiducial mark must be determined to be able to determine the position of the PCB.

To estimate the repeatability (σ) of the board alignment the repeatability of each module (σ_{module}) in the metrology loop will be added quadratically as shown in Equation 2.3. Where n is the number of modules in the

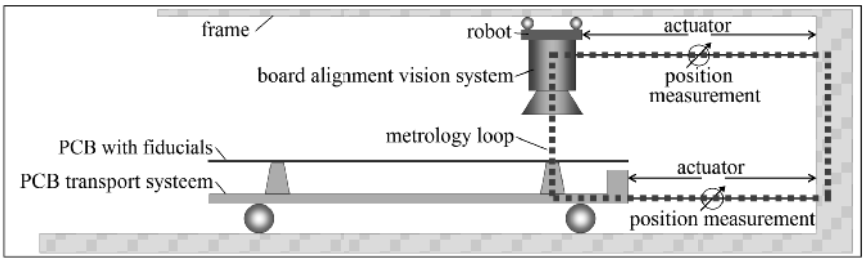

Figure 2.4: *Model of a board alignment system of a pick-and-place machine including a printed circuit board (PCB) transport system. The PCB has fiducials available for board alignment. The dotted line indicates the metrology loop during board alignment*

metrology loop.

$$\sigma = \sqrt{\sum_{i=1}^{n} \sigma_{module}(i)^2} \tag{2.3}$$

This equation can only be used if the repeatability of each module is uncorrelated of the repeatability of other modules. Therefore during the design it must be verified that the repeatability is uncorrelated.

Pick-and-place machine repeatability

Equation 2.4 is used to determine the repeatability of the overall P&P machine. The repeatability of each process in the P&P cycle is estimated and than added quadratically. This is allowed as long as the repeatability of each P&P processes is uncorrelated with respect to the other processes. In this case n is the number of processes that take place in the P&P cycle.

$$\sigma_{P\&Pmachine} = \sqrt{\sum_{i=1}^{n} \sigma_{process}(i)^2} \tag{2.4}$$

2.3 Design of integrated alignment systems

The components and PCBs must be aligned. Therefore P&P machines are equipped with two alignment systems, one for board alignment and one for component alignment. In this section several board alignment and component alignment strategies are discussed.

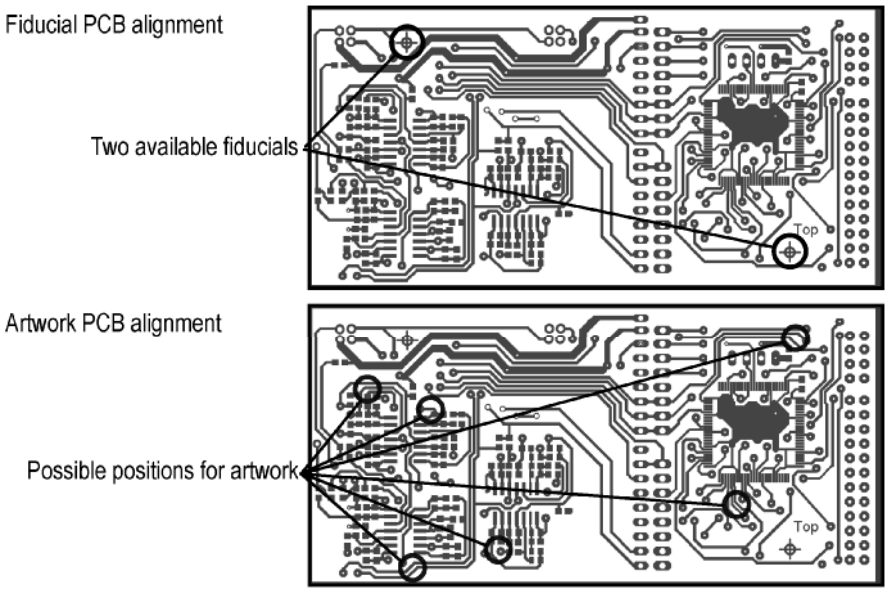

Figure 2.5: *The same PCB but different board alignment features are depicted. Top: The PCB with two fiducials that can be used for board alignment. Bottom: The PCB with possible positions that can be used for artwork board alignment*

2.3.1 Board alignment

A PCB is a plate with copper artwork, consisting of wires, vias, lands and fiducials etched on it. The position of this artwork, with respect to the mechanical properties of the PCB are not meeting the required repeatability. Consequently, it is not possible to use mechanical board alignment. Therefore, the position of the artwork of the PCB is nowadays determined by means of a vision system.

To determine the position of each footprint would take too much time for board alignment. Instead, during board alignment the position of specific features from the layout are used by the board alignment system. With the assumption that the expansion or shrinkage of a PCB will be linear over the board, the position of the features measured can be fit on the expected positions of these features. Hereafter, with the help of the CAD-files the positions of the lands of each component can be calculated.

There are two different methods used during board alignment: fiducial or artwork recognition. Figure 2.5 shows the layout of artwork on a PCB. For fiducial recognition (top PCB in Fig. 2.5) fiducial marks are added at the perimeter of the patterned area. This results in the requirement to be able to determine the position of all fiducials before a component is placed. Artwork recognition (bottom PCB in Fig. 2.5) uses wires, lands and vias

of the patterned board. Jong [57, pg.111-113] describes artwork properties that have to be taken into account to be usable for artwork board alignment. The benefit of artwork recognition is that local information can be used to determine the position of the PCB.

The usability of the alignment strategies depends on the layout of the PCB and not on the P&P machine strategy. Therefore it is decided that preferable board alignment system must be designed in such away that both methods are feasible. The consequences will be discussed in the next chapters.

2.3.2 Component alignment

During the component alignment process the aim is to determine the position of the component's terminations, which can be positioned at the outline of the body or at the bottom side[1]. To determine the position of the terminations vision systems are used.

There are multiple strategies to implement vision based component alignment systems. These strategies can be divided into two groups when taking account the velocity difference between the component and the vision system. A difference in velocity can result in motion blur that influences the repeatability.

In Figure 2.6 five component alignment strategies are presented. A short description of each strategy is presented in the next list.

1: stop-and-go-vision the P&P robot, holding the component, moves to a vision system, stops above the vision system, an image is taken. Then the P&P robot moves to the PCB to place the component. There is no velocity difference between the vision system and the component to be aligned.

2: vision-on-the-fly the P&P robot, holding the component, moves over a vision system and the image is taken. While taking the image there is a velocity difference between the vision system and the component to be aligned.

3: vision-on-the-beam the P&P robot is equipped with a vision system. While the P&P robot moves from the pick to the placement position an image is taken. Because the vision system is mounted on the P&P robot there is no velocity difference between the vision system and the component.

4: laser-alignment the P&P robot is equipped with a laser alignment system. While the P&P robot moves from the pick to the placement

[1] More information on the component range and the specifications will be discussed in the next chapter

Comparison of component alignment strategies		
Description	**Process time[1]**	**Repeatability[2]**
1: stop-and-go-vision	−−	0
2: vision-on-the-fly	+	−
3: vision-on-the-beam	0	0
4: laser-alignment	++	−−−
5: look-while-place	−	−−

Table 2.4: *Expected influence of component alignment strategies on process time and repeatability; the alignment strategies are compared with the benchmark: vision-on-the-beam; 1: −− means maximum extra time, ++ means minimum influence on P&P cycle time; 2: −−− lowest repeatability, 0 means highest repeatability*

position the component is rotated inside a laser beam. The shadow produced by the rotating component is measured combined with the angular position of the component the position of the component can be determined. Because the system is mounted on the P&P robot there is no speed difference between the vision system and the component. On the right side of Fig. 2.6 strategy 4, an image is shown of the laser beam and the shadow created by the component. If the terminations are the edges of the component then the termination positions are measured directly, otherwise the housing is measured.

5: look-while-place the vision system looks downward during the placement of the component; the scene contains the position of the component (from top side) and information of the position of the footprint of the component is measured. The benefit of this idea is the direct visual coupling between the component and the placement position. But to realise such a setup there are demands on the PCB and components. The image contains information about the position of the component and the PCB. When the leads are not visible from above an additional measurement station must be added to determine the position of the leads of the bottom side of the component with respect to the housing of the component.

In table 2.4 the five strategies are compared with respect to each other on two performance indicators: process time and repeatability. The vision-on-the-beam strategy is used as the benchmark for the other strategies and is thereby neutral.

Taking into account the influence on process time the laser-alignment strategy is preferred. The only extra movement is the rotating during the move process but it is to be expected that there is no extra time required. Vision-on-the-fly needs extra distance during the move process,

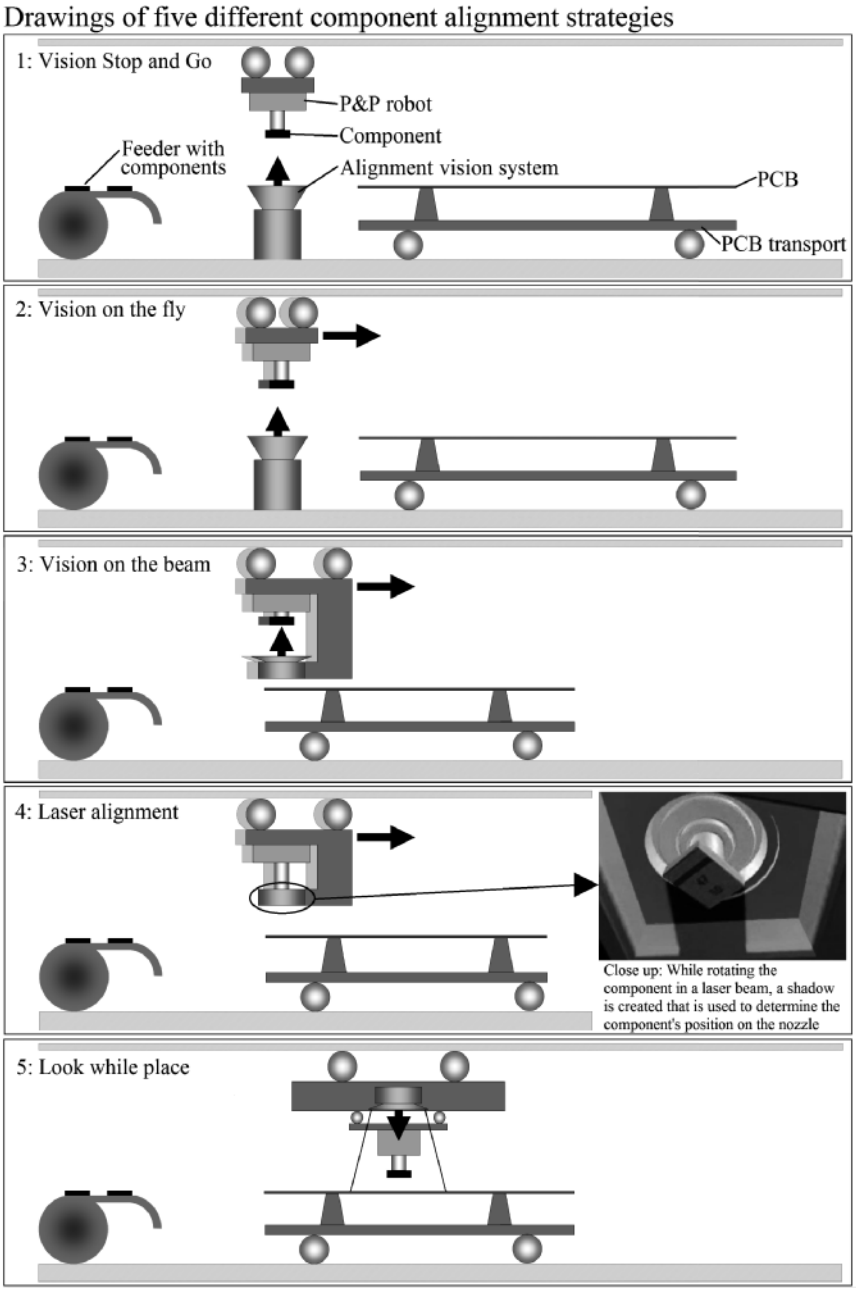

Figure 2.6: *Five drawings of component alignment strategies; 1: stop-and-go-vision, the P&P robot stops above the vision system. 2: vision-on-the-fly, the P&P robot moves over the vision system. 3: vision-on-the-beam, the vision system attached to the P&P robot takes an image of the component. 4: laser-alignment, the vision system attached to the P&P robot measures the shadow of the rotating component using a laser beam. 5: look-while-place, the vision system attached to the P&P robot makes an image of the scenery that includes the component and board features*

where vision-on-the-beam needs some extra distances to be able to have a vision system under the component. look-while-place needs most time to determine the artwork or footprint and then the component must be moved into the field of view of the vision system. Finally stop-and-go-vision requires additional time for stopping, settling and starting, which results in an increased P&P cycle time.

Comparing the five strategies with respect to the repeatability requirement results in the estimation that stop-and-go-vision and vision-on-the-beam will perform equal. In both situations the vision system and component are not moving with respect to each other. vision-on-the-fly is next, although this depends on the amount of displacement when taking the image. This displacement leads to motion blur, which will decrease the repeatability. look-while-place can probably perform well but will fail if the terminations are at the bottom side of the component. Finally, laser-alignment will not perform at all if a component has terminations at the bottom side of the component.

The conclusion of this analysis is that the stop-and-go-vision concept can not be used. The time needed to stop, measure and move again will major influence the time of the total P&P cycle. The requirement to be able to align also components with terminations at the bottom of the component leads to the conclusion that laser-alignment and look-while-place both can not be used as alignment strategies. So the two most feasible vision strategies are vision-on-the-fly and vision-on-the-beam meaning that these two alignment strategies are used during the integration of the alignment systems.

2.4 Realisation of the alignment system

Using the requirements from the previous chapters in Chapter 5 the modules for the alignment systems are determined. The use of commercial available modules to realise the alignment systems is preferred. If commercial available modules do not meet the requirements, these modules must be designed and built.

2.5 Demonstrator design considerations

In this section the general design considerations made for the demonstrator are discussed per module.

2.5.1 Shuttle

Figure 2.7 shows the main idea of the shuttle concept P&P machine. The top drawing shows a schematic layout of a P&P machine without a shuttle; the P&P robot picks a component from the feeder moves to the component

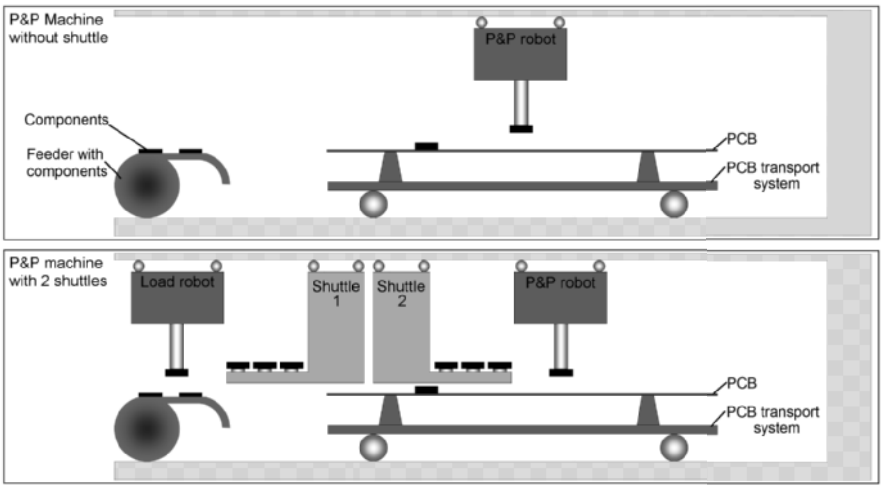

Figure 2.7: *Top: schematic layout of a P&P machine. Drawn a feeder with a reel containing components. A PCB transport system containing a PCB. Also shown is the coordinate system used in this thesis. Bottom: schematic layout of a P&P machine with two shuttles, a load robot and a P&P robot*

placement position, places the component and moves back to the feeder. In the bottom drawing a layout of a P&P machine containing two shuttles and a load robot is shown; the P&P robot moves from the pick position on the shuttle to the component placement position, places the component and moves back to the shuttle. While the component is placed by the P&P robot, the shuttle moves to stay close to the P&P robot. More information on this design can be found in Appendix A.

Figure 2.8 shows why it is required to have two shuttles. A load robot in the shuttle concept P&P machine enables the possibility to fill one shuttle while the other P&P robot will empty the second shuttle.

The study on throughput has resulted in requirements that must be met to realise the estimated throughput increase. It has been concluded that the increase of throughput can only be realised when three main properties are taken into account: the size of the shuttle, the travel distances of the P&P robot and the time required for processes. Goede et al. [40] discusses the design of the shuttle. The component carrying shuttle is used to reduce the distance from the pick to the place location and hence travel time is reduced. The shuttle will be placed between the PCB and the P&P robot that is why the height of the shuttle will add a distance in the z-direction. From the analysis it is concluded that the overall height of the shuttle can be 10 mm at max. The sizes that are presented for the shuttle are 50 $mm\times$ 50 $mm\times$ 10 mm (x×y×z).

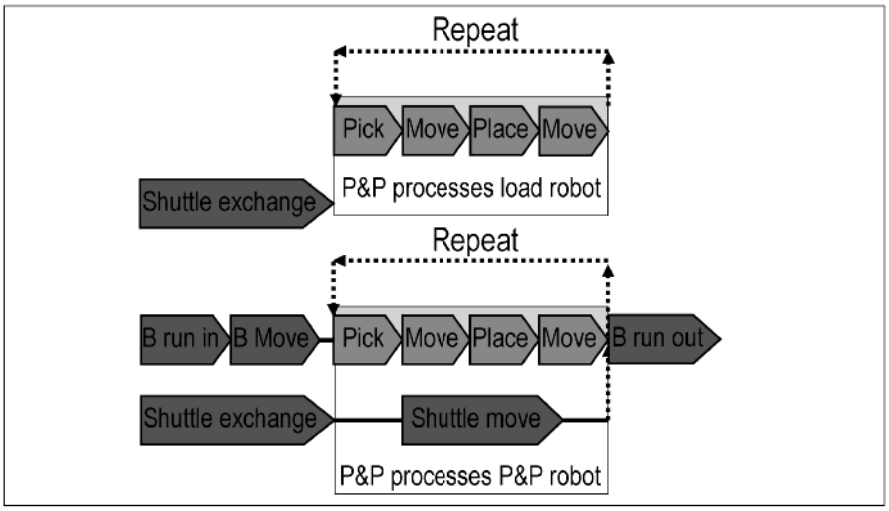

Figure 2.8: *The P&P cycle of the load robot filling the shuttle while concurrently the P&P robot picks components of the shuttle and places the components on the PCB*

2.5.2 Load robot

Depending on the design of the alignment systems, a load robot can influence the repeatability. If the load robot becomes part of the alignment system then the load robot will be designed equal as the P&P robot. It is decided that the design of the load robot will not be a part of this research.

2.5.3 Pick-and-place robot

To realise a test setup for the integrated alignment system a shuttle concept P&P machine must be designed including the P&P robot. In this section some considerations on the design of the P&P robot as part of the test setup are briefly discussed. The limited time available in the shuttle concept P&P machine for the movements, combined with the repeatability has led to the consideration for some other design concepts. From Appendix A the working area of the P&P robot is adopted being 80 mm×500 mm×26 mm (x×y×z) and a ϕ-axis that is able rotate 2π rad. To be able to place components in this working area the space to build a P&P robot is limited in the x-direction to 120 mm. This limitation comes from the requirement that multiple P&P robot must be able to move in parallel. The other directions are not limited.

In general, it is preferred to keep the mass of the P&P robot as low as possible, due to the accelerations up to 50 m/s^2 in x- and y-direction, which must be achieved. The mass of the shuttle is less critical as the accelerations for this part are limited to 10 m/s^2. Consequently, it is preferred to add the alignment systems to the shuttle and not to the P&P robot.

It is a requirement that the shuttle must be able to move within the working area of the P&P robot. This means that during the design of the P&P robot the design of the shuttle is taken into account.

Macro shuttle robot with micro pick-and-place robot

The functionality of the P&P robot, which should be fast and have a high repeatability, and a shuttle robot that is slow and requires limited repeatability generates the idea to use the macro/micro concept. Sharon et al. [95] state that a macro/micro manipulator system, consists of a large (macro) robot carrying a small (micro) high performance robot. The first concept in Fig. 2.9 shows the main idea. A micro manipulator with a limited stroke but high repeatability, is stacked onto the macro manipulator, which has a long stroke but limited repeatability. The macro manipulator holds in this design not only the P&P robot but also the shuttle.

This concept is a well known concept used in different industries [24, 46, 47, 66, 67]. The main idea is that the weight of a micro robot is low compared to the weight of the total robot, resulting in better dynamic behavior.

Research where a micro manipulator is attached to a macro manipulator to place surface mounted device (SMD) components has been carried out. Hollis et al. [48] present a macro/micro system where the micro robot has a stroke of 0.9 mm with an accuracy of 0.5 μm. The stroke of the micro manipulator does not fit the required stroke of minimum 50 mm of the P&P robot in the shuttle concept P&P machine. Baartman et al. [6] show a design where a look-while-place macro/micro concept is designed. In this design the micro system is able to make a stroke of 1 mm. Lee [70] has realised a macro/micro system but is only adding a micro system to control the forces in the z-direction. The x- and y-positioning is done by the macro system.

As can be concluded the stroke of micro manipulators is often considered to be small when it is in the order of a millimeter or less. In the shuttle concept, the stroke of the micro manipulator has to be more than 50 mm (size of the shuttle). Therefore the realisation of the micro manipulator requires probably the same measurement and actuation modules that will be used to build a macro manipulator.

For this reason the macro/micro concept is rejected.

Shuttle robot combined with a parallel mechanism pick-and-place robot

Parallel mechanism robots are used for fast P&P processes [11, 8, 78]. Therefore this concept seems useful in the shuttle P&P machine where the P&P robot has to be fast.

Liu [73] shows several parallel mechanisms layouts where the majority of mass is attached to the solid world and linkages are used to move the end

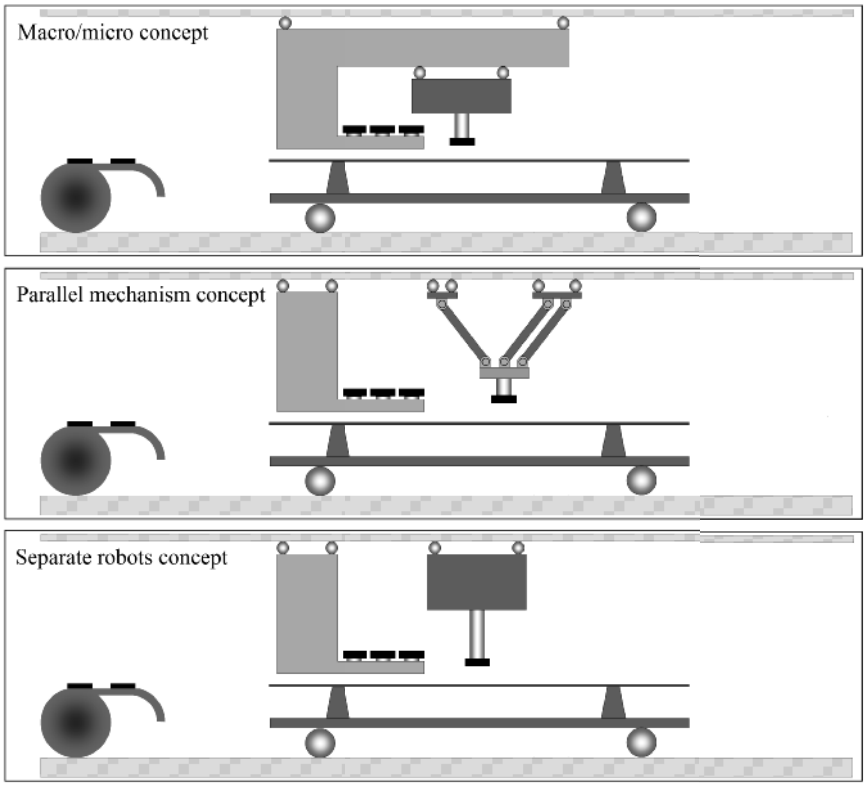

Figure 2.9: *Three concepts combining a P&P robot with a shuttle. Top: the shuttle is the macro manipulator where the P&P robot is the micro manipulator. Middle: a parallel mechanism robot is combined with a separate shuttle. Bottom: a P&P robot is combined with a separate shuttle on the same linear bearing. the last concept is selected*

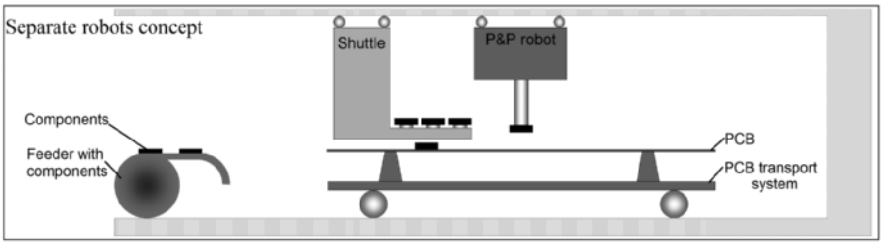

Figure 2.10: *The selected shuttle concept layout combines a P&P robot with a separate shuttle on the same linear bearing*

effectors. When parallelograms are added to a parallel mechanism robot, the end-effector can be kept horizontal without adding an active linkage. The middle image in Fig. 2.9 shows a two DOF parallel mechanism robot able to move in the x- and z-direction while maintaining the end-effector horizontal by using a parallelogram. This robot has two actuators moving in the y-direction. Via two linkages placed on these actuators a movement in the y-direction or the z-direction or a combined movement in these directions can be realised.

A case study for this parallel mechanism P&P robot is presented in Appendix B. This study proves the feasibility of such a P&P robot.

The second concept in Fig. 2.9 shows the parallel mechanism P&P robot combined with a shuttle. As can be seen, combining this concept with a shuttle robot becomes difficult due to required length in y-direction to realise the z-stroke of the parallel mechanism robot. The shuttle must be able to present the components close to the end-effector of this robot, which seems not very feasible.

This design is therefore rejected.

Shuttle robot combined with a pick-and-place robot

This concept uses two separate robots, one robot to carry the shuttle and one P&P robot. The P&P robot needs four DOFs to be able to place a component. The layout of a four DOFs can be combined in several ways. Because the y-axis can be used by both robots, the shuttle robot and the P&P robot this will be the first axis. The other three directions are stacked onto this axis. First x-axis then z-axis and finally the ϕ-axis. Hereby it is easy to rotate the nozzle with the component.

Figure 2.10 shows the selected concept using a shuttle robot and a P&P robot.

2.5.4 Position measurement

Each axis position must be measured with respect to a reference. Kunzmann et al. [65] compare scales with interferometers and concludes that

for resolutions in the range of 0.1 μm to 10 μm scales are mostly more reasonable than interferometers for integration into machines. Also Probst [83, pg 28-29] concludes that for position measurement, scales are the only cost effective system for P&P machines. In this design each axis will be equipped with a scale. The term encoder is used for the position measurement systems, where an encoder consists of a readhead and a scale. For the encoder calibration and the validation of the repeatability performance additional interferometers are used in the demonstrator.

2.5.5 Actuators

During the design of the demonstrator, the actuators for the x- and y-direction have to be chosen. Examples in literature [12, 52] show that P&P machines can be equipped with spindle drives but in this application where the shuttle robot as well as the P&P robot will perform the same linear movement in the y-direction the use of a linear actuator is preferred.

The choice of an actuator will mainly come from the acceleration and velocity specification, but the actuator can also influence the repeatability. In general gearboxes and spindles will influence the repeatability because play, backlash and friction will be present. To avoid these non-linearities, direct drive actuators can be used. However, direct drive actuators can have non-linear behavior such as cogging when iron is used inside the moving part of the actuator. Several studies [90, 81, 55] are performed to improve the repeatability of an iron core machine. But for this demonstrator it is preferred to use actuators with minimal non-linearities so an iron-less linear actuator will be selected.

As shown in Figure 1.2 a narrow P&P robot has a width of 120 mm. The UC3 actuator meets the required dimensions because the magnet track of this actuator has a length of 118 mm[100]. The moving coil has a length of 34 mm and is able to produce 10 N continuously.

For both y-axes, shuttle and the P&P robot, an equal motor concept is chosen. This ironless linear actuator is larger, the coil length is 78 mm and is capable of producing 22 N. The magnet track will be placed onto the frame, the coils will be moving.

To be able to place a component P&P robot moves to the desired position above the PCB. Then the component must be positioned in the ϕ-direction and finally the component is moved downwards to be placed on the PCB. The rotation and downwards movements are often combined in one module. In this research a commercial available zϕ-module is used. This module is equipped with a voice coil DC motor for the z-stroke and an AC-synchronous motor to move the ϕ-axis. Both axes have an optical encoder to determine the position.

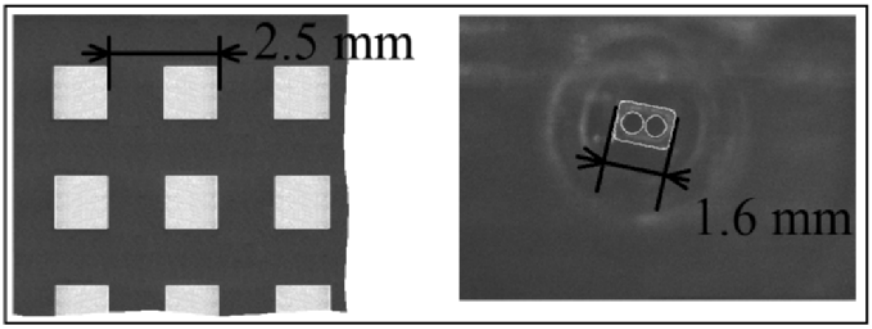

Figure 2.11: *For repeatability validation are two reference systems used: Left: portion of the calibration plate used for board alignment. Right: nozzle used for component alignment*

2.5.6 Machine control

The machine controller must perform several tasks. The main tasks are: motion control for multiple axes, position measurement, creation of the alignment trigger and the homing sequence. The choice is made to realise the overall machine control with help of a PC program and a commercial available motion control platform, which is designed for semiconductor machines [36, 21]. This motion control platform has a modular architecture where up to five modules can be placed into a backplane. The first module is a CPU module able to control multiple other modules. The other slots can be used for drives that can drive one or two axes. A maximum of eight axes can be driven by this motion control platform. This motion control platform will be discussed in more detail in Section 6.1.4.

2.5.7 Image processing software

Halcon [39] is commercial available machine vision software to process images including an integrated development environment to develop sequences using image processing algorithms. This software is also capable to control a camera. After the development of the image processing sequences it is easily possible to interface with the overall machine control software.

2.6 Validation of the alignment system

As stated in Section 1.4, one of the goals is to validate the repeatability of the integrated alignment systems. A common way to test the board alignment system's repeatability is to replace the PCB by a calibration plate [85, 108]. A calibration plate is a glass plate with squares etched onto it (step 2.5 mm). This plate is produced and measured afterwards, a repeatability of -0.12 μm per step and -0.64 μm in total is measured. In the left picture

of Fig. 2.11 two of the edged squares of the calibration plate are shown. Later it will be discussed that round PCB features are preferable for the repeatability, because the calibration plate is available this plate is used.

To determine the repeatability of the component alignment system the component is replaced by a reference nozzle for a 0603 component. The advantage is that the nozzle is stable attached to the P&P robot what eliminates the chance of moving during repeatability tests. This hollow nozzle takes a component with help of vacuum. In the right picture of Fig. 2.11 the reference nozzle is shown including in white the reference model used for the image processing software. The reference model contains two circles and the rectangular outline. The angle of the nozzle is arbitrary but will remain on the shown position due to the homing sequence of the zϕ-module. The disadvantage is that this reference model has more information than a rectangular component, what can influence the analysis of the repeatability tests.

To present the repeatability, histograms will be used and the 1σ value will be determined.

2.7 Conclusion

The performance indicator repeatability will be used during the design of the concepts. Later in this thesis, repeatability will also be used to determine the performance of subsystems and to analyse the performance of the subsystems. Using repeatability as the accuracy performance indicator, implies that calibration is possible. Otherwise, the average value ($\bar{X}$) has also be taken into account. During the analysis of the demonstrator calibration will be discussed.

Figure 2.2 showed a V-model where the chapters are added for this thesis. In Chapter 3 the requirements will be determined. In Chapter 4 an iterative method is used to design the integrated board alignment and component alignment for a shuttle concept P&P machine. In Chapter 5 the modules are selected for the alignment systems. Then in Chapter 6 the demonstrator is presented that is used to perform the measurements, which are presented in Chapter 7.

Chapter 3

Requirements

Using the competitive engineering method as introduced in Section 2.2 means that a requirement is specified by eight attributes. In this chapter the two requirements pick-and-place cycle time and repeatability are defined using this method.

3.1 Pick-and-place cycle time

In appendix A the shuttle concept P&P machine is selected to improve the throughput. The shuttle concept minimises the distance between component pick position and the position on the PCB where the component must be placed. The throughput is calculated by taking the inverse of the algebraic sum of the individual P&P cycle times. The P&P cycle time is determined by adding the process time of each succeeding process. In appendix A it is estimated that adding a shuttle to the selected P&P machine will decrease the P&P cycle time from 450 ms to 225 ms. The P&P cycle time requirement is presented in Table 3.1 using the eight requirement attributes.

Requirement attributes	
Tag	P&P cycle time
Gist	average time to execute a P&P cycle
Rationale	this time will influence the throughput of the P&P machine
Scale	ms
Meter	adding the time required for each process in the P&P cycle
Past	> 450 ms (see appendix A)
Must	225 ms
Plan	< 200 ms

Table 3.1: *The P&P cycle time requirement is specified using eight attributes*

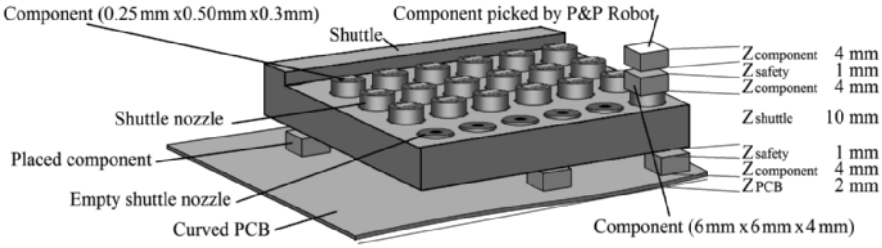

Figure 3.1: *Specifications of distances in z-direction for the shuttle from Fig A.17 the shuttle has 24 nozzles that can carry one component each. The largest components are 6 mm×6 mm×4 mm. The P&P robot must be able to pick a component and move over other components on the shuttle. The total required stroke of the P&P robot in z-direction is determined*

Trajectory

For motion planning trajectories are used [74, 69]. These trajectories are described by parameters as: acceleration, velocity and the distance. To minimise the P&P cycle time, acceleration for movements should be maximised. On the other hand the accelerations are limited due to the use of a vacuum nozzle and the settling time for the P&P robot. The analysis presented in Appendix A uses a maximum acceleration of 50 m/s^2 and a maximum velocity of 2 m/s to determine the time required for the distances that the P&P robot can travel in a shuttle concept P&P machine.

Distances in x- and y-direction

By using the limited values for acceleration and velocity and a maximum P&P cycle time of 225 ms , it can be calculated that the maximum average distance between pick and place should be 50 mm(Appendix A). This dimension will be a requirement for the design of the integrated shuttle concept alignment system.

Distances in z-direction

The mechanical dimensions from the shuttle design are shown in Fig. 3.1. From the component specification it is known that the height of a component can be maximum 4 mm. This means that the shuttle must be positioned on a height with respect to the PCB to move over the non-flat PCB containing components, $Z_{PCB} + Z_{Component} + Z_{Safety}$ is 7 mm. The shuttle has a height of 10 mm. Then on the shuttle a component is placed and another component must be safely transported over components on the shuttle. This means that above the shuttle a distance of $Z_{Component} + Z_{Safety} + Z_{Component}$ being 9 mm is required. So the total stroke in the z-direction is minimal 26 mm.

3.2 Repeatability

The terminations of components will prescribe the required repeatability but different component types can have different terminations like end-caps or leads. The component types that will be handled by a shuttle concept P&P machine are components that fit in a maximum component volume of 6 mm×6 mm× 4 mm as shown in Section 1.3. Two groups of components that fit within this volume are passive components with two end-caps as termination and ICs with leads. The repeatability requirements for the passive components and ICs will be determined in the next paragraphs.

In Section 1.3 is stated that in literature the required repeatability to place a 0.254 mm×0.508 mm (0201) component is 15 μm (1σ).

Other components that fit in the envelop of 6 mm× 6mm× 4 mm are ICs. The terminations of ICs can be side leads or balls in a grid at the bottom side (Ball grid Array (BGA) components). In literature [1, 33] it can be found that the smallest pitch between the side leads is about 300 μm. Using the IC's bottom side, with a larger area compared to side leads, has as the advantage that the pitch of the balls can be equal or larger than the pitch between the side leads. Therefore it can be expected that the pitch between the side leads of a component will specify the required repeatability. In literature [33, 35] it is stated that the repeatability for components with a side lead pitch of minimal 300 μm can be placed with P&P machines with a repeatability of 17 μm (1σ).

To verify the feasibility of the "must" requirement, the attribute "past" value is determined using a benchmark machine. For repeatability the AX-5 as shown in Fig. 1.2 is used as a benchmark machine, which is capable of a repeatability of 13 μm (1σ)[82]. Due to the fact that the repeatability is depending on the components to be handled, the "plan" attribute only has to be improved when the types of components will change. Therefore this attribute is set equal to the "past" attribute. All requirement attributes are presented in Table 3.2

Requirement attributes	
Tag	repeatability in x- and y-direction
Gist	measure for placement accuracy
Rationale	the x-, y- and ϕ-repeatability are measures used for placement accuracy
Scale	μm (1σ)
Meter	multiple measurements are performed to determine the repeatability (when feasible)
Past	13 μm (1σ)
Must	15 μm (1σ)
Plan	15 μm (1σ)

Table 3.2: *The repeatability requirement is specified using eight attributes*

Although there can be a difference in the repeatability requirement in x- and y-direction, it is chosen to present during specification only one value, which is the maximum of the both directions. During validation the repeatability in y-direction will be determined. In the next section the repeatability requirement for the individual P&P processes is discussed.

3.2.1 Process repeatability contributions

In the previous section the machine repeatability requirement is determined. In this section this requirement is divided over the separate P&P processes presented in Fig. 1.3. For each separate P&P process is the influence on repeatability described and a value is determined.

The repeatability values of the individual P&P processes are determined and used to calculate the overall P&P machine concept. When the overall repeatability is lower than the repeatability specification the remaining repeatability can be used for unforseen influences.

The feasibility of the "must" values are compared with the benchmark machine "past" values [82].

3.2.2 Board handling

Board handling contains three processes: Board Run In, Board Move and Board Run Out used to load, move and unload the PCB from the machine. Loading the PCB into the machine and transport it to the board alignment area will not influence the repeatability because the PCB's position is determined after these process steps. The movement of the PCB to the component placement area by a PCB transport system will influence the repeatability. This influence can be eliminated if board alignment can be performed in the placement area. This is only feasible when the PCB position information is within the placement area and the board alignment system can work in this area. While it is not possible to guarantee that BA can be performed after board transport, it is assumed that the transport will contribute to the final repeatability.

Another effect that can influence the placement repeatability is the effect of the shift of pre-mounted components caused by accelerations of a PCB. Therefore the accelerations of the PCB must be limited, so no component shift will occur.

The benchmark P&P machine uses a walking-beam PCB transport system, which is able to transport the PCB with a repeatability of 4 $\mu m\,(1\sigma)$. This result is added to Table 3.3.

Redesigning the board handling system will not be part of this research meaning that the repeatability contribution of board handling is adopted from the benchmark P&P machine.

Error budget Description	Repeatability [$\mu m\,(1\sigma)$] "past"	"must"
Board handling	*4.0*	*4.0*
Total repeatability	*4.0*	*4.0*

Table 3.3: *Repeatability requirement "past" and "must" values for Board handling*

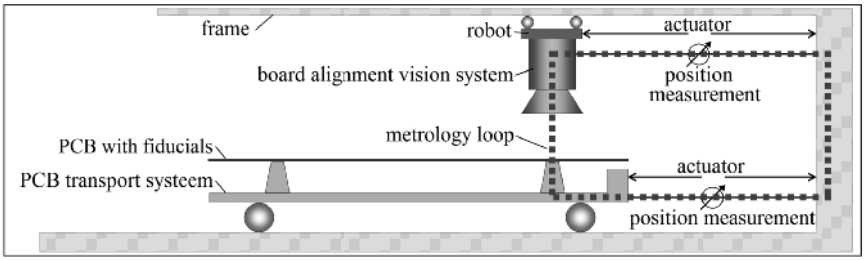

Figure 3.2: *Model of a board alignment system of a P&P machine including a PCB transport system. The dotted line indicates the metrology loop during board alignment*

3.2.3 Board alignment process

A board alignment (BA) process is added to the P&P machine to determine the position of the PCB. State of the art BA systems contain a digital vision sensor, lenses, illumination and image processing software to determine the PCB position [23].

Figure 3.2 shows a BA system, which is attached to a robot that is able to move the BA system to the position where a fiducial or artwork is positioned on the PCB. An image is taken and processed to determine the PCB's position in the image. Using a metrology loop indicated by the dotted line the position of the PCB in the machine can be determined. The metrology loop contains the frame, the position sensor of the robot, the mechanical dimensions of the robot, the vision system, the PCB features, the dimensions of the PCB transport system, the mechanical dimensions of the transport system, the position sensor of the transport system, back to the frame. For the analysis all mechanical parts of the metrology loop are considered stiff minimising the influence on repeatability. The influence of board handling is already estimated in the previous section. To determine the repeatability of the BA system the contribution of all other parts of the metrology loop will be discussed.

Robot position measurement system

The BA vision system is mounted on a robot to be able to move over the PCB. For this robot a linear encoder is used for position measurement

(Section 2.5.4). The scale of the linear encoder is attached to the frame and the readhead is mounted to the robot to determine the relative position reading the scale.

In this research standard available optical encoders [87, 88] are used. Depending on the readhead this linear optical encoder can realise resolutions from 50 nm to 5 μm. The scale has a linearity of $\pm$ 0.75 μm/ 60 mm and ± 3 $\mu m/m$. Using calibration techniques, it is expected that the non-linearity of the scale of 3 $\mu m/m$ can be compensated for meaning that the remaining repeatability will be 0.75 μm (1σ).

Board alignment vision system

A BA vision system consists of a camera containing the sensor, a lens, illumination and image processing software and is movable. To be able to determine the requirements of the vision measurement system starts with the determination of the field of view (FOV). The FOV of the board alignment camera system must cover the area where a feature, fiducial or artwork, can be positioned. This area can be determined taking into account the maximum deviation of the PCB after board run in and the deviation of the artwork with respect to the PCB. Although the repeatability of the transport system is 4 μm (1σ), the mean can be much higher and is in millimeter range. Taking into account the inaccurate placement of the PCB and the patterns on the board, a board vision alignment must have a FOV of 4 $mm \times 4$ mm to determine the features. The size and number of the pixels of the sensor and the magnification of the lens can be used to determine the pixel size at the object position.

To perform board alignment, the vision system must be able to take images of the fiducials or artwork. The position of these fiducials or the artwork that is selected for board alignment can be anywhere on the PCB. This results in the requirement that the board vision system of the board alignment system must be able to move over the working area in x- and y-direction. Moving a BA camera will result in vibrations. To eliminate the influence of the camera's vibrations, the stop-and-go-vision strategy is applied in such a way that the images are acquired after applying a settling time. Hereby the influence of the vibrations can be neglected.

As shown in the shuttle design in z-direction, a PCB is not always an ideally flat substrate and consequently the vision module must be able to work accurately when height difference of ± 2 mm occur due to curvature of the PCB. The lens must be able to correct for the difference in heights.

For vision sensors Super Video Graphics Array (SVGA) (800 pixels $\times$600 pixels) and Extended Graphics Array (XGA) (1024 pixels $\times$768 pixels) are common sizes. Using a SVGA sensor a FOV 4 $mm \times$ 5.3 mm will be divided into 600$\times$800 pixels. This means that a pixel covers about 6.7 $\mu m \times$ 6.7 μm image side. The repeatability depends also on the PCB features, so the

repeatability will be determined in the next paragraph.

PCB features

The PCB features will be measured using the vision system. Jong [57] describes some requirements that have to be taken into account during the selection of artwork that can be used for board alignment. The minimum size of fiducials or artwork that should be used is about $2{\times}2\ mm$.

Other studies [6, 7, 22, 79, 101, 109] show that a round shaped fiducial is preferable and that there is a minimum size to realise subpixel repeatability. Using a round shaped fiducial with a minimum radius of 20 pixels can result in a repeatability of 0.17 pixel after image processing. Increasing the size of the fiducial will not increase the repeatability significantly.

Using image processing software the position can be determined on subpixel level of 0.17. Combined with the number of pixels and FOV, this results in a maximum repeatability of 1.2 $\mu m\ (1\sigma)$.

Feasibility Board Alignment

To be able to determine the feasibility of the repeatability requirement table 3.4 shows the determined contributions of the systems of the BA system. To be able to design the board alignment system, a budget for design is added. This budget was determined when the contribution of all known influences were determined.

Error budget	**Repeatability** $[\mu m\ (1\sigma)]$	
Description	**"past"**	**"must"**
Board Alignment process	3.8	
Vision System (FOV 4 $mm{\times}4\ mm$)		1.2
Position measurement		0.75
Design budget		5.8
Total estimated repeatability	3.8	6.0

Table 3.4: *Repeatability requirement "past" and "must" values for Board Alignment*

3.2.4 Component pick process

The P&P cycle shows that component alignment takes place after component pick what means that the pick process will not influence the P&P machine's placement repeatability The contribution to the P&P machine's placement repeatability is 0. As long as the alignment takes place after pick, this process will not influence the repeatability.

Error budget	**Repeatability** $[\mu m\,(1\sigma)]$	
Description	**"past"**	**"must"**
Component pick process	*0*	*0*
Total estimated repeatability	*0*	*0*

Table 3.5: *Repeatability requirement "past" and "must" values for Component pick process, while component alignment takes place after picking the component this process will not contribute to the repeatability*

3.2.5 Component move process

The move process of the P&P robot starts with picking a component using a vacuum nozzle, then the P&P robot moves to the component alignment system where the position of the component is determined and in succession the P&P robot moves to the component placement position above the PCB. During the movements after alignment, the component may not shift with respect to the nozzle.

Due to the use of a vacuum nozzle, the accelerations are bounded to avoid component shift or lost. The allowed acceleration in the x- and y-direction compared with the z-direction is different due to the fact that in the x- and y-direction the force holding the component on the nozzle includes the friction coefficient between the nozzle and the component. Where in the z-direction only the forces created by the vacuum nozzle are influencing the holding force.

By bounding the accelerations in the x- and y-direction to 50 m/s^2 component shift will not occur and therefore there will be no contribution of component move process to the repeatability.

Error budget	**Repeatability** $[\mu m\,(1\sigma)]$	
Description	**"past"**	**"must"**
Component move process	*0*	*0*
Total estimated repeatability	*0*	*0*

Table 3.6: *Repeatability requirement "past" and "must" values for Component move process, the component may not shift during movements what means that this process will not contribute to the repeatability*

3.2.6 Component alignment process

The component alignment process is added to the P&P cycle to increase the final placement repeatability. Using a vision system, the positions of the component's terminations are determined. Comparable to the board alignment, the total system consists of a digital vision sensor, lenses, illumination and image processing software. In Fig. 3.3 a vision-on-the-beam

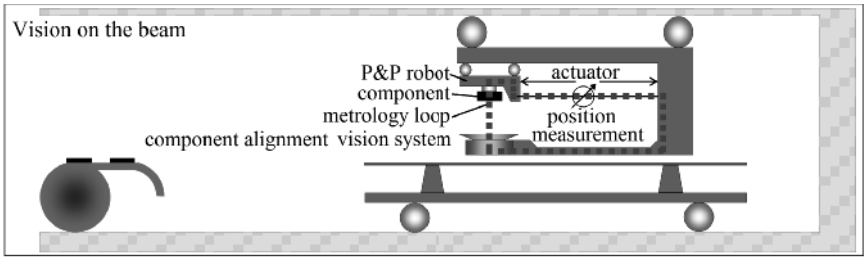

Figure 3.3: *Model of a vision-on-the-beam component alignment system. The dotted line indicates the metrology loop during component alignment*

component alignment system is presented where the P&P robot can move to a position where component alignment is performed. The metrology loop during component alignment includes a local measurement frame, position measurement system, component, sensor, illumination and lens. A vision-on-the-beam system means that the component is moved above a component alignment system. In analysis a stop-and-go-vision method is applied, where the influence of the dynamics is minimised while acquiring the image after a settling time.

Component

The range of components that will be handled by the P&P machine is discussed. It is mentioned that terminations can be at the edge or at the bottom side of the component. The alignment system must be able to handle both termination positions.

Component alignment vision system

The component alignment consists of a camera containing the sensor, a lens and illumination. The size of the components determines the FOV of the component alignment system. Taking into account the maximum size of the components of 6 $mm\times$ 6 mm can be used to determine the FOV. The components can be picked of center and with a rotational offset resulting in the demand that the $\text{FOV}_{component}$ must be larger then the size of the component is set to 7 $mm\times$ 7 mm.

Using the SVGA sensor as selected for the BA system means that a pixel represents 11.8 $\mu m\times$ 11.8 μm at object side, a XGA sensor results in a pixel representing 9.2 $\mu m\times$ 9.2 μm at object side.

Using a XGA sensor means that minimal 27 pixels are used for one side of a passive 0201 component. Efrat et al. [22] show that the maximum repeatability of a square aligned with the pixel grid is 0.5 the size of a pixel. The shape of components terminals other then BGAs will terminals rectangular. So a factor 0.5 is the maximum that can be achieved, resulting

in 4.6 μm.

To be able to determine the position of all components the illumination during component alignment must create the highest contrast between the terminals and the environment. Several different illumination systems are required depending on the component's shape. In the next chapter these illumination systems will be designed.

Component alignment position measurement system

In Fig. 3.3 a vision-on-the-beam alignment system is presented. The position measurement system of the P&P robot is part of the metrology loop. There for this position measurement system will influence the repeatability. The position measurement system used for this P&P robot will be equal to the position measurement system as discussed for the BA system. So the repeatability is expected to be 0.75 μm (1σ).

Feasibility component alignment

The most important contributions to the repeatability of the CA are estimated and summarised in table 3.7. Also to the component alignment process a design budget was added.

Error budget	**Repeatability** $[\mu m\,(1\sigma)]$	
Description	**"past"**	**"must"**
Component Alignment process	6.8	
Vision System (FOV 7 $mm \times 7\,mm$)		4.6
Position measurement		0.75
Design budget		7.0
Total estimated repeatability	6.8	8.5

Table 3.7: *Repeatability requirement "past" and "must" values for Component Alignment*

The influence on repeatability will mainly be determined by the vision system and the position measurement system. Other errors such as temperature, linear guidance system flatness, mechanical stability of the robot and the frame will influence the component alignment repeatability also but the influence on repeatability is not estimated.

3.2.7 Component place process

During the component place process, the component is placed on the PCB corrected with the data gathered during board and component alignment.

Component placement means that the P&P robot moves in the x- and y-direction. Meanwhile, the component is positioned in the ϕ-direction. At

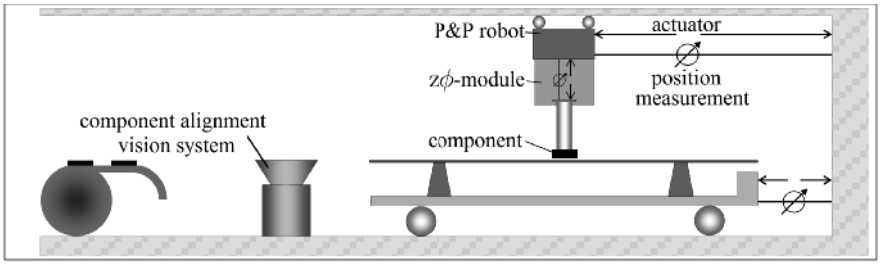

Figure 3.4: *Component placement. The P&P robot and the zϕ-module will influence the placement repeatability*

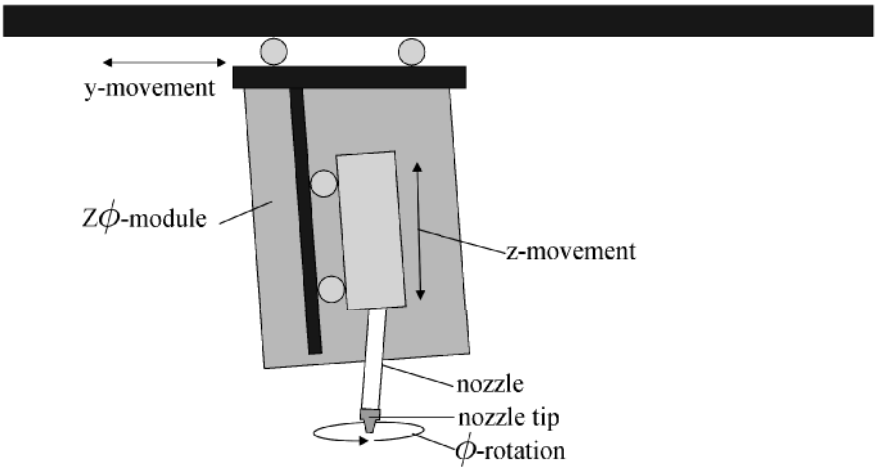

Figure 3.5: *Influences of z- and ϕ-axis positioning of the zϕ-module on placement repeatability*

the required corrected position, the P&P robot stops and the component is moved in the z-direction, until the component is pressed into the solder paste or glue. A dwelling time is required to let the solder paste or glue deform. Concurrent the vacuum is released. In Appendix A it can be found that the time for moving down will be 25 ms; the dwelling time 10 ms; moving up will take 25 ms.

During component placement two modules are used (Fig. 3.4):

- The P&P robot containing the zϕ-module, moves the component in the x- and y-direction
- The zϕ-module rotates the component and moves the component in the z-direction

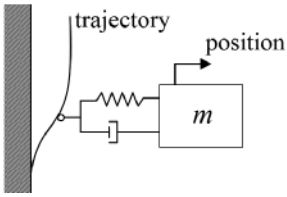

Figure 3.6: *Simple P&P robot second order representation*

zϕ-module

The zϕ-module will influence the repeatability in the x- and y-directions. While the nozzle is moved down, various effects will occur that influence the component placement repeatability in x- and y-directions. Figure 3.5 shows the influence of axis misalignment. If the z-axis is not perpendicular to the x- and y-axis, this will result in a deviation in x- and/or y-direction where the deviation is depending on the position of the z-axis. The height of the PCB will vary (± 2 mm) and is unknown, which will result in a contribution to the deviation of the placement repeatability. The rotating ϕ-axis will also influence the placement repeatability. When this axis is not centered with respect to the z-axis, depending on the ϕ-position, there will be a x- and y-deviation. To be able to pick and place the complete range of components, the nozzle tip has to be exchanged. The exchange of a nozzle tip can introduce an extra possible influence on the repeatability.

The design of a zϕ-module is not part of the research so data from the AX-5 P&P machine is used to estimate the total influence of the zϕ-module on the component placement repeatability and is set to 8 μm (1σ)[82].

Dynamic behavior pick-and-place robot

During the move process the P&P robot moves from the component pick position or component alignment position to the x- and y-position above the PCB where the component will be placed. The place process starts by moving the nozzle downward to place the component. During the movement in z-direction, the P&P robot has to settle in the x- and y-direction. This dynamical behavior of the P&P robot will influence the placement repeatability. An estimation is used to determine the settling time.

For an estimation it is assumed that the P&P robot can be modeled by a free moving mass (Fig. 3.6) that is controlled by only a feedback controller. A second order trajectory is used to create a position setpoint. This setpoint is used to move the mass via a proportional controller represented by the spring and a derivative controller represented by the damper.

The maximum acceleration of a_{max} (50 m/s^2) is prescribed by the application. It is assumed that the bandwidth of the P&P robot position controller (f_c) is in the range of approximately 50 Hz.

Using maximum acceleration a_{max} and controller bandwidth ω_c the maximum position overshoot amplitude after acceleration can be estimated:

$$A = \frac{a_{max}}{\omega_c^2} \approx 200\mu m \tag{3.1}$$

For the discussed place process, the P&P machine must be settled within a range of 5 μm in 25 ms. The decay rate of the exponential envelop is described by (3.2). Where ζ represents the damping factor.

$$c(t) = Ae^{-\zeta\omega_c t} \tag{3.2}$$

Takin into account the settling time (25 ms) and the allowed error (5 μm), the maximum allowed value for the decay rate at the settling time can be determined.

$$c(25ms) \leq \frac{allowed\ position\ error}{A} \leq 0.025 \tag{3.3}$$

Combining (3.2) and (3.3), ζ can be determined. It must be higher than 0.6, which is a reasonable value that can be achieved. In additional, feed-forward controllers are usually applied in these machines, which will result in a better performance. However, non-linearities as non constant friction will influence the performance too. This analysis shows that it is feasible to assume that final positions within a range of 5 μm can be achieved within a settling time of 25 ms. Taking into account the maximum accelerations of 20 m/s^2, an estimation on the repeatability will be 5 μm (1σ).

Error budget	**Repeatability** $[\mu m\ (1\sigma)]$	
Description	**"past"**	**"must"**
Component Place process		
zϕ-module	*8*	*8.4*
P&P robot	*5*	*5.3*
Total estimated repeatability	*9.8*	*10.0*

Table 3.8: *Component place influence on P&P machine repeatability*

The design of the component place process is not part of this thesis.

3.2.8 Feasibility repeatability

In Table 3.9 the values for the attributes "past" and "must" are presented. Using only the determined "must" values for each process results in a repeatability of 12 μm (1σ). The overall "must" requirement is 15 μm (1σ). The remaining budget is mainly divided over the two alignment processes. This budget will be used during the design.

Error budget	**Repeatability** $[\mu m\,(1\sigma)]$		
Description	**"past"**	**"must"**	**"design"**
*Board handling**	*4.0*	*4.0*	*4.0*
Board alignment process	3.8	6.0	
Vision System (FOV 4 mm×4 mm)			1.2
Position measurement			0.75
*Nozzle exchange**	*0*	*0*	*0*
*Component pick process**	*0*	*0*	*0*
*Component move process**	*0*	*0*	*0*
Component alignment process	6.8	8.5	
Vision System (FOV 7 mm×7 mm)			4.6
Position measurement			0.75
*Component place process**	*9.8*	*10.0*	*10.0*
Total estimated repeatability	13	15	12

Table 3.9: *Repeatability requirement values "past" from AX-5 machine data [82] and "must" estimation used as requirements for the V-model; *italic values will not be determined in this thesis*

3.3 Conclusion

In this chapter two requirements, P&P cycle time and repeatability, were introduced and defined using the competitive engineering method. The P&P cycle time requirement has resulted in additional specifications for the maximum distance between the shuttle and the P&P robot. The repeatability requirement is determined using the characteristics of the components that are within the range of components that will be placed by a shuttle concept P&P machine.

The repeatability specification is divided. For each process that takes place in the P&P cycle the "past" attribute is determined using a benchmark P&P machine. The "must" requirement attributes are estimated using some preliminary design data. This has resulted in an error budget for the processes and the overall P&P process. These values will be used in the next chapters as requirements for system design.

It can be concluded that the repeatability requirement is feasible by comparing the values for the "past" attribute with the values determined for the "must" attributes.

Chapter 4

Design of the integrated alignment system

In Chapter 3 the requirements for a shuttle P&P machine with integrated alignment systems are discussed. This chapter starts with the analysis of the best timing for board and component alignment within the P&P cycle. After the determination of the best moment of the board and component alignment, four shuttle P&P machine concepts with integrated alignment systems are presented. Followed by the selection of a concept. Finally, the repeatability for this concept is estimated and the requirements for the realisation of the integrated alignment system are summarised.

4.1 Integration of alignment systems with a shuttle concept

The integration of the alignment systems with the shuttle concept P&P machine means that the influence of the alignment processes on the process time must be minimised while realising the required repeatability. A solution to minimise the influence on the process time is to execute alignment concurrent with another process. In the next sections the alignment moments for board and component alignment are determined and then the influence on the P&P machine repeatability is estimated.

4.1.1 Integration of the board alignment system

Board alignment is required to determine the position of the PCB inside the machine before components can be placed onto the PCB. In this section the position of board alignment within the P&P cycle of the shuttle concept P&P machine is determined.

Figure 4.1 shows for both board alignment methods, fiducial and artwork alignment, possible time moments within the P&P cycle. The position of

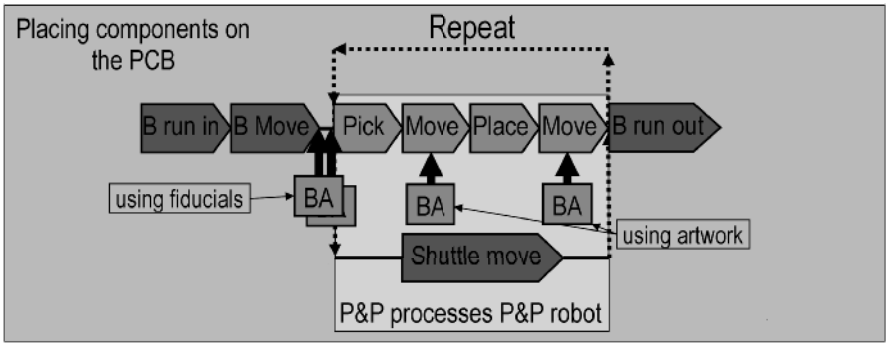

Figure 4.1: *Board alignment can take place on various moments in the P&P cycle. If fiducial alignment is used the position of minimal two fiducials must be available before the first component is placed. If artwork is used, before the first component is place information must be available of the board position but during the P&P process new information on the board position can be gathered*

the PCB must be determined before a component can be placed on the PCB. Therefore, the first moment to perform board alignment is when the board has been moved inside the P&P machine. When artwork is used in stead of, or in addition to fiducial alignment, it is can be required to add some extra board alignment steps to the P&P cycle. Two logical moments to add board alignment are after a component is picked and after a component is placed. This means that the board alignment will take place during the movements of the P&P robot. Therefore, no extra time is added to the P&P cycle time.

The moment of board alignment in the P&P cycle will not influence the repeatability as long as the board position information is available before a component is placed.

4.1.2 Integration of the component alignment system

To be able to integrate the component alignment system with the shuttle concept P&P machine, the moment of component alignment within the P&P cycle must be determined. In Fig. 4.2 there are four moments depicted where component alignment can take place in a shuttle P&P machine. In Fig. 4.3 shows also the four moments of CA.

In the next list the four moments of CA are described. In general it can be stated that for the repeatability it is preferable to minimise the number of processes after CA. The disadvantage is that the available time between the component alignment and the component placement on the PCB will decrease.

CA moment 1: before placing a component on the shuttle The load robot starts by picking the component from the feeder, then it moves

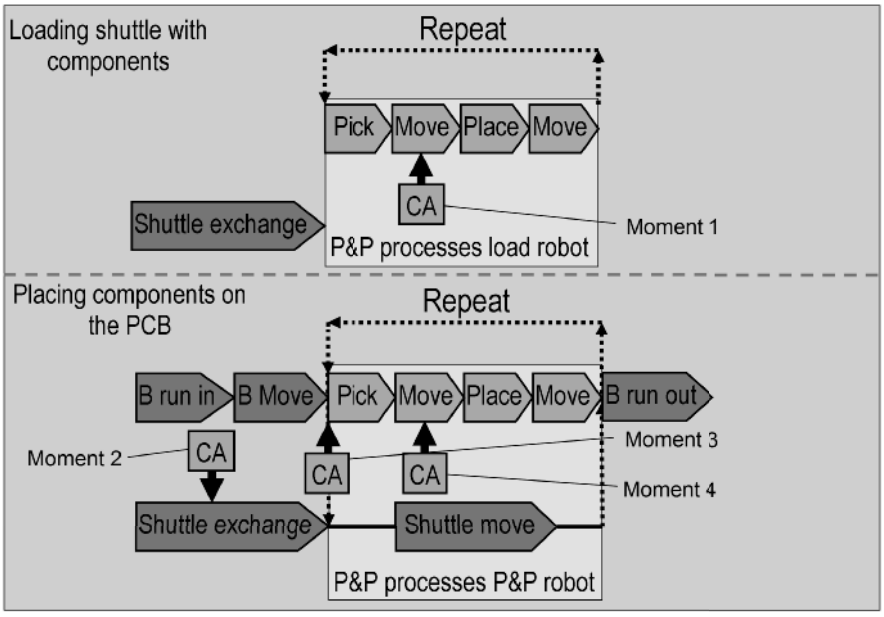

Figure 4.2: *In a shuttle concept P&P machine two P&P cycles are present. Top: the P&P cycle to load the shuttle. Bottom: the P&P cycle to place components on the PCB. Component alignment can take place on four moments of the two P&P cycles*

with the component over the component alignment camera where the component is aligned and then the component is placed on the shuttle. All processes except component pick of the load robot will influence the repeatability

CA moment 2: when a component is on the shuttle After the component has been placed on the shuttle, the component position is determined. The movements of the shuttle and the processes performed by the P&P robot will influence the repeatability

CA moment 3: before picking a component from the shuttle The component is aligned before the component is picked from the shuttle. The influences of the load robot and the shuttle movements will not influence the repeatability

CA moment 4: after picking a component from the shuttle Only the processes after component pick in the P&P cycle will influence the repeatability.

By using the "past" repeatability values from table 3.9 a first estimation on the influence of the repeatability of the four CA moments can be made. In table 4.1 the total estimated repeatability of the four positions is presented.

Influence on P&P machine repeatability				
Description	**xy-direction** [$\mu m\ (1\sigma)$]			
	m1	m2	m3	m4
Board handling	4.0	4.0	4.0	4.0
Board alignment process	3.8	3.8	3.8	3.8
Load robot				
Component pick process	0	0	0	0
Component move process	0	0	0	0
Component alignment process	6.8	6.8	0	0
Component place process	9.8	0	0	0
Shuttle movement	3.6	3.6	0	0
P&P robot				
Component pick process	9.8	9.8	9.8	0
Component alignment process	0	0	6.8	6.8
Component move process	0	0	0	0
Component place process	9.8	9.8	9.8	9.8
Total estimated repeatability	19	17	16	13

Table 4.1: *Estimated repeatability of the shuttle concept P&P machine with component alignment on four different moments within the P&P cycle using "past" values*

The table shows that the repeatability requirements of the parts of the shuttle concept P&P machine, load robot, shuttle and P&P robot, depends

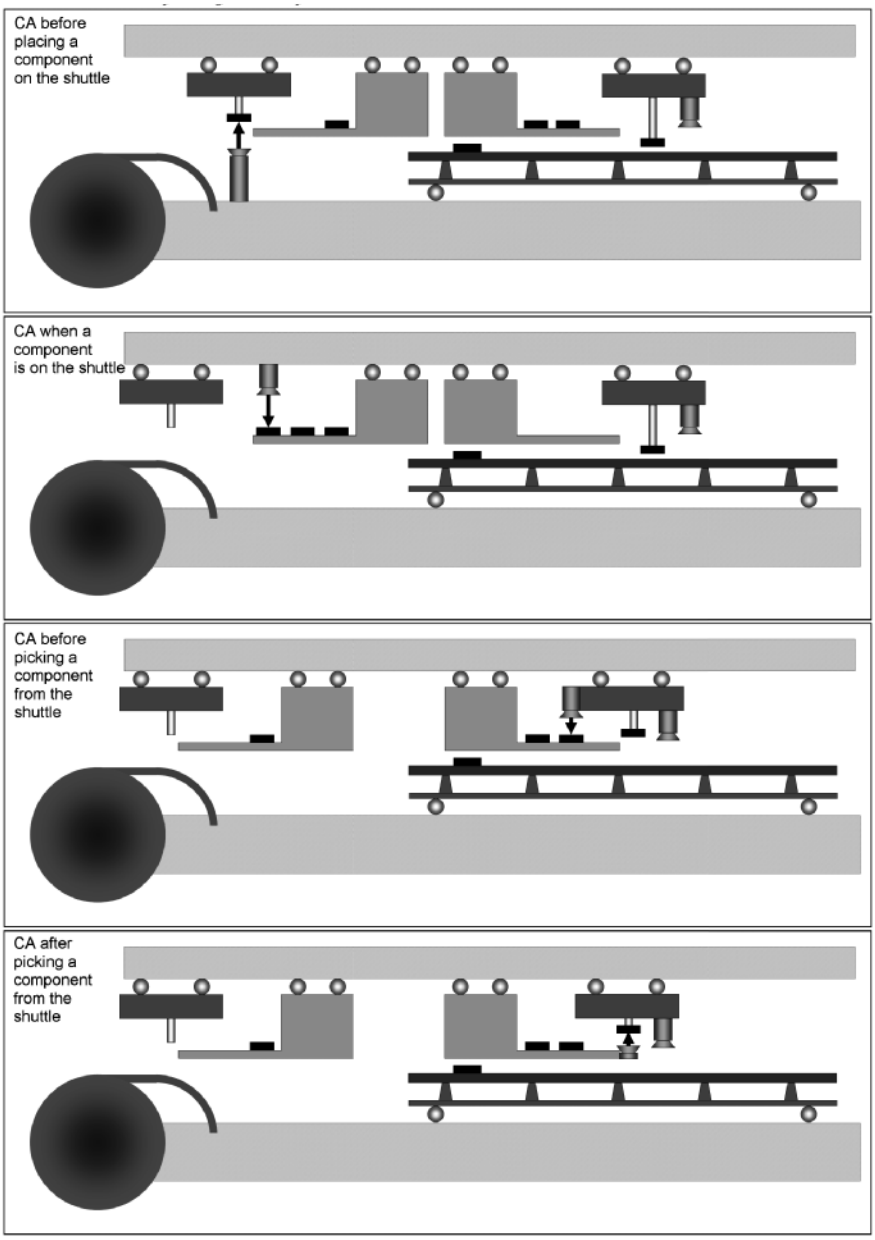

Figure 4.3: *Four moments where component alignment can take place in a shuttle concept P&P machine. Component alignment during the P&P cycle to load the shuttle. Component alignment while the components are on the shuttle. Component alignment before a component is picked from the shuttle. Component alignment after a component is picked from the shuttle*

on the moment that component alignment takes place in the P&P cycle. As can be expected, component alignment at the end of the total P&P cycle results in the best P&P machine repeatability. Furthermore, when component alignment is done after picking the component from the shuttle, the repeatability requirements of the load robot and shuttle will decrease. Finally, this decrease of requirements will probably result in a cheaper load robot and shuttle. The conclusion is that it is preferable to add the component alignment process after the component has been picked from the shuttle.

The disadvantage of performing component alignment after picking the component from the shuttle is that the time available for image processing is the shortest. The component alignment has to take place after the upwards z-movement of the nozzle holding the component and the downwards z-movement. Using the data shown in appendix Fig. A.20, the available time for the complete component alignment process will be in the range of 20 - 80 ms, depending on the exact implementation of the component alignment system. Taking into account the first estimated value for component alignment of 55 ms (appendix table A.5) it can be concluded that it will be feasible to perform component alignment after the component is picked from the shuttle.

4.2 Design of integrated alignment systems

In this section, four integrated alignment systems for shuttle concept P&P machines will be discussed. The discussion will address the layout of the integrated alignment system including the metrology loop.

The first P&P machine concept with integrated alignment systems is designed with the idea to keep the mass for the P&P robot as low as possible. Hereby, both alignment systems are added to the shuttle. The component alignment system is attached to the shuttle, the strategy used for component alignment will be vision-on-the-fly.

The second P&P machine concept with integrated alignment systems shows a layout where the component alignment system is placed on the shuttle and the board alignment system is attached to the P&P robot.

The third P&P machine concept has the board alignment system attached to the P&P robot, the component alignment system is split up in two parts. One part of the component alignment system is connected to the P&P robot, while the other part is attached to the shuttle. Taking into account the working principle, the used component alignment strategy meets the vision-on-the-fly strategy the best.

The fourth P&P machine concept consist of two alignment systems that both are split up in two parts. The first part is a single-camera that can be used for both alignment systems and is attached to the P&P robot. The second part consists of mirrors that are attached to the shuttle. Both alignment systems use the vision-on-the-fly strategy.

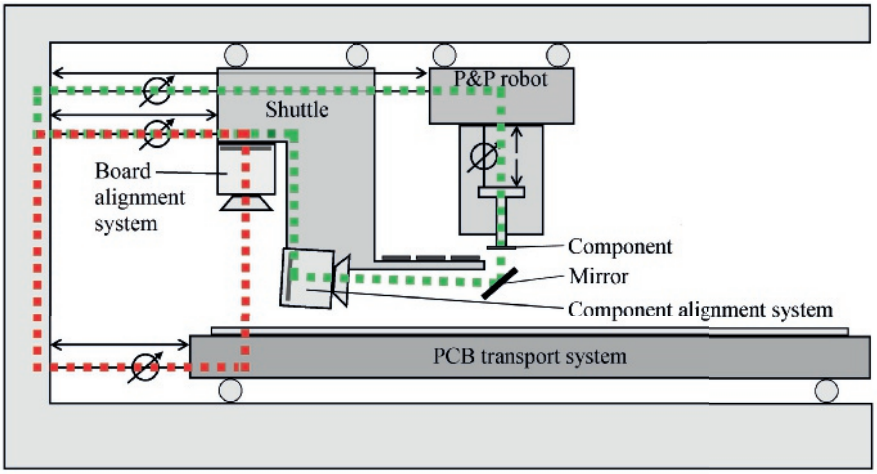

Figure 4.4: *Setup A: Low moving mass P&P robot. The shuttle contains two alignment systems. The red dotted line shows the metrology loop during board alignment. The green dotted line shows the metrology loop during component alignment*

4.2.1 Setup A: component and board alignment system on the shuttle

The basic idea for setup A is to keep the moving mass of the P&P robot low. Therefore the board and component alignment systems both are added to the shuttle. Figure 4.4 shows a schematic overview of this setup.

Board alignment

The shuttle is able to move in the y-direction over the PCB. By adding the board alignment system to the shuttle it can move in the y-direction over the PCB. To be able to move also in the x-direction, an x-axis has to be added to the shuttle.

Component alignment

By mounting the component alignment system on the shuttle, it is possible to align the components close to the P&P robot. The P&P robot with component moves over the camera right after a component has been picked from the shuttle. Figure 4.5 shows the top view of a possible movement of the P&P robot. The camera is placed on the shuttle at the center of the x-axis. The P&P robot must move with the component to the center of the x-position and then to the placement position. The x-movement from the pick position to the component alignment position can increase the P&P cycle time.

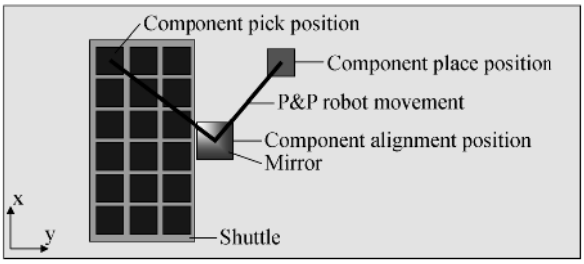

Figure 4.5: *Top view on shuttle and mirror for component alignment. In black a possible movement of the P&P robot is drawn*

The dimensions of the lens and the camera, used in a component alignment system, are too large to place this system at the position where the components are aligned. Therefore, a small mirror is added to the shuttle. Hereby, it is possible to position the camera and lens on another position on the shuttle. Consequently, the distances added to the P&P cycle are less compared to the system where a complete camera system is at the alignment position.

Metrology loop

In Fig. 4.4 two metrology loops are drawn by dotted lines. The red dotted line shows the metrology loop that is used during board alignment. The board alignment metrology loop contains the board alignment camera, which is used to take an image of the board. With help of software this image is processed and the position of the feature is determined with respect to the sensor. By knowing the position of the sensor with respect to the camera and hereby to the shuttle the metrology loop can be created. So, the metrology loop exists of the sensor in the camera, the PCB transport system including the position sensor, the frame, the position sensor of the shuttle and the shuttle itself.

The green dotted line indicates the metrology loop during component alignment. The component metrology loop starts with the camera on the shuttle by taking an image of the bottom side of the component via a mirror. The image is processed and the position of the component is determined with respect to the sensor inside the camera. The total metrology loop exists of the camera with sensor inside, the mirror, the P&P robot including the nozzle holding the component, the dimensions of the P&P robot, the P&P robot's position measurement system, the frame the shuttle's position system and the dimensions of the shuttle.

Finally, the data from the board alignment and component alignment is used to correct the position of the P&P robot for the deviations measured. In this concept the position of the shuttle, the PCB and the P&P robot will influence the repeatability.

The alignment of the board and component will not happen concurrently. First the position of the board with respect to the frame is determined, afterwards the position of the component is determined also with respect to the frame. Finally, it is possible to calculate the corrected placement position to place the component with the required repeatability.

Conclusion setup A

Advantage There is no mass added to the P&P robot for component alignment and board alignment. For component alignment a mirror is added that increases the movement distance. The estimated size of this mirror will be in the range of the FOV of the camera.

Disadvantage The use of a mirror influences the repeatability. The P&P robot must move to the alignment position in both the x- and y-direction. The shuttle must be equipped with an x-motor to move the board alignment camera. The position of the shuttle must be measured accurately because it has become part of both metrology loops.

4.2.2 Setup B: component alignment camera on the shuttle, board alignment camera on the pick-and-place robot

In the previous proposed setup an additional linear axis is added on the shuttle to move the board alignment system in the x-direction. The P&P robot is already able to move in the x- and y-direction. Adding the board alignment camera to the P&P robot has the advantage that no motor has to be added to the shuttle. The disadvantage is the increase of the P&P robots mass. Figure 4.6 shows a schematic overview of the setup where the board alignment system is attached to the P&P robot.

Board alignment

The board alignment camera is attached to the P&P robot. The camera thereby can move over the PCB in x- and y-direction.

Component alignment

The component alignment system will have the same layout as used in setup A. So the P&P robot moves to the alignment position at the center of the x-stroke to align the component. The x-movement to the component alignment position must be realised before the y-stroke from component pick position to mirror position has been finished. It is expected that this x-movement towards the mirror can add additional time to the P&P cycle.

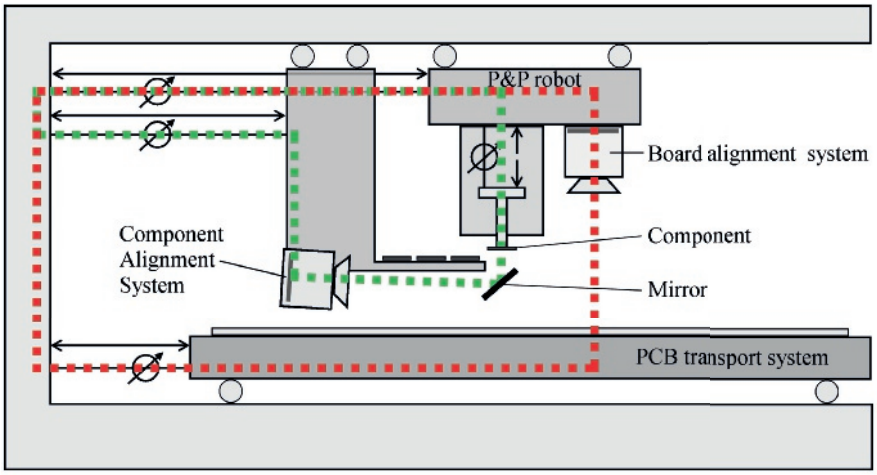

Figure 4.6: *Setup B: shuttle and P&P robot both holding an alignment camera system. The shuttle with the component alignment system attached to it. The P&P robot with the board alignment system attached to it. The red dotted line shows the metrology loop during board alignment. The green dotted line shows the metrology loop during component alignment*

Metrology loop

In Fig. 4.6 two metrology loops are drawn. The green dotted line, indicating the metrology loop for component alignment, is the same as in setup A.

The red dotted line shows the metrology loop used during board alignment. The board alignment camera is mounted onto the P&P robot. The metrology loop for board alignment starts at this camera on the P&P robot. Here, an image of the PCB is taken, processed and the coordinates with respect to the sensor are calculated. These coordinates are transferred to the P&P robot position. The component metrology loop starts with the camera on the shuttle that via a mirror an image takes of the bottom side of the component. The image is processed and the position is determined with respect to the sensor. The position of the shuttle. The data is used to correct the position of the P&P robot with the measured data. In this concept the position of the shuttle, the PCB and the P&P robot will influence the repeatability.

Conclusion setup B

Advantage The mass of the component alignment system is added to the shuttle. The added distances are the sizes of the component. There is no extra motor required for board alignment on the shuttle.

Disadvantage The use of a mirror gives an extra part, which influences the repeatability. The P&P robot must move to a position in the

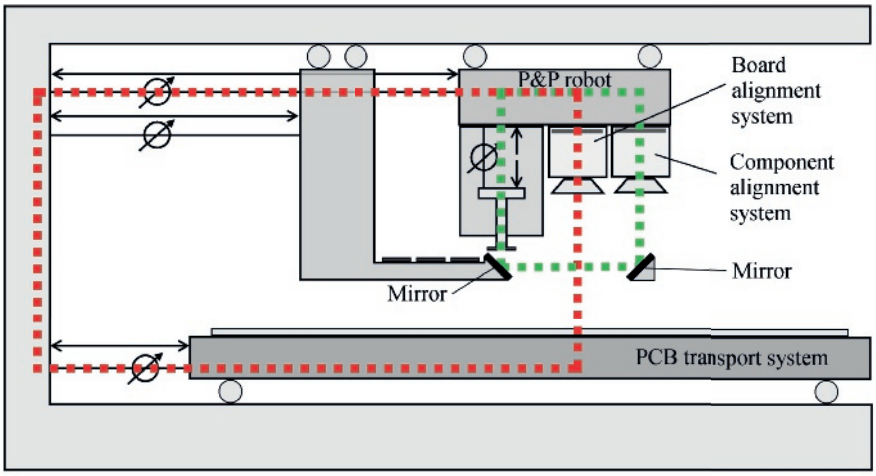

Figure 4.7: *Setup C; P&P robotwith two camera's. The P&P robot contains a board alignment camera system and a component alignment camera system. The shuttle holds two mirrors for component alignment. The red dotted line shows the metrology loop during board alignment. The green dotted line shows the metrology loop during component alignment*

x-direction before the image of the component can be taken what can influence the P&P cycle time. The mass of the board alignment system is added to the P&P robot.

4.2.3 Setup C: component and board alignment cameras on the pick-and-place robot

A major disadvantage of proposed setup A and B is the additional time required to move the P&P robot to the alignment position in the x-direction. This movement can influence the throughput of the shuttle concept. To eliminate the movement in the x-direction it is preferable to be able to perform component alignment on every x-position. To do so, the component alignment camera must be able to move in the x-direction. In this setup both cameras are mounted onto the P&P robot. Figure 4.7 shows a schematic overview of this setup.

Board alignment

The board alignment camera is, as in setup B, attached to the P&P robot. This camera can move over the PCB in x- and y-direction.

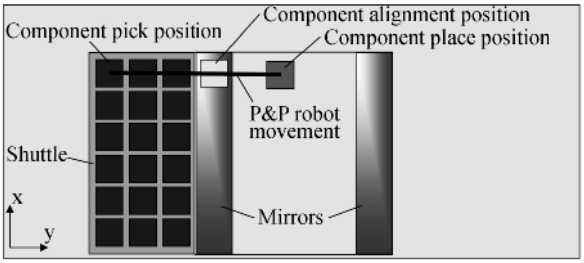

Figure 4.8: *Top view on shuttle and mirror for component alignment. In black a possible movement of the P&P robot is drawn on every x-position component alignment is possible*

Component alignment

The component alignment camera is mounted to the P&P robot. The shuttle is equipped with two mirrors that cover the total x-dimension. Figure 4.8 shows a top view of the shuttle and the two mirrors. The use of the mirrors makes it possible to take images of the component bottom side. Because the camera is placed on the P&P robot and the mirrors cover the total x-direction, it is possible to take an image on every x-position.

Metrology loop

The metrology loop used during board alignment is drawn in Fig. 4.7 as a red dotted line and is equal to the metrology loop in setup B.

The metrology loop used during component alignment is drawn in Fig. 4.7 as a green dotted line. This loop starts with the camera that looks to the bottom side of the component via two mirrors that are attached to the shuttle. An image is taken and processed. The position of the component is determined with respect to the sensor inside the camera. The metrology loop for component alignment consists of the camera, the mirrors attached to the shuttle and the dimensions of the P&P robot. Although in this proposed metrology loop the position of the P&P robot and the position of the shuttle are not included, the position of the P&P robot with respect to the shuttle does influence the position measurement and has to be taken into account.

Conclusion setup C

Advantage The x-position for component alignment is not prescribed; so no additional time is added to the P&P cycle.

Disadvantage The two mirrors used will influence the repeatability. Two cameras are attached to the P&P robot, which increases the mass.

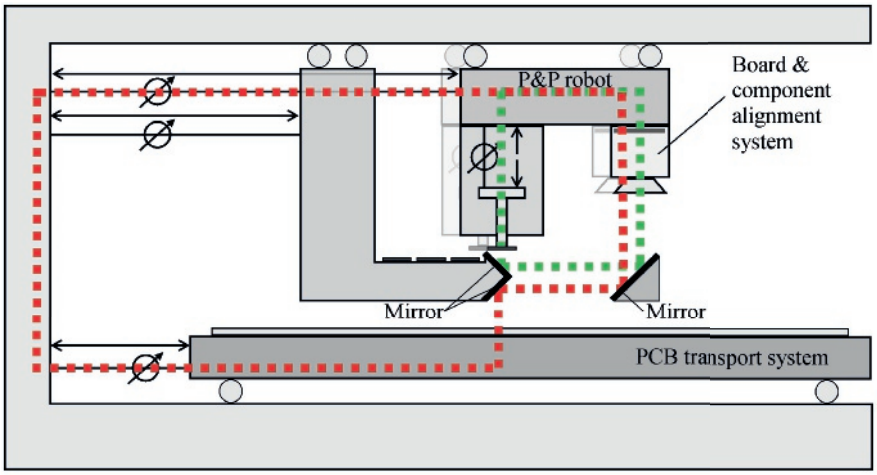

Figure 4.9: *Setup D: Single-camera-concept. This selected concept has a P&P robot that holds one single-camera used for component and board alignment; the shuttle holds three mirrors. The red dotted line shows the metrology loop during board alignment. The green dotted line shows the metrology loop during component alignment. Although the position of the shuttle, holding the mirrors, is not in the metrology loop, the position of the shuttle will influence the repeatability*

4.2.4 Setup D: single-camera for component and board alignment on the pick-and-place robot

The previous setup has two cameras attached to the P&P robot both looking downwards. The reason to use two cameras is because the optical working distance of the two cameras is different. So if it is possible to keep the working distance the same for both systems, one single-camera can be used for both alignment systems. Figure 4.9 shows a schematic overview of a setup where an extra mirror is added to the shuttle. The working distance for both alignment systems has become equal what makes it possible to take images from the component and the board with one single-camera.

Metrology loop

In Fig. 4.9 two metrology loops are shown. The P&P robot is drawn during component alignment and the green dotted line indicates the metrology loop during component alignment. The component alignment setup is equal to the setup proposed by setup C.

If the P&P robot is moved to the left (drawn in light grey) the red dotted line indicates the metrology loop used during board alignment.

The red dotted line board alignment metrology loop starts with the camera that looks to the PCB via two mirrors that are attached to the

shuttle and the image is taken. The position of the feature is determined with respect to the sensor inside the camera. The metrology loop for board alignment consists of the camera, the mirrors attached to the shuttle, the PCB transport system, the position measurement system of this transport system, the frame, the dimensions of the P&P robot and the P&P robot's position measurement system. Similar to the component alignment of setup C, the position measurement of the shuttle does not influence the metrology loop. Theoretically, for the board alignment this is true. If the mirrors are well positioned with an angle of 45°, the exact position of the shuttle will not be important. Knowing that there are always deviations, it is probably required to use the actual shuttle position as information for board alignment.

Conclusion setup D

Advantage Only one camera is added to the P&P robot; Minimal time is added to the P&P cycle.

Disadvantage The use of mirrors will influences the repeatability. One camera is attached to the P&P robot, which increases the mass.

4.2.5 Selected board and component alignment setup

The shuttle concept is based on short distances within a P&P machine. Consequently, it is necessary to design a component alignment system that is situated close to the P&P robot and the shuttle. The availability of the shuttle has resulted in four alignment concepts where the complete or parts of the alignment systems have been attached to the shuttle.

The requirements to measure after the shuttle pick and minimising the distances has resulted in the addition of at least one mirror because the size of the vision system is too large.

The repeatability of this alignment system, which is divided over two moving parts, the shuttle and the P&P robot, is worth to investigate. The repeatability of the alignment system depends on the position of the shuttle and the position of the P&P robot, which adds extra requirements of the trajectory control and/or position measurements.

The idea of only using one camera and mirrors also is economically interesting. A literature study on this concept has resulted in patents of Sony [92, 93]. There is a difference in the setup but the main idea described in these patents is the same. If this concept violates the patents this should be investigated before commercial use of this concept.

Setup D is selected as the most promising alignment concept and its feasibility will be investigated further.

4.3 Repeatability of a single-camera alignment system

In this section the repeatability of the single-camera component and board alignment system is estimated. This repeatability is estimated with help of the values presented in Chapter 3. The integrated alignment system has mirrors attached to the shuttle and the vision system attached to the P&P robot and is thereby split over two moving systems. The addition of separately moving mirrors is the main differences between the component and board alignment systems used during the requirement and the integrated alignment system proposed.

The design of the integrated alignment system will influence the error budget for repeatability. In the next list the differences that influence the repeatability are listed.

- Mirror stability
- Vision-on-the-fly strategy means that the images are taken while the P&P robot and/or shuttle are moving. Movements during image taking causing motion blur
- The positioning of the mirrors and the P&P robot with attached the vision system. As a result of the design, the influence of the positioning will be different for board and component alignment
- Movement synchronisation, using a shuttle moving the mirrors and a separately moving vision system requires the synchronisation of the movements
- Vibrations of the shuttle and the P&P robotinfluence the repeatability
- Vision system board alignment, the vision system for board alignment will change because using a single-camera requiring a FOV that is the same for component and board alignment.

These six items will be discussed in more detail in the next subsections. Where possible requirements will be determined.

Mirror stability

As shown in Fig. 4.9 the mirrors are part of both metrology loops and used to reflect the image of the component or the PCB feature. Ideally the mirrors are mounted on an angle of 45° with respect to central axis of the vision system but a constant deviation in the angle will introduce a systematic error. After this measurement the data can be analysed and used for calibration. More important than an exact angle is the stability of the mirrors. When the mirrors are mechanically stable it is possible to

use calibration for compensation. Instability of the mounting of the mirrors will introduce random errors that will affect the repeatability.

Vision-on-the-fly strategy

The use of vision-on-the-fly will influence the repeatability. Motion blur will occur due to the fact that an image is taken while the component is moving causing blurred images. Two ways to handle motion blur are discussed.

Several restoration techniques for blurred images are described as example: image deconvolution and blind image deconvolution [64]. Where image deconvolution expects to know the motion profile, blind image deconvolution starts with estimating the motion profile (point spread function). In case of vision-on-the-fly it is possible to record the motion profile during the time the image is taken, meaning that image deconvolution is probably possible. The deconvolution of the image will take time and can thereby influence the process time. Minimising motion blur is another preferable solution.

Reducing the shutter opening time during alignment can be used to reduce the motion blur. If the shutter opening time is infinitive short, the influence of motion blur on the repeatability will become zero. Another way to reduce the influence of motion blur can be realised by shorten the illumination time by using short high-powered light flashes. In a rather dark environment it is allowed to open the shutter longer while this shutter opening time will not determine the motion blur but the length of the light flash will do.

The goal is to keep the motion blur within one pixel at the sensor side, which means that a point in the image may not move more than the size of one pixel. As determined in the previous chapter, a component alignment systems' pixel will represent $9.2 \times 9.2 \mu m$. This means when the distance is less then $9.2 \mu m$ the contribution to the error budget for motion blur will be $4.6\ \mu m\ (1\sigma)$.

$$t_e = \frac{d_{max}}{v_{max}} \tag{4.1}$$

The exposure time (t_e) can be calculated using Equation 4.1. A velocity of $2.5 m/s$ (Appendix A) and a distance of one pixel $9.2\ \mu m$ results in a maximum exposure time of about $3.7 \mu s$.

Positioning of the shuttle and pick-and-place robot

In the single-camera alignment system a deviation of the position of the P&P robot or the shuttle containing the mirrors, will give different position deviations for board or component alignment.

Figure 4.10 shows four situations where the P&P robot or the shuttle with the mirrors have a position deviation during board or component alignment.

The top left drawing shows what happens when the P&P robot has a position deviation during board alignment. The black line shows the optical alignment axis when the P&P robot is at the optimal position. This optimal position means that the camera is centered with respect to the left mirror used during board alignment. In gray, the P&P robot is drawn with a position deviation. This results in a new optical axis, drawn in gray. The deviation results in a feature shift equal to the deviation of the P&P robot.

The top right drawing shows the P&P robot during component alignment. The black line shows the optimal optical alignment axis. This optimal position means that the center of the camera is centered with respect to the nozzle of the P&P robot. In gray, the P&P robot is drawn with a position deviation. This results in a new optical axis, drawn in gray. This deviation results in a shift of the component equal to the deviation of the P&P robot but in the opposite direction compared to board alignment.

The bottom left drawing shows the influence of mirrors position deviation during board alignment. The black line shows the optical alignment axis when the P&P robot is at the optimal position. In gray, the mirrors are drawn with a position deviation. This results in a new optical axis, shown in gray. The deviation does not influence the repeatability, because the feature remains on the position at the camera of the P&P robot.

In the bottom right drawing the influence of a position deviation of the mirrors during component alignment. The black line shows the optimal optical alignment axis. In gray, the mirrors are drawn with a position deviation. This results in a new optical axis, shown in gray. This deviation results in a shift of the component twice the deviation of the mirrors. So, a position deviation of the shuttle will influence the component alignment.

Taking into account that the position measurement must be calibrated and can have a calibration residue of 0.75 $\mu m\,(1\sigma)$, the influence of the calibration residue on the repeatability can be calculated with help of Equations 4.2 and 4.2. The calibration residue of the P&P robot and shuttle can result in a contribution to the repeatability of 1.7 $\mu m\ (1\sigma)$ for component alignment (CA) and 1.1 $\mu m\ (1\sigma)$ for board alignment (BA).

$$\Delta Y_{BA} = \sqrt{{\Delta Y_{Shuttle}}^2 + {\Delta Y_{P\&Probot}}^2} \approx 1.1\mu m \tag{4.2}$$

$$\Delta Y_{CA} = \sqrt{(2 \times \Delta Y_{Shuttle})^2 + {\Delta Y_{P\&Probot}}^2} \approx 1.7\mu m \tag{4.3}$$

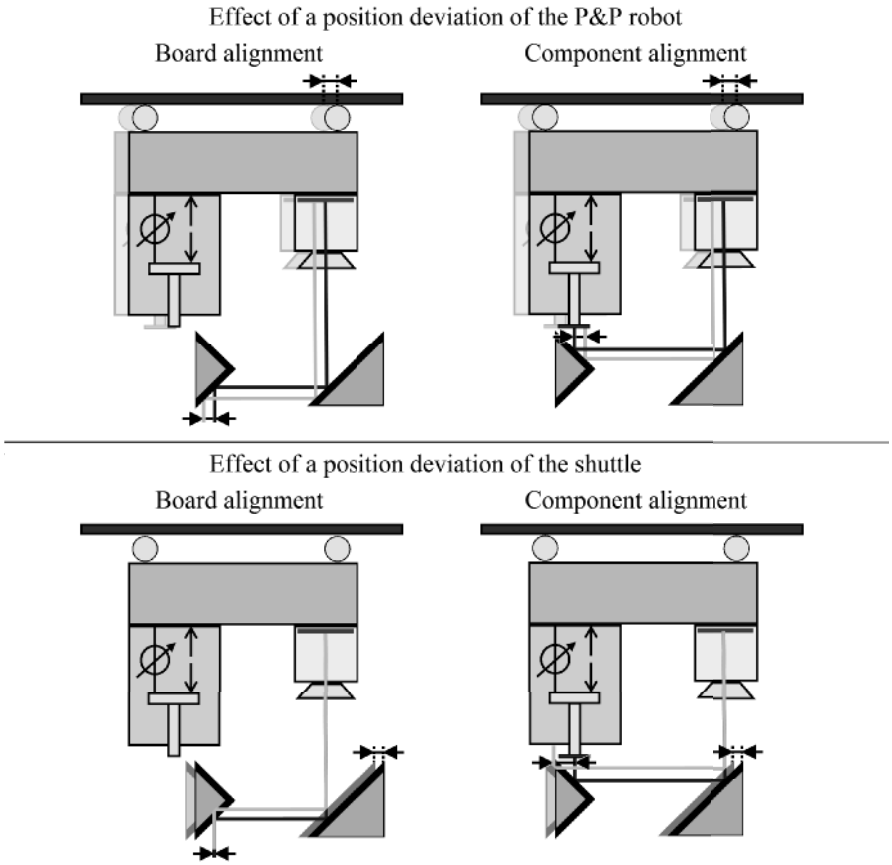

Figure 4.10: *Top left: Board alignment, in black and grey two possible optical axes during alignment, the shift of the P&P robot results in a equal shift on the PCB. Top right: Component alignment, in black and grey two possible optical axes during alignment, the shift of the P&P robot results in a equal shift in the opposite direction on the component. Bottom left: Board alignment, in black and grey two possible optical axis during alignment, the shift of the mirrors has no influence on the board alignment. Bottom right: Component alignment, in black and grey two possible optical axes during alignment, the shift of the mirrors results in a shift twice the deviation of the mirrors*

Movement synchronisation

To minimise the influence of misalignment of the P&P robot and shuttle the position deviation between the two systems must be minimised. Therefore an alignment trigger must be created. This trigger must be generated when the mirrors and the P&P robot are aligned and triggers the vision system to take the image. There are two solutions for the alignment trigger. The first solution is to create an alignment trigger at the moment that the P&P robot and the mirrors (on the shuttle) are aligned. The second solution is to record the actual positions when the vision system takes the image. In both situations the acquired information can be used to correct the image for actual positions of the shuttle and P&P robot.

The alignment trigger is generated when the position of the shuttle and the P&P robot are aligned. The timing of this trigger will influence the repeatability of the alignment systems. Therefore this trigger must have a small delay and minimum jitter. The comparison of the two position can be realised in hardware meaning that the delay will be small and jitter under 0.5 μs can be easily realised, while clock frequencies over 2 MHz are for electronic hardware not a problem. Taking into account the maximum speed of 2.5 m/s, the contribution on repeatability of the alignment trigger is calculated to be to 1.25 μm (1σ).

Vibrations

The dynamic behavior of the P&P robot influences the repeatability during alignment while the P&P robot is holding the vision system. The shuttle is part of the metrology loop and the dynamic behavior of the shuttle can also influence the repeatability.

In Fig. 4.11 a dynamic representation of the P&P robot is shown where the bearings used at the top of the system are replaced by springs with limited stiffness. Due to this limited stiffness and the forces induced by the actuator, the P&P robot will rotate around the center of mass, which results in the rotation of the camera and the component.

The specification of the P&P robot is set to realise a controller bandwidth of 50 Hz. The mechanical eigenfrequency of the P&P robot is preferable above this frequency and a mechanical eigenfrequency of 150 Hz for the P&P robot is preferable. Although it can be expected that the P&P robot can be realised with the required eigenfrequency, the deflection of the P&P robot still will influence the repeatability.

Using an exposure time of 4.7 μs means that all dynamic movements up to $\approx$ 210 kHz will influence the repeatability. The light flash will freeze the position of the P&P robot at the time the image is acquired. The frequencies above 210 kHz will appear as noise. It is required that the dynamics of the P&P robot is taken into account.

The rotation of the vision system depends on eg. forces, size, mass,

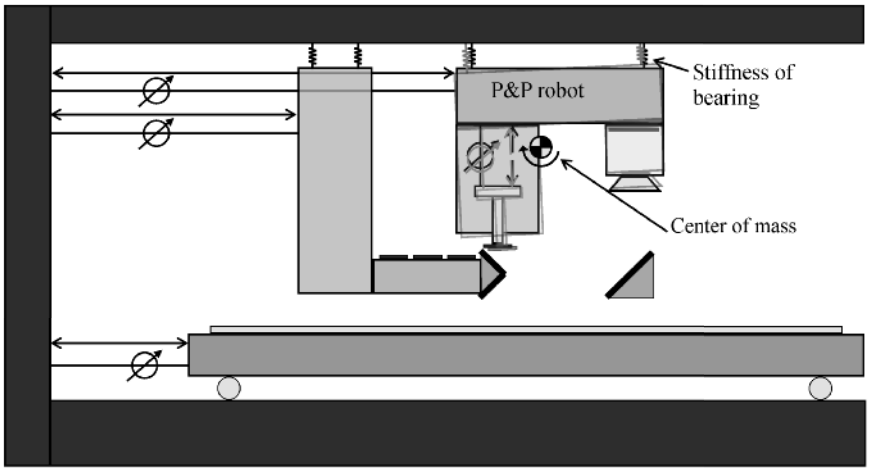

Figure 4.11: *Rotation of the P&P robot around the center of mass (COM) as a result of introduced forces and the limited stiffness of the bearings*

center of mass, stiffness of the bearings and is without a design hard to estimate. Therefore no estimation is made, but during the test a sensor must be added to measure the rotation.

In addition due to the process cycle of the shuttle, the shuttle can settle before images are taken. Because of these two reasons it is to be expected that the influence on repeatability will be negligible.

Vision system board alignment

The contribution of the board alignment system to the repeatability in a shuttle concept P&P machine must be adjusted with respect to the sequential P&P machine. The FOV of the board alignment system has to increase due to the fact that one single-camera is used for both board and component alignment. This means that the FOV is adjusted to 7.0 $mm \times 7.0$ mm. The used camera has a XGA resolution sensor meaning that it has 1024 pixels $\times 768$ pixels. This results in an estimated repeatability of 1.6 $\mu m\,(1\sigma)$ when subpixel level of 0.16 can be achieved.

4.4 Error budget integrated alignment system

From this analysis the error budget for the single-camera alignment system can be estimated. In table 4.2 the determined values are added. This results in a total repeatability 14 $\mu m\,(1\sigma)$, which is smaller than the requirement of 15 $\mu m\,(1\sigma)$.

Error budget	**Repeatability** $[\mu m\,(1\sigma)]$		
Description	**"past"**	**"must"**	**"design"**
*Board handling**	*4.0*	*4.0*	*4.0*
Board alignment process	3.8	6.0	
Vision System (FOV 7 mm×7 mm)			1.6
Motion blur\Movements			4.6
Position measurement			1.1
Alignment trigger			1.3
*Nozzle exchange**	*0*	*0*	*0*
*Component pick process**	*0*	*0*	*0*
*Component move process**	*0*	*0*	*0*
Component alignment process	6.8	8.5	
Vision System (FOV 7 mm×7 mm)			4.6
Motion blur\Movements			4.6
Position measurement			1.7
Alignment trigger			1.3
*Component place process**	*9.8*	*10.0*	*10.0*
Total estimated repeatability	13	15	13.8

Table 4.2: *Repeatability requirement "must" values (as total value for adapted from table 3.9) and the "design" requirement values for the single-camera alignment system; *italic values will not be determined in this thesis*

4.5 Conclusion

In this chapter the optimal moment in the P&P cycle for component and board alignment was determined. Taking into account the repeatability the component alignment must be added after the component has been picked from the shuttle. Hereby, the load robot and shuttle do not contribute to the final repeatability.

Four integrated alignment concepts have been presented. Finally, the choice is made for the concept where only one single-camera mounted on the P&P robot is used for both component and board alignment. To be able to use a single-camera, mirrors were added to the shuttle. The repeatability of the single-camera alignment system was estimated and excepted.

Chapter 5

Realisation of the alignment module

In the previous chapter the layout for a shuttle concept with a single-camera integrated alignment system was introduced, requirements were determined and the repeatability was estimated. In this chapter the requirements are used to realise the modules for the alignment system. The modules are selected or built when not standard available. Finally, the modules are validated.

5.1 Specification

The alignment system is based on vision technology to determine the position of object, in this case the component or PCB features. Often, the term vision system is used for a complete system that is able to acquire and process images, meaning that a vision system exists of more modules then only a camera. In general, a vision system consists of a camera holding the vision sensor, a lens, an illumination system and image processing software. The integrated alignment system requires also mirrors, which will be mounted onto the shuttle. Finally, in this concept, the choice for vision-on-the-fly results in the demand for an alignment trigger. When the P&P robot and the mirrors are aligned, this trigger must be generated. In the next list the vision system's requirements are summarised:

Vision sensor From the repeatability analysis it has been concluded that the Charge Coupled Device (CCD) camera must contain a vision sensor with a minimum of 700 pixels $\times$ 700 pixels.

Lens The lens must magnify the FOV of 7 $mm\times$ 7 mm to the light sensitive area of the vision sensor. It is required that the lens is able to handle a PCB height difference of ± 2 mm

Illumination Illumination is required to take images

Mirrors The mirrors must reflect the images of the objects

Alignment trigger The alignment trigger must be generated when the P&P robot is aligned with the mirrors

Image processing software The image processing software is used to determine the position of the object

In the next subsections the various modules of the vision system for the single-camera alignment systems are designed or selected.

5.1.1 Vision sensor

The vision sensor is used to transfer the image of the object to data that can be used by image processing software to determine the position.

Various vision sensors with different sizes, technology, layout are available on the market. With respect to layout, these sensors can be divided into two groups: 1D- and 2D-sensors.

1D-sensors have only a single line of pixels. Although, an image of these sensors consists of one line of pixel information, these sensors can be used to construct a 2D-image by combining several 1D-images. This means that the 1D sensor must move over the object or the object must move over the 1D-sensor to build up an 2D-image. The choice of the vision-on-the-fly concept, where the image is taken during movement gives the opportunity to use a 1D-sensor.

2D-sensors can also be used in the alignment system. If the object is completely in the FOV, only a single image has to be acquired of the object.

To realise the estimated repeatability for the alignment system, the pixel size on the object side has been determined. During accuracy analysis it is determined that the object pixel size has to be 10 $\mu m \times$ 10 μm. Taking into account the FOV of 7 $mm \times 7$ mm, this results in a sensor resolution of minimal 700 pixels $\times$ 700 pixels.

Line scan sensor (1D)

From the requirements it is known that adding distances will increase the process time. A line scan camera takes images of only one single line so theoretical the added distance is only the distance of one pixel at the object side resulting in a distance of 10 μm. Considering only this property, it is beneficial to use a line scan camera. But later it will be shown that to realise a 2D-image, 700 lines must be taken. This results in the requirement that the movement is synchronised while the images are taken by the 1D-camera.

Available 1D-sensors can have various pixels per line. Several companies have a range of 1D-sensors with 1024, 2048, 4096 pixels per line. These sensors have different pixel sizes like 10 $\mu m \times$ 10 μm or 14 $\mu m \times$ 200 μm[19, 28].

If a 1D-sensor with a pixel size of 10 $\mu m \times$ 10 μm is used, this results in the requirement that a line must be sampled when the object has moved with 10 μm. Equation 5.1 shows that a sample rate of 250 kHz is required during the maximum velocity of 2.5 m/s.

$$Line\ rate\ time = \frac{Pixel\ size}{V_{max}} = 4\ [\mu s] \tag{5.1}$$

To realise the 2D-image, each line acquired must be digitised and transported to memory. While sampling at 250 kHz, the 1D-sensor must be able to acquire an image and transport the data within 4 μs. Even the very fast line scan cameras can not meet this requirement [30, 59]. Therefore, it seems not feasible to use a 1D-sensor due to the high rate of line scans required.

Full area sensor (2D)

A full area sensor contains a 2D pixel area, which takes an image of the total object. There are several standard sensor resolutions available like VGA, SVGA and XGA. The XGA-sensors contain 1024 pixels $\times$ 768 pixels but there are other standard sensor that have even higher number of pixels. To realise the determined sensor resolution of minimal 700 pixels $\times$ 700 pixels the XGA-sensor or better can be used for this alignment system.

After an image is taken, the image must be digitised and transported. Because only a single image is taken, the time for digitising and transporting an image can be larger than the 4 μs calculated for the 1D sensor. The total time available for digitising, transport and image processing is maximal 55 ms [from Appendix A].

The time for digitising and transporting the image using a 2D-sensor seams feasible. Sensor are available with the required resolution. A disadvantage is the required mirror size to be able to acquired an image of the complete scenery. Concluding, a 2D-sensor can be used and the implementation of the total vision system seams feasible.

A disadvantage of a 2D-sensor with respect to a 1D-sensor is the requirement that the total object must be in the FOV at the moment an image is taken. This results in the requirement that the mirrors need at least the size of the FOV.

CCD or CMOS sensor

Vision sensors commercially available are: Charge Coupled Device (CCD) and Complementary Metal Oxide Semiconductor (CMOS) sensors. In general, it can be stated that in 2004 the light sensitivity of a CCD sensor was higher than a CMOS sensor [71, 30, 63]. The reason that a CCD has

a higher light sensitivity can be explained taking into account the difference between the implementation of the pixels on a CCD or CMOS chip. The total area of a pixel (ie. 10 $\mu m \times$ 10 μm) of a CCD sensor contains light sensitive material where a pixel of a CMOS sensor has also electronics added resulting in an area where no light sensitive material can be placed. To increase the signal output, a CMOS sensor can have a per pixel built-in amplifier. These amplifiers will have gain differences with respect to each other resulting in additional pixel to pixel noise.

A standard CCD sensor can be used with frame rates up to 60 frames per second fps due to the restriction on the analog to digital converter (ADC) speed. A frame rate of 60 fps means that taking an image and transport the data to the processing unit takes maximal 17 ms. In this application the maximum process time was set to 55 ms. This means that a 60 fps CCD sensor is sufficiently fast.

In this application, the requirement that images have to be taken in 4 μs will result in little light on the sensor. It is therefore preferable that the sensor used has a high light sensitivity. There are two solutions to ensure that the image is acquired in maximum 4 μs. Firstly, a camera with a shutter able to open and close in 4 μs. Secondly, using flashing illumination system.

The alignment system will be integrated with the P&P machine, which limits the allowed sizes of the camera. The P&P robot must be able to travel a distance in x-direction of 80 mm where a maximum width of 120 mm is allowed in the x-direction, meaning that the width in the x-direction of alignment system is limited to 40 mm. The dimensions of the alignment system in the y- and z-direction are not specified.

An overview of the sensor requirements can be found in table 5.1.

Parameter	**Required**	**Unit**
Sensor resolution	$>$ 700×700	$pixels$
Sensor technology	CCD	
Data transport time	$<$ 50	ms
Size x-direction	$<$ 40	mm
Optional: shutter opening time	$<$ 4	μs

Table 5.1: *Sensor parameters*

5.1.2 Lens

In a vision system the lens is used to magnify the object FOV_{object} to fit the FOV_{sensor} size. But there are more lens parameters then magnification. In the next list the most relevant lens parameters are discussed.

Magnification magnification of the FOV_{object} to FOV_{sensor}

Working distance (WD) nominal distance from the lens to the object

Effective F-number effective F-number of a lens specifies the loss of light inside the lens; If the F-number increases, the amount of light lost in the lens increases

Distortion specifies the deviation that the lens will introduce on images

Focus depth describes the deviation with respect to the WD where the object is still in focus

Mass Mass of lens

These parameters must be determined for the alignment system. The magnification can be calculated when the sensor is selected. The FOV_{object} is set to 7 $mm\times$ 7 mm. The lens WD of the lens must be in the range of 70-120 mm to match the shuttle design. Due to the fact that only limited time ($4\mu s$) is available to acquire the image the F-number must be low. Distortion will influence the repeatability and should be as low as possible. Focus depth must meet the requirement for board alignment, which is ± 2 mm. Although mass is not a strict requirement it is preferable to have the mass as low as possible.

Lens type selection

When a single lens is used in a measurement system this can result in measurement errors [75]. The upper graph in Fig. 5.1 shows a single lens in a measurement system. The object (solid arrow) is positioned and appears on the sensor. If the same object is moved towards the lens, the object appears to be larger on the sensor and out of focus. Because the height of the PCB in this application can variate, this can result in measurement deviations if no precautions are taken.

To solve this problem a telecentric lens, shown in the lower graph of Fig. 5.1 can be used. A telecentric lens has a range where the magnification is constant resulting in an object that will keep the same size at the sensor even when the WD differs. To realise a telecentric lens different lenses are combined and an aperture is added [106, 80]. There are disadvantages to use a telecentric lens in the shuttle concept P&P machine.

Due to the fact that a telecentric lens is realised by combining multiple lenses and an aperture, the F-number will increase. By the increasing F-number more illumination is required during the image acquisition. The telecentric lens has a higher mass then a single lens. The increase of maas of the lens is not preferable because the lens is mounted onto the camera that is attached to the P&P robot.

Despite the disadvantages a telecentric lens is required to be able to determine the PCB features.

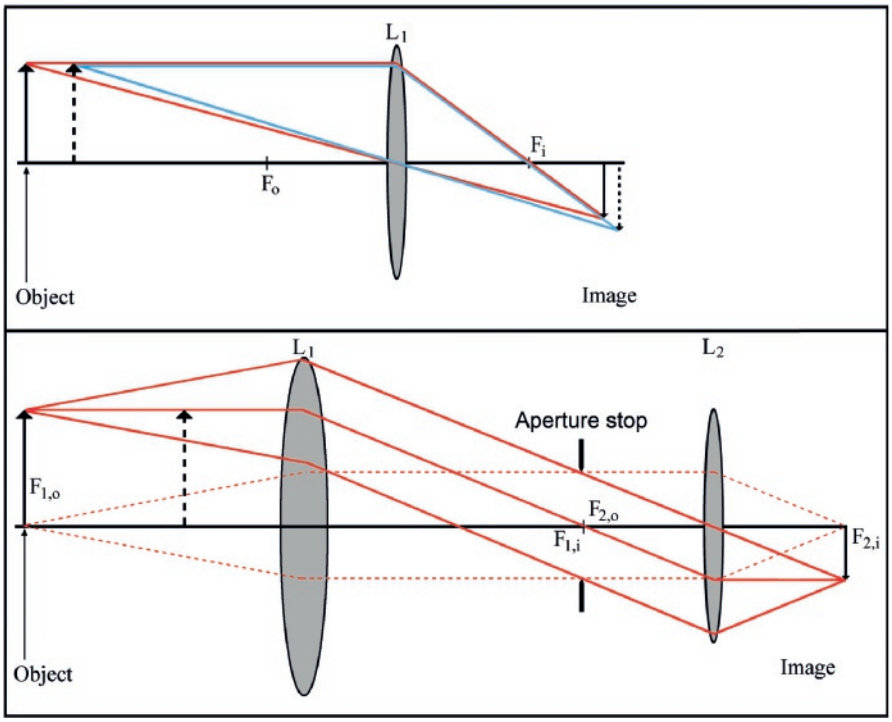

Figure 5.1: *Upper drawing: single lens; when the object shifts towards the lens, the image becomes larger. Lower drawing: a telecentric lens contains to lenses and an aperture; when the object shifts towards the lens, the image will have the same size. Drawings adapted from [94, pg. 611, 625]*

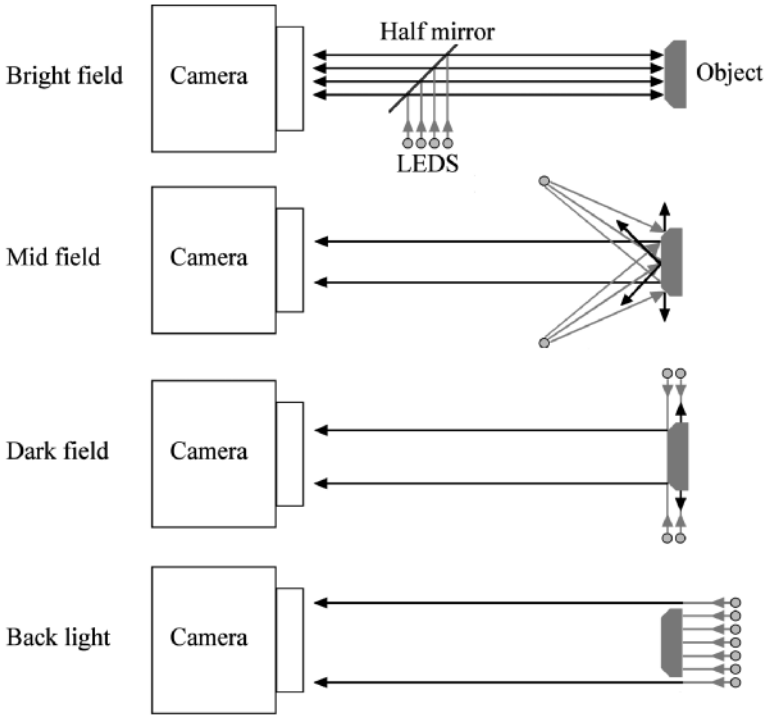

Figure 5.2: *Four different illumination direction used in machine vision*

5.1.3 Illumination

In general it can be stated that to determine the position of an object is more easy when the image is rich of contrast. This means in this application that for example the leads of a component should be clearly detectable with respect to the component and the background. Therefore the illumination must be designed in such a way that a high contrast image is acquired.

Heek [42] presents four possible illumination fields as presented in Fig. 5.2. The top image shows a bright field illumination. Light comes from the front and illuminates the object. To realise a bright field (0° with respect to the optical axis of the camera) illumination, often a half mirror is used. The second image shows a mid field illumination (45°). Light is send to the object with an angle of about 45°. The third image shows the dark field illumination. Light is send under an angle between 80 and 90°. This illumination field will result in an image where the edges have a high contrast with respect to the surrounding. Finally, the fourth image shows a back light illumination field. In this situation the light comes from behind the object. In this case the object will become black with respect to the bright background. Various combinations of these illumination fields must be used in P&P machines to realise full contrast images[62, 60, 84].

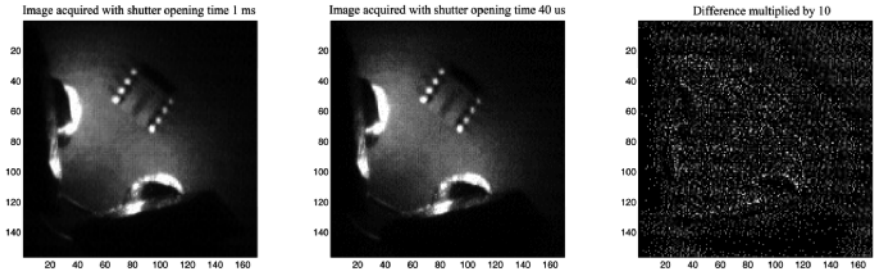

Figure 5.3: *Pulsed power LEDs (4 μs pulse duration) used to illuminate a component. Left: camera shutter time 1 ms. Middle: camera shutter time 50 μs. Light: difference between two images multiplied by 10*

In the shuttle concept P&P machine, three illumination fields will be implemented to realise high contrast images of components being: bright field, mid field and dark field. Combinations of these illumination fields will be sufficient to be able to acquire high contrast images of all the specified components. To acquire high contrast images, the intensity of the illumination fields with respect to each other must be adjusted. Therefore, every single illumination field must be adjustable and capable of producing enough light to illuminate the component.

To illuminate the PCB features only bright field illumination is required. To acquire high contrast images of the features, the intensity of the bright field must be adjustable.

In addition to the optical properties of the objects, the amount of light that must be generated by the illumination system depends also on other parts used in the vision system. The light sensitivity of the camera, the F-number of the lens and the reflectivity of the mirrors will influence the required amount of light.

Proof of principle: images in 4 μs

As discussed to decrease the influence of motion blur because of the use of vision-on-the-fly, the image must be taken in a maximum time of 4 μs. One solution is to use a camera with a shutter that can be opened and closed in 4 μs. Another solution is to generate illumination pulses with the specified time and keeping the camera shutter open for a longer time. To validate the feasibility of this idea, a simple setup to proof the principle was realised.

The performance of Light emitting diodes (LEDs) was and still is improving. Power LEDs are powerful light sources that can probably solve the problem to create enough light in a short time. The test setup realised uses two power LEDs and a high speed camera. To prove that illumination during 4 μs can function as shutter the shutter of the high speed camera is changed from 50 μs to 1 ms. When the illumination determines the im-

age no difference between these two images may be visible. During 4 μs a current pulse of 10 A drives two power LEDs.

In Fig. 5.3 three images are shown. The left image is acquired using a camera shutter opening time of 1 ms. The middle image is acquired using a camera shutter opening time of 50 μs. Because the LEDs only generate light during 4 μs, it is expected that the duration of the shutter opening time will not influence the image. The right image shows the difference between the first and second image multiplied by 10. The third image shows a noisy image, which leads to the conclusion that the opening time of the shutter does probably not influence the amount of light. From this test it can be concluded that it seams feasible to use LEDs to illuminate a component in 4 μs and that LEDs can be used as a shutter.

Wavelength

The amount of light required depends on the reflection/absortion of light by the parts in the optical path. In this concept the parts involved are: the illumination, the object of which an image is acquired, two mirrors, the lens and finally the sensor inside the camera. But the reflection of light depends also on the wavelength of the illumination.

All parts in the optical path can be chosen for a certain wavelength except the components and the PCB features. The components and features do not require a special wavelength and so there is no special need to use a certain wavelength.

5.2 Realisation

In this section the following modules will be selected or designed and built: vision sensor, illumination, mirrors, alignment trigger and illumination controller, image processing software.

5.2.1 Vision sensor

The majority of cameras does not meet the requirement for the size in x-direction combined with the sensor resolution. In 2004 Sony introduces new CCD cameras in a small housing (29 $mm\times$ 29 $mm\times$ 42 mm) and XGA resolution [98]. The pixel size is 4.65 $\mu m\times$ 4.65 μm resulting in a FOV_{sensor} of 4.8 $mm\times$ 3.6 mm. The shutter time can be programmed between 10 μs and 250 ms. Although the 10 μs shutter time is higher than the requirement it has been proven that flash illumination can be used to decrease motion blur. In table 5.2 the Sony camera is compared with the determined requirements. The size combined with the resolution has resulted in the decision to use this camera.

Parameter	Required	Sony	Unit
Sensor resolution	$\geq$ 700×700	1034×779	$pixels$
Sensor technology	CCD	CCD	
Data transport time	$\leq$ 50	$\leq$ 30	ms
Size x-direction	$\leq$ 40	29	mm
Optional: shutter opening time	$\leq$ 4	10-250000	μs

Table 5.2: *Vision sensor parameters*

5.2.2 Lens

With help of the FOV_{sensor}, the magnification of the lens can be calculated using Equation 5.2.

$$Magnification = \frac{FOV_{sensor}}{FOV_{object}} \tag{5.2}$$

A small investigation in commercial available telecentric lenses resulted in two applicable lenses. The first lens is a lens from JENMetar, the second comes from CCS. The lens properties of these two lenses are summarised in table 5.3.

Description	Required	JENMetar	CCS	unit
FOV_{object}	7x7	7.9×6.0	9.5×7.1	mm×mm
Magnification	0.51	0.6	0.5	
Working Distance	70-120	94	107	mm
Effective F-number	-	12	5.9	
Distortion	0	0.05	0.001	%
Focus depth	±2	4.8	1.92	mm
Mass lens	-	200	29.6	g

Table 5.3: *Specification of two lenses (JENMetar and CCS)*

The CCS lens covers the FOV_{object}. In addition the effective F-number and distortion of the CCS lens are lower compared to the JENMetar lens. The main disadvantage of the CCS lens is the focus depth. The JENMetar has a focus depth of about 5 mm, where the focus depth of the CCS is about 2 mm, which does not meet the requirements. For this research it is possible to work with the CCS lens despite the limited focus depth. The FOV_{object} is more important and therefore the CCS lens is selected and used in the demonstrator.

5.2.3 Illumination

As discussed, three illumination fields for component alignment and one illumination field for board alignment must be realised.

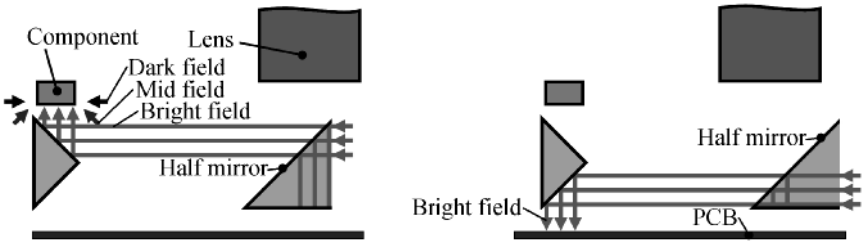

Figure 5.4: *Left: component illumination using dark field, mid field and bright field illumination. Right: PCB illumination using bright field imagination*

Bright field illumination

The bright field illumination can, in general, be generated with two setups. The first method is a ring light positioned around the lens. This results in an illumination field that illuminates the object with an angle of almost 0°, where this angle depends on the working distance and the size of the lens. In case of the suggested alignment layout it is not possible to use a ring light. The light coming from the ring light must be reflected by the mirrors to be able to illuminate the component or PCB. The size of the mirrors will function as a diaphragm, so most of the light will not be reflected resulting in almost no light to illuminate the component or PCB.

The second method is adding a half mirror. Via this half mirror the angle of the bright field illumination will be 0°. The design of the integrated alignment system contains three mirrors. In Fig. 5.4 the bright field is created by changing one of the mirrors in a half mirror. The LEDs are placed behind this half mirror.

A disadvantage of a half mirror is the loss of light. A half mirror with a reflective coefficient of 50% means that half of the generated light of the bright field illumination will go through the mirror, the other half will be reflected. The same holds for the light that comes from object illuminated meaning that the light reflected by the object will half go through the mirror and the other half will finally reach the lens of the camera. At the end only 25% of the illumination will reach the camera.

The loss of 75% of the bright field illumination, or 50% of the mid and dark field illumination is high taking into account the illumination time of 4 μs. To determine the reflectance factor experiments on reflectiveness and illumination have been performed and have resulted in the conclusion that a mirror with a reflectance factor of about 80% is preferable to create enough contrast.

The mirrors used are produced by depositing a thin layer of aluminium on a glass plate. By adjusting the layer thickness, the reflectance of the mirror can be changed. With help of this technique three mirrors are produced,

where the half mirror has a thin aluminium layer resulting in about 80% reflectance. The reflectance of the other mirrors is estimated to be 95%.

The LEDs used to produce the bright field illumination are mounted on the shuttle. Therefore, the mass and size of the illumination system is not important. The bright field illumination exists of two series of LEDs. A portion of the light from the LEDs will be reflected towards the bottom of the housing containing the LEDs. To prevent reflecting light into the lens, this surface has to be non reflective.

Dark and mid field illumination

To realise the dark and mid field illumination an illumination module must be attached to the P&P robot. Adding distances in the z-direction for the illumination unit will influence the process time. Therefore the dark and mid field illumination module should be as small as possible. The dimensions of the box where the dark and mid field illumination units must fit in are: x-direction maximal 40 mm, z-direction as small as possible but maximal 10 mm and the y-direction is not critical and is expected to have a maximum of 80 mm.

For realising the dark and mid field illumination, several illumination systems have been designed and examined. These systems are discussed below.

Power LEDs with fibers A commercial version of a dark field illumination system is shown in Fig. 5.5. Power LEDs illumination systems are available. These systems exists of three different parts. The first part is a unit in which one or more power LEDs can be placed. From this unit a glass fiber will guide the light into the light distribution unit. The third part is the light distribution unit. The light distribution unit will distribute the light to create a homogenous light spot. To realise this spot, this distribution unit contains lenses. There are two reasons why this system can not be used. First, the homogeneous illumination spot is not large enough for all components. Second, the distribution unit does not meet the mechanical requirements. The spot size and the mechanical dimensions have been subject of discussion with the manufacturer, but could not be adjusted. This solution is rejected.

Power LEDs with plexiglass guidance Figure 5.6 shows a system where the light of the LEDs are guided with help of plexiglass. The idea is to realise the dark field with one or two power LEDs in combination with a plexiglass light guidance system. This guidance system has preferably a rectangular shape due to the shape of most components. A rectangular light guidance system is built and tested. The problem with this system is to create a homogenous light spot. It is visible

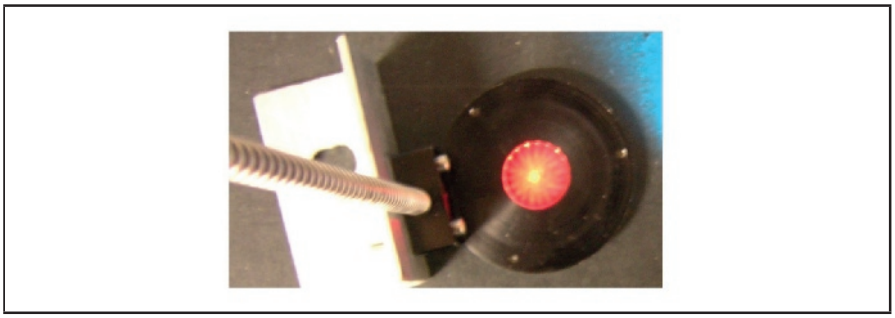

Figure 5.5: *Commercial dark field unit of CCS. Light of Power LEDs is distributed via fibers to a light distribution unit*

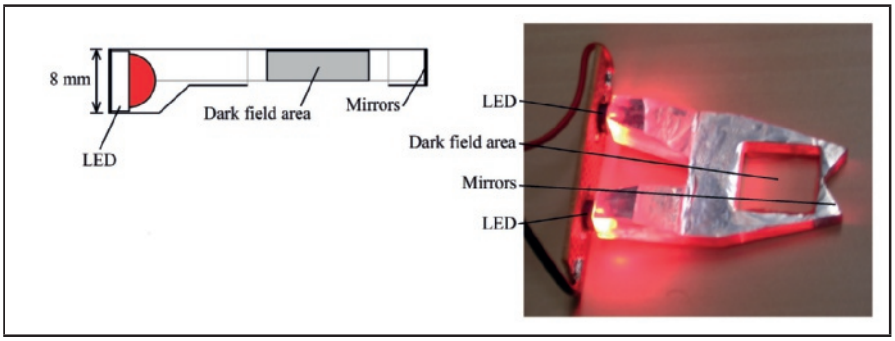

Figure 5.6: *Functional model of a dark field unit of plexiglass with Power LEDs*

by eye that the side where the LEDs are mounted gives more light intensity than the opposite side. Because of the problems with homogeneousness the research to create a plexiglass light guidance was stopped.

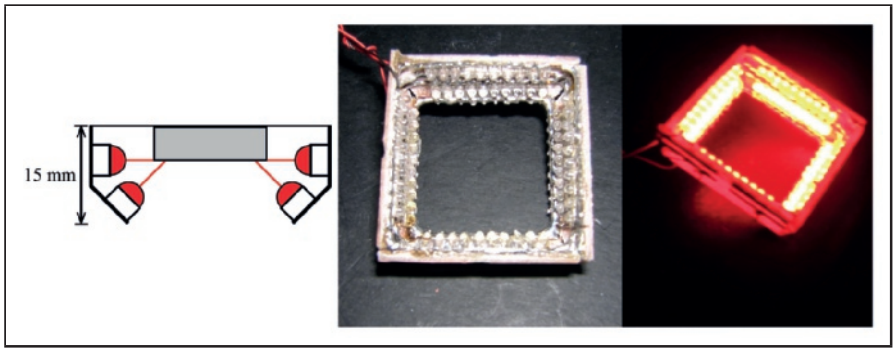

Figure 5.7: *Selected illumination system Left: Drawing of setup; Middle: Functional model of a dark and mid field system using direct SMD LEDs. Right: Same system illuminated*

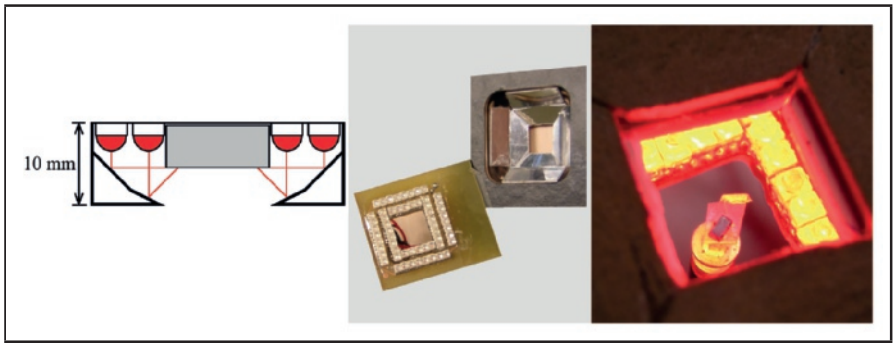

Figure 5.8: *Left: Drawing of setup. Middle Functional model of a dark and mid field system using SMD LEDs and mirrors. Right same system illuminating a component*

Small LEDs Figure 5.7 shows a system where SMD LEDs are used to create a mid and dark field illumination system. The upper row of LEDs are used to realise the dark field, the lower row of LEDs are used to realise the mid field. As can be seen from the left figure, to realise the 45° angle for the mid field, the size of the illumination system in z-direction is larger than 10 *mm* and can therefore not be used.

Small LEDs combined with mirrors In Fig. 5.8 a system is shown where the height of the illumination system is reduced. This design is realised with LEDs and mirrors. The left drawing shows the setup. The middle image shows the mirrors and the PCB with the LEDs. The right image shoes the complete system illuminating a component.

The choice is made to realise an illumination system for mid and dark field with help of SMD LEDs and mirrors. This design fits in the space reserved for the illumination. In Fig. 5.9 the total illumination setup in-

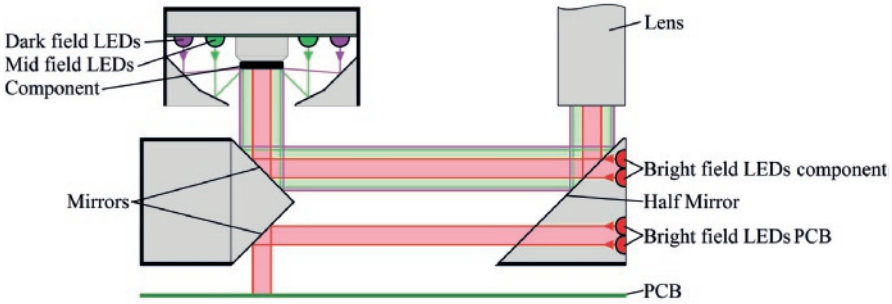

Figure 5.9: *The camera takes an image of the component; the dark and mid field illumination is generated close to the component; the bright field is generated behind a half mirror. The bright fields also illuminates the PCB*

cluding the mirrors is shown.

Illumination current controller

The next step is to realise an adjustable illumination controller that is able to generate a homogeneous illumination field.

Multiple LEDs are used to create one single illumination system. The dark field illumination system contains 32 LEDs, the mid field illumination system contains 28 LEDs and the bright field contains 32 LEDs. Although multiple LEDs are used, the goal is to create a homogenous illumination field. This requires that each LED generates the same amount of light and the amount of light of a LED is proportional to the current through the LED. Consequently, it is preferable that each LED is driven with the same current. Placing all LEDs in series is a solution, but this will result in a high forward voltage. If all LEDs are placed in parallel, this will result in a non homogenous field because the current through the LEDs will depend on the specific properties of each LED (the diode characteristics).

The solution is to connect four LEDs in series what averages the diode characteristics. These lines with four LEDs are placed in parallel. Finally, these illumination systems can be driven with high currents (up to 10 A) with reasonable voltage (maximum 100 VDC). To realise the amount of light required, the LEDs used will be driven with higher currents than the recommended currents.

The current per illumination system must be adjustable from 0 to 10 A. The expected pulse length is 4 μs but to be able to find the ideal situation for various components it is preferred that the pulse length is programmable between 1 μs and 15 μs. Taking into account the minimum pulse duration and the maximum current, the slew rate can be calculated. A slew rate of 20 $A/\mu s$ is required.

The functional overview of the current controller is shown in Fig. 5.10. The capacitor (C) is charged via a current limiting resistor (R1). If the

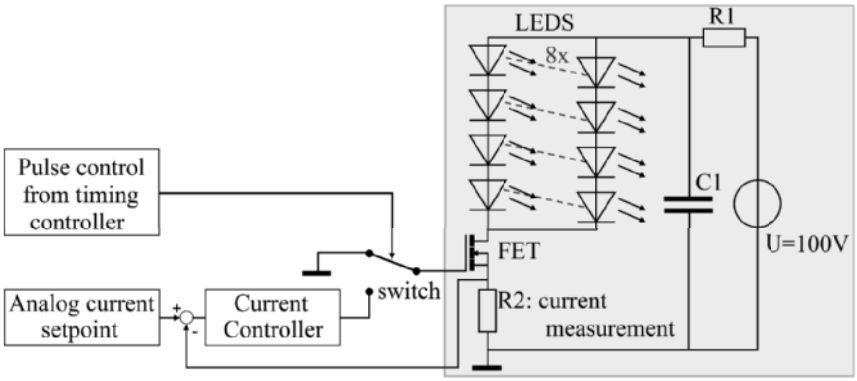

Figure 5.10: *Control strategy for illumination control; Right electronic schematic inside the gray box: an the current for eight times four serial LEDs comes from C1; C1 will be charged via R1 limiting the charging current; the FET is used to control the current through the LEDs; R2 is a resistor used as current sensor. Left schematic representation: Pulse control: an external digital signal coming from the illumination timing controller can switch on/off the current controller and controls hereby the light flash length. When light is required the timing controller switches the switch; the measured current is compared with an analog setpoint set by the system controller*

switch is closed, the current setpoint is compared with the measured current using a current sensor (R2) and the current is controlled via the FET (Field Effect Transistor) creating a P-controller. To create the pulse length, the switch is digitally controlled. If there is no current required, the input of the FET is kept at 0 V. Each illumination system has its own current controller.

5.2.4 Mirrors

The vision sensor and lens are now chosen, meaning that the WD and FOV are known. With help of these parameters the total layout of the alignment system can be determined.

A schematic overview of this layout is presented in Fig. 5.11. Drawn are the camera, CCS lens and the mirrors. The mirrors are drawn with the angle of 45°. With help of Equations 5.3, 5.4, 5.5, 5.6 the distances in the P&P machine can be calculated where the CCS lens has a WD of 107 mm. The 7 mm comes from the FOV_{object}.

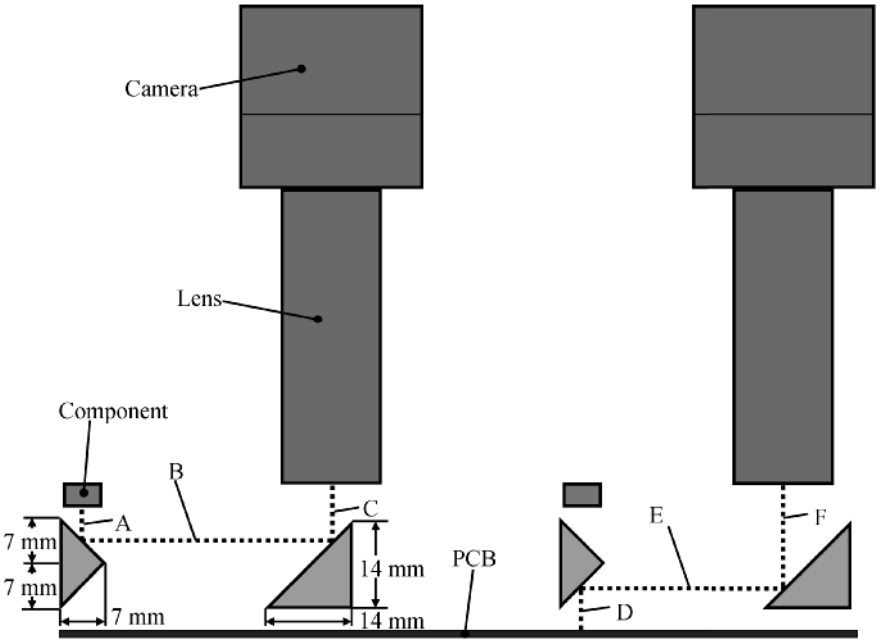

Figure 5.11: *Left: distances during component alignment. Right: distances during PCB alignment*

$$WD = A + B + C \tag{5.3}$$
$$WD = D + E + F \tag{5.4}$$
$$F = C + 7\,mm \tag{5.5}$$
$$E = B - 7\,mm \tag{5.6}$$

It can be concluded that A must be equal to D. The height of the mirrors above the PCBis known from Fig. A.17 and when the distance between the mirrors is determined the design can be drawn.

Mirror stability

The mechanical stability of the mirrors with respect to each other is an important requirement. Figure 5.12 shows the mirror rack that was designed to hold the mirrors. On the left side of the image a precise machined block is mounted holding two mirrors. On the right side a holder for the half mirror is visible. Behind the half mirror is a chamber to place the LEDs required for the bright field illumination.

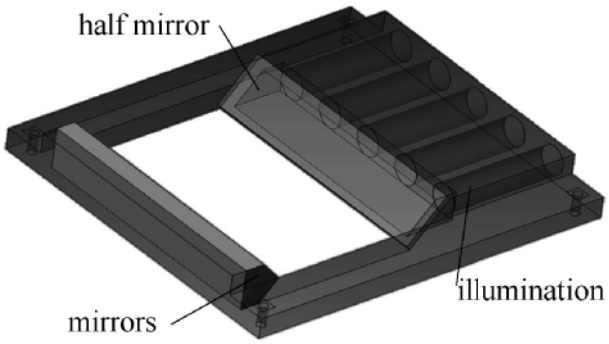

Figure 5.12: *Drawing of mirror rack. The mirrors are attached to this rack. The space behind the half mirror is used to mount the bright field illumination*

5.2.5 Alignment trigger

When the shuttle holding the mirrors is aligned with the P&P robot the motion must create an alignment trigger. This alignment trigger will then be used synchronous all processes required for image acquisition. This function is performed by the illumination timing controller.

Illumination timing controller

The illumination timing controller has two functions and uses the alignment trigger as the input. The first function is to generate a pulse to control the camera shutter and hereby the image acquisition. The second function is to generate three pulses for the current controllers, each controlling an illumination field (Current On/Off in Fig. 5.10).

The illumination timing controller to realise these pulses will be realised in dedicated hardware. For the moment it is assumed that the alignment trigger can be generated when the P&P robot and the mirrors are aligned. The realisation of the alignment trigger will be discussed later.

The illumination timing controller must be able to generate pulses to synchronise the opening of the camera shutter, the duration of the light per illumination field and starting the data transfer and image processing. Figure 5.13 shows a timing diagram that must be realised by the illumination timing controller. An alignment trigger is received. The next step is to open the camera shutter, the illumination will flash, the shutter is closed and finally a trigger will be generated that the data is available and can be transferred and processed.

Figure 5.14 shows a scheme of the programmed illumination timing controller. The illumination timing controller is implemented in a complex programmable logic device (CPLD). With help of eight counters four outputs are created. Three outputs are used to control the illumination, the

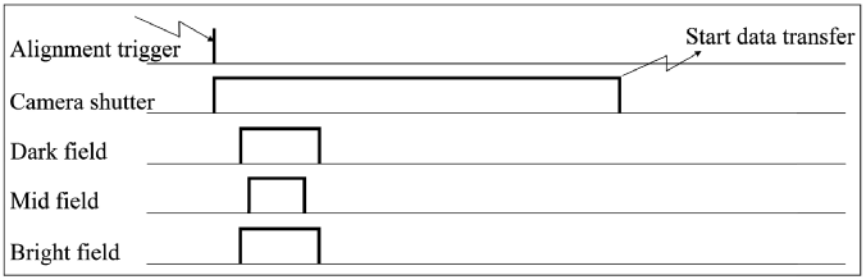

Figure 5.13: *Timing diagram; when an alignment trigger is received, the shutter is opened when the shutter signal is high; control signals for the dark field, mid field and bright field light flashes are generated; the shutter closes and the pc receives a trigger to start data transfer and after transfer start the processing of the data*

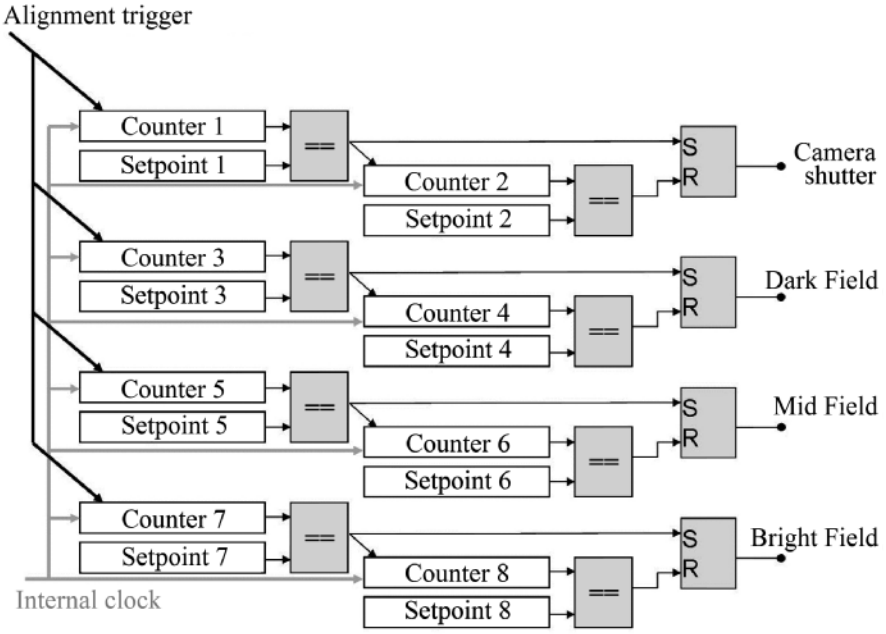

Figure 5.14: *Illumination control overview: The illumination controller obtains setpoints. When an external alignment trigger is received four pulses that can be adjusted with respect to each other in length and delay will be generated*

fourth output is used to control the camera shutter. Four parallel counters start to count after the external alignment trigger is received. As can be seen in the figure, all counters receive the same internal clock, which ensures synchronisation of the four outputs. When the counter value is equal to the setpoint, the output is set and a second counter starts counting. When the second counter has reached its setpoint the output is reset again. Via this implementation the different pulses can be adjusted to each other with respect to start time and length.

This clock is not synchronised with the alignment trigger. This will result in jitter with respect to the alignment trigger. This jitter will influence the repeatability. In this design the jitter is maximal 160 ns. Improvements can be realised when the internal clock frequency is increased.

Finally, an embedded processor is added to the illumination controller used to program the setpoints into the CPLD and to create analog setpoints for the illumination current controller. Hereby, the illumination system can be integrated into the overall machine control.

5.2.6 Image processing software

After the transfer of the image data, this data must be processed to determine the position of the object. The repeatability analysis has resulted in the requirement that the position must be determined with subpixel level.

In P&P machines pattern matching is used to determine the position of the object. Pattern matching algorithms determine the position of an object by fitting a known pattern, called reference model in Halcon, onto the image that is been acquired. The standard pattern matching algorithm finds the best fit of the reference model on the image and is therefore used in this research. The result of this pattern matching are four values: the position in x-direction [subpixels]; the position in y-direction [subpixels]; the rotation ϕ [rad] and a value between 0 and 1 that represent the reliability of the fit. As discussed the rotation will not be part of the investigation.

For each object a reference model must be created. Figure 5.15 shows on the top left the reference model for the nozzle. On the top right an image of this nozzle is shown with in white the position where the nozzle is found using pattern matching. Figure 5.15 shows on the bottom left the reference model for the calibration plate and on the bottom right an image of the calibration plate with in white the position where the square is found using pattern matching.

Tests with the Halcon pattern matching algorithms have shown that the position can be found in less than 5 ms for general objects as resistors, capacitors and nozzles. The repeatability of this algorithm will be discussed later. The same tests have shown that the illumination realised can generate enough light. The images of the nozzle and components can be taken using a light flash with a duration of 1 μs.

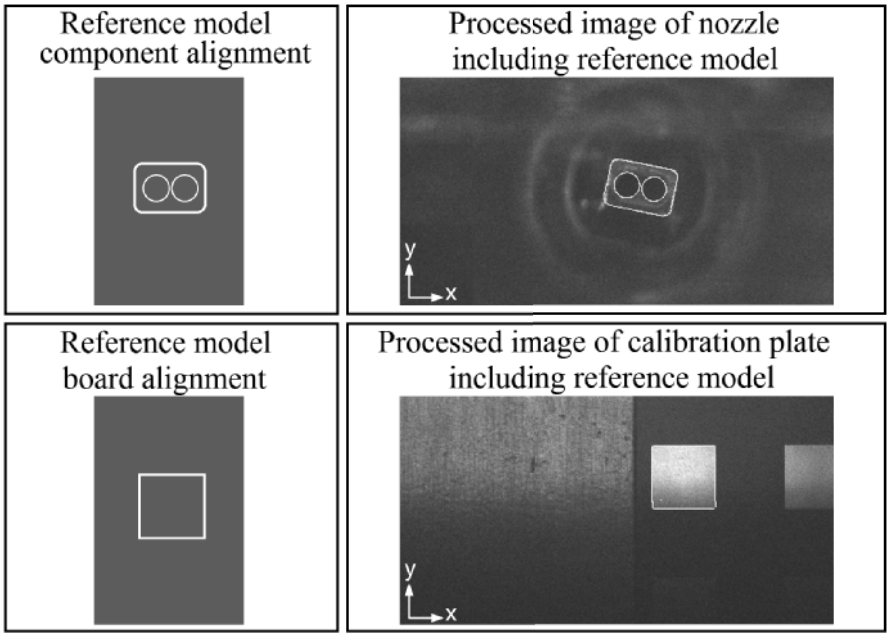

Figure 5.15: *Top left: Nozzle reference model component alignment. Top right: Image of nozzle; in white the nozzle reference model drawn by the image processing software at the determined position. Bottom left: Square reference model board alignment. Bottom right: Image of edge of calibration plate; in white the square reference model drawn by the image processing software at the determined position*

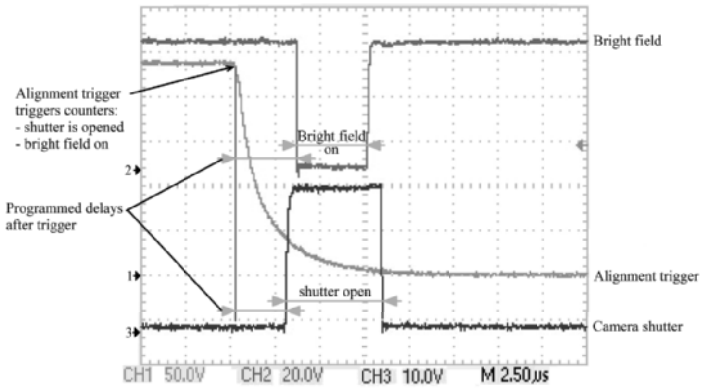

Figure 5.16: *Illumination timing controller: measured signals: alignment trigger, camera shutter, bright field illumination*

During this research Halcon's pattern matching algorithm will be used to process the images and to determine the positions.

5.3 Validation

After the modules selection and design validation tests on the different modules of the alignment systems need to be done according to the V-model. These validation tests have been divided in a two general tests. First, a part validation test is performed on the illumination timing controller. Second, validation tests are performed for the submodules: component and board alignment.

5.3.1 Illumination timing controller

The validation of the illumination timing controller can be performed by creating an input signal and measuring output signals. Fig. 5.16 shows three signals. The input signal to the illumination controller is the alignment trigger. Two outputs signals are measured: bright field and camera shutter. The alignment trigger is external generated and triggers the counters and after a delay, which was communicated to the timing controller. The shutter of the camera is opened for 250 ns before the illumination pulse is created with the desired length of 4 μs. Finally, the camera shutter is closed. More validation tests were performed and it was proven that the illumination timing controller is able to control the three illumination fields and the camera shutter.

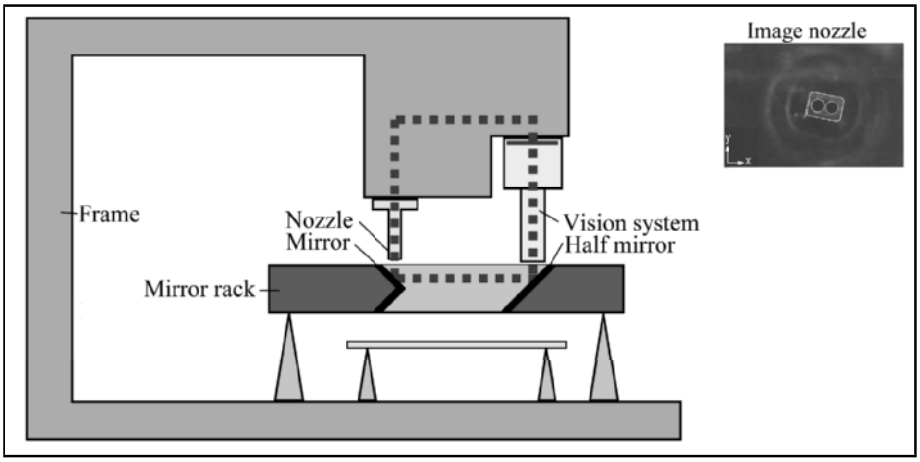

Figure 5.17: *Static test setup for CA; images of the nozzle are taken and the position of the nozzle is determined. The dotted line is the metrology loop involved; shown is an image of the nozzle (without a component)*

5.3.2 Vision system

The validation of the vision system is performed using the camera, the lens, the illumination system and the image processing software. Static setups are build used to perform the validation tests of the component alignment and board alignment system.

Component alignment test

The performed validation test has as goal to determine the repeatability of the component alignment system. The test setup is shown in Fig. 5.17. The camera and nozzle are mounted to a frame. The mirror rack is also placed on this frame. The dotted line indicates the metrology loop used during the test. Although, the CA system is used to determine the position of the component, images are taken of the nozzle. Hereby, the influence of components is avoided.

For the validation test, 1,000 alignment triggers are generated. For each trigger, the illumination controller will create light flashes, open the camera shutter and the camera will acquire one image. The image is processed using the reference model of the nozzle to determine the position in x- and y-direction of the nozzle within the image.

The result is the determined position of the nozzle in the x- and y-direction. These determined positions are presented in Fig. 5.18 as a histogram. Using Equation 2.2 the repeatability is calculated. The x-position has a repeatability of 1.0 $\mu m\,(1\sigma)$, and the y-position has a repeatability of 0.7 $\mu m\,(1\sigma)$. These values are added to table 5.4. The difference in x- and y- direction can be the result of the shape of the nozzle. This repeatability

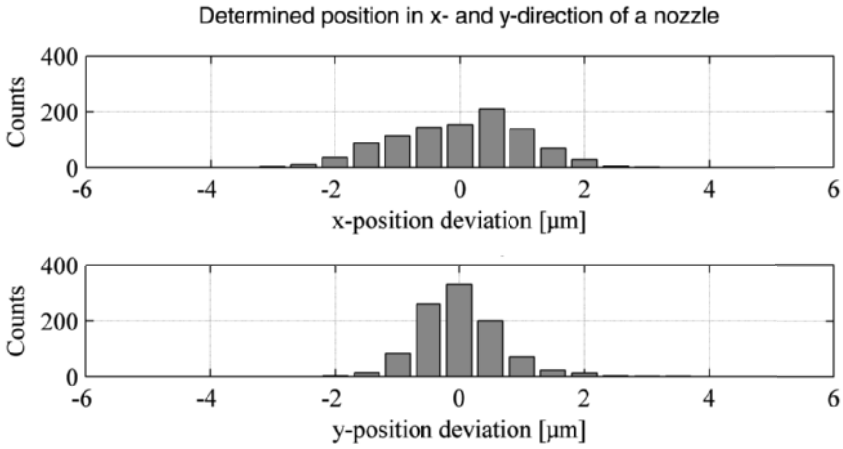

Figure 5.18: *Position in x- and y-direction of the nozzle of 1,000 images; x-direction 1.0 μm (1σ); y-direction 0.7 μm (1σ); both within the expected range of 4.6 μm (1σ)*

shows that the vision system is able to determine the position of the nozzle at subpixel level because the object pixel size is 9.3×9.3 μm.

Taking into account the repeatability budget of 4.6 μm (1σ) it can be concluded that the vision system will meet the specification in the x- and y-direction.

Board alignment test

In Fig. 5.19 the test setup for board alignment repeatability is shown. The mirror-box and the P&P robot are positioned by hand in such a way that a square of the calibration plate is visible. A thousand images are acquired and these images are processed to determine the position in x- and y-direction of a square on the calibration plate. The results of this test are the x- and y-position of the square, presented as a histogram in Fig. 5.20.

From these measurements it can be calculated that the x-direction repeatability of the vision system for board alignment is 1.0 μm (1σ) and the y-direction repeatability is 0.6 μm (1σ). These values are added to table 5.4.

A possible reason why the repeatability in the x-direction is worse than in the y-direction can be the positioning of the calibration plate with respect to the pixels in the camera. Although adjusting the settings for the illumination or changing the position of the mirror-box and/or P&P robot did not change this result.

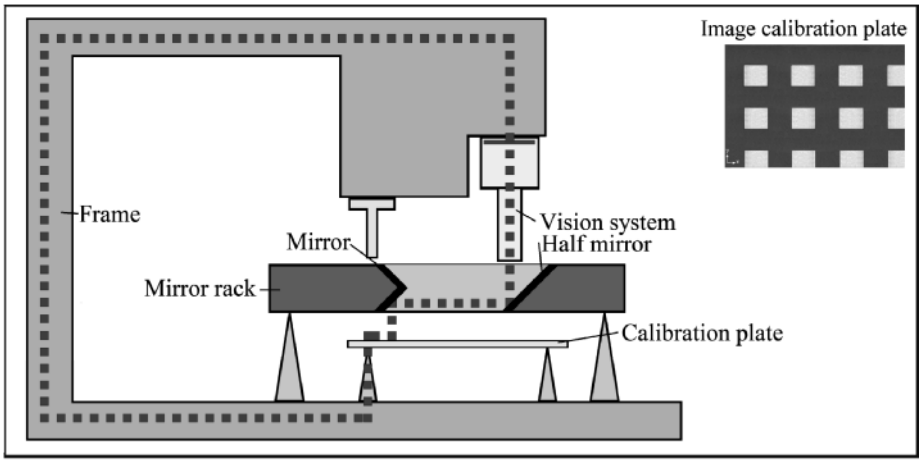

Figure 5.19: *Static test setup for BA; images of the calibration plate are taken and the position of a calibration square is determined. The dotted line is the metrology loop involved; shown is an image of the calibration plate*

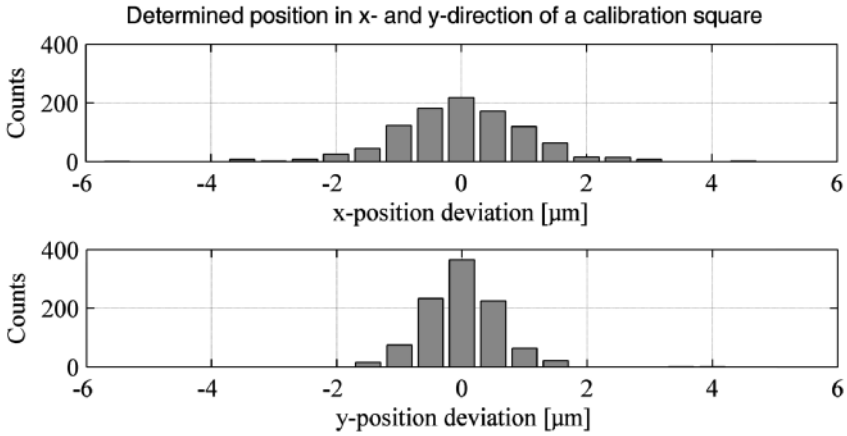

Figure 5.20: *Positions in x- and y-direction of a calibration plate square of 1,000 images; x-direction 1.0 µm (1σ); y-direction 0.6 µm (1σ); both within the expected range of 1.7 µm (1σ)*

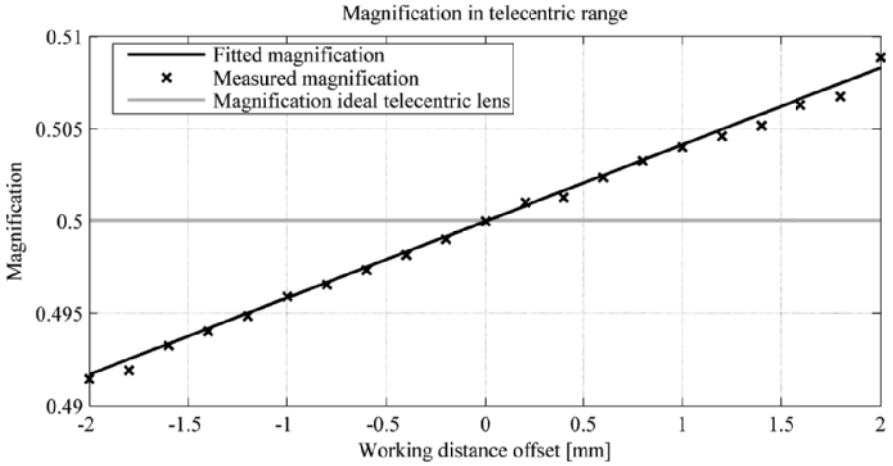

Figure 5.21: *The magnification of the lens with respect to the working distance offset being the height of the PCB (Working Distance = 107 mm)*

Influence of the lens on repeatability

Since a PCB is not flat, the distance from the top of the PCB to the lens varies. When using a single lens this results in a change of magnification. Therefore a telecentric lens is selected to avoid this change in magnification with a focus depth of 1.92 *mm*.

The magnification of the telecentric lens used is tested. For this test, the calibration plate is placed at the WD of the lens. The height of the calibration plate is then changed from -2 *mm* to +2 *mm* with respect to the WD, while the image processing software is used to determine the size of the square of the calibration plate. When the magnification of the lens is constant, the size of the square will be constant. It can be expected that the magnification will change when the height is outside the telecentric range of -0.96 *mm* and +0.96 *mm*.

The results of this test is shown in Fig. 5.21 where the magnification as function of the calibration plate height is shown. From this figure it can be concluded that the lens' magnification is not constant when the WD changes. A curvature of the PCB leads to a changing WD and hereby to a changing magnification. Due to the fact that the WD is unknown, the changing magnitude will influence the repeatability.

From the measurement it can be determined that the relative variation in magnification will be -0.0075 to 0.0075. This will result in a deviation of $\pm$ 0.0075 * 7 $mm \approx \pm 53\ \mu m$. Hence this lens does not fulfill the requirements and precautions must be taken during tests with this lens.

Error budget **Description**	**Repeatability** [μm (1σ)] **"design"**	**"demonstrator"**
*Board handling**	*4.0*	*4.0*
Board alignment process		
Vision System (FOV 7 mm×7 mm)	1.6	1.0 (Fig. 5.20)
Motion blur\Movements	4.6	To be determined
Position measurement after calibration	1.1	To be determined
Alignment trigger	1.3	To be determined
*Nozzle exchange**	*0*	*0*
*Component pick process**	*0*	*0*
*Component move process**	*0*	*0*
Component alignment process		
Vision System (FOV 7 mm×7 mm)	4.6	1.0 (Fig. 5.18)
Motion blur\Movements	4.6	To be determined
Position measurement after calibration	1.7	To be determined
Alignment trigger	1.3	To be determined
*Component place process**	*10.0*	*10.0*
Total estimated repeatability	13.8	To be determined

Table 5.4: *Repeatability requirement values "design" (adapted from table 3.9) and the achieved values during the "static" validation; *italic values will not be determined in this research*

5.4 Conclusion

In this chapter the requirements of the various modules used to realise the alignment system were determined. The component and board alignment system consists of a camera system with a vision sensor, lens, mirrors, illumination, alignment trigger and image processing software.

A commercial available Sony 2D camera was chosen to be used in the alignment system. This camera has a CCD vision sensor, a reasonable size.

The CCS lens that will be used in the demonstrator has telecentric properties to overcome the PCB height differences. The working distance is 107 mm and the effective F-number is relative low (5.9) compared to the other selected lens. During the validation tests it was shown that changing the working distance changes the magnification of the lens. This has to be taken into account during further testing.

The total illumination system consists of three illumination fields being: dark field, mid field and bright field. Illumination systems were designed and built. The illumination fields were created with help of LEDs. A current controller and timing controller were designed to meet the specifications.

The use of vision-on-the-fly results in the requirement that the images must be taken in 4 μs. With a power LED setup, it was shown that it is possible to take images in 4 μs.

A camera link interface card will be used to interface with the selected camera. Dedicated image processing software of Halcon will be used for image processing. This software is also able to control the camera link interface card. Finally, pattern matching algorithms as implemented by Halcon will be used to determine the position of the objects. Therefore reference models of the objects have been created.

Chapter 6

Demonstrator

Using the V-model method means that the designed subsystems are validated before assembly of the total system. To be able to validate the repeatability of the integrated alignment system a demonstrator was realised, which is presented in this chapter. This chapter starts with the explanation of the total layout of the demonstrator. Afterwards, the various subsystems are shown and explained. Finally, some properties of the demonstrator are presented.

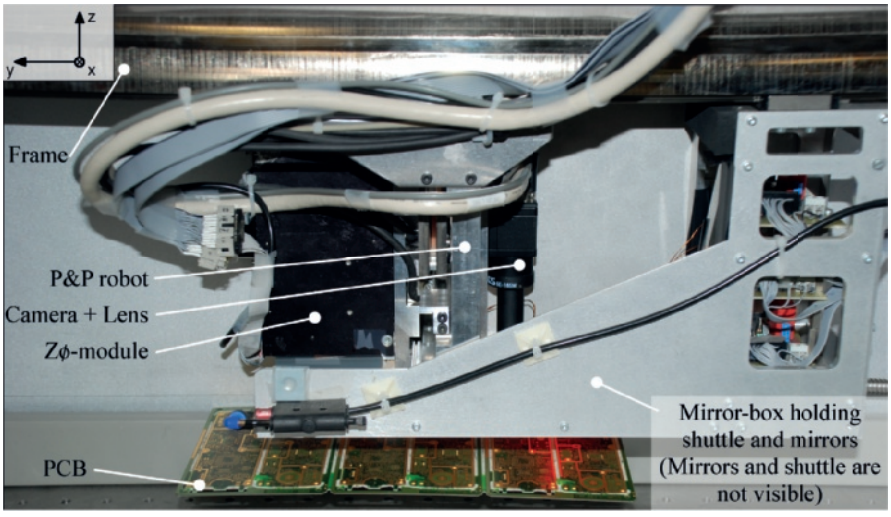

Figure 6.1: *Picture of realised demonstrator*

6.1 Demonstrator modules

Figure 6.1 shows the realised demonstrator with a frame, P&P robot containing the camera and lens, zϕ-module. In front the mirror-box holding a

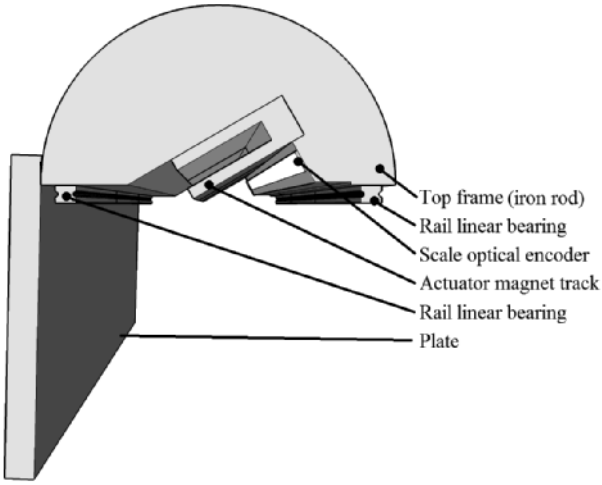

Figure 6.2: *Drawing of the frame including the magnet track of the actuator, two sliders of the linear bearings and the optical scale encoder*

shuttle and the mirrors. In the next sections each module of the demonstrator is explained.

6.1.1 Frame

Figure 6.2 shows a drawing of the frame. The frame supports two rails of linear bearings. In between these two rails the magnet track of the linear motor is mounted under an angle. The optical encoder scale is mounted onto the frame. Both the P&P robot and the mirror-box will use the actuator magnet track, rail and the encoder scale.

The total length of the frame is 0.6 m. The top frame is built out of a iron rod and has a mass of about 50 kg. On the side of the top frame a plate is screwed that is attached to the base.

As can be seen in Fig. 6.1 the cables of the complete system have not been integrated into the frame. To integrate all the cabling inside the frame and modules would take much effort. Taking into account the goal to prove the repeatability, it is not required to integrate the cabling inside the demonstrator. Therefore, the choice is made to place the cables outside the machine.

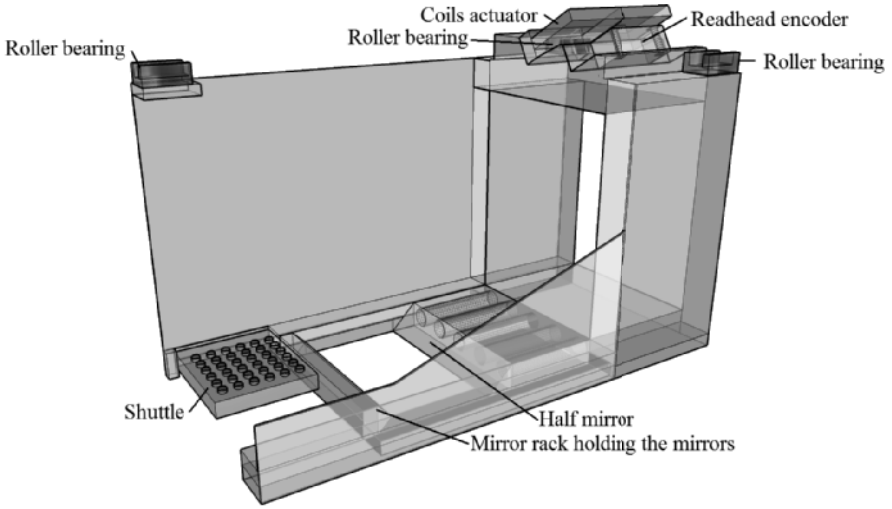

Figure 6.3: *Drawing of the mirror-box holding the shuttle and the mirror rack containing the mirrors and a half mirror*

6.1.2 Mirror-box

Figure 6.3 shows the mirror-box that is used in the demonstrator to hold a shuttle and the mirror rack. The used open box structure explains the term mirror-box for this robot. The mirror-box uses the magnet track, encoder scale and the rails that are mounted on the frame. On top of the mirror-box three roller bearings, the actuator coils and the readhead of the encoder are mounted.

As can be concluded from Appendix A an acceleration of 10 m/s^2 and a velocity of 1 m/s is required for the mirror-box to be able to follow the P&P robot. With this design these requirements are met.

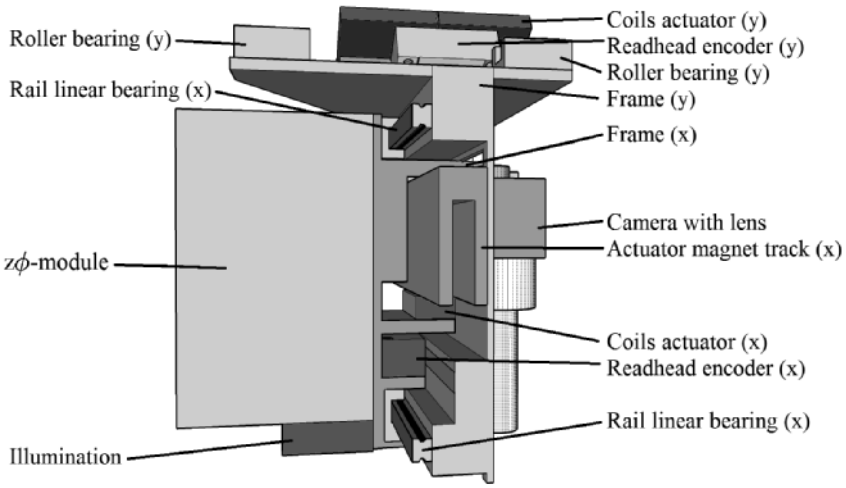

Figure 6.4: *Drawing of the P&P robot; the camera with lens and the zϕ-module are attached to the frame that can move in x-direction*

6.1.3 Pick-and-place robot

Figure 6.4 shows a drawing of the P&P robot. At the top of the P&P robot the actuator coil for the y-direction is placed. This coil will move through the magnet track mounted on the frame. Also on top, three roller bearings and the encoder readhead. On the left the zϕ-module with attached to it the module to generate the dark and mid field illumination. On the right, the camera and lens. In the middle the actuator, encoder and linear bearings for the x-direction. The magnet track of the actuator, the optical encoder scale and the linear guidance are attached to the frame that moves in the y-direction. The coil of the x-actuator, the roller bearing cages and the encoder read head move in the x-direction. Attached to this frame are the camera and the zϕ-module. The moving mass in x-direction is about 1.5 kg. The moving mass in y-direction is about 3 kg.

As stated it is required to calibrate the linear encoders to realise a repeatability lower than 0.75 μm (1σ). To calibrate the encoder system an interferometer system has been added to the demonstrator. Figure 6.5 shows the two positions where the mirrors are added for the interferometers. The interferometer used to calibrate the encoder is placed along the same axis as the encoder and as close to the position where the read head determines the position [9]. If this principle is not met, the contribution of angular motions or rotations will influence the measurement. In this system it is not (easy) possible to add an interferometer mirror at the position where the encoder readhead is positioned. To keep the distances between the encoder readhead and the interferometer mirror, as small as possible to reduce the effect of angular motions, the mirror of the calibration reference interferometer is

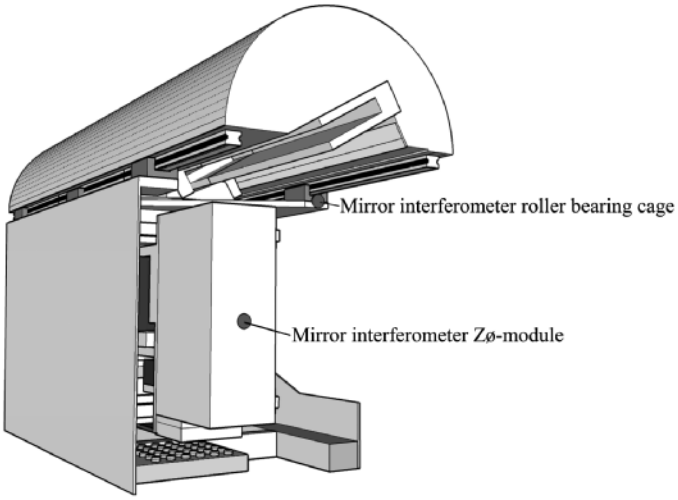

Figure 6.5: *For encoder calibration a interferometer mirror is added to the roller bearing cage; a second mirror to measure the zϕ-module dynamics is added to the zϕ-module*

attached to the roller bearing cage of the P&P robot.

A second interferometer is added to be able to measure the rotational movements of the P&P robot. This interferometer measures the position in the y-direction of the zϕ-module.

6.1.4 Demonstrator control

In Fig. 6.6 the machine control layout is presented. Top left: Three current controllers are present to control the three illumination fields. The setpoint and timing for the current controllers comes from the illumination controller. This illumination controller controls also the shutter.

Top right: A PC is used as the overall machine controller. The software sends setpoints to the illumination controller, the camera and the motion control platform. Via the camera link interface the images are imported. The software will process these images and save the results as data for later analysis and could finally use this data to perform setpoint correction.

As stated in Chapter 2 a commercial motion control platform is used to control the five moving axes of the demonstrator. The Nyce 4000 motion control platform consist of a backplane, one Nyce 4110 CPU board and four Nyce 4120 2-axes motion controllers.

The first position in the backplane is used by the Nyce 4110 CPU board. This 4110 CPU board is equipped with firewire to communicate with a PC. This CPU board communicates with four Nyce 4120 2-axes motion controllers using an internal bus on the backplane. The next four positions on the backplane are occupied by four Nyce 4120 2-axes motion controllers. One Nyce 4120 2-axes motion controller drives the x-axis and switches the vacuum valve for picking up and release components. A second Nyce 4120 2-axes motion controller drives the two axes of the zϕ-module. A third Nyce 4120 2-axes motion controller is added to measures the position of the two y-axes using two interferometers. A fourth Nyce 4120 2-axes motion controller drives the y-axis of the P&P robot and the y-axis of the mirror-box. This motion controller also generates the alignment trigger.

The Nyce 4110 CPU module is the interface between the PC and the motion controllers. It is used to sample data from the various axes and to synchronise the motion of the axes. The maximum sample frequency is 8 *kHz* for one axis, when eight axes are used a maximum sample frequency of 2 *kHz* can be achieved.

The Nyce 4120 2-axes motion controller is a dual axes motion controller with integrated drive. This module is equipped with a Field programmable gate array FPGA that is programmed with two separate motion controllers. Both motion controllers have a sample frequency of 32 *kHz*. Although, the two controllers are programmed in a FPGA, the motion controllers can not communicate with each other and have no shared memory.

Encoder inputs

The readhead of the optical encoders generates after interpolation pulses when the readhead moves. In general it can be stated that it is preferable to have the highest resolution but there is an important restriction on the highest resolution that can be used. This is the number of pulses per second

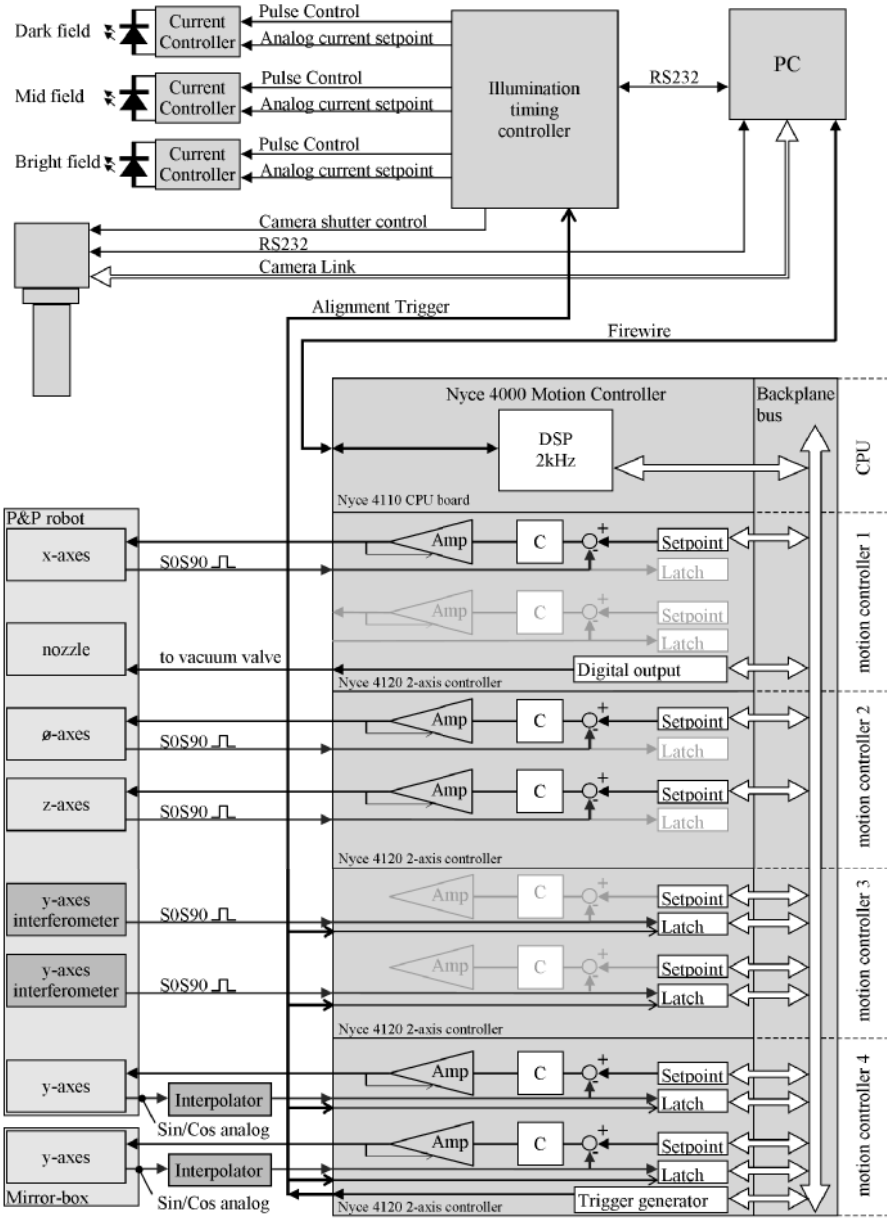

Figure 6.6: *Machine controller layout used for the demonstrator. A PC is used as overall system controller; communication with the illumination timing controller, the camera and the Nyce 4000 motion controller. The illumination timing controller is controlling three current controllers and the camera shutter; the Nyce 4000 Motion Controller contains one Nyce 4110 CPU board and four Nyce 4120 2-axes motion controllers; the fourth Nyce 4120 2-axes motion controller generates the alignment trigger*

that can be created meaning that the resolution is also depending on the maximum velocity of the system. For the x-axis a S0S90 encoder with a resolution of 200 nm is used. Both y-axes are equipped with an analog sin/cos encoder. With help of an interpolator are the analog signals transformed in digital S0S90 200 nm signals [1].

The x- and y-axis have a 200 nm encoder that generates pulses every 200 nm displacement. Combining the resolution of 200 nm with the maximum speed of the axes the required minimum counter frequency of the encoder input of the motion controller can be calculated.

$$Counter\ frequency > \frac{2.5m/s}{200nm} = 12.5MHz \tag{6.1}$$

This frequency applies to the motion controller's encoder input specification of 40 MHz.

Motion control

A motion controller runs with a 32 kHz sample frequency and has a feedback controller PID controller, programmable filters and a feedforward controller.

Each axis of the demonstrator is controlled using this motion controller. The x- and y-axis of the P&P robot are tuned to have a bandwidth of about 50 Hz. This is sufficient for the repeatability tests. Further third order trajectories are used as setpoints.

Alignment trigger

As discussed an alignment trigger must be generated when the P&P robot and the mirror-box are aligned. So it is not the position of one axis, but the difference between two axes that is important for the generation of the alignment trigger. This means that the difference between two positions must be calculated and when this difference has become a predefined value the trigger must be generated. As specified the trigger may only add 1.25 μm to the error budget. Resulting in a maximum allowed time delay and jitter of 0.5 μs.

The motion controller is equipped with a task to generate a trigger depending on an axis position. Below the specifications of this trigger task and feasibility to use it as an alignment trigger are discussed.

A 4120 2-axes motion controller is capable of controlling two axes, but it is not possible to exchange data between the two motion controllers. This means that it is not possible to calculate the difference between two axes. Taking into account that the mirror-box will not move during alignment makes it possible to measure the mirror-box's actual position and use this data to determine the position where the P&P robot is aligned with the mirror-box. Consequently, it is possible to generate the alignment trigger

[1] There were some practical reasons to use these two axes analog sin/cos encoders.

by only monitoring the actual position of the moving P&P robot. When the P&P robot has reached its position an alignment trigger must be generated using a high speed output.

Although, the high speed output is controlled by the motion controller's FPGA, it is not possible to monitor the P&P robot's position in realtime and generate the trigger. The standard solution implemented in the 4110 CPU board is to predict the moment when the trigger must be generated using actual axes position and the calculated trajectory movement. This expected moment is sent to the FPGA and that will generate the trigger on the calculated time with a jitter of 100 ns max. To determine if this solution will be within the requirements the calculations performed are discussed more in depth.

On CPU sample k the estimation is calculated for the position (x) of the axes on sample moment $k+2$ and $k+3$ (Equation 6.2, Equation 6.3). As inputs for these equations the actual position, the setpoint velocity (v_{sp}) and the CPU sample time TS_{CPU} (0.5 ms) are used.

$$x(k+2) = x(k) + 2 \times v_{sp} \times TS_{CPU} \tag{6.2}$$

$$x(k+3) = x(k) + 3 \times v_{sp} \times TS_{CPU} \tag{6.3}$$

If the desired trigger position will pass in between these two calculated positions, the hardware trigger time is calculated and programmed in the FPGA. At the calculated time the FPGA will generate the trigger with hardware accuracy, depending on the clock frequency of the FPGA, but expected within 100 ns.

The alignment trigger timing will be correct if the setpoint velocity (v_{sp}) is constant, but if the robot is accelerating the displacement caused by accelerating should also be taken into account (Equation 6.4).

$$x(k+2) = x(k) + 2 \times v_{sp} \times TS_{CPU} + 0.5 \times a_{sp} \times (2 \times TS_{CPU})^2 \tag{6.4}$$

The maximum deviation caused by this term can be calculated taking the difference between Equation 6.2 and 6.4.

$$\Delta x(k+2) = 0.5 \times a_{sp} (2 \times TS_{CPU})^2 = 0.5 \times 50 \times (2 \times 0.0005)^2 = 25\,\mu m \tag{6.5}$$

This means that the trigger can have a deviation of 25 μm due to the fact that the acceleration is not taken into account. This alignment trigger will not fulfill the repeatability requirement of < 1.25 μm. To met the repeatability requirement, latches are used. These latches are introduced in the next paragraph.

Latches

The alignment trigger is not accurate enough to meet the requirements but accurate enough with respect to the FOV available compared to the size of

the component or the PCB features. A solution to meet the requirements is to save the actual positions at the moment the alignment trigger is generated and use the latched positions to correct the measurements. So, if the positions of the mirror-box and the P&P robot can be measured when the alignment takes place, it is not required to have a very accurate alignment trigger.

The motion controller modules are equipped with latches. These latches are memory places where the actual position of an axis can be stored. Storing a position is initiated by an external trigger. The latches are implemented in hardware, meaning that the external trigger directly, there is no software involved, saves the actual position into the latch what makes these latches is very fast. The actual position will be saved within 100 ns after the hardware trigger. Taking into account the maximum velocity of 2 m/s this results in a maximum position error of 0.2 μm.

The solution is to use the alignment trigger to save the actual y-axis positions of the P&P robot using the encoder and the two interferometers, to save the actual y-axis position of the mirror-box and to activate the illumination controller that will activate the camera to acquire an image. Afterwards the latched positions will be used to correct the positions calculated from the image by the vision software.

Machine control

The demonstrator overall machine control is implemented using a PC. The developed software running on this PC is used to send commands to the motion controller, the illumination controller and the camera. Machine initialisation including the homing sequences for all axes is programmed. During operation the software communicates with the motion controller. The software sends position setpoints to the axes controller, requests the positions saved by the latches and processes the images. During the repeatability tests, the results of the image processing software together with the latched positions are stored. Additional, with a sample frequency of 2 kHz actual axes data such as: trajectory setpoints, position, velocity, acceleration, position error is stored. This data will be used in the next chapter to determine the overall repeatability of the shuttle concept P&P machine.

6.2 Vibration of the demonstrator

With help of Finite Element Method (FEM) calculations, the first mode of the P&P robot is determined.

Figure 6.7 shows in light gray the P&P robot. In dark gray the calculated first mode shape of the P&P robot during y-acceleration is drawn. This mode in y-direction will rotate and displace the camera and zϕ-module. The eigenfrequency of this mode is calculated to be about 200 Hz and results

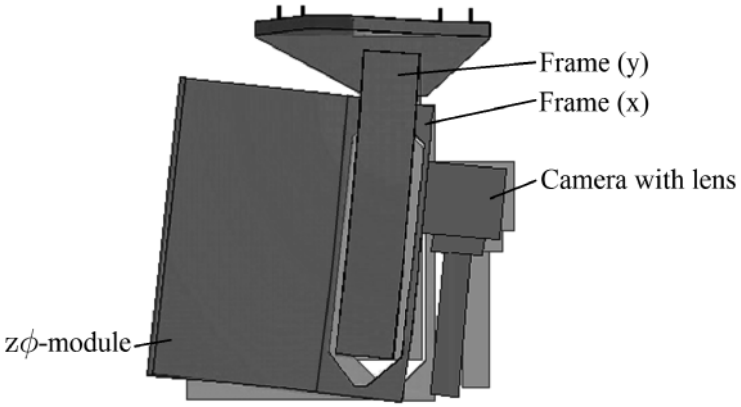

Figure 6.7: *Image of deformation of first mode of P&P robot in y-direction. This mode will introduce a rotation around the x-axis. This rotation will influence the repeatability of the alignment system*

in a bend around the x-axis. This bend around the x-axis is introduced by a gap in the y-frame required to connect the zϕ-module with the camera. This limited stiffness causes a deflection of the y-frame when acceleration forces are applied.

Now the demonstrator is built, the mechanical vibrations can be measured. The frequency response of the P&P robot in y-direction is measured. The bode diagram of the y-axis shows the first eigenfrequency at 200 *Hz*. The frequency response changes only slightly when the x-position of the P&P robot changes.

The frequency response was measured using an external drive analog connected to the Nyce 4120 motion controller what results in an additional delay. The delay is measured as an additional phase shift. To eliminate this delay the internal drive of the Nyce 4120 controller is used during repeatability tests.

Friction

The x- and y-direction both have two parallel linear bearings, resulting in an over-constrained system. The demonstrator has no adequate solution to overcome the problem of an over-constrained system. The total length of 0.6 m makes it difficult to adjust the guidance in such a way that the linear bearings are perfect parallel. The linear bearings being not perfectly parallel results in a position dependant varying friction. Later during the repeatability tests, this will influence the repeatability.

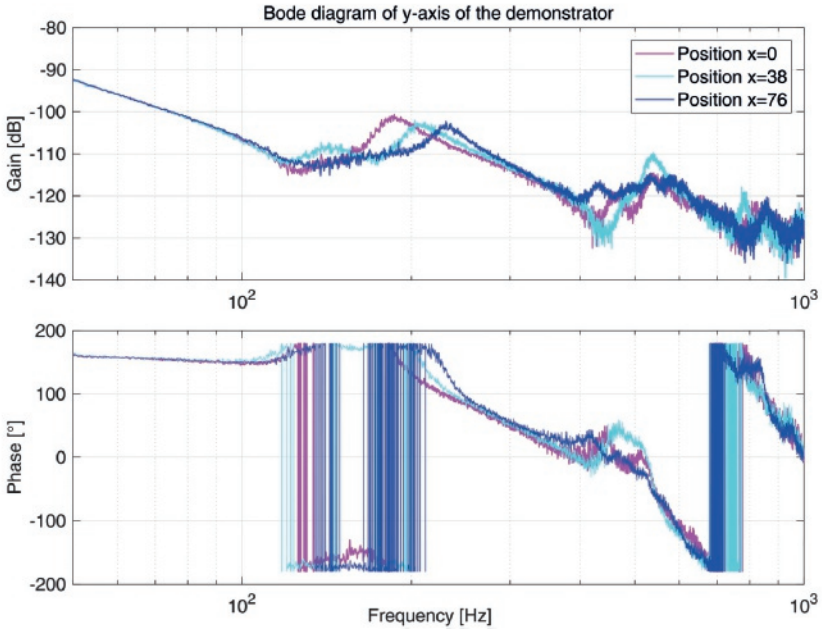

Figure 6.8: *Bode diagram of P&P robot in y-direction (from y-actuator to y-encoder): the first eigenfrequency is about 200 Hz. The eigenfrequency is slightly depending on the position of the robot in x-direction*

6.3 Conclusion

The demonstrator built has four main parts being: frame, P&P robot, mirror-box holding the shuttle and mirrors and the machine controller. The fully functional P&P robot contains a zϕ-module, camera with lens mounted on a x-axis.

Overall machine control software was implemented on a PC. The overall machine control software sends setpoints to the illumination controller, the camera and the Nyce 4000 motion platform. The image processing software was integrated into the machine control software. The illumination controller controls the shutter of the camera and generates the setpoints for the current controllers. The motion controller controls the axes, and creates the alignment trigger. Furthermore position latches will be used to be able to compensate for the inaccurate alignment trigger.

The modes of the P&P robot were estimated and validated. These modes will influence the repeatability of the shuttle concept P&P machine.

With help of this demonstrator the repeatability of the shuttle concept with integrated alignment systems will be validated.

Chapter 7

Validation of the alignment system

In this chapter the accuracy feasibility of the proposed integrated alignment system (see Chapter 4) is validated using the realised demonstrator (see Chapter 6).

Two types of component placement errors exist: systematic and random. Systematic errors can be compensated by calibration where random errors are unpredictable and cannot be compensated for. In Section 1.3 it is defined that accuracy will contain the random errors (repeatability) and the calibration residue (offset) remaining after compensation for systematic errors. The influence of both errors - repeatability and offset - were estimated for the P&P processes during the design of the alignment system. To validate the accuracy feasibility, first the calibration feasibility is determined followed by the repeatability feasibility study.

To be able to realise the throughput requirements the proposed alignment system is based on the vision-on-the-fly alignment strategy where the alignment images are acquired while moving. To enable vision-on-the-fly the board and component alignment system consists of two moving subsystems: the P&P robot with the vision system and the shuttle with the mirror rack. The relative position of these subsystems enables alignment measurements for the board and the components (see Figure 5.11).

The three parameters: distance between the component pick and the place position, the maximum allowed acceleration and maximum allowed velocity are used to determine the P&P robot's trajectory. While the P&P robot is moving from the "pick" to the "place" position, a trigger is generated to acquire an image of the component or board fiducial/artwork. The timing of this trigger influences the repeatability. The trigger timing depends on two system properties: the trajectory parameters and on jitter and delay of the used controller components that are used to generate the alignment trigger. Also the dynamic behavior of the P&P robot will influence the repeatability. In this chapter compensations for jitter, delays,

mechanical rotations and vibrations will be applied.

Due to the fact that the mirror-box only moves in y-direction it is decided that most of the measurements and results will be presented in the y-direction only.

In Section 7.1 the calibration feasibility will be determined. The first step is the calibration of the linear y-encoder of the P&P robot using the two interferometers. The calibration data is acquired while slowly moving (constant velocity $< 0.01\ m/s$) the P&P robot to minimise dynamic effects. The processed data is used for P&P robot encoder calibration.

The second step for the alignment system calibration is to include the mirrors of the mirror-box. Therefore a calibration plate is added to the demonstrator. The P&P robot and mirror-box are moved in the y-direction over the calibration plate. On multiple y-positions the vision system acquires images of the calibration plate. These images are processed and the data is used for calibration of the alignment system.

The third step is to determine the calibration feasibility of the mirrors. An image is acquired from the nozzle without a component via the mirrors. This image is processed and then the P&P robot is moved to another position. This sequence is repeated multiple times to create a grid of data points. These data points show the errors and are used to determine calibration-polynomials of the mirrors in x- and y-direction. After applying the calibration-polynomials a calibration residue or offset will remain. This residue will be added to the single camera alignment system's repeatability.

In Section 7.2 the single camera alignment system's repeatability will be determined. The proposed design of the alignment system is realised by using the motion controller to generate the alignment trigger. The motion controller uses the P&P robot's encoder and the mirror-box's encoder to determine the position of both systems. When the P&P robot and mirror-box are aligned the alignment trigger is generated. The timing of the alignment trigger is influenced by two properties: delays in the position measurement systems and the timing jitter of the motion controller generating the alignment trigger. To determine the repeatability of the alignment trigger timing a test is performed where the P&P robot executes several times a P&P movement. This test is then repeated using four different movement trajectories.

To realise the P&P robot's movements the P&P robot is accelerated and decelerated. The forces induced to accelerate and decelerate the P&P robot will also deform the P&P robot due to mainly stiffness. The deformation results in the rotation of the P&P robot part where the nozzle and camera are mounted. The interferometers are used to measure the rotation Rx. The influence of this rotation on the repeatability is determined.

The repeatability measurements show that the repeatability is not within

the specifications. Analysis of the measurements show the presence of additional systematic errors such as alignment trigger timing and delays in the position measurement system, which can be compensated. Applying these compensations improves the repeatability.

Finally this chapter ends with the conclusions in Section 7.3 where the measurements are compared with the design specifications. It is concluded that calibration is feasible and that the repeatability is within design specification.

7.1 Calibration

In this section, the tests to determine the calibration feasibility of the single camera alignment system are described.

Subsection 7.1.1 contains the description of the calibration of the y-encoder of the P&P robot. The y-position of the P&P robot is determined using an encoder and two interferometers. A calibration-polynomial is determined and applied.

In Subsection 7.1.2 calibration of the mirror-box mirrors and the P&P robot with vision system is performed. To include the mirrors and the vision system a calibration plate containing squares is added to the demonstrator. The images from the calibration plate are acquired and processed. The data is used for calibration.

In Subsection 7.1.3 the calibration feasibility of the mirrors is determined by a test where the P&P robot moves in x- and y-direction while acquiring images of the nozzle of the P&P robot.

In Subsection 7.1.4 the calibration residue is determined.

7.1.1 Pick-and-place robot calibration using interferometer

For calibration two interferometers are added to the demonstrator. One interferometer measures the position of a bearing of the P&P robot and one interferometer measures the position of the zϕ-module as shown in Fig. 6.5. The information of the two interferometers can be used to determine the position and the Rx-rotation of the P&P robot.

The first calibration step is to calibrate the P&P robot's y-direction encoder. To calibrate the P&P robot encoder, the P&P robot is moved in the y-direction while the position is measured using the encoder and the two interferometers. To minimise the dynamical influence the P&P robot is moved with a constant low velocity ($< 0.01\ m/s$).

The first graph of Fig. 7.1 shows the measured positions by the encoder and two interferometers with respect to time. In this graph, for readability, offsets are applied to the position measured with the bearing's interferometer and the zϕ-module's interferometer.

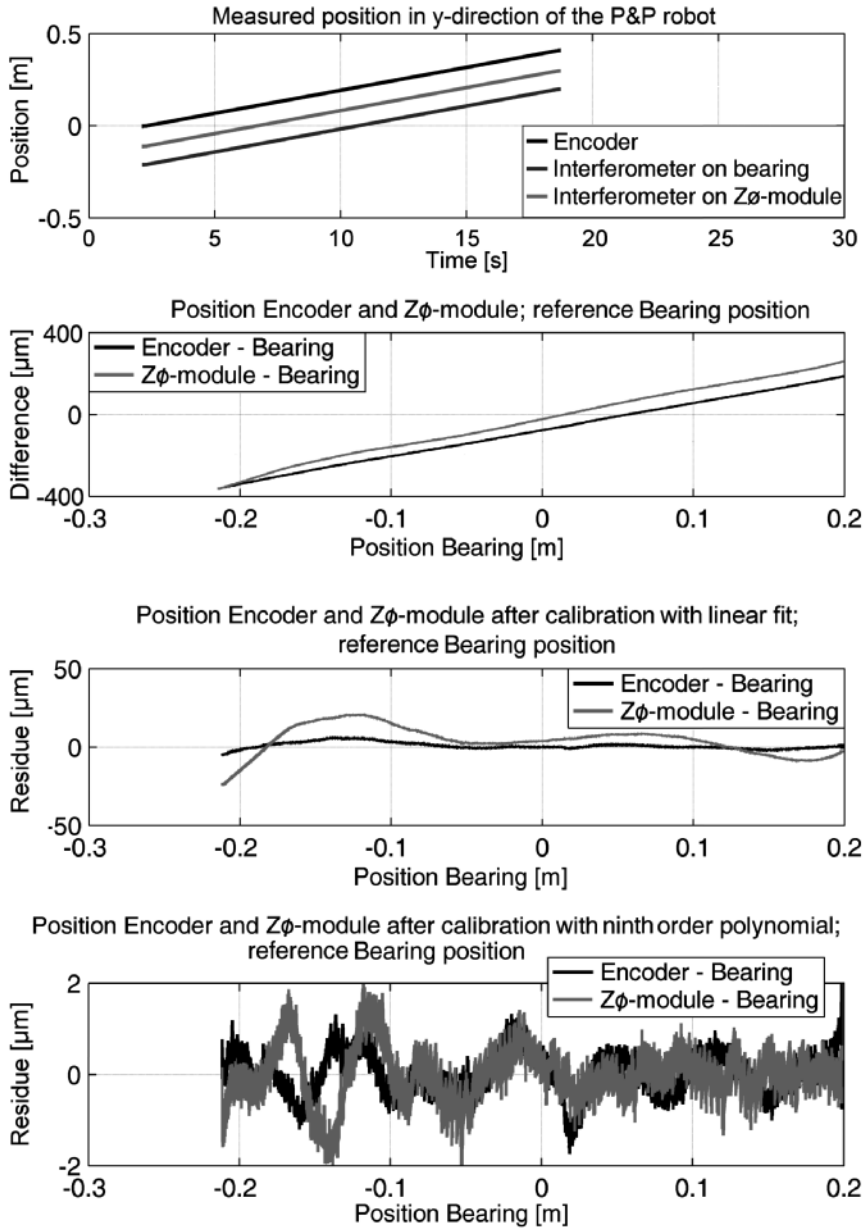

Figure 7.1: *P&P robot encoder calibration in y-direction; plot 1: position data measured in time: P&P robot position measured with encoder, bearing position measured with an interferometer, zϕ-module position measured with an interferometer. Plot 2: Encoder and zϕ-module position with respect to the bearing position. Plot 3: Encoder and zϕ-module position with respect to the bearing position, applying a linear calibration. Plot 4: Encoder and zϕ-module position with respect to the bearing position applying a ninth order polynomial calibration*

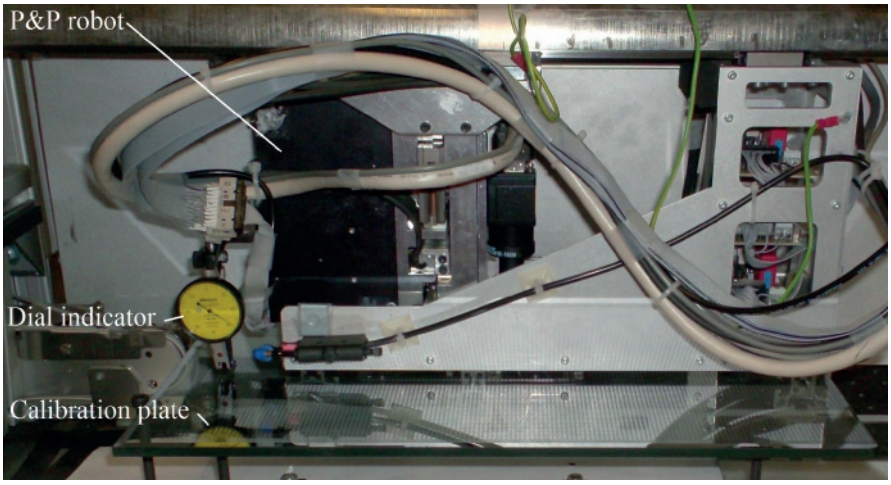

Figure 7.2: *A dial indicator is attached to the P&P robot to measure the height of the calibration plate. After adjusting the plate a height difference less than 100 μm over the working area is realised. The calibration plate contains multiple squares as presented in Fig. 2.11*

In the second graph the bearing's interferometer position is used as the reference for the encoder position and the zϕ-module position.

The third graph shows the residue after calibration using a linear fit of the position encoder and the zϕ-module interferometer with the bearing interferometer as reference. The calibration residue is not yet within specifications.

The fourth graph shows the calibration residue after applying a ninth order calibration polynomial of the encoder position and zϕ-module position with respect to the reference interferometer. It can be seen that the residue of the interferometer with the mirror on the zϕ-module after calibration is within ± 2 μm. The residue after calibration of the encoder will be within ± 1.8 μm. This value will be used for the accuracy of the position measurement in table 7.1.

7.1.2 Pick-and-place robot and mirror-box calibration using a calibration plate

To determine the calibration feasibility of the alignment system, a calibration plate is added to the demonstrator. The vision system attached to the P&P robot acquires via the mirrors images of the calibration plate's squares. These images are processed and this data is used for calibration.

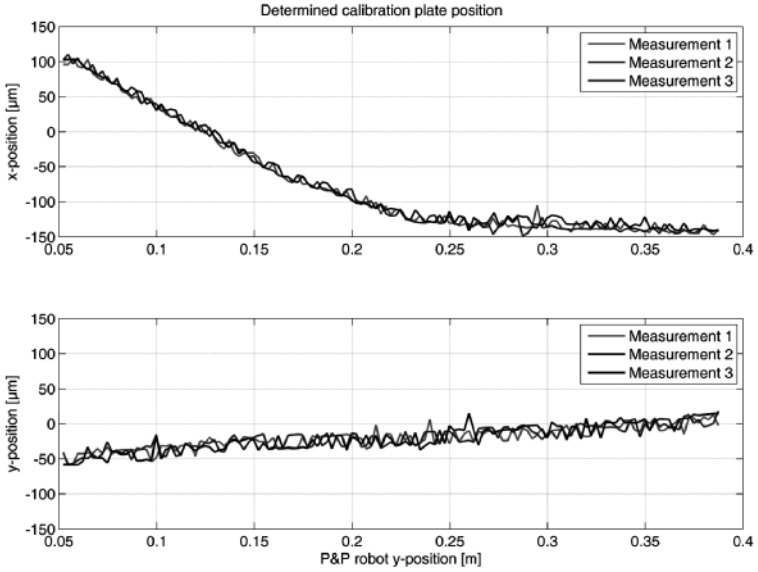

Figure 7.3: *Determined x- and y-positions of the "calibration plate squares" with respect to the y-position of the P&P robot. The top graph shows the determined x-position. This line shows a deviation with respect to a straight line due to the mechanical design poor straightness of the frame. The bottom graph shows the determined y-position and is a straight line*

Calibration plate height adjustment

The validation of the lens has shown that the lens' magnification is not constant when de distance from object to lens changes (Section 5.3.2). This effect has to be minimised during the tests performed for calibration. Therefore the height of the calibration plate is mechanically adjusted with respect to the P&P robot.

Figure 7.2 shows a picture of the P&P robot with a dial indicator attached to it that measures the calibration plate's height. To ensure a constant distance between the object (calibration plate) and the camera the calibration plate's height is mechanically adjusted using the dial indicator. This adjustment results in a height deviation between the P&P robot and the calibration plate within $\pm$ 50 μm. The height deviation will result in a x- and y-direction deviation of $\pm$ 0.75 μm max. This is larger then the specification but taking into account that the height deviation will change linear, this will contribute to the measurements as a linear changing offset. It is possible, if required to compensate for this.

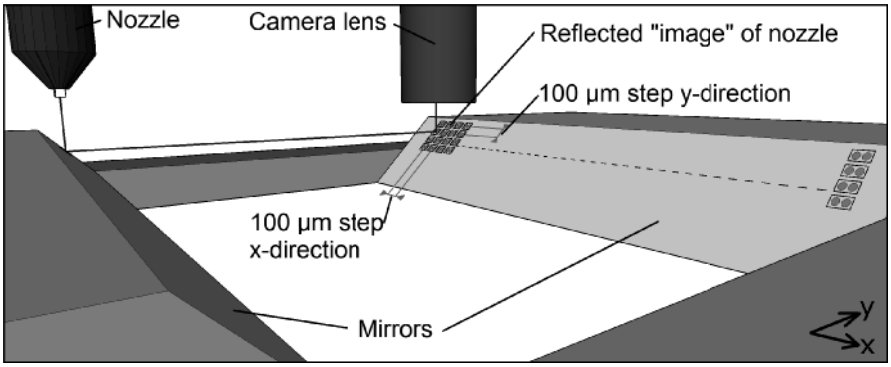

Figure 7.4: *Detail drawing of mirror rack inside the mirror-box, nozzle and lens. The "combined" mirror flatness is determined by acquiring images of the nozzle via the mirrors. After each acquisition, the nozzle and camera (attached to the P&P robot) are moved 100 µm in y-direction. When the nozzle is not present in the image, a movement in the x-direction is performed and the measurements start in the y-direction again. Finally, this results in a grid of the determined nozzle position in the x- and y-direction showing the flatness of the mirror. This data is used for calibration*

Measurements using calibration plate

Three tests have been performed where the P&P robot and mirror-box move in the y-direction acquiring an image of a square etched on the calibration plate. After acquiring the images, the images are processed and the x- and the y-position of the squares is presented as a measurement.

Figure 7.3 shows the determined positions in the x- and the y-position of calibration plate squares with respect to the P&P robot y-position. Expected is a straight line, but in the x-direction a bend in the line is visible. This bend is caused by poor straightness of the frame holding the linear guides. This influences the position of the P&P robot and results in a rotation around the y-axis, resulting in a deviation in the x-direction. Improvement of the frame or calibration will solve this.

7.1.3 Mirror flatness calibration

In the previous subsections two calibration tests have been performed, while using the total stroke in the y-direction. The mirror flatness calibration test is focussing on the calibration feasibility of the mirrors. The size of the mirrors determines the area in x- and y-direction of the mirror flatness test.

Figure 7.4 shows a drawing of the test setup and sequence performed to determine the feasibility of mirror flatness calibration. In this test, the vision system attached to the P&P robot is moved by the P&P robot in the x- and the y-direction over the mirrors while the mirror-box stands still.

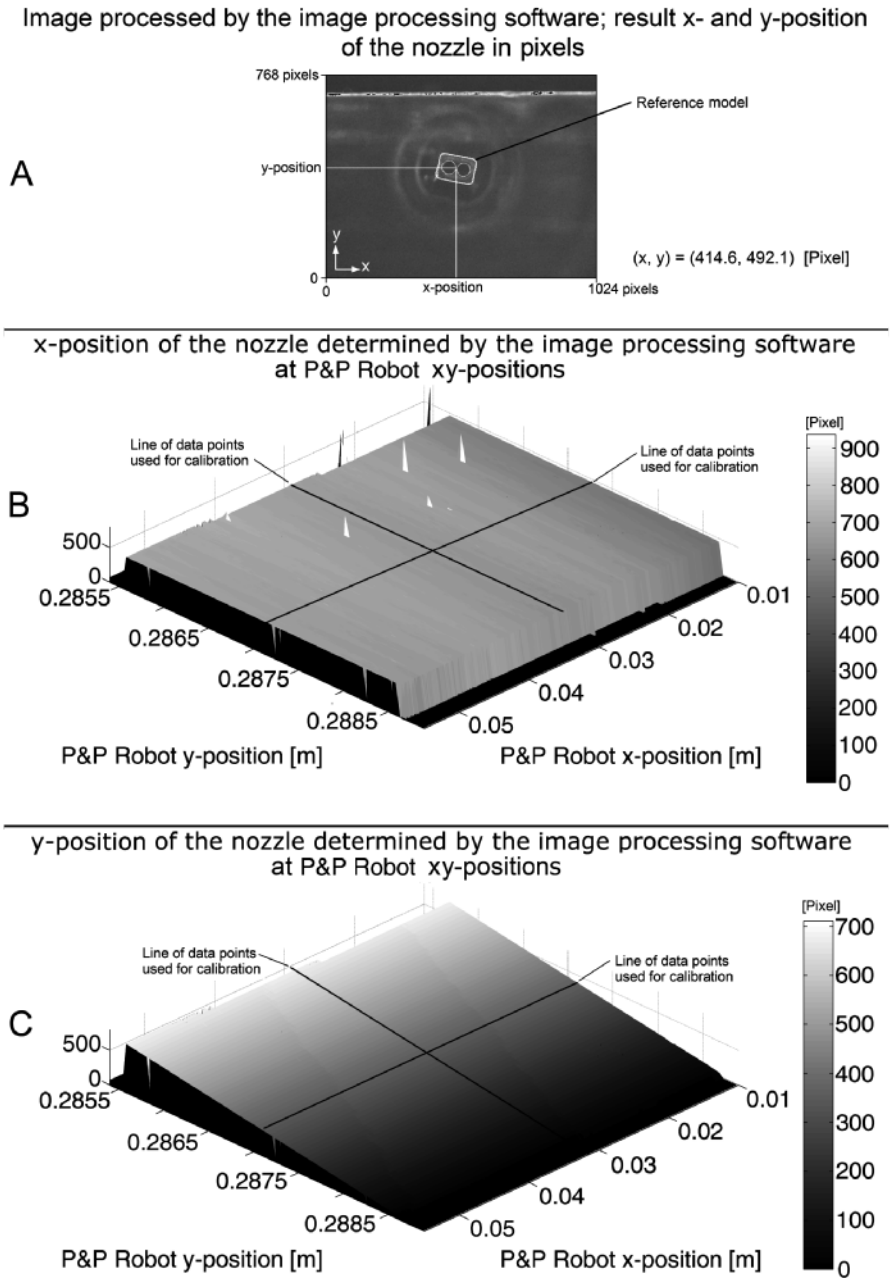

Figure 7.5: *Row A: An image as acquired by the camera and afterwards processed by the image processing software; as result the image processing draws the reference model in the image and determines the position of the nozzle in x- and y-direction. Row B: the determined nozzle x-positions at various P&P robot positions. Row C: the determined nozzle y-positions at various P&P robot positions*

The P&P robot moves in steps over the mirrors. The step size is 100 μm in the x- and y-direction. At each position an image of the nozzle is acquired. After the completion of this test, the P&P robot and the mirror-box are moved 100 mm in the y-direction and the test is repeated to determine the dependency of y-position on the results. Therefore is this calibration test repeated around four different y-positions being: 0.087, 0.187, 0.287 and 0.387 m with respect to the P&P robot home position. The images acquired are processed by the image processing software to determine the nozzle's x- and y-position. The result of this test is a matrix of x- and y-positions of the nozzle determined by the image processing software.

Figure 7.5 shows in row A an image acquired during the test. In white the image processing software has drawn the reference model (See also Fig. 5.15). The x- and y-position of the reference model within the image is the result of the image processing software. The graphs show the x- and y-positions as a result of the test around an y-position of 0.287 m.

In row B of Fig. 7.5 the determined x-position of the nozzle is shown. In x-direction the P&P robot moves 45 mm, from 0.010 m to 0.055 m. In y-direction the P&P robot moves 4 mm, from 0.2850 m to 0.2890 m what covers the mirror in y-direction as explained in Fig. 4.10 (component alignment).

The stroke in y-direction is larger than the size of the mirror. The nozzle is only reflected in the mirror when the P&P robot's y-position is in between the 0.2855 m and 0.2887 m. When the nozzle is not visible the image processing software gives for the x- and y-position (0,0). Therefore, a steep edge is visible at the y-positions 0.2855 and 0.2887. The spikes shown are measurement errors. The images were afterwards checked and it was shown that the image processing software found the reference model on the wrong position. The edges of the mirrors caused this problem and for future use the mirrors must be improved to overcome this problem.

In row C of Fig. 7.5 the determined y-position of the nozzle is shown. The determined y-position of the nozzle depends on the y-position of the P&P robot. As expected the nozzle moves from one side of the image (pixel 0) to the other side of the image (pixel 700). This results in the slope. Also for the y-direction a steep edge is visible at 0.2855 m.

To reduce the amount of data for the mirror flatness calibration, for each P&P robot movement direction a line of data points is selected containing the determined nozzle position. Four lines of data points are selected. These are drawn in rows B and C of Fig. 7.5. These data points are used for the mirror flatness calibration.

X-direction mirror calibration

In Row A of Fig.7.6 the determined nozzle's x-position and nozzle's y-position at a P&P robot x-position are shown. Each line represents the

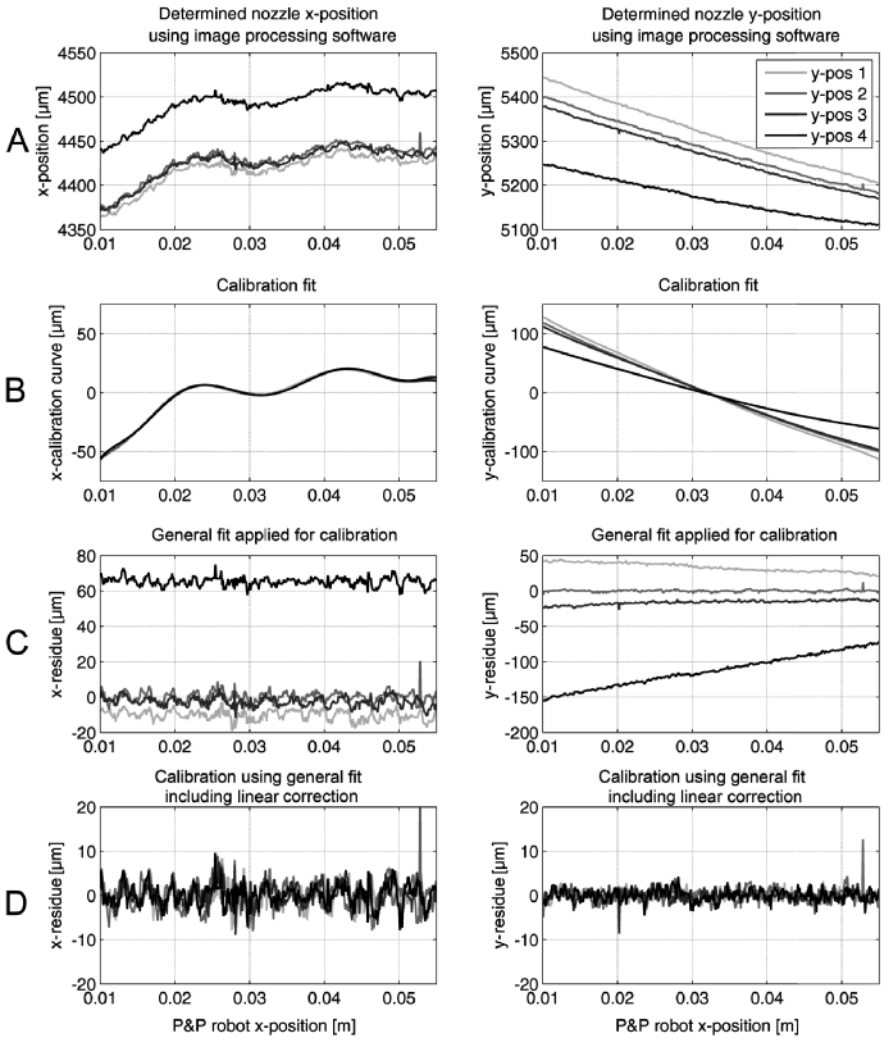

Figure 7.6: *The determined nozzle x- and y-positions on four y-positions. The P&P robot moves in the x-direction. Images are acquired and processed. The graphs in row A show the nozzle x- and y-position determined by the image processing software. Row B shows the calibration curves calculated using a polynomial fit. Row C shows the measurements after applying a general fit, calculated by taking the mean of the four determined calibration curves. The graphs in row D show the measurements calibrated using a general fit and applying a linear fit. The flatness of the mirror in the x-direction shows a residue of* ± 10 *µm*

data at an y-position ("y-pos 1" = 0.087, "y-pos 2" = 0.187, "y-pos 3" = 0.287, "y-pos 4" = 0.387 m).

The left graph of row A shows the determined nozzle's x-position with respect to the x-position of the P&P robot moving from 0.01 m to 0.055 m around the four y-positions. The right graph of row A shows the determined nozzle's y-position with respect to the x-position of the P&P robot around the four y-positions.

In Section 7.1.2 it is mentioned that the P&P robot rotates due to the frame flatness around the y-position ("y-pos 4"). In these measurements this is also visible as an offset in the measurement compared with the other three measurements. This offset is removed from measurement.

A least square fit is used per data line to determine the calibration polynomial. The determined calibration-polynomials are plotted in row B. The y-position calibration curves show for each position another slope.

Using these four calibration-polynomials one general calibration polynomial is calculated. This general curve is applied to the measured data and shown in row C. Applying this general curve does not result in a calibration within the specifications.

The left graph in Row D shows the x-residue after applying the general calibration curve to each data line and a linear correction for the frame's poor straightness. A calibration residue of ± 10 μm in the x-position of will remain, when two measurement faults are ignored.

The right graph in Row D shows the y-residue after applying the general calibration curve and linear correction. A calibration residue of 3.2 $\mu m\,(1\sigma)$ in the x-position will remain.

The maximum of the two residue values is added to table 7.1 for board and component alignment. To improve the ± 10 μm x-residue a more extended calibration can be used. Another option is to improve the mirror quality.

Y-direction mirrors calibration

Figure 7.7 shows the plots when the P&P robot is moving in the y-direction. The y-stroke is 3.5 mm due to the size of the mirrors in the y-direction. In the upper row the two graphs show the determined nozzle's x- and y-position. Shown in row B, the calibration curves calculated using a linear fit. The universal calibration curve is calculated by taking the mean of these calibration curves. In the row C the calibrated measurements using linear fit calibration curves are shown. In row D the calibrated measurements are shown when the linear fit including offsets are used for calibration. A calibration residue of ± 2 μm will remain, which is five times better than the residue when moving in the x-direction.

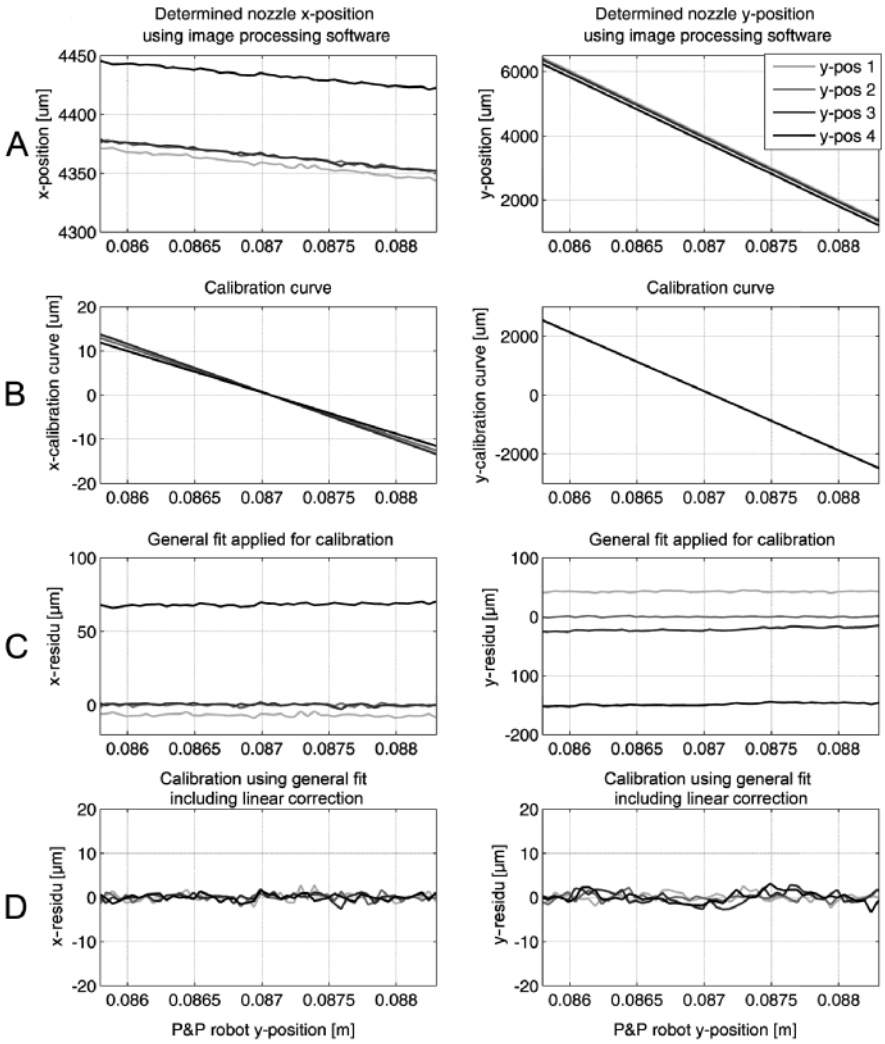

Figure 7.7: *The determined nozzle x- and y-positions within the image when the mirror-box is positioned on four y-positions. The P&P robot moves 3.5 mm in the y-direction around the four positions. Images are acquired and processed. The graphs in row A show the nozzle x- and y-position by the image processing software determined. Row B shows the calibration curves calculated using a linear fit. Row C shows the measurements after applying a general fit, calculated by taking the mean of the four determined calibration curves. The graphs in row D show the measurements applying a full calibration*

7.1.4 Conclusion

The calibration tests performed have shown that the system is not within specification without calibration. Therefore the feasibility of calibration of the systems is validated. The measurement data is used to determine the required compensations. Using compensation the systematic errors are reduced.

In Section 7.1.1 the encoder calibration with the interferometers has shown that a polynomial can be used to decrease the systematic position error of the P&P robot. The data from the second interferometer shows that the P&P robot does not rotate around the x-axis when moving slowly.

In Section 7.1.2 a calibration plate is added to the demonstrator and has shown that the P&P robot rotates around the y-axis when moving in the y-direction. This results in a deviation in the x-direction. Correction for this deviation is required or the frame straightness should be improved.

In Section 7.1.3 images are acquired of the nozzle via the mirror surface to determine the mirror flatness. This test is repeated around four different mirror-box and P&P robot y-positions. These tests have shown that it is required to calibrate the mirrors. Applying the determined general fit does not reduce the systematic errors within design specifications. To reduce the offsets further in the y-direction, a position dependant offset correction is required. To reduce the offsets in the x-direction, more extended calibration or improving the mirror's quality is required.

7.2 Repeatability

In this section the feasibility of the repeatability is validated. During the alignment system design the choice has been made to use an alignment trigger that depends on the P&P robot and mirror-box position measurement systems to trigger the vision system to acquire images while moving. The influence of this system design choice on repeatability is determined.

First the influence of the timing of the alignment trigger on the repeatability is determined. The motion controller calculates the alignment trigger moment using the trajectory parameters, acceleration and velocity. The alignment trigger is used to trigger the vision and illumination system and to trigger a system that uses latches to store the actual encoder position of the P&P robot and the actual position of the mirror-box. This section starts with the determination of the influence on the repeatability of the timing of the motion controller generating the alignment trigger.

The second test is performed to determine the influence of the position measurement systems on the repeatability.

The third test is to determine the influence of acceleration of the P&P robot on the repeatability. Forces are applied to accelerate the P&P robot.

Repeatability in y-direction [μm (1σ)]		
Description	**"design"**	**"demonstrator"**
*Board handling**	*4.0*	*4.0*
Board alignment process		
Vision System (FOV 7 $mm \times 7$ mm)	1.6	0.6
Motion blur/Movements	4.6	to be determined
Mirror flatness (Calibration residue)	-	3.4
Position measurement (Calibration residue)	1.1	1.8
Alignment trigger (Latch used)	1.3	to be determined
*Nozzle exchange**	*0*	*0*
*Component pick process**	*0*	*0*
*Component move process**	*0*	*0*
Component alignment process		
Vision System (FOV 7 $mm \times 7$ mm)	4.6	0.7
Motion blur/Movements	4.6	to be determined
Mirror flatness (Calibration residue)	-	3.4
Position measurement (Calibration residue)	1.7	1.8
Alignment trigger (Latch used)	1.3	to be determined
*Component place process**	*10.0*	*10.0*
Total estimated repeatability	13.8	12.1

Table 7.1: *Repeatability requirement values "design" (adapted from table 5.4) and the achieved values during the calibration feasibility study of the "demonstrator"; *these values will not be determined in this research*

The P&P robot will also deform due to these forces. This deformation results in a rotary displacement around the x-axis of the lower part of the P&P robot that holds the nozzle and the alignment camera. Two interferometers are used to measure the deformation of the P&P robot displacement and rotation around the x-axis.

The results from the previous tests are combined to improve the calibration and to determine the feasibility for repeatability of the alignment system design. Finally this section ends with a conclusion.

7.2.1 Alignment trigger jitter

In Section 6.1.4 it is explained that the alignment trigger moment is calculated by the motion controller. The fact that the alignment trigger moment is calculated and not realtime determined from the encoder values of the P&P robot and mirror-box can introduce time jitter. Meanwhile the

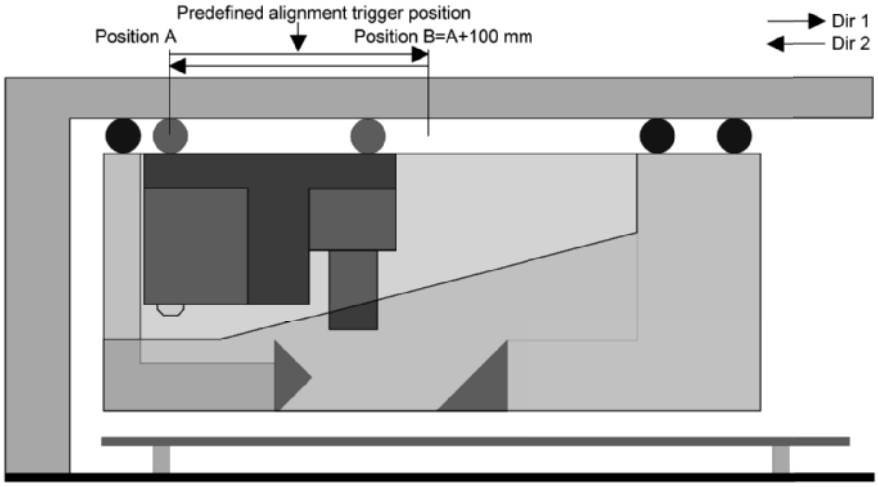

Figure 7.8: *The P&P robot moves from position A to position B and visa versa. The mirror-box is kept on a steady position. The alignment trigger is generated at the moment that the P&P robot moves over the predefined alignment trigger position*

position of the P&P robot and mirror-box are stored (latched) simultaneously with the acquisition of the image. This test is used to investigate the performance of the alignment trigger generation and the use of latches to determine the influence on the repeatability.

To test the alignment trigger and the latches, the mirror-box is positioned on a fixed y-position. The P&P robot moves from position A to position B, realising an y-stroke of 100 mm and back from position B to position A as shown in Fig.7.8. In Fig.7.9 the created third order trajectory setpoint is shown. The maximum setpoint velocities used are 0.25, 0.5, 0.75 and 1 m/s, although a velocity of 1 m/s will never occur because of the combination of the maximum acceleration and the distance. Other parameters, such as position and acceleration, are kept at the same values.

During this test the motion controller generates an alignment trigger when the P&P robot passes over a predefined position. This predefined position is equal for both directions. When the alignment trigger is generated, the positions of the P&P robot and the mirror-box will be stored. Due to the fact that the trigger position is equal for both directions, the latched encoder position should be constant.

With help of the latched positions, the predefined alignment position and the velocity setpoint of the P&P robot, the time jitter and delay of the alignment trigger for four different velocities can be determined. Figure 7.10 shows the determined alignment trigger moment. If there would be no delays or jitter, all alignment triggers would occur at time is zero.

The first two graphs of Fig. 7.10 show the measurements with a veloc-

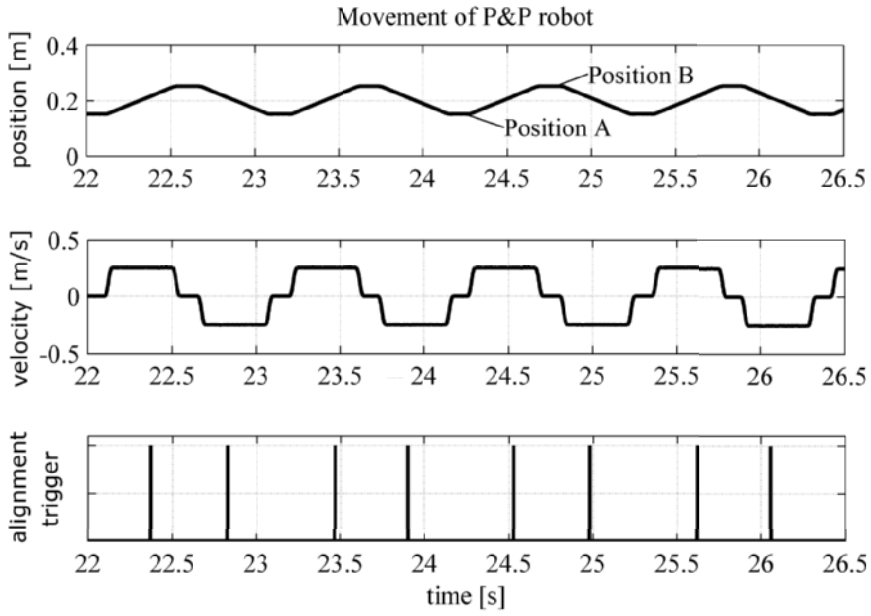

Figure 7.9: *The movement of the P&P robot. The first plot shows the displacement of the P&P robot. The second plot shows the velocity of the P&P robot. The third plot shows the alignment trigger. When the P&P robot passes a predefined y-position an alignment trigger is generated. This position is equal for both directions*

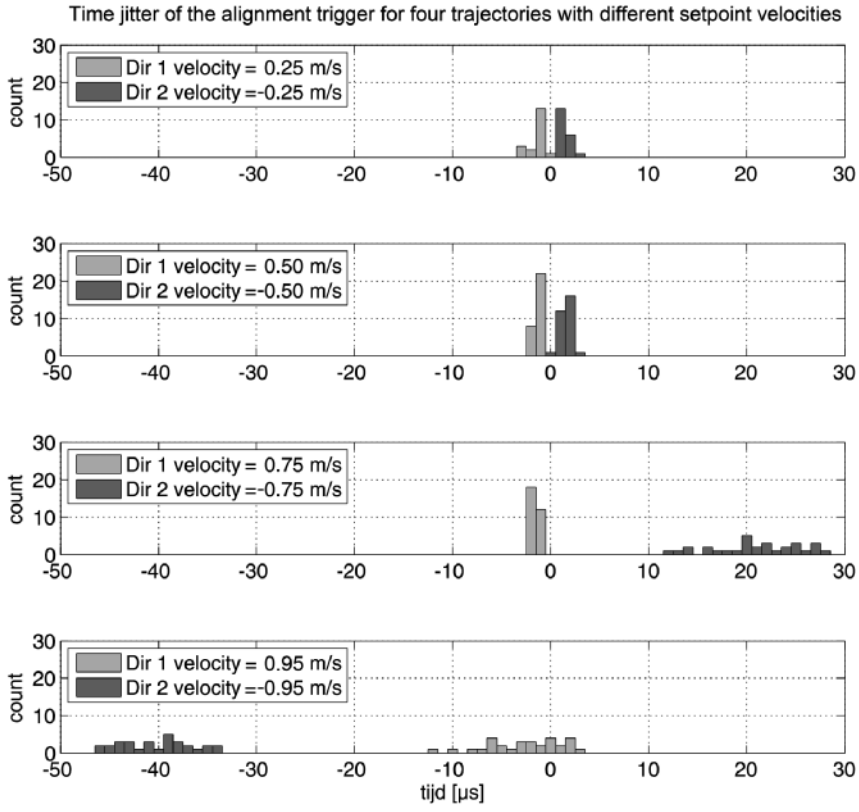

Figure 7.10: *The determined time jitter and delay of the alignment trigger for four velocities in two directions where Dir 1 are movements in the positive y-direction and Dir 2 are movements in the negative y-direction. The time jitter increases for three trajectories: Dir 2 velocity =-0.75 m/s, Dir 1 velocity = 0.95 m/s, Dir 2 velocity =-0.95 m/s. This jitter increases because the alignment trigger is generated when the velocity is not constant*

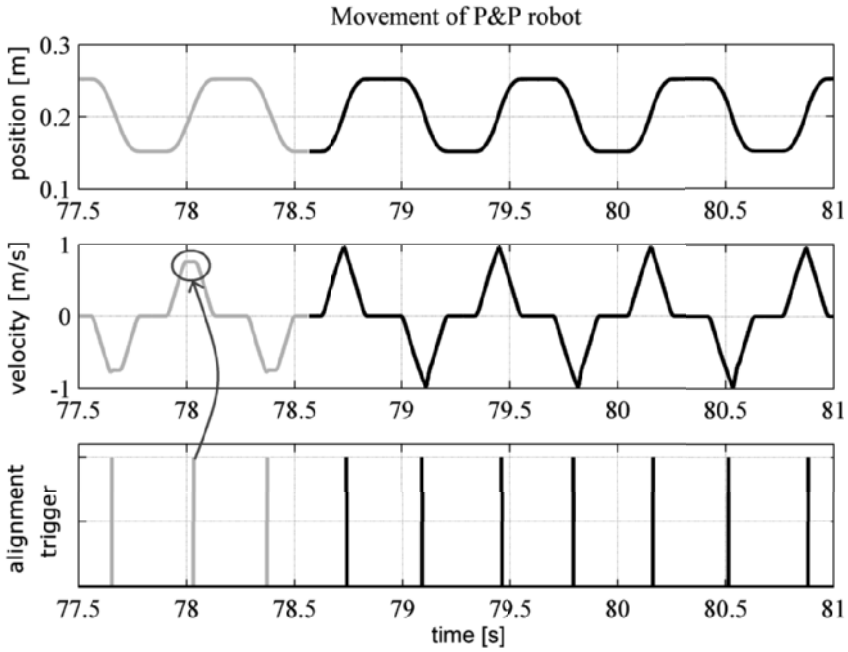

Figure 7.11: *P&P robot moves with maximum absolute velocity of 0.75 m/s or maximum absolute velocity of 0.95 m/s. The first graph shows the displacement of the P&P robot. The second graph shows the velocity of the P&P robot. The third graph shows the moment the alignment trigger is generated. Only the alignment trigger at 78.05 s is generated when the velocity is constant. Note that the predefined alignment trigger position is the same for both directions*

ity of 0.25 m/s and 0.5 m/s. These graphs show an offset depending on the direction combined with a distribution around the offset. The offset is caused by a delay where the distribution around this offset is introduced by jitter.

The delay seems equal for both directions. In the manual of the motion controller it can be found that the high speed output, which is used for the alignment trigger, has an maximum switch time of 2 μs[21]. Measured is a switch time of 3 μs. Figure 5.16 showed that the time to switch the alignment trigger output is about 1 μs. In combination with the switch time of the motion controller high speed output, a delay of 3 μs can be expected.

The alignment trigger timing distribution for multiple measurements show a distribution of 1 μs. It can be concluded that the alignment trigger has little time jitter being smaller than 1 μs.

The third and fourth graphs in Fig. 7.10 show the time jitter at velocities of 0.75 m/s and 0.95 m/s. The time jitter increases significant at these velocities. To understand this increase of time jitter a better look must be

taken at the moment the alignment trigger is generated. Figure 7.11 shows a part of the trajectory of the P&P robot where the velocity is 0.75 m/s or 0.95 m/s. In the top graph of Figure 7.11 the position of the P&P robot is shown, in the middle graph the velocity of the P&P robot is shown. In the lower graph the moment when the alignment trigger is generated is shown. In these graphs the grey part are the movements where the P&P robot reaches a maximum velocity of 0.75 m/s and in black the movements where the P&P robot reaches a maximum velocity of 0.95 m/s. In the gray part of the movement only the second alignment trigger (at 78.05 s) is generated when the P&P robot is moving with a constant velocity of 0.75 m/s.

All other alignment triggers are generated during a non-constant velocity period. During the non-constant velocity period, the actual velocity differs from the setpoint velocity. Meanwhile the alignment trigger is generated using the setpoint velocity.

Taking a closer look at the moment that the alignment trigger is generated it can be seen that the first trigger (at time stamp: ≈ 77.65 s) is generated when the P&P robot just reaches 0.75 m/s. The second trigger is generated when the P&P robot is moving at a constant speed. The third trigger is similar to the first trigger. This explains why the time jitter at a velocity of 0.75 in the positive y-direction (Dir 1) is smaller than the time jitter when the P&P robot is moving in the negative y-direction (Dir 2).

This test proves that the implemented calculated alignment trigger can not be used without the use of latches because the time jitter is to high.

7.2.2 Position measurement delay

The P&P robot with vision system and the mirror-box with the mirrors must be aligned when the image is acquired. Therefore the measured position will influence the repeatability.

To determine the influence of the encoder system on the repeatability the encoder values are latched at the moment an image of the calibration plate is acquired. This image is processed and the y-position of the calibration plate's square is determined. Afterwards the determined image position is corrected for the delay and jitter found in the previous test. After correction it is to be expected that y-position determined by the image processing software is constant and not depending on the direction or the velocity of the P&P robot. If these positions are not equal a delay or jitter must be present in the position measurement system.

The top left graph of fig. 7.12 shows the determined y-position when the P&P robot moves with a velocity of 0.25 m/s. The bottom left graph shows the determined y-position when a velocity of 0.5 m/s is used. As can be seen the determined y-position depends on the direction and the velocity of the P&P robot. The presence of an offset in both directions with respect position 0 (the position where the P&P robot passes over the predefined

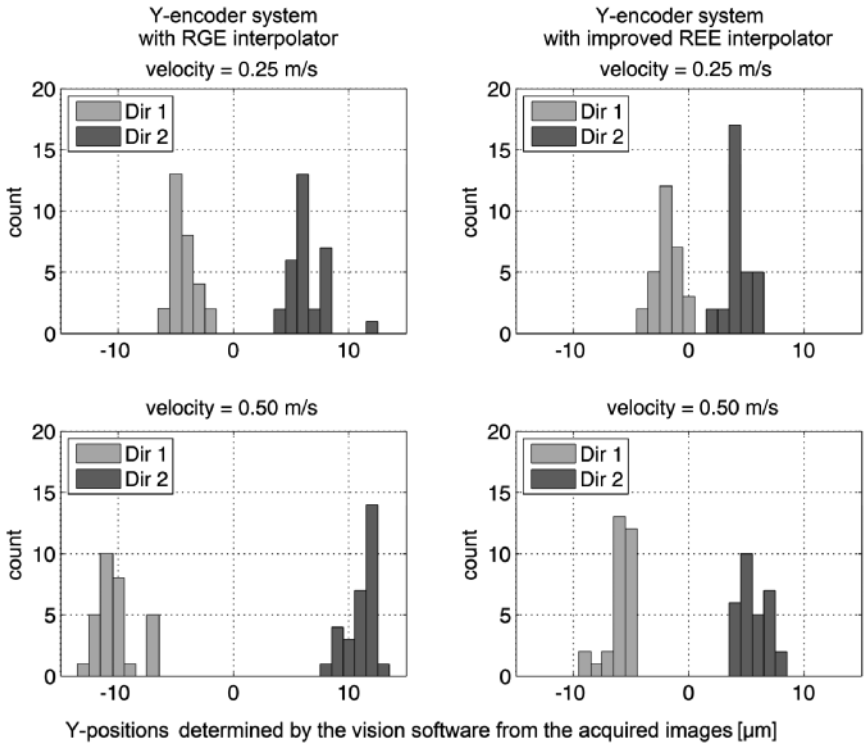

Figure 7.12: *Influence of the encoder system's delay on the alignment system. The image processing software determines the y-position of a calibration plate square. This position depends on the velocity and direction of the P&P robot. The two left plots are determined using a RGE Interpolator. The two right plots are determined using an improved REE interpolator. The position changes when the interpolator is changed, which proves that the encoder system has a delay*

alignment trigger position) indicates the presence of a delay in the encoder system. To validate that the delay is created by the encoder system the encoder system is adapted.

The encoder system exists of an encoder readhead and a separate interpolator. There are two types of interpolators that can be used with the encoder: type 1: RGE [86] and type 2: REE [89]. The REE-interpolator's maximum analog input frequency and minimum counter clock frequency are improved with respect to the RGE-interpolator. When the delay is depending on these parameters, the delay will depend on the interpolator type used.

The left graphs in Fig. 7.12 are measured using the RGE interpolator. The right graphs are measured using the improved REE interpolator. It can be seen that the determined y-position changes when the interpolator

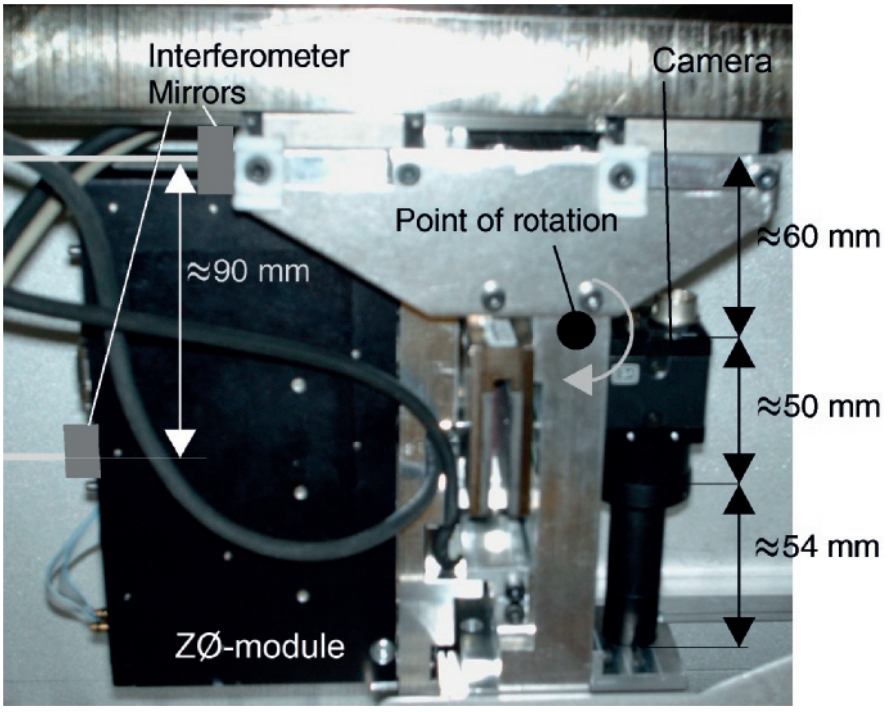

Figure 7.13: *The P&P robot's mechanical design has a limited stiffness at the point of rotation. The result is that the lower part of the P&P robot holding the zϕ-module and P&P robot rotates with respect to the point of rotation introducing a deviation in the y-direction. The dimensions of the P&P robot are shown. With help of these dimensions the influence of the rotation of the P&P robot on the alignment images can be estimated)*

is changed.

This test shows that the encoder system has a delay influencing the repeatability. Taking into account that the delay has a constant offset, it is possible to correct for this delay.

7.2.3 Pick-and-place robot dynamics

The P&P robot is accelerating, moving and decelerating from pick to place position. The forces required for acceleration and deceleration will introduce vibration and rotation of the P&P robot. This vibration and rotation of the P&P robot is present in the image acquired when the P&P robot moves over the mirrors and can effect directly the component and board alignment repeatability.

As showed in Section 6.2, the first mode of the demonstrator rotates around the x-axis what results in the camera rotating around the x-axis. Consequently, this will influence the repeatability. To measure the rota-

tion of the P&P robot, the two interferometers are used. In figure 7.13 the position of the two mirrors of the interferometer are shown. The top interferometer mirror is used to measure the position of the roller bearing cage. The lower interferometer mirror measures the position of the zϕ-module.

In Fig. 7.13 the mechanical layout of the P&P robot is shown. From the determined mode it is known that the P&P robot will rotate around a position depicted in the figure with "Point of rotation". Because the two interferometers are used to measure the rotation of the P&P robot, the position of the mirrors of the interferometers with respect to the "Point of rotation" will determine the sensitivity of measurement system. Another dimension that has to be taken into account is the working distance of the lens (107 mm).

The rotation of the P&P robot around the "Point of rotation" will influence the y-position determined after image processing. With help of the mechanical layout and working distance of the lens the y-position deviation after image processing can be determined. The total distance from rotating point to object is 107+54+50 = 211 mm. The rotating point is half way the interferometer distances. The gain will then be about $\frac{211\ mm}{45\ mm} \approx 4.7\times$ meaning that a deviation of the P&P robot measured with the interferometers will be magnified 4.7 times. With help of this gain the image y-position deviation, as a result of the rotation of the P&P robot, can be calculated.

With help of the same test sequence as before, the influence of the dynamics of the P&P robot on the repeatability is determined. The motion controller used to record the position data of the interferometers is also equipped with latches. These latches latch the y-position of the interferometers and will be controlled by the alignment trigger. Hereby, the y-position of the P&P robot measured with the encoder and the two interferometers are saved at the time the image is acquired.

With help of the latched interferometer y-positions it is possible to calculate the rotation of the P&P robot. Using the calculated rotation combined with the determined gain it is possible to calculate the deviation of the y-position of the calibration plate square in the images. In Fig. 7.14 the y-position deviation is shown at four velocities. These y-position deviations are determined using the measured rotation of the P&P robot. This figure shows that a rotation of the P&P robot results in a deviation in the y-direction up to 50 μm.

7.2.4 Extended calibration for improved repeatability

In this section the repeatability feasibility of the alignment system is determined. This repeatability is effected by the jitter of the alignment trigger, the delay of the position measurement system and the P&P robot dynamics. The repeatability measurements performed show not only random errors but also systematic errors appearing as offsets with respect to zero. These

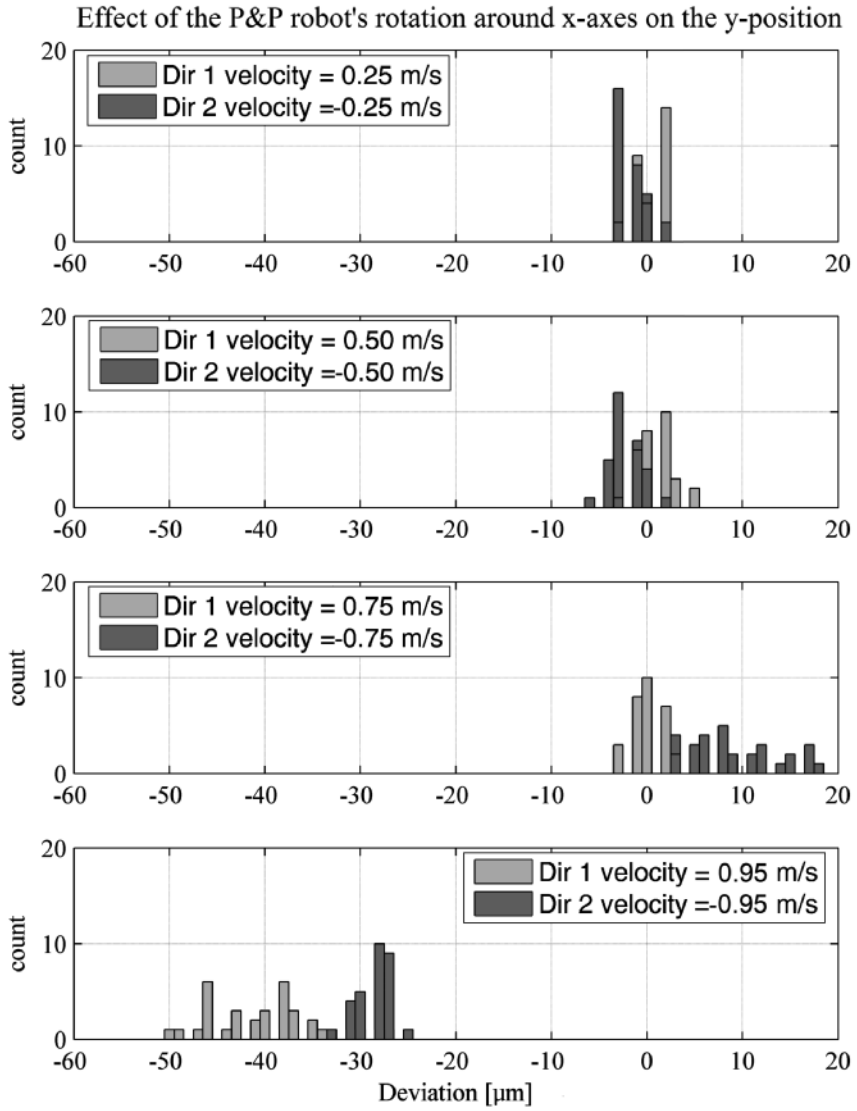

Figure 7.14: *Calculated deviation of the y-position of a calibration plate square due to the rotation of the P&P robot*

systematic errors are correlated to effects as the accelerations, velocities, delays and the mechanical rotations of the P&P robot. In this subsection the repeatability is determined when compensating for these systematic errors.

To determine the improved repeatability after correction for systematic errors a test is performed where the P&P robot moves multiple times from point A to B and visa versa with a predefined acceleration and maximum velocity. After several movements the maximum velocity is increased and the tests are repeated. In total four different maximum velocities are used. Figure 7.15 shows the measured data where the left graphs are determined when the P&P robot is moving in direction 1, and the right columns shows the data when the P&P robot is moving back (direction 2). In row A left graph each point represent the setpoint velocity of a complete movement from position A to B. It can be seen that the P&P robot moved 20 times in direction 1 with a setpoint velocity of 0,25 m/s, followed by 30 movements with a setpoint velocity of 0,5 m/s. Then 30 at 0.75 m/s and finally 30 movements with 0.95 m/s. In row A right graph the opposite direction is showed.

Figure 7.15 shows five rows of graphs, which are discussed in the following list:

Graphs in row A show the maximum velocity achieved by the P&P robot. Each point is the setpoint velocity for one movement from position A to B (left graph) and vice versa (right graph)

Graphs in row B show the latched encoder position when the alignment trigger is generated with respect to the predefined alignment trigger position. When the trigger position is equal to the predefined position, the difference is zero. As shown before, when the velocity is above 0.5 m/s, the jitter on the alignment trigger timing can increase causing an deviation with the predefined alignment trigger position. This is because the velocity is not constant at the alignment trigger time. In the left graph the deviation starts at sample 51. In the right graph it starts at sample 81.

Graphs in row C show the calculated rotation of the lower part of the P&P robot using the latched P&P robot y-positions measured with the two interferometers; these graphs show that the P&P robot rotates more during acceleration than during constant velocity

Graphs in row D show the determined position of the nozzle in the image determined by the image processing software

Graphs in row E show the repeatability if the data from graph D: the determined position of the nozzle corrected by the data from graph A, B and C.

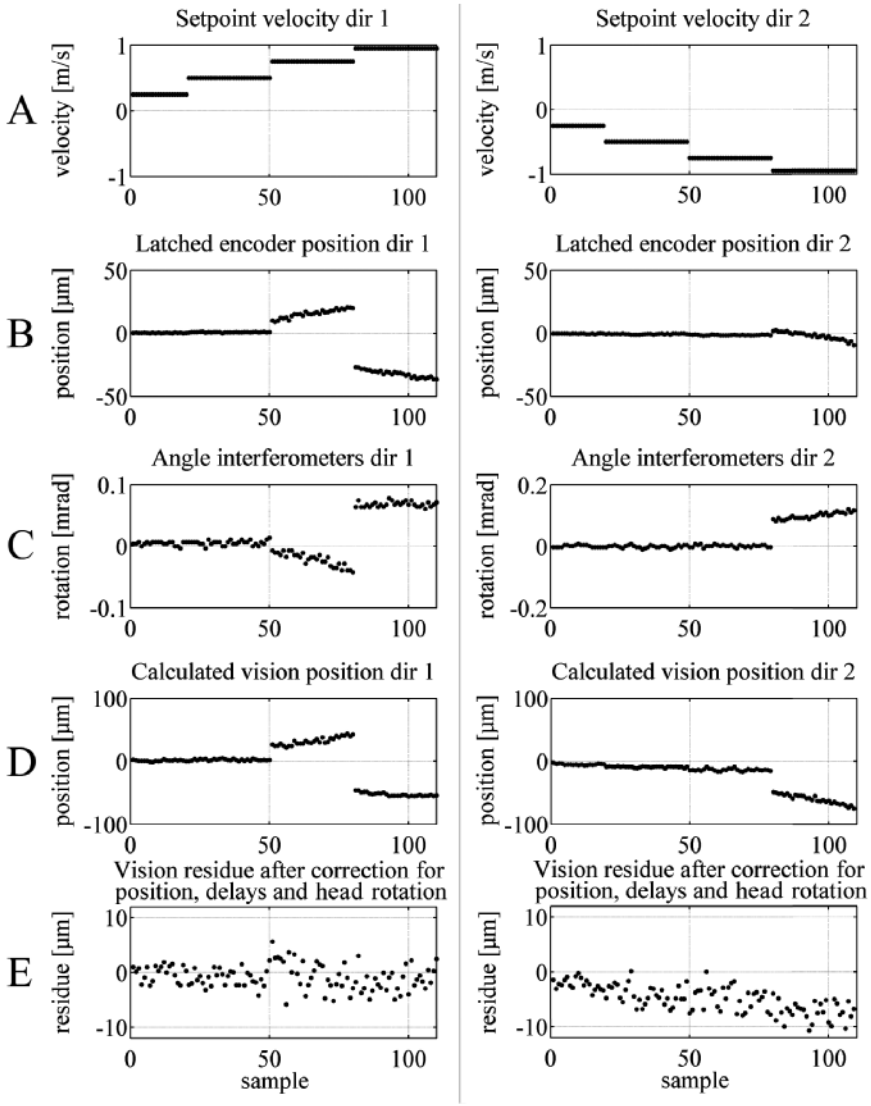

Figure 7.15: *110 samples of 110 P&P-Movements. The left column shows the measured data while the P&P robot is moving in direction 1, the right column shows the measured data while the P&P robot is moving back (direction 2). Row A: the graphs show the maximum velocity of the P&P robot. Row B: difference between the predefined alignment trigger position and the real alignment trigger position. The graphs show the latched encoder positions of the P&P robot. Row C: the graphs show the rotation calculated from the latched interferometer positions. Row D: the graphs show the calculated y-position from the images by the image processing software. Row E: the graphs show the residue when the calculated vision position is corrected with the measured trigger position, delays and head rotation*

To determine the repeatability after applying the corrections, the measurements shown in row E are grouped per velocity and plotted in histograms. These histograms are shown in Figure 7.16. Each histogram shows the deviation of the position after correction, depending on velocity and direction.

Correction for alignment trigger

During the tests a latch is used to sample the encoder position at the time the alignment trigger is generated. These latches can be used in a P&P machine and the required data for correction is available at the moment the y-position is determined. If this technique will be used it is required to sample also the position of the mirror-box.

On the other hand, another implementation of the alignment trigger in hardware can also be used to decrease the jitter. In this case it is required that the position of the P&P robot is determined with respect to the mirror-box because the alignment trigger must depend on positions of the mirror-box and the P&P robot. In this case a high speed position comparator must be realised.

Correction for encoder delay

If delays are constant, correction is possible. A delay in a moving system results in a position deviation depending on the velocity. In the test sequence of the demonstrator, at higher velocities (0.75 m/s and higher) the image is acquired while the P&P robot is accelerating meaning that the velocity is not constant. It is advisable to realise also latches for the actual velocity. With the actual velocity it is possible to compensate for delays. The selected motion controller can not latch the velocity. The actual velocity can continuously be sampled and this data can be used for correction.

Correction for rotations of the pick-and-place robot

The mechanical deformation of the P&P robot has a large influence on the repeatability. The rotation of P&P robot holding the camera influences the position repeatability. The conclusion is that the vibrations and rotation of this P&P robot will influence the repeatability in such a way that the repeatability specifications will not be met. In the demonstrator interferometers were added to investigate the movements and rotation of the P&P robot. The rotation of the P&P robot can not be measured or calculated from the encoder data and the interferometers will not be available in a P&P machine. Adding extraadditional sensors or redesign of the P&P robot is required to correct for the rotations of the P&P robot.

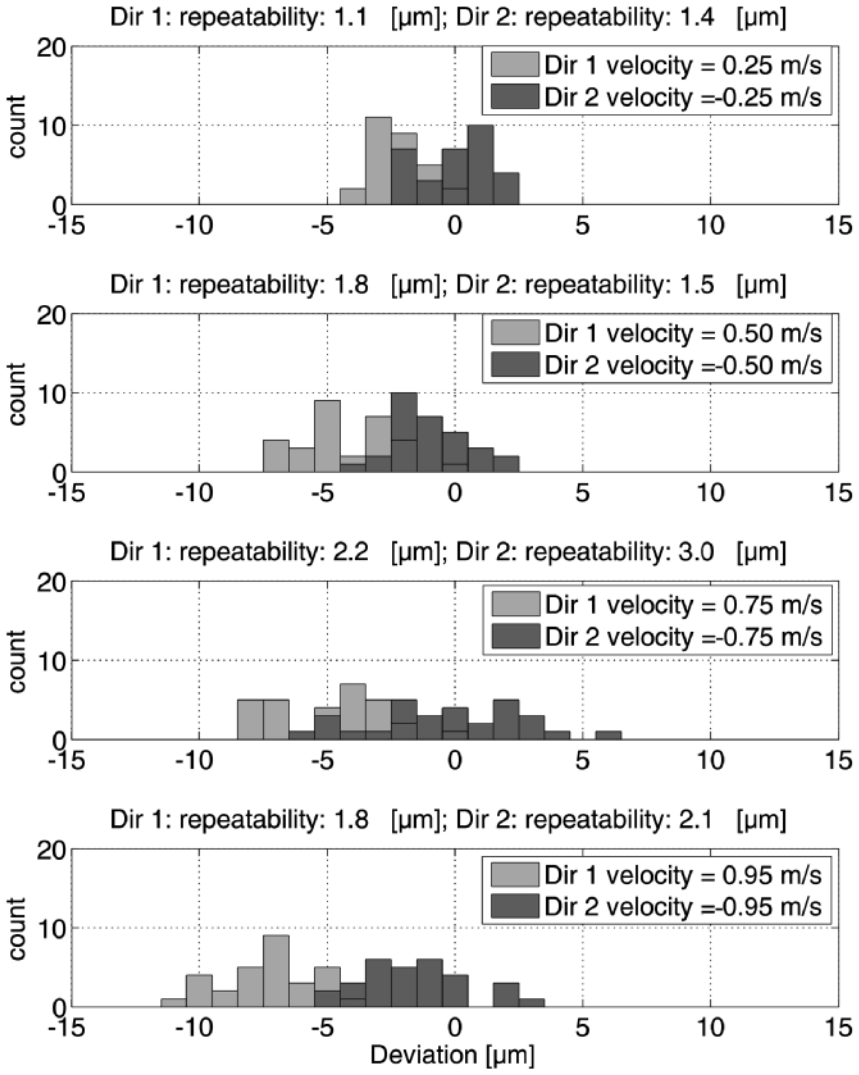

Figure 7.16: *The repeatability of the alignment system when corrected for trigger jitter, delays and the dynamics of the P&P robot. The histograms are calculated for four velocities and two directions with a final repeatability of 3 µm (1σ)*

Repeatability in y-direction [μm (1σ)]		
Description	**"design"**	**"demonstrator"**
*Board handling**	*4.0*	*4.0*
Board alignment process		
Vision System (FOV 7 mm×7 mm)	1.6	0.6
Motion blur/Movements	4.6	3.0
Mirrors flatness (Calibration residue)	-	3.4
Position measurement (Calibration residue)	1.1	1.8
Alignment trigger (Latch used)	1.3	0
*Nozzle exchange**	*0*	*0*
*Component pick process**	*0*	*0*
*Component move process**	*0*	*0*
Component alignment process		
Vision System (FOV 7 mm×7 mm)	4.6	0.7
Motion blur/Movements	4.6	3.0
Mirrors flatness (Calibration residue)	-	3.4
Position measurement (Calibration residue)	1.7	1.8
Alignment trigger (Latch used)	1.3	0
*Component place process**	*10.0*	*10.0*
Total estimated repeatability	13.8 (<15)	12.9

Table 7.2: *Repeatability and calibration residue requirement values "design" (adapted from table 5.4) and the achieved repeatability values during the validation of the "demonstrator"; *values will not be determined in this research*

7.3 Conclusion

In this chapter the accuracy of the integrated alignment system for the shuttle concept P&P machine was analysed. The tests performed have shown that calibration for systematic errors is required. After compensating for systematic errors the accuracy contains random errors and the calibration residue.

In Section 7.1 the compensation for systematic errors with help of calibration polynomials was discussed. The linear y-encoder was calibrated using an interferometer. The P&P robot was moved while measurements were performed using two interferometers and the P&P robot's encoder. These measurements were used to determine the calibration polynomial. The alignment system also uses a moving mirror-box holding the mirrors.

The mirror-box also requires a calibration. A calibration plate was added to the demonstrator. Measurements were performed where the alignment system's camera acquired images of the calibration plate. These measurements were used to determine the calibration polynomial. The flatness of the mirrors in the mirror-box was measured by acquiring images of the nozzle of the P&P robot. These images were processed and the x- and y-position of the nozzle was determined. A polynomial to compensate for systematic errors, which were present in the mirror was determined. Finally the calibration residue was determined. The calibration feasibility measurements show that calibration is possible. The systematic deviations of the encoders and the mirror's mechanical alignment are compensated using low order (<10) polynomial functions. The calibration residue after compensation was added to the repeatability budget.

In Section 7.2 the repeatability feasibility was discussed. The vision-on-the-fly strategy will influence the repeatability. More specifically the repeatability will be influenced by the delays introduced by the position measurement system, the jitter of the alignment trigger and dynamics of the P&P robot. Therefore tests were performed where the alignment system was moved while acquiring images. These measurements were analysed to determine the repeatability of the integrated alignment system. Analysis of the repeatability measurements showed that these measurements contained systematic errors. It was possible to compensate for these systematic errors using latches that saved the actual positions of the shuttle and P&P robot when the image of the component or board was acquired. These images were processed and corrected for delays and jitter. The addition of two interferometers to the demonstrator enabled the possibility to compensate for the rotation of the lower part of the P&P robot. After compensating the systematic errors the repeatability is within the design specifications. Due to the fact that the interferometers will not be present in a P&P machine, it is recommended to adapt mechanical design of the P&P robot to minimise the rotations.

Table 7.2 shows the repeatability after compensation. The column "design" shows the repeatability design values determined in Chapter 4. Column "demonstrator" shows the repeatability values measured in this chapter after applying compensations for systematic errors. For the integrated single camera alignment system a repeatability of 12.9 $\mu m\,(1\sigma)$ was realised.

Chapter 8

Discussion and conclusion

8.1 Discussion

In this thesis the V-model method was used to design an integrated component and board alignment system. The benefit of using this method is that a complex mechatronic system will be divided in smaller subsystems and these subsystems are divided in modules. For these subsystems and modules clear requirements are determined. Additionally, tests are designed to validate these requirements. During integration of the system these validation tests are executed before integrating modules into subsystems and subsystems into the system. In this thesis the subsystems and modules were designed using an iterative design cycle.

A drawback of the V-model method can be the straight-forward design approach. The method assumes that a system can be divided in subsystems and modules and that the requirements for a subsystem or module can be determined and met during the design phases. When a requirement of a module cannot be met a subsystem specification redefinition is required. Hence, a specification change can be required what can result in a redesign to meet the requirements. In case of doubt of the feasibility of a specification it is advised to validate this specification during the V-model's design phase using preliminary tests. In addition the V-model method expects that module tests are performed before the modules are integrated into subsystems, which ensures successful integration.

As an example, in this thesis the lens did not fulfill the module requirements. During the lens module test this problem was addressed and as a result the integration tests were adjusted. Although this adjustment solved the problem for the integration tests, a redesign of the vision module mounted on the P&P robot would be required to meet all the alignment subsystem's requirements. Performing a requirement validation test could have helped to indicate this requirement mismatch before the design of the module was started.

The use of the V-model method requires strict and feasible requirement specifications for systems, subsystems and modules. In this thesis the competitive engineering approach described by Gilb [37, 38] was used. The competitive engineering requirements description advises to use many attributes to specify a requirement. In this thesis two main requirements: repeatability and throughput were specified using nine attributes. These attributes were split into two types: attributes to describe the requirement and attributes to measure the requirement. and to indicate the requirement's feasibility.

The use of the competitive engineering specification method enforced an unambiguous definition for the two requirements throughput and repeatability selected from the IPC-9850 standard [53]. This standard was used to determine the attributes to describe the requirements. To make the requirement's values measurable, the AX-5 was selected as the benchmark P&P machine. The determination of state-of-the-art benchmark values for the attributes helped to define feasible specifications.

8.2 Conclusions

This study addresses the general competing demands of high throughput versus repeatability. In particular the P&P machine under study was designed to realise a maximum cycle time of 225 ms for picking a component and placing it onto the PCB and move back to the pick position. The component placement repeatability was better than 15 μm (1σ).

In this thesis a shuttle concept P&P machine was proposed with a two times higher throughput with respect to ultra high speed P&P machines. The shuttle decreases the distance between the component pick position and the component place position and so the P&P cycle time is reduced by at least a factor of two.

To maintain the placement repeatability two vision based alignment systems using a single camera were added to the P&P machine shuttle concept without compromising the short distances and thereby the P&P cycle time.

A vision alignment concept study has resulted in a proposition where the board and component alignment system were realised using a single camera attached to the P&P robot combined with mirrors attached to the independently moving shuttle. Additionally the required illumination systems were added to the P&P robot and shuttle. The introduction of the shuttle enables this concept vision concept.

To minimise the alignment systems' influence on the P&P cycle time, the alignment images were taken while the P&P robot is moving. Motion blur was kept within the repeatability error budget using flashing LEDs.

The alignment system with independently moving mirrors introduced additional requirements for the machine controller. The machine controller must be able to generate a trigger when the position difference between

the shuttle and P&P robot is within micrometers. This requirement was found to be hard to implement in the machine controller due to the high velocities. In this thesis a concept was proposed where the trigger was inaccurately generated. So, to meet the final repeatability, a correction was required after processing the image of the component or board features. To be able to correct the data from image processing for the inaccurate trigger, the position information of the P&P robot and shuttle was measured and stored at the moment the image was taken. With help of this information and data correction afterwards it was demonstrated that the repeatability of the alignment system was within specification.

Calibration of the mirrors was required to determine the offset. For the component and board alignment mirrors the offset was determined in the two directions on four different positions of the P&P robot and shuttle using a quasi static measurement. During this measurement a 100 μm step size in both directions was used. The mechanical properties of the mirrors were stable, which allowed the use of an universal calibration polynomial to reduce the repeatability error. Applying a calibration for the mechanical characteristics of the moving P&P robot and shuttle resulted in a repeatability error of at most 4 μm. Thus, it was concluded that it seems feasible to meet the repeatability requirements using calibration for the characteristics of the P&P robot and shuttle.

Using an illumination flash time of 4 μs or less to minimise motion blur has consequences for the requirements of the system's vibrations. Due to the short illumination time the image taken contains also the movements of the vibrating systems, especially the P&P robot. The mechanical layout of the P&P robot was analysed and the center of rotation was determined. Interferometers were added to measure the rotation of the P&P robot when the alignment image was taken. The measured rotation was used to correct the data from the image processing. This resulted in a maximum repeatability error of less than 3 μm (1σ).

This thesis presents the design and realisation of a new concept for a single-camera alignment system. This concept is validated regarding its feasibility for calibration and repeatability. The gathered information such as: shuttle position, P&P robot position, actual machine status, calibration data is combined with the images acquired to determine the position of the component or board alignment feature. After the implementation of correction algorithms the maximum repeatability error is less than 3 $\mu m(1\sigma)$. The offset after calibration resulted in a repeatability of 12.9 μm (1σ), which is within the required 15 $\mu m(1\sigma)$. It is concluded that the proposed alignment concept in a P&P machine is feasible.

The data gathering strategy proposed for the machine concept could also be used in other situations. In this thesis the chosen alignment system concept required a position dependent alignment trigger. To simplify the

implementation of this alignment trigger, it was implemented accepting a position deviation with respect to the ideal trigger position, but this resulted in an unacceptable repeatability error if no additional measures were taken. It was shown that by sampling additional machine data including the actual positions of the moving parts a correction can be performed afterwards.

The strategy to accept an inaccurate trigger was feasible in this concept due to the fact that the moment of data sampling was at least 15 ms before the moment the data is required. Within this time frame the final placement position can be determined by the image processing software using the additional sampled data.

To enable the use of this concept in other designs implies that two requirements must be met. Firstly, there must be sufficient time available between data sampling and the moment the data is used to execute the data processing to combine all information. Secondly, it must be possible to sample all relevant data of the various machine systems that influence the final correction values. If both requirements are met then this concept can be applied in other designs.

Appendix A

Throughput analysis of pick-and-place machine concepts

A.1 Introduction

This appendix presents a study on new P&P machine concepts to improve the throughput P&P machines. It starts with analysing a sequential P&P machine. In this machine concept all required process steps take place sequential. The throughput of this machine concept is used as a benchmark for the design and validation of the other machine concepts.

A.1.1 Throughput indicator

Figure A.1 shows the P&P process that take place in a P&P machine.

- **Board Run In**: the PCB is fed into the P&P machine with limited accuracy
- **B(oard) Move**: the PCB is transported to the area where the P&P robot can place the components onto the PCB

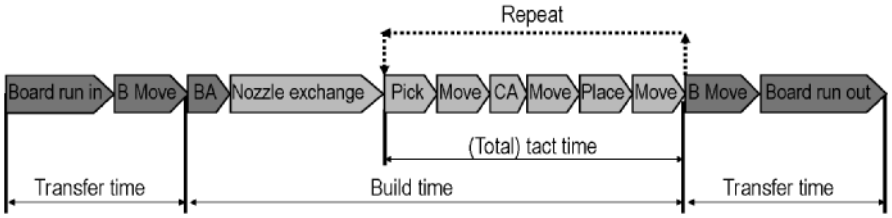

Figure A.1: *P&P processes that take place during the transfer time, build time and (Total) tact time according to the IPC-9850 standard [53]*

- **BA (Board Alignment)**: the position of the PCB is determined and is mostly realised using a vision system
- **Nozzle exchange**: depending on the component to be handled the required nozzle is picked from the nozzle storage position
- **Pick**: the P&P robot picks a component from one of the feeders; the pick process consists of moving downward to the component, build up vacuum, pick a component and then move upward; this is the process where the P&P cycle starts
- **Move**: the P&P robot moves to the component alignment position
- **CA (Component Alignment)**: the position of the component is determined and is mostly realised using a vision system
- **Move**: the P&P robot moves to the place position above the PCB
- **Place**: the P&P robot places the component on the required position on the PCB
- **Move**: the P&P robot moves to one of the feeders to pick a new component; this is the process where the P&P cycle stops
- **B(oard) Move**: the PCB is transported to the area to unload the PCB
- **Board Run Out**: all components are placed by the P&P robot(s) so the PCB runs out

Also shows Fig. A.1 the definitions used in the IPC9850.

- Build time (Time required for BA, nozzle exchange and the P&P cycle)
- Transfer time (Time required for board movement)
- Tact time (Time required for one P&P cycle)

The IPC-9850 defines two performance indicators for throughput being: net throughput and throughput. Net throughput can be calculated with help of the transfer time, build time and the number of components placed. Throughput can be calculated using the total tact time and the number of components placed.

$$Throughput = \frac{\#placed\ components \times 3600}{Total\ tact\ time} \tag{A.1}$$

In this analysis, throughput is used as performance indicator. Although, board alignment and nozzle exchange will influence the machine throughput, during the first analysis the influence of the other processes will dominate. The average P&P cycle of a component on the AX-5 P&P machine will

take about 450 ms. The IPC-9850 [53, pg.6] prescribes a minimum of components to be placed: 30 components for larger IC's up to more than 100 components for small components. The time required for BRI, BM and BRO, using a walking-beam transport system will be about 1 s and board alignment will take about 2 s [33, pg.217]. This means that for small components the contribution of board handling and board alignment will be less than 10%. Additionally, the new concepts will all be compared using throughput as performance indicator. During comparison, the influence of board handling and board alignment can be neglected for all concepts. Finally, the throughput is defined in components per hour but an addition is required. Taking into account that a multi-station will have more than one station, this means that several P&P robots can operate in parallel; resulting in a higher throughput. Therefore the throughput is defined per station
P&P robot.

A.2 Process throughput time contribution

The processes that were presented in Fig. A.1 will be explained in the next paragraphs. In order to estimate the throughput, the time required per process must be determined.

Board Run In, Board Move, Board Run Out

Board run in, Board move (B Move) and Board Run Out are the processes used to handle the PCB. The time required for board handling depends on the layout of the P&P machine. Because very high-volume P&P machines, above 40,000 *cph* per machine, have often a walking-beam transport system [107], this board handling system is also in this study used as transport system.

Figure A.2 shows a walking-beam transport system. The top graph of the figure shows a P&P machine with six P&P robots. Four PCBs are placed on the walking-beam transport system. If all six P&P robots have finished the placement of the components, the PCB has to move to the next position. The walking-beam transport system will perform an index step. Hereby, all PCBs move concurrently. The bottom graph of Fig. A.2 shows the same P&P machine, with the same four PCBs, after the walking-beam transport system has performed an index step. Concurrently to the board movement, a new board can be fed into the machine and an assembled board can be unloaded from the machine. Hereby, the total contribution of the three processes, Board run in, board move and Board run out, to the P&P cycle is equal to the longest time required for the board handling processes.

During Board Move and Board run out, a PCB contains pre-mounted components. The components are pre-mounted using the solder paste or

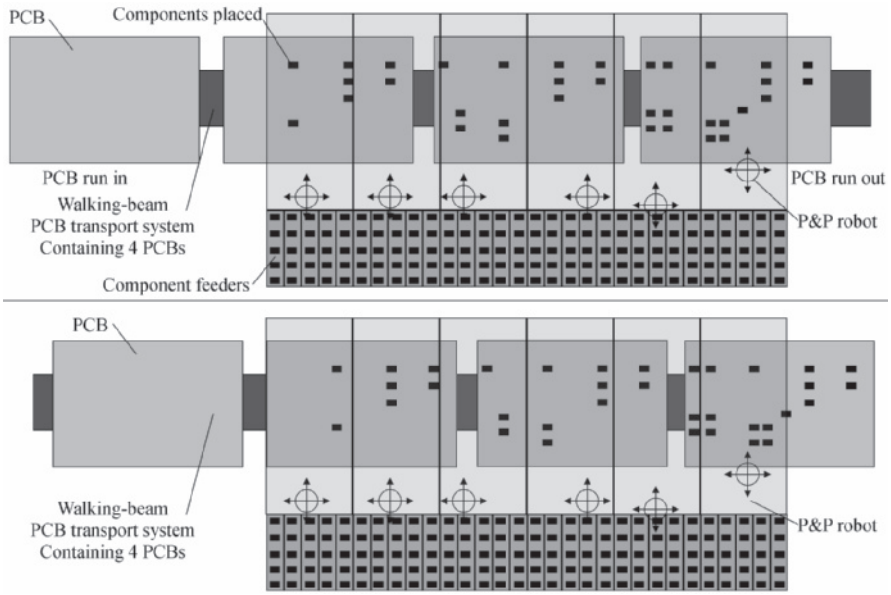

Figure A.2: *A walking beam transport is used in very high-volume machines. In this figure 6 P&P robot are present. Top: 4 PCBs on the walking beam transport system at the moment all P&P robots have placed the components. Bottom: Same 4 PCBs on the walking beam transport after an index step has been made. The P&P robots start with component placement. All PCBs move concurrently*

glue. The acceleration of the PCB must be limited to ensure that the pre-mounted components maintain their position [31]. A maximum acceleration of 15 m/s^2 is adopted for PCBs with pre-mounted components. This results in a practical maximum estimated time required for board handling of 2 s [33, 51, pg.217].

Board run in, board move, board run out	
Description	**time [s]**
Board move time	2

Table A.1: *Estimated transfer time*

Board alignment process

The process board alignment (BA) is used to determine the position of the PCB in the machine. The moment of board alignment can differ for machine concepts. If a walking beam PCB transport system is used combined with a separate board alignment module in the P&P machine, board alignment can take place concurrently to component placement. Normally, the total tact time will be larger than the maximum time that is required for board alignment.

To acquire, transfer and process an image takes maximal 50 ms [23]. As discussed, the position of minimal two features has to be determined. This means that the board alignment system has to been moved to various positions above the PCB. This movement can result in a board alignment time of 1 s [33, pg.217]. If the time required to acquire an image (50 ms) is compared with the time required to move the camera (1 s), the time for movement is larger. Therefore, the time for board alignment is set to 1 s.

Board alignment	
Description	**time [s]**
Board alignment time	1

Table A.2: *Board alignment time*

Component pick process

The pick process (Pick) is the process where the component is picked from a feeder by the P&P robot. The total pick process can be divided into three main steps. The first step is moving down towards the component. The second step is the actual pick of the component and the third step is moving upwards to a safe height.

The typical time for the total pick process is 60 ms [33, 51, pg.217]. This time is divided in 25 ms for the movement downwards, 10 ms for picking

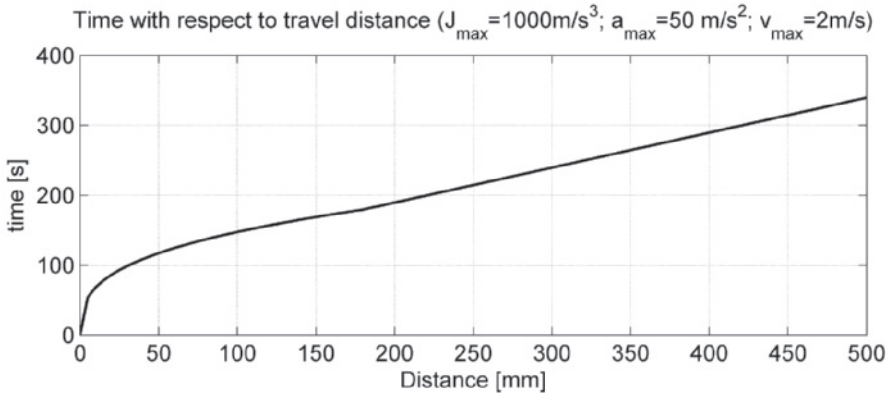

Figure A.3: *Time depending on the distance using a third order trajectory for movements in the horizontal plane*

the component and 25 ms for the upward movement.

Component pick time	
Description	**time** [ms]
Component pick process	60

Table A.3: *Contribution of the component pick process to the tact time*

Component move process

During the move process, the P&P robot moves from the position where a component is picked to the position where the component is placed on the PCB and back. Moving to the component alignment position between pick and place can be required. This means as shown in Fig. A.1 that the move process step appears three times in the P&P cycle.

To determine the contribution of the move processes to the tact time, analysis of the move process is required. To determine the time of a move process the move trajectory can be used. Nowadays, movements of a P&P robot are programmed using a third order trajectory. Hereby, this trajectory is described by the maximum allowed jerk, acceleration and velocity. The maximum allowed acceleration in x- and y-direction for a P&P machine are a result of the vacuum nozzle used to hold the component.

Figure A.3 shows the time required by the P&P robot to travel over distances between 0 and 500 mm when the jerk is limited to 1,000 m/s^3, the acceleration to 50 m/s^2 and the velocity to 2 m/s.

The influence of distance, velocity and acceleration on the throughput in the machine will be investigated during the design of new P&P machine concepts. Meanwhile, for a trajectory between 0 and 500 mm a time between 0 and 340 ms is calculated.

Component move time	
Description	**time** $[ms]$
Component move process, depends on distances	0 - 340

Table A.4: *Contribution of the component move process to the tact time*

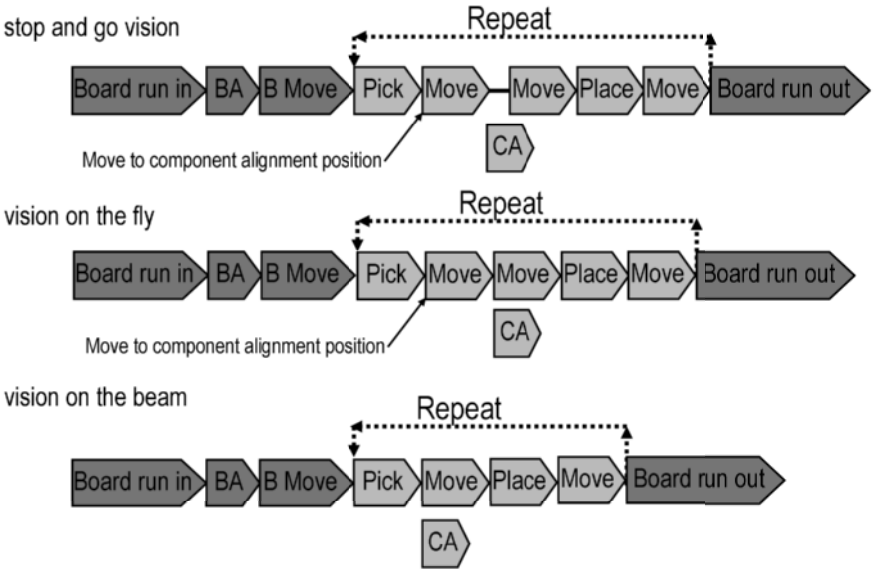

Figure A.4: *Overview of three P&P cycles. Each cycle contains a different component alignment strategy, resulting in another total tact time. CA = Component Alignment*

Component alignment process

Depending on the architecture of the P&P machine, component alignment (CA) can take place on various moments within the P&P cycle, which results in other timing diagrams. Also various ways of implementing a component alignment system are possible. As an example, there is a major difference between performing component alignment while moving or at stand-still. Consequently, all these differences will influence the time required for component alignment.

According to Gastel et al. [33, pg.147] there are three vision system strategies for component alignment used in P&P machines. The next list presents these three strategies with help of four known concepts to implement component alignment using a vision system. These four concepts differ with respect to the implementation of the component alignment system with respect to the integration with the P&P machine layout. The integration with the P&P machine results in two different strategies: the component moves or stands-still during component alignment.

1. **Stop and go vision:** This method uses a component alignment system that is on a fixed position within the P&P machine. The first graph of Fig. A.4 shows the P&P cycle of stop-and-go-vision. The P&P robot, holding a component, moves to the CA camera, stops above the camera, an image is acquired and the P&P robot moves to the component placement position. When the image of the component is acquired, the P&P robot is not moving, resulting in an extra delay indicated by the line after the move process. The P&P robot starts moving again after the image is acquired, the processing of the image can take place during the P&P robot movement, which explains that part of CA takes place during movements.

2. **Vision on the fly:** The component alignment system is on a fixed position within the P&P machine. The P&P robot, holding a component, moves over the component alignment camera. By using a pulsed illumination or camera shutter - to prevent motion blur - an image is acquired of the component while moving. The second graph in Fig. A.4 shows the P&P cycle of vision-on-the-fly. The two move steps indicate that the P&P robot must move from the pick position to the component alignment position and then, without stopping, moves towards the component placement position.

3a. **Vision on the beam:** A vision system is mounted on the P&P robot and determines the position of the component while the P&P robot moves from the pick position to the placement position. Because the camera is attached to the P&P robot, there will be no speed difference between the component and the camera. Therefore, a flash light or shutter is not necessary. The third graph of Fig. A.4 shows the P&P cycle. Since the camera is attached to the P&P robot, no extra movements have to be made.

3b. **Laser alignment:** A laser alignment module is mounted on the P&P robot and used to determine the position of the outline of the component, while the P&P robot is moving from the pick position to the placement position. Because the laser alignment system is attached to the P&P robot, no extra movements have to be made. The same P&P cycle as shown by vision-on-the-beam can be used for laser-alignment.

As can be concluded from Fig. A.4, stop-and-go-vision will require the largest alignment time. The P&P robot has to move to the component alignment position, stop there before the image can be acquired. Taking into account the settling time of the P&P robot during the P&P process, it can be expected that settling time has to be larger than 25 ms for the required repeatability. The use of the stop-and-go-vision strategy is not preferred because the stop time will increase the tact time and thereby decrease the throughput.

For all strategies it is required that after acquiring the image, this image has to be transferred and processed to determine the terminations' position. The estimated time for image processing is 55 ms [51].

Except for stop-and-go-vision the time required for component alignment is estimated to be 55 ms. taking into account that the image can be transferred and processed concurrently to the movements of the P&P robot.

Component alignment time	
Description	**time** $[ms]$
Component alignment process	
stop-and-go-vision	105
vision-on-the-fly(concurrently with movement)[1]	> 55
vision-on-the-beam(concurrently with movement)	55
laser-alignment(concurrently with movement)	55

Table A.5: *Component alignment process contribution to the tact time*

Component place process

During this process (Place) the component is placed on the PCB. This process can be divided into three main steps. Moving the nozzle from the upper position to the PCB, Placing the component and moving to the upper position.

From the upper position the nozzle with component moves towards the PCB with a maximum velocity. Two millimeter above the nominal PCB position, the velocity is reduced. Hereby, the component approaches the PCB with a "low" velocity until the component touches the PCB. After touchdown the component has to be placed by pushing the component's terminations into the solder paste or glue.

While pushing the component into the solder paste or glue, the solder paste or glue will deform and hold the component. Concurrently the vacuum is switched off. The required time for this process is about 10 ms [51].

The total average time of these three steps is about 60 ms [33, pg.217]; this time will be used in the timing model.

Component place time	
Description	**time** $[ms]$
Component place process	60

Table A.6: *Component place process contribution to the tact time*

Estimated throughput for a sequential pick-and-place machine

In this subsection a timing model will be presented that can be used to estimate the throughput of machine concepts. Initially, general assumptions will be presented. Finally, the results of the timing model of the generic P&P machine will be described.

The throughput of machines can differ dramatically due to variations in machine layout, machine parameters as distances, acceleration, velocity, vacuum process time and software processing time to perform board or component alignment. Process parameters as the size of the PCB, the position of the components on the board, positions of the components in the feeders and number of components to be placed will also influence the throughput. To determine the influence of parameters on throughput of a machine a timing model is made. This timing model will use the timing values of the P&P processes determined in the previous subsections.

The first timing model that will be determined is based on the layout of a sequential machine that is also used during repeatability analyses. This sequential machine has one nozzle, a stationary PCB and stationary feeders. The component alignment is assumed to be vision-on-the-beam or laser-alignment. Component alignment will start after the pick of a component from the feeders and will be performed during the movement of the robot to the place position. Image acquisition, image transfer and image processing time of the component alignment process takes place concurrently to the move process.

In the previous subsections time values were determined for the P&P process. In table A.7 these time values are summarised up.

Process time overview	
Description	**time** $[ms]$
Pick process (T_{pick})	60
Move process, depends on distances (T_{XYmove})	0 - 340
Component alignment, concurrent with move (T_{CA})	55
Place process (T_{place})	60
Move process, depends on distances (T_{XYmove})	0 - 340

Table A.7: *Time determined per P&P process*

Equation A.2 shows that the tact time can be calculated by adding the time of all processes required for a component placement.

$$T_{tact} = T_{pick} + T_{XYmove} + T_{CA} + T_{XYmove} + T_{place} + T_{XYmove} \qquad \text{(A.2)}$$

The time required picking a component consists of the required time for the movements in z-direction and the time required to perform the actual

component pick. The place process time consists of the z-movements and the required dwelling time. Hereby, all z-movements are covered by the pick or place process. Consequently, the move process contains only the simultaneous movements in x- and y-direction.

The influence of the move processes time depends on positions in the P&P machine. Calculating T_{XYmove}, the required time for the movement in the x- and y-direction, means calculating the time for both x- and y-direction movements separately, taking into account the distances between the pick and place position. When these two times have been calculated the largest time has to be taken because this will be the largest influence:

$$T_{XYmove} = \begin{cases} T_{Xmove}(j, a, v, x) & \text{if } x\text{-}distance \geq y\text{-}distance \\ T_{Ymove}(j, a, v, y) & \text{if } x\text{-}distance < y\text{-}distance \end{cases} \quad \text{(A.3)}$$

Image processing, required for component alignment, can take place concurrently with the move process. The timing model has to be adjusted such that always the time required for image processing is taken into account. In other words, if the move process time is less than the image processing time, the image processing time has to be used instead of the move time.

Finally, the tact time for one component can be calculated summing the time of every process contribution taking into account either the move or the alignment time (Equation A.4). To calculate the total tact time, the tact time of every component picked and placed, must be summed:

$$T_{tact} = \begin{cases} T_{pick} + T_{CA} + T_{place} + T_{XYmove} & \text{if } T_{CA} \geq T_{XYmove} \\ T_{pick} + T_{XYmove} + T_{place} + T_{XYmove} & \text{if } T_{CA} < T_{XYmove} \end{cases} \quad \text{(A.4)}$$

The realised timing model can be represented as a flow model and is shown in Fig. A.5. After Start, the time required for pick is added to the P&P cycle. Next step is to retrieve the placement xy-position and calculate the maximum time required for this movement (Equation A.3). The maximum time is compared with the time required for component alignment. The maximum time of the move process or component alignment is added to the P&P cycle. Next step is to add the time required for placement. A feeder position is retrieved and the maximum move time is calculated again and added to the total tact time.

As shown in the flow diagram, the component position of the feeder and the component position on the PCB are used in this timing model. Some assumptions have been made for the PCB and the component feeders.

Using the working area of the AX-5 P&P robot, the size of the PCB is defined to be 80×500 *mm* (x×y). Over this area 800 components are uniform distributed (Fig. A.6). During the simulations the sequence of

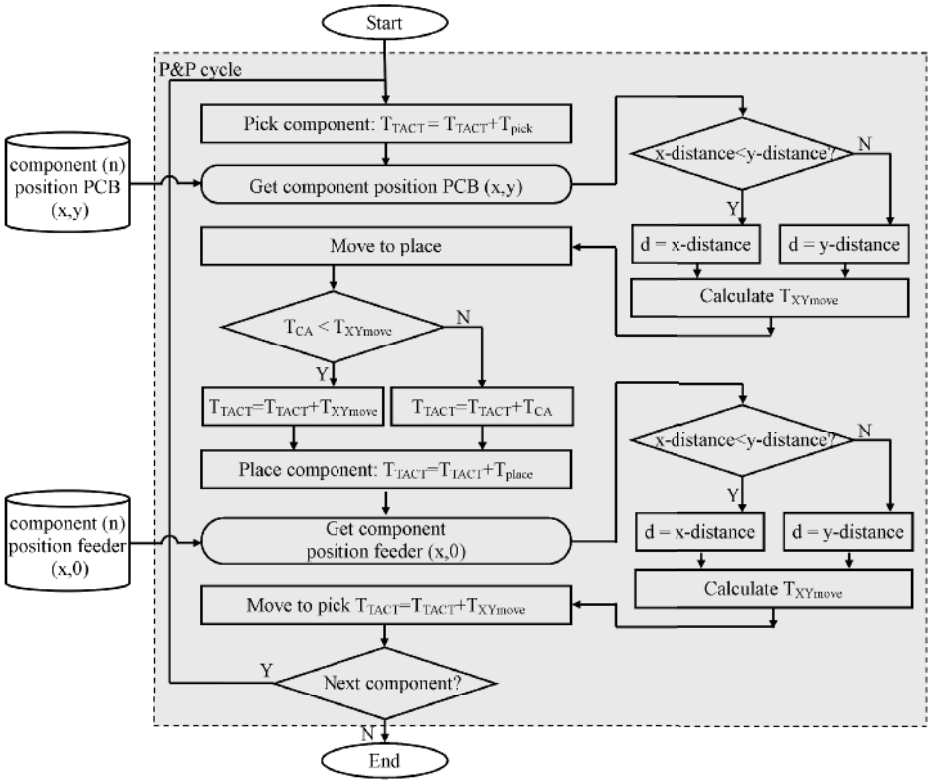

Figure A.5: *Flow diagram of the timing model used for the sequential machine*

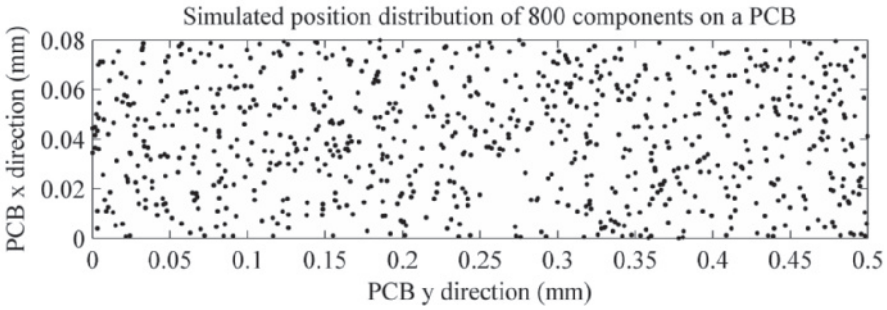

Figure A.6: *Distribution of components on a PCB during simulations*

placing components is sorted with respect to the y-direction. This will not influence the throughput because the timing is not depending on the sequence of placements but on the tact times. The tact time will not change by using a different sequence.

For the component feeders, there are six x-positions defined evenly spread over the total x-distance, where the components can be picked. The y-position is equal for all feeder positions. During simulations the feeder positions from where the component must be picked, are a uniform distributed over the six possible feeder positions.

Figure A.7 shows the influence of the P&P machine processes on the tact time. The travel distance in the y-direction is varied (the x-distance is set to zero for this graph). As expected only the movements, Move to Pick and Move to Place depend on the size of the PCB. The processes pick, place and CA are independent of the movements in the horizontal plane. If the distances in the P&P machine are minimised to 0 mm the maximum throughput of the machine will be 20500 cph due to the fact that the processes pick, place and CA together take 175 ms when performed sequentially.

As mentioned, the influence of all the movements to the total tact time can be 70% depending on the size of the PCB. Figure A.8 shows the influence of the maximum acceleration and maximum velocity on the throughput of the machine. The top graph of the figure shows the throughput of the sequential P&P machine, with default parameters. The second graph shows the throughput when the acceleration is changed. A high acceleration is helpful for small distances. It can be concluded that for small PCB sizes the acceleration should be increased. If the distances become larger, the maximum velocity is the limiting factor. The third graph shows the throughput change depending on the maximum velocity. For larger PCBs increasing the velocity will help to increase the throughput.

Increasing acceleration and velocity can be a solution to increase the throughput. On the other hand, decreasing the travel distance, increases the throughput also. The influence of changing more parameters at the

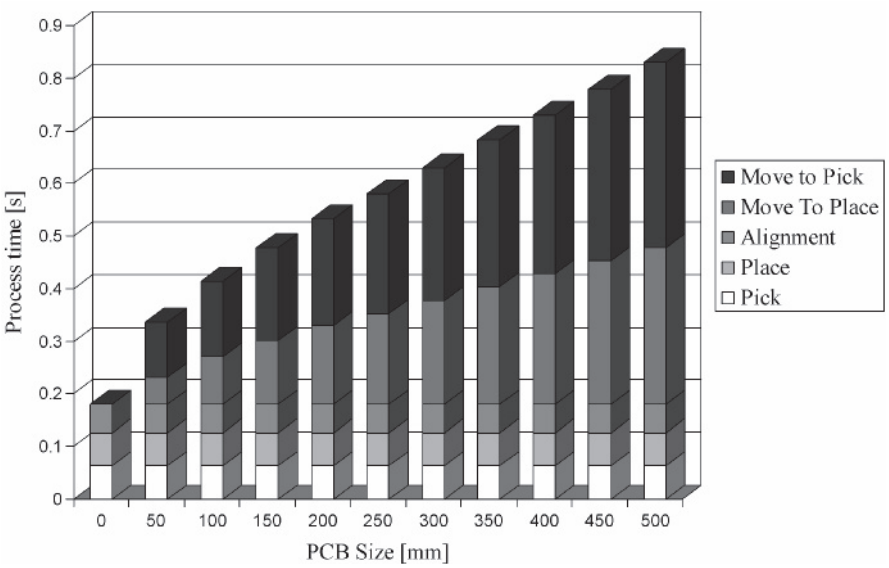

Figure A.7: *Tact time of a sequential P&P machine with respect to PCB size; acceleration horizontal plane = 20 m/s^2*

same time is discussed in the next chapter.

A.2.1 Conclusion

The performance indicator throughput is derived from the indicator costs. The throughput indicator is expressed in the number of components placed per hour per P&P robot. To determine the throughput of a P&P machine, the required time for the P&P machine processes in the P&P cycle is estimated. For the pick and place process a fixed time is determined. The image processing time, needed for component alignment, is estimated on maximal 55 ms. However, data transfer and processing can take place concurrently with movements. The movements depends on the travel distance of the P&P robot and can take up to 70 % of the total tact time. The time required for movements is calculated using third order trajectory setpoints.

A timing model is realised, taking into account the travel distances in x- and y-directions. The required alignment time is compared to the move time and the maximum time is used in the timing model.

With help of the timing model, the first estimations on throughput have been shown. This timing model will be used during the analysis of new concepts.

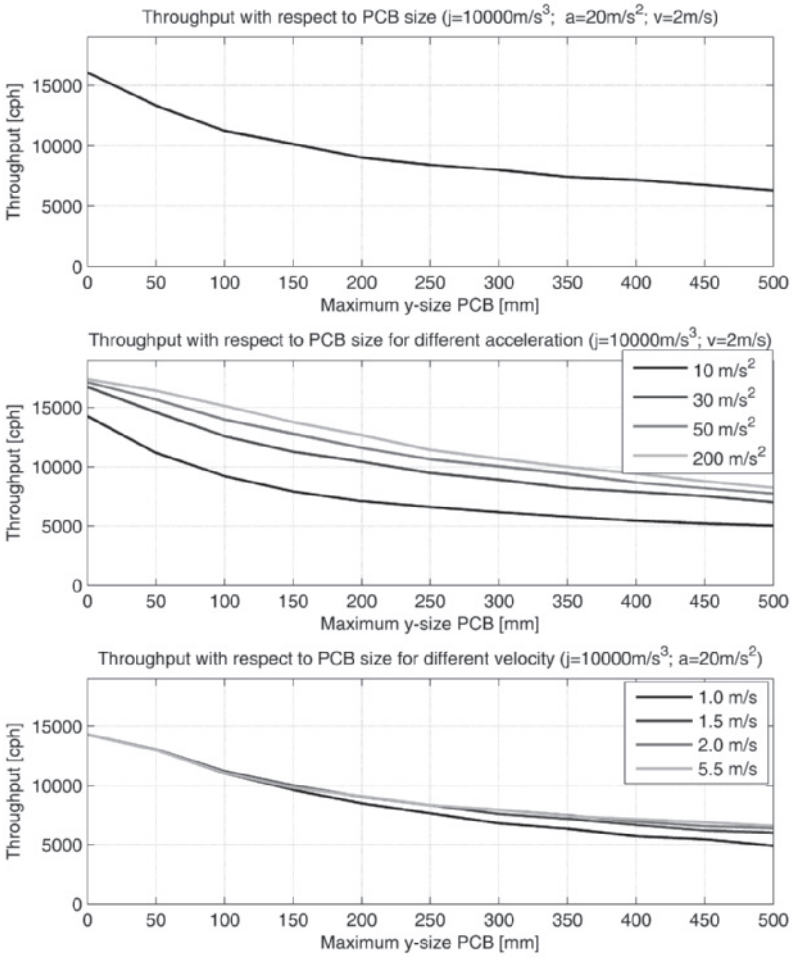

Figure A.8: *Influence of acceleration, velocity, distance on the throughput of a sequential P&P machine*

A.3 Introduction new concepts

Several new P&P machine concepts are described and the throughput of these concepts is estimated with help of timing models.

This section starts with a general analysis of possible throughput improvement strategies. Three strategies are presented and with the help of these strategies nine new P&P machine concepts are generated. Next, the nine concepts are described and a first estimation on feasibility is added. With help of the feasibility estimation three concepts are selected and a estimation on throughput is presented. The estimated throughput and expected feasibility have result in the choice for the shuttle concept P&P machine.

Next a layout of a shuttle concept P&P machine is presented and a more accurate timing model is realised. With help of this timing model, machine parameters are determined, which will be used during the design of the demonstrator. Finally, a conclusion ends this chapter.

A.4 Strategies for throughput improvement

As discussed the performance of a P&P machine on throughput means the number of components placed per hour per P&P robot. Increasing the throughput can be realised by decreasing the time required to place a component. In addition time required to place a component is the summation of the time required for each P&P process. By eliminating a process the time will decrease, but also by reducing the time required for a process the throughput can be increased.

Another way to decrease the overall time required to place a component is performing processes in parallel to each other. This can increase the number of components placed without changing the time for each individual component. As an example performing component alignment while moving decrease the overall time required without changing the process time of a process.

With the previous analysis, three strategies can be found to decrease the total tact time.

Reduce the time of a process When the time of a single process is reduced, the Tact Time for a component will decrease. The time of a process depends on the machine and process parameters. Therefore, analysis of the processes is required to determine the possible reduction of the process time.

Eliminate processes Because the Tact Time depends on the time required for each process, eliminating a process will decrease the Tact Time and hereby increase the throughput. The only required process of the P&P process is the place process. A P&P machine is built to

place components on the PCB. If all other processes could be eliminated the machine will still perform its task.

Processes parallel When processes can be executed parallel the Total Tact Time will be reduced. If all processes of the P&P process are performed in parallel, the largest process time will determine the Tact Time.

Taking these three strategies into account, nine new P&P machines concepts have been created.

A.5 Pick-and-place machine concepts

In table A.8, nine P&P machine concepts are presented. The first column of the table shows a short description/name of the concept. In the second column the used strategy is described. The third column explains the concept and comments on the feasibility are added. Taking into account the feasibility, the last three concepts in the table are selected and these will be analysed in the next section.

description	strategy	explanation
shoot components 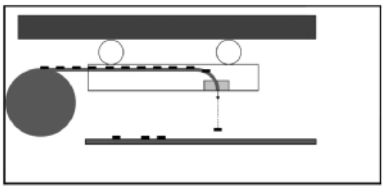	eliminate processes	A solution is to shoot all components directly from the feeder to the PCB. The throughput of this machine should be very high. A challenge of this concept is to keep the orientation of the components during flight. This solution results in a research question on components' air dynamics and is therefore rejected.
use multiple separate heads 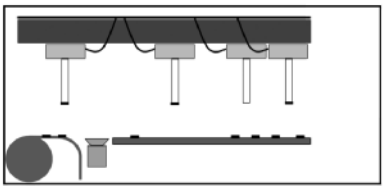	processes parallel	Several robots, with planar motors, are moving into xy-direction, hanging above the PCB. Each robot will pick and place components concurrently. For the distribution of power, vacuum and signals the robot is wired to the base. The determination of the trajectories, without crossing cables of other robots and still be able to reach all pick and place positions will be difficult. The available space will probably be insufficient. This concept is rejected.
feed components through tubes 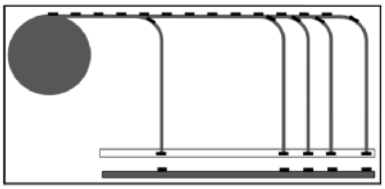	processes parallel	Tubes are positioned above the PCB. A component will fall down through a tube onto the PCB. The accurate positioning of the components will be difficult. This system is not flexible (a mask for every different PCB is required) or very complex (an actuator for each tube is required). It will difficult to realise the repeatability. It is therefore rejected.
fast inaccurate placement afterwards position repeatability 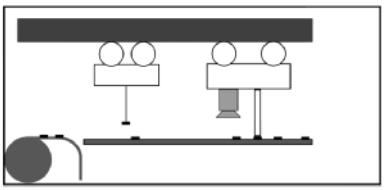	reduce time of a process step/process parallel	Accurate placement of components requires an accurate system. These systems should be stiff and are probably heavy. A fast, inaccurate, lightweighted robot places components. A second, slow robot positions the components accurately, afterwards. Moving components afterwards in solder paste or glue can result in broken components. This concept seems not feasible and is rejected.

description	concept	explanation
rolling mill 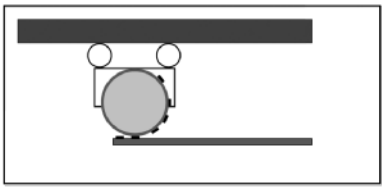	reduce time of a process	Components are placed on/in a mill. This mill rolls over the PCB to place the components on the PCB. There are two general problems. Firstly, the difference in height of components is difficult to handle. Secondly, to place components on the mill, still a P&P robot is necessary; the problem is only displaced. This concept is rejected.
typewriter machine 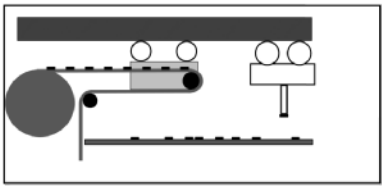	reduce time of a process	The idea is to reduce the distances for the move process. The tape, containing the components, will move into the machine close to the P&P robot. This concept uses a tape to transport the components. Because not all components are packed in tapes this concept is rejected.
formula-1 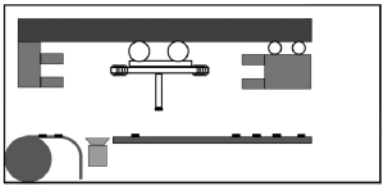	reduce time of a process	Increase the acceleration, beyond 50 m/s^2 and increase velocities of the P&P robot. The name refers to the fast formula-1 cars. The problem to be solved is holding components. This idea will be further discussed as concept 1.
shuttle 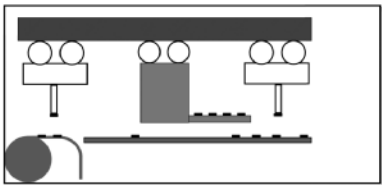	reduce time of a process	The idea is to reduce the time used for the move step by decreasing the distances. A part (shuttle) containing the components moves close to the P&P robot. The components must be handled twice so a second robot is necessary. This idea will be presented as concept 2.
small feeder robots 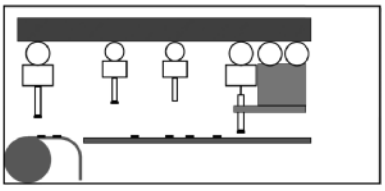	process in parallel	Instead of multiple separate heads there is only one P&P robot. But for every component feeder there is a separate simple robot, which can transfer the component from feeder to the P&P robot. The move steps can now be performed in parallel. This idea will be analyzed as concept 3.

Table A.8: *Generated P&P machine concepts*

The analysis of the nine concepts has resulted in the conclusion that three concepts are promising concepts. Further analysis of these three concepts is required to make a final choice. The next section will discuss this analysis.

A.6 Analysis of three concepts

The selected concepts are:

Concept 1: Formula-1 extreme accelerations and speeds decrease the time required for the move process

Concept 2: Shuttle an external part, called a shuttle, is added to the P&P machine. This shuttle brings the components nearby the P&P robot. The travel distances of the P&P robot will decrease resulting in a decrease of the time required for the move process

Concept 3: Small feeder robots every component feeder will get a small robot to bring a component to the P&P robot. The move process is divided over the small robots. This results in the decrease of the distances that the P&P robot must travel.

In the next subsections timing models are designed and used to analyse the concepts with respect to throughput. The presented timing model for the sequential machine is used as the bases for the timing models for the three concepts.

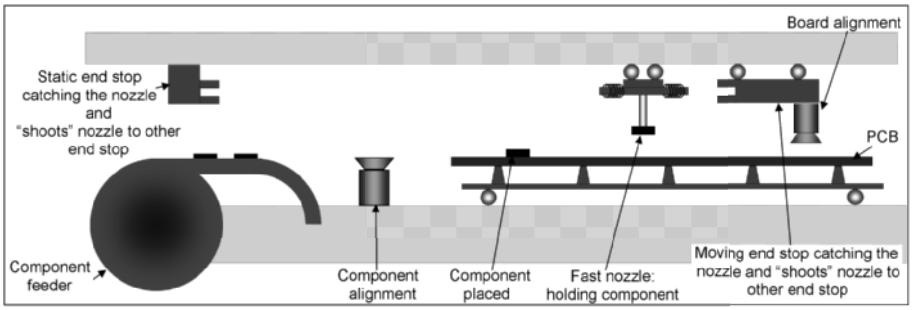

Figure A.9: *Concept 1: Formula-1: the nozzle is bounced between two end stops*

A.6.1 Concept 1: Formula-1

The strategy used for this concept is the decrease of the move process time. To reduce this process time, the maximum acceleration and velocity of the P&P robot in the x- and y-direction are increased. Although, the maximum acceleration and speeds are limited due to the use of a vacuum nozzle for holding the component, it is probably possible to solve this problem by changing the nozzle direction during acceleration.

Figure A.9 shows a schematic overview of the formula-1 concept. The fast moving nozzle is bounced, in y-direction, between two end stops. The end stops contain a nozzle gripper and an actuator to perform the z-movement. To create the movements in the x-direction, the complete system containing the guidance of the nozzle and the end stops has to move in the x-direction.

Throughput

The timing model of the sequential P&P machine is used to predict the throughput of this concept. The process and machine parameters are not adjusted except the maximum acceleration and maximum velocity. For the test the maximum y-size of the PCB is changed in steps of 50 mm from 0 to 500 mm, the x-size of the PCB is 80 mm. The throughput for this concept is calculated using combinations of maximum acceleration and maximum velocity for the P&P robot x- and y-direction.

Figure A.10 shows the estimated throughput depending on combinations of maximum acceleration, maximum velocity and maximum PCB y-size. From this figure it can be concluded that an acceleration of 150 m/s^2 and a maximum speed of 50 m/s will realise a throughput of approximately 12,000 cph with a PCB y-size of 500 mm. But even when the PCB y-size is reduced still the maximum throughput will be 16,500 cph.

The maximum throughput is limited due to the fact that firstly, the time required for the processes: pick, component alignment and place in total is

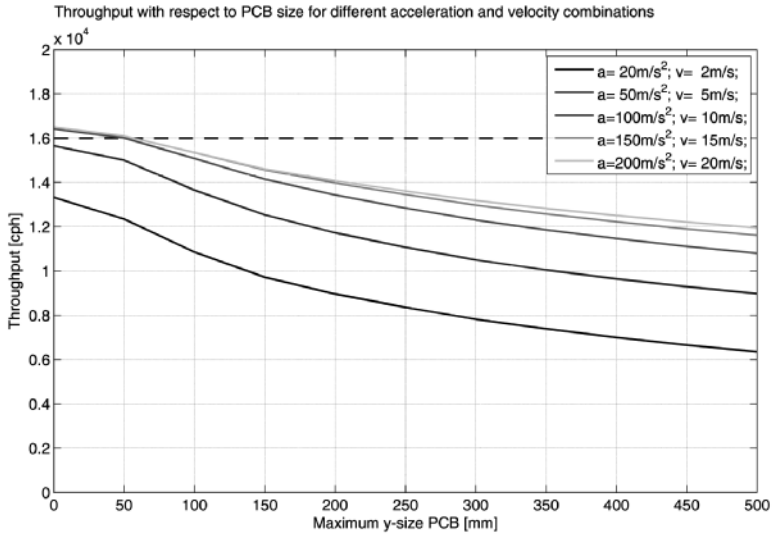

Figure A.10: *Throughput of concept 1: Formula-1: the throughput depends on the maximum acceleration, maximum velocity and PCB size*

175 *ms* and secondly, the x-size of the PCB is set to 80 *mm* what results in a limited throughput even when the y-size is set to zero. To increase the throughput, the time required for component pick, component place and component alignment has to be decreased.

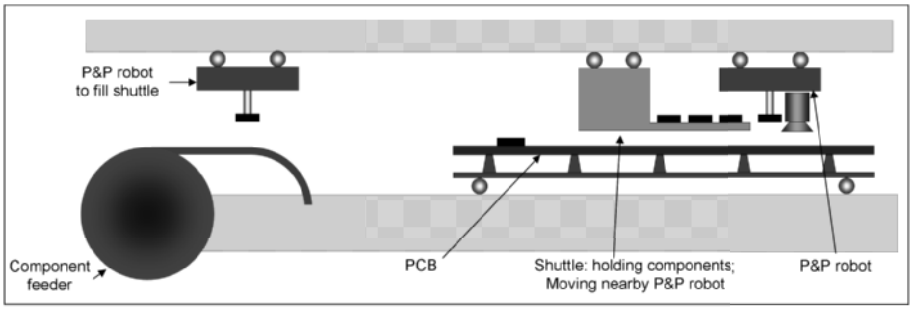

Figure A.11: *Concept 2: Shuttle: the shuttle brings components close to the P&P robot*

A.6.2 Concept 2: Shuttle

This concept is based on the idea to reduce the time required for the move process by reducing the traveling distances between the position where the component is been picked and the position where the component must be placed onto the PCB. To reduce the distances, the P&P machine is extended with a part, called shuttle, which carries several components. This shuttle follows the P&P robot what results in shorter traveling distances between the component pick position and place position, thus the time required for the move process will decrease. Figure A.11 shows an overview of the shuttle concept.

Throughput

To predict the throughput of this concept the sequential machine timing model from Section A.2 can be used. Figure A.12 shows the throughput of the sequential machine with a maximum acceleration of 20 m/s^2 and a maximum velocity of 2 m/s. The maximum y-size of the PCB is 500 mm.

This figure can also be used to estimate the throughput of the shuttle concept. The main idea to follow the P&P robot within a certain range to decrease the travel distance can be simulated using a smaller y-size PCB. The shuttle will follow the P&P robot from the beginning of the PCB to the end. Hereby, the traveling distance from the position where the component is picked from the shuttle to the position where the component is placed will be reduced. From the figure it can be concluded that the throughput of the shuttle concept can be higher than 12,000 *cph* when the shuttle will follow the P&P robot within a range of 50 mm of the P&P robot.

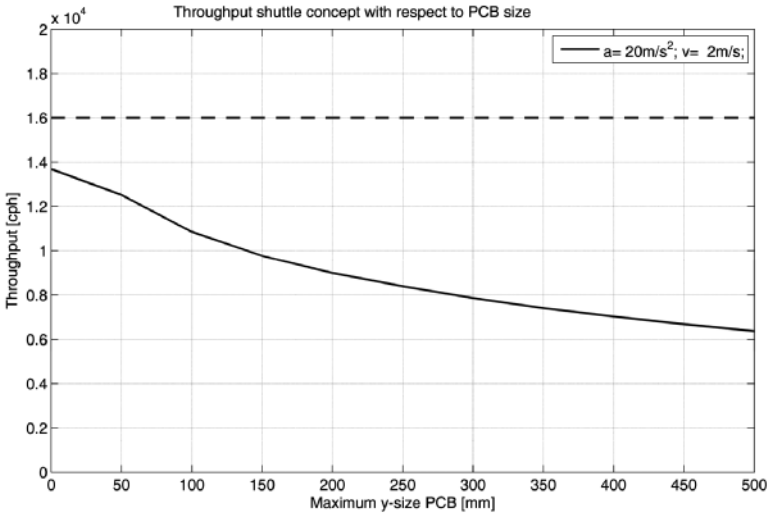

Figure A.12: *Throughput of concept 2: Shuttle: the throughput depends on distance between the shuttle and the P&P robot*

A.6.3 Concept 3: Small feeder robots

The basic idea of this concept is to reduce the P&P robot time required for the move process by performing several move processes in parallel. Six small feeder robots are used to bring components to the P&P robot. Figure A.13 shows an overview of the small feeder robot concept. A small feeder robot is able to transport a component from the feeders to the P&P robot. The P&P robot can grip the nozzle of the small feeder robot and places the component on the PCB. Afterwards, the small feeder robot will return to the feeders to pick the next component. Meanwhile, another small feeder robot has arrived at the P&P robot. With help of this setup, six components can

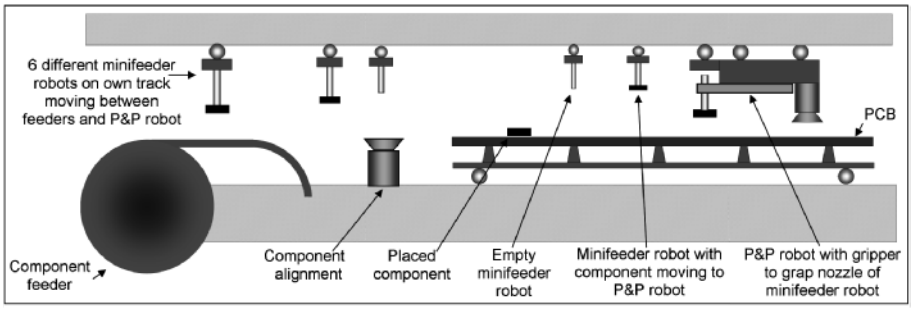

Figure A.13: *Concept small feeder robots: 6 different feeder robots bring components close to the P&P robot*

be brought to the P&P robot concurrently. As a result, the move process times will overlap.

To be able to move the robots in both directions independently, these robots must be small (a maximum of 20 mm width in x-direction is allowed) and long (500 mm is the minimum range that must be covered in the y-direction). Because of the layout, these small feeder robots are called snake robots in literature [110]. OCRobotics shows the feasibility of these robots [10]. They have build a robot with a length of 500 mm and a diameter of 6 mm. It can handle a payload of 10 g.

Throughput

To predict the throughput of this concept the timing model of the sequential machine can not be used so to calculate the throughput of this concept a new timing model must be realised.

To be able to model this concept, the dependency between the six small feeder robots and the P&P robot must be taken into account. The dependency can be explained as follows. The P&P robot can only place a component when the proper small feeder robot is arrived at the position of the P&P robot so the P&P robot must wait for that specific small feeder robot to be arrived. Next, the P&P robot can place the component and the small feeder robot has to wait until the nozzle is released by the P&P robot, which means that the small feeder robot must wait in the timing model for the feedback signal from the P&P robot. When the P&P robot has released the nozzle, the small feeder robot can go to the pick position to get the next component.

To be able to model this interaction between different robots, feedback signals between the different parts in the timing model are used [105]. In Fig. A.14 an overview of the interactions between the P&P robot and the small feeder robots is presented.

In the timing model for the small feeder robots, there are several feedback signals. One from the P&P robot to all the small feeder robots and six signals from the small feeder robots to the P&P robot.

The timing model is realised using a state machine that calculates the actual positions at a certain moment for the small feeder robots and the P&P robot. The time used for the component pick and place processes are taken into account in the timing model.

To calculate the throughput of this system, some assumption have been made. First, there is no optimisation used for the sequence of components. This can result in the situation that a component from the same feeder and thus from the same small feeder robot is placed multiple times in a row. This results in longer waiting times because the P&P robot will wait for this specific component. Second, component alignment is not in the timing model. The assumption is made that there is enough time, due to parallel

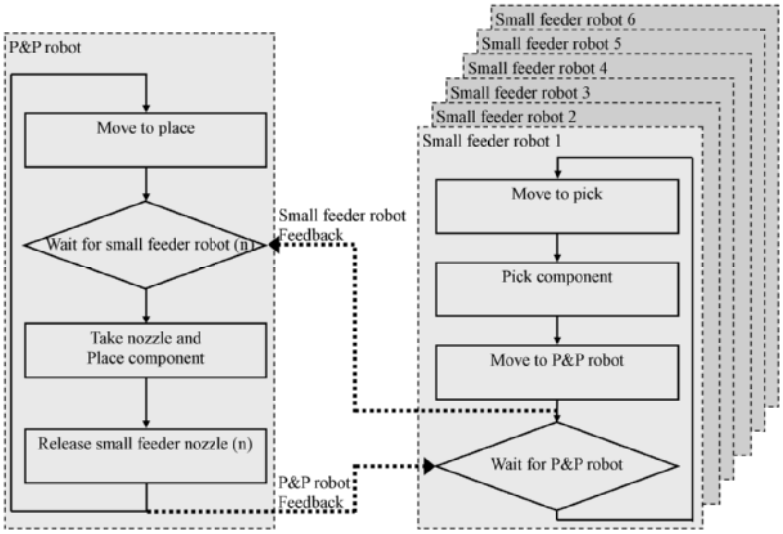

Figure A.14: *Concept 3: Small feeder robots: overview of timing model, the different small feeder robots give feedback to the P&P robot and visa versa*

processing, to realise component alignment while the small feeder robots are moving.

The P&P robot moves with a maximum acceleration of 20 m/s^2 and a maximum velocity of 2 m/s. To see the influence on the throughput, the maximum acceleration and maximum velocity of the small feeder robots are varied.

Figure A.15 shows the estimated throughput of the small feeder robot concept. It can be concluded that using an acceleration of 10 m/s^2 and a velocity of 2 m/s a throughput of about 12,000 *cph* can be expected. When the size of the PCB is small, the throughput increases. Note that the CA time is not taken into account. This will decrease the throughput for small PCBs.

A.6.4 Evaluation of the three concepts

The timing models used for the estimation of the throughput of the three concepts shows for all three concepts a throughput of approximately 12,000-13,000 *cph* when the PCB has a y-size of 500 mm. In the timing models a fixed time is used for the pick process (60 ms), component alignment (55 ms) and the place process (60 ms). This results in a maximum throughput of 20,500 *cph* without any movements. To be able to compare the three concepts, the throughput that can be realised for a PCB with a y-size of 500 mm is considered.

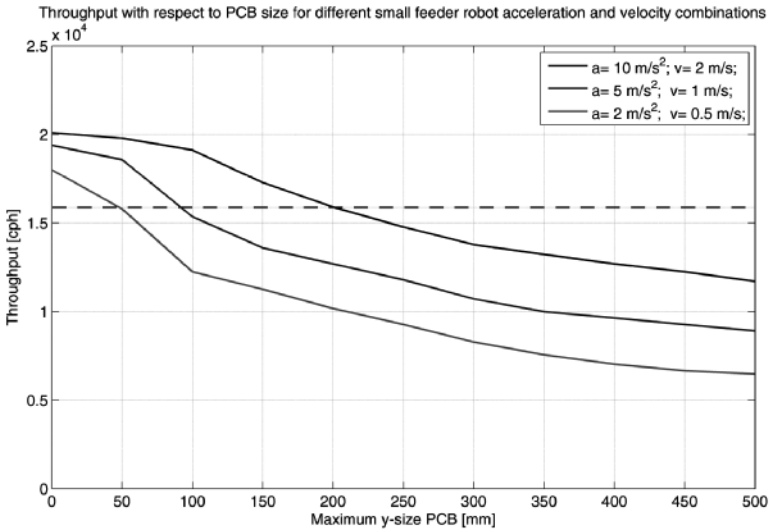

Figure A.15: *Concept 3: Small feeder robots: simulated throughput using 6 small robots*

Concept 1: Formula-1

The formula-1 concept can reach a maximal throughput of 13,000 *cph* with a maximum acceleration of 200 m/s^2, and a maximum velocity of 20 m/s. Note that holding a component, using a vacuum nozzle, with this acceleration can become a problem. The integration of the movement in the x-direction, by moving the total system that is holding the guidance of the fast moving nozzle and the end stops, can become a problem.

Concept 2: Shuttle

The Shuttle concept can reach a throughput of 12,000 *cph* when the shuttle can follow the P&P robot within a range of 50 mm. During this simulation the maximum acceleration of 20 m/s^2 and the maximum velocity of 2 m/s are used for the P&P robot. The conclusion for this concept is that by adding a shuttle to the sequential machine, the throughput can be up to 12,000 *cph*. The major disadvantage of this concept is that every component will be handled twice, first by a loading station to place the components on the shuttle, second by the P&P robot taking the component from the shuttle and placing it on the PCB. This can influence the reliability of the P&P machine.

Concept 3: Small feeder robots

The small-feeder-robots concept is able to realise a throughput of approximately 12,000 *cph*, when six small feeder robots are used with a maximum acceleration of 10 m/s^2 and a maximum velocity of 2 m/s. The small-feeder-robots concept has two major disadvantages. Firstly, the mechanical construction of the small feeder robots can be difficult, the width of a single robot can only be 20 mm, while the length must be 500 mm. Secondly, the number of parts added and the control of the overall system will become a complex system.

Conclusion

All three presented concepts are able to realise a throughput of approximately 12,000-13,000 *cph*. The goal of in this thesis is to realise a minimal throughput of 16,000 *cph*. This means that not only the estimated throughput is important but also to increase the throughput even further more, the potential of the concept has to be taken into account.

From the three concepts, the shuttle concept appears to be the most promising concept. The increase of throughput is substantial without extreme requirements. The formula-1 concept has high requirements on the acceleration of the nozzle, the small feeder robot concept will result in a complex system from the mechanical and control perspective.

By only adding a shuttle to a P&P robot, the throughput will be increased and if the maximum acceleration of the P&P robot is increased to 50 m/s^2 the throughout will increase even further, but still no extreme acceleration is required. This analysis has resulted in the conclusion that the shuttle concept is the most promising concept and is therefore selected.

A remark on adding a shuttle to a P&P machine has to be placed. When a shuttle is added to a P&P machine, new logistic possibilities can be realised. These possibilities are not discussed in this thesis, but can be further examined in the future.

A literature study on the use of a shuttle in a P&P machine has not resulted in any references. Based upon this observation a world patent on the shuttle concept has been filed [32].

Now the concept is selected, a first machine layout can be made for this concept. This layout can be used to update the timing model and an more precise estimation of the throughput of the shuttle concept can be determined.

A.7 Layout of a pick-and-place machine containing a shuttle

In this section a layout of a P&P machine containing a shuttle is described. Two possible implementations of the shuttle in the P&P machine will be shown. A choice will be made and the requirements for the P&P machine as result of this choice will be discussed.

A.7.1 Shuttle integration

The first timing model showed that a throughput of 12,000 *cph* seams feasible. The target for the design of the complete shuttle concept is a minimum throughput of 16,000 *cph*. This means that the P&P process must be analysed to improve the throughput. To estimate the throughput of the shuttle concept a new timing model must be realised. This timing model must be able to model the movement of the P&P robot but also the movements of the shuttle.

To be able to design a shuttle for the shuttle concept P&P machine, the specification for this shuttle must be determined. In general the shuttle has three main functions in the shuttle concept:

Move components The shuttle must follow the P&P robot to reduce the traveling distance from the position where the component is picked to the position where the component is placed. This requirement results in the demand that the shuttle can move close to the P&P robot in the y-direction This requirement shows that the shuttle must be positioned close to the P&P robot but it is not connected to the P&P robot.

Hold components During acceleration of the shuttle the components must remain on their position. The orientation of the components can be important and this information should not be lost. The shuttle must be able to hold components with various mechanical layouts

Release components When the P&P robot picks a component from the shuttle, the holding force of the shuttle must be reduced so that the P&P robot can pick the component from the shuttle using a vacuum nozzle

The first step to come to a P&P machine layout with a shuttle is to determine the position of the shuttle in the total P&P machine. The P&P robot moves above the PCB and is able to place components on the top side of the PCB. The most common position of the shuttle is next to the P&P robot, also above the PCB as presented in Fig. A.16. Adding a shuttle in the horizontal plane is a simple addition to the current P&P machines. Therefore it is decided is that the shuttle concept in this thesis will contain a shuttle in the horizontal plane.

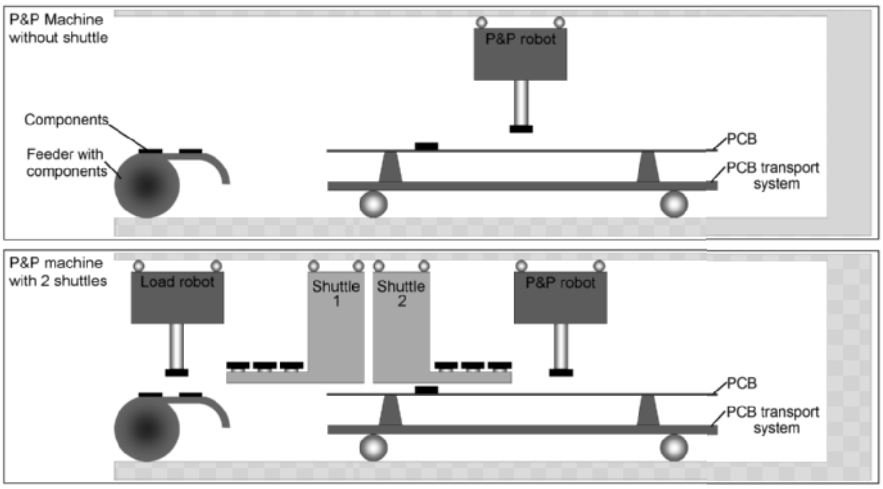

Figure A.16: *Concept design of a P&P machine with two shuttles, a load robot and a cartesian style P&P robot*

A.7.2 Number of shuttles

As described in the previous section, the shuttle is inside the P&P machine close to the P&P robot. Therefore, it is not possible to load the shuttle with new components while the P&P robot picks components from this shuttle. Thus, the only moment to load the shuttle is when this shuttle is not used by the P&P robot. In the total P&P machine processes cycle, the P&P robot can not place during board handling ($1s$). If only one shuttle is used, this means that there is only a maximum of one second to place all components on the shuttle. To overcome this problem a second shuttle can be added. One of the shuttles can be loaded in the same time as the other shuttle will emptied by the P&P robot. As a consequence a second P&P robot is required to load the shuttle.

A.7.3 Shuttle dimensions

The overview of the concept can be used to estimate the dimensions of the different parts. Adding a shuttle above the PCB will influence the z-distances. Figure A.17 shows the contribution of the different parts to stroke in z-direction. The total z-stroke exists of different distances:

- 2 mm curvature of the PCB
- 4 mm maximum height of a component placed
- 1 mm safety distance between placed components and the shuttle

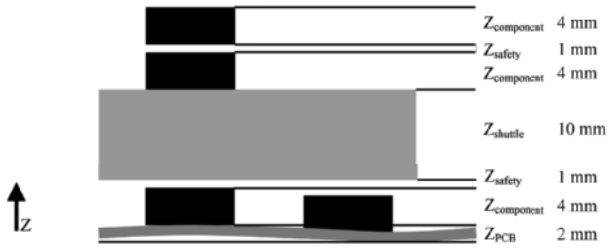

Figure A.17: *Estimation of distances in z-direction for a P&P robot with a shuttle*

- 10 *mm* estimated mechanical height of shuttle. It can be difficult to create a shuttle with a height of 10 *mm* that can hold and release components
- 4 *mm* maximum height of a component placed on the shuttle
- 1 *mm* safety distance above the shuttle
- 4 *mm* picked component, this distance is only required if the nozzle can move above the shuttle over components present on the shuttle

With help of these distances the movement of the nozzle in z-direction during the pick and place processes can be calculated. The maximum z-stroke is 26 *mm*.

A.8 Shuttle concept pick-and-place machine modeling

From the previous analyses of the P&P machine shuttle concept, a throughput of 12,000 *cph* can be expected. To realise a final throughput of 16,000 *cph* or more, not only a shuttle must be added but also the time required for the P&P process must be decreased. In this section the move, pick and place processes are discussed and new specifications for the P&P process will be determined.

The timing model used for the sequential machine, used a constant time for the pick process (60 *ms*), the component alignment process (55 *ms*) and the place process (60 *ms*). Adding a shuttle to the P&P machine changes the z-distance during component pick process and component place process. It is therefore necessary to adjust the timing model of the pick and place processes, taking the traveling distance in z-direction into account. In addition, the acceleration of the nozzle in the z-direction can be increased.

Pick process

The pick of a component from the shuttle can be divided in three steps. First, the nozzle moves from the upper position to a position just above the component. The next step is building up vacuum and pick the component from the shuttle. The third step is the movement of the nozzle upwards to the position that the component can move over other components that can be on the shuttle.

The time required for the downward and upward movements during the pick process can be calculated using a third order trajectory. The time required to build up vacuum and to pick a component is set to 10 ms.

Pick-and-place robot move process

The time required for the x- and y-movement of the P&P robot can be calculated with help of a third order trajectory. The maximum allowed acceleration of the P&P robot during x- and y-direction movements can be increased up to 50 m/s^2. The influence of these adjustment has to be included in the timing model.

Component alignment process

The time required for component alignment is still kept 55 ms, where the component alignment takes place during the P&P robot movement in x- and y-direction. This means that a minimum time of 55 ms is required after component pick and before component place.

Place process

From Fig. A.17 the z-distance for the place process can be determined and is set to 26 mm. The time required to travel this distance can be calculated using a third order trajectory. The dwelling time, the time required for solder paste or glue to deform and hold the component, is set to 10 ms. The total place process time can be calculated adding time required for the downwards z-movement, the dwelling time and the upwards z-movement.

Shuttle movement

In the shuttle concept P&P machine the shuttle has to be close to the P&P robot and during a component pick the P&P robot will be above the shuttle. To estimate the throughput of the shuttle concept P&P machine, the movement of the shuttle will influence the throughput. Smaller distances between the P&P robot and the shuttle will increase the throughput.

Figure A.18 shows the movements of the P&P robot and the shuttle. The top graph shows the P&P robot picking a component from shuttle.

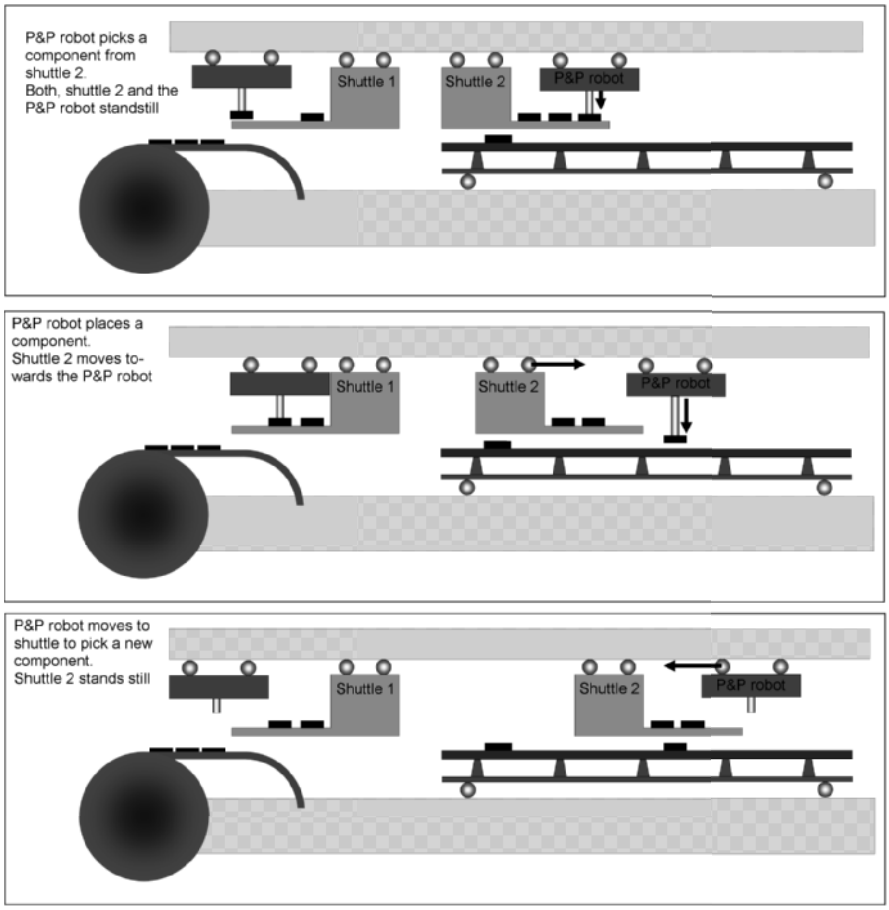

Figure A.18: *Shuttle and P&P robot movements in a shuttle concept P&P machine. Top: P&P robot picks a component from the shuttle. The P&P robot and the shuttle are standing still. Middle: The P&P robot places a component, meanwhile the shuttle moves towards the P&P robot. Bottom: The shuttle stands still, the P&P robot moves towards the shuttle to pick a component*

Both, the P&P robot and the shuttle are not moving in the x- and y-direction. In the second graph the P&P robot places a component on the PCB, meanwhile the shuttle moves towards the P&P robot. It will stop close to the P&P robot and waits there. The third graph shows how the P&P robot moves to the shuttle to pick the next component. Meanwhile, the shuttle remain on its position.

In the shuttle concept P&P machine, the pick position is a combination of the shuttle position and the position of the component on the shuttle. This input is used for the calculation of the y-movements of the P&P robot.

The maximum acceleration and the maximum velocity of the shuttle will be limited. From the fact that the components have to be picked from the shuttle by the P&P robot using a vacuum nozzle, it can be expected that the forces to hold the components on the shuttle have to be lower than the force that is generated by a vacuum nozzle. A maximum acceleration of 10 m/s^2 and a maximum velocity of 1.5 m/s are used to calculate the time required for the y-movement of the shuttle.

A.8.1 Shuttle concept pick-and-place machine model

As the basis for the timing model for the shuttle concept P&P machine, the sequential machine timing model can be used. Figure A.19 shows the flow diagram that is used for the modeling of the shuttle concept P&P machine. Firstly, this model is extended with the calculations for the time required for the component pick and component place process. Secondly, the calculations for the movement of the shuttle are added.

As can be seen in the flow diagram, the shuttle can influence the throughput. If the P&P robot requires a shorter time for move to place and component place then the time required by the shuttle to move to the new position, the time required by the shuttle movement will be used and the Tact Time will increase.

With help of this timing model the movement of the P&P robot in y-direction and the movement of the nozzle in the z-direction can be determined.

Figure A.20 shows the movement of the P&P robot in the y-direction and the nozzle movement in the z-direction for different parameters. The two left graphs of Fig. A.20 show the movement of the P&P robot and the nozzle. The settings for the P&P robot are a maximum y-acceleration of 20 m/s^2 and a maximum velocity of 3 m/s. For the nozzle the maximum z-acceleration is limited to 50 m/s^2 and the maximum velocity is set to 2.5 m/s. A component of 4 mm height is picked and placed. The distance between the pick position on the shuttle and the place position on the PCB is 50 mm. These settings result in a P&P cycle time of 410 ms. The maximum throughput in this case is approximately 8800 *cph*.

The goal is a throughput of 16,000 *cph*. From the previous P&P cycle

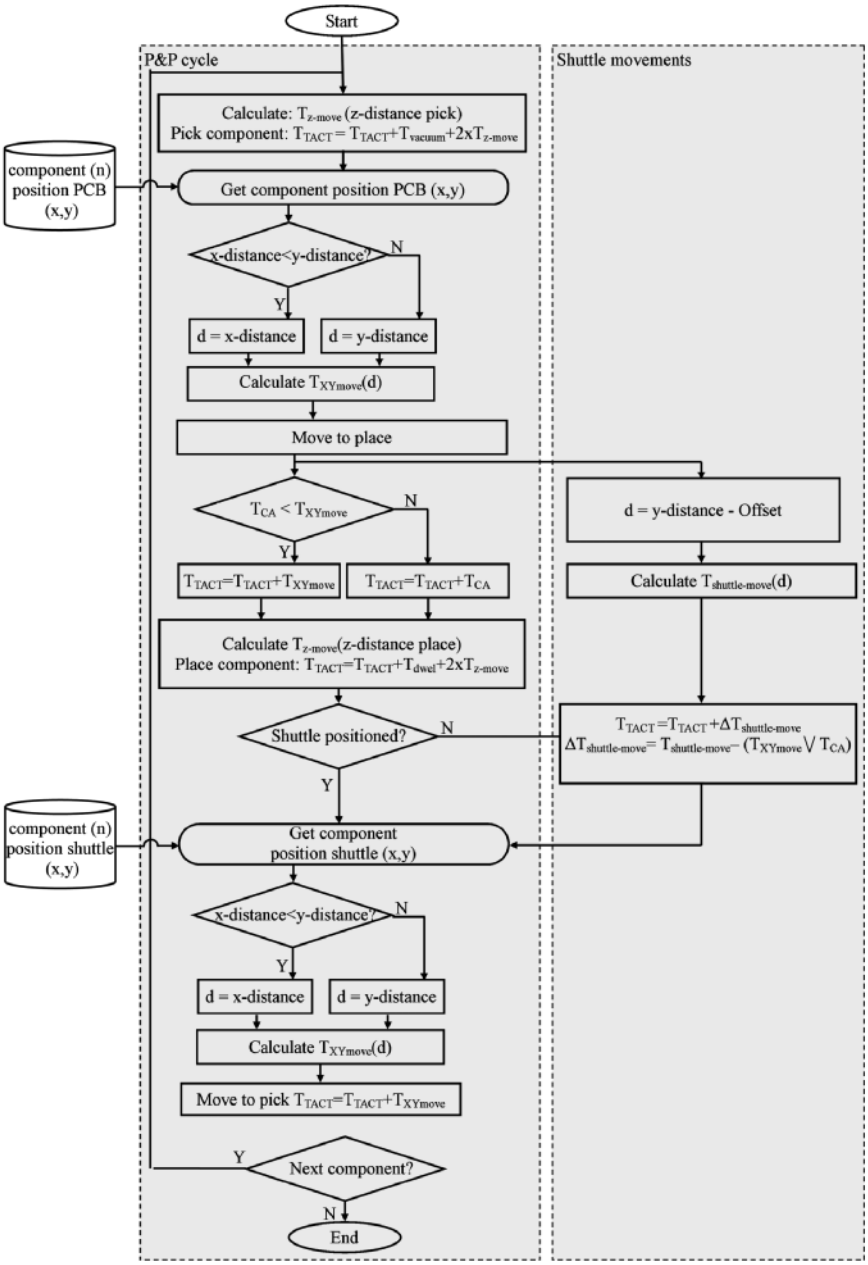

Figure A.19: *Flow diagram of the timing model used for the shuttle concept P&P machine*

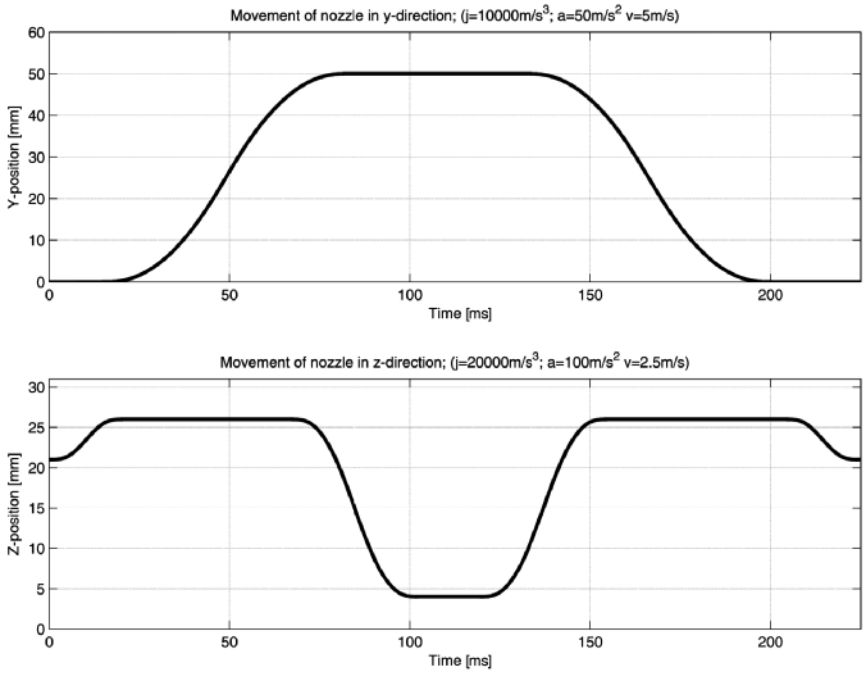

Figure A.20: *Movement of the P&P robotcontaining the nozzle in y- and z-direction; a P&P cycle time of 225 ms is realised*

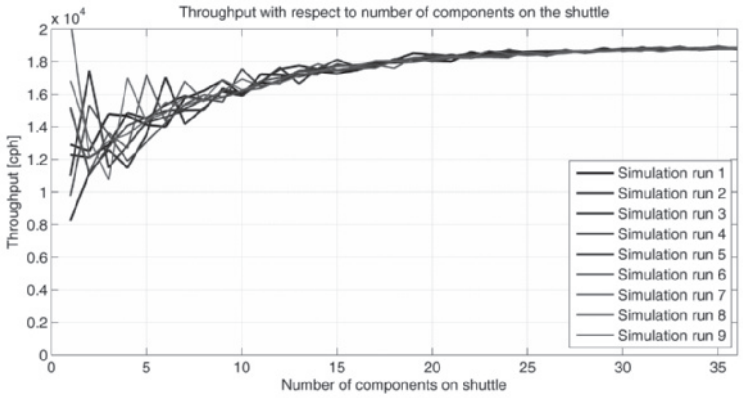

Figure A.21: *Throughput with respect to number of components on a shuttle*

it can be concluded that both movements, in y- and z-direction, take too much time. The acceleration in y-direction can be increased to 50 m/s^2. It is then still possible to use a vacuum nozzle. The maximum acceleration of the P&P robot in y-direction is set to 50 m/s^2. The next step is to decrease the time required for the z-movement. It can be determined that an acceleration of 100 m/s^2 and a maximum velocity of 2.5 m/s is required to realise a P&P cycle time of 225 ms. The two right graphs of Fig. A.20 show the movement of the P&P robot in the y-direction and the movement of the nozzle in z-direction with these adjusted parameters.

From this analysis it can be concluded that the requirements for the z-movement results in the design of a high dynamic z-axis.

A.8.2 Number of components on the shuttle

It is to be expected that there is a minimum number of components on the shuttle required to achieve an optimal performance. With help of the timing model the influence of the number of components on the shuttle can be determined.

During this simulation, the number of components present on the shuttle is varied between 1 and 36. Nine PCB layouts are randomly generated. Figure A.21 shows the estimated throughput of the concept with different number of components on the shuttle.

If only a few components are placed on the shuttle, the estimated throughput is highly depending on the positions of the component on the PCB. If this component position is close to the feeder position the estimated throughput will be higher. This effect explains the high difference in throughput if the number of components is under eight components. If the number of components increases, this effect decreases.

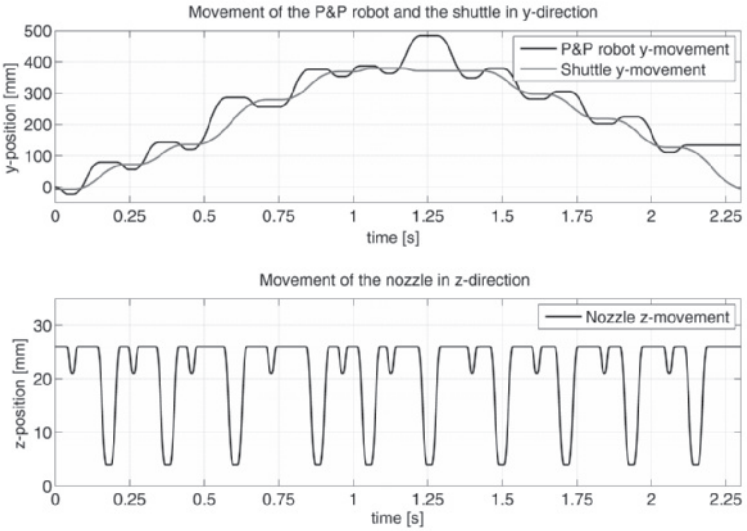

Figure A.22: *Top: Movements of the P&P robot and the shuttle in y-direction while placing 10 components on a PCB. Bottom: The movement of the nozzle in z-direction, picking a component from the shuttle (z=21 mm) and placing it on the PCB (z=4 mm). During the pick of a component the P&P robot and shuttle are both standing still. The shuttle moves when the P&P robot places a component*

The results of the simulations show that the maximum throughput of the shuttle concept will be approximately 19,000 *cph* when 36 components are available on the shuttle. A throughout of 16,000 can be realised when 10 components are available on the shuttle.

To check if number of components required on the shuttle will fit in the mechanical dimensions of a P&P machine, the minimal dimensions of the shuttle can be estimated. Taking into account the maximum sizes of a component (6×6 *mm*) and the number of components on the shuttle (minimal 10), can result in a shuttle with 2 rows with 6 component (during the simulations six feeders in parallel are used). The of the shuttle size will be minimal 12×36 *mm*.

A.8.3 Estimated shuttle concept throughput

The last test performed with the timing model is a complete P&P cycle where ten components are picked from the shuttle and placed onto the PCB. In Fig. A.22 the movements of the P&P robot and shuttle are shown. The first graph of this figure shows the y-movements of the P&P robot and the shuttle. The second graph shows the movement of the nozzle in the

z-direction. As can be seen in the second graph the component is picked from the shuttle (height 21 mm above the PCB), moves up to a safe height 26 mm, and places the component on the PCB (height 4 mm). During this simulation the shuttle starts to move after the component has been picked from the shuttle.

The v-shape movement is selected to end with the shuttle at the starting point. On this position the shuttle can be loaded or exchanged. The pick and place of ten components takes approximately 2.25 s, meaning a throughput of 16,000 cph can be realised.

A.9 Conclusion

Analysing the P&P machine and the P&P cycle has shown three throughput strategies to improve the throughput: decrease the time for the P&P process, eliminating P&P process, and perform P&P process in parallel. With help of these strategies nine concepts have been generated. Three concepts have been analysed and the shuttle concept is selected. The shuttle concept has as its main objective to reduce the time used for the move process step by decreasing the distances.

The different parts in the machine are described and the main requirements are determined. The total machine concept exists of the following parts:

Shuttles Two shuttles are added to the P&P machine. One shuttle follows the P&P robot within a distance of 50 mm carrying a minimum of 10 components. The second shuttle will be loaded during the time the P&P robot is emptying the first shuttle. The mechanical dimension in the z-direction is maximal 10 mm.

P&P robot The P&P robot picks the components from the shuttle and places them on the PCB. Accelerations in horizontal plane 50 m/s^2, bounded by the choice for vacuum to hold components. The maximum velocity will be 2.5 m/s. The acceleration in z-direction must go up to 100 m/s^2.

Load robot A second robot is required to load the shuttle. The design of this robot seems feasible but not arbitrary.

To maximise the benefits using this concept, the integration of the different parts, shuttle, alignment systems and P&P robot, is required to achieve an optimal system. Meaning that the component and board alignment must be integrated with the shuttle concept without adding extra time to the P&P cycle or distances to the P&P move processes. Only then a throughput of 16,000 cph can be realised. This means that the P&P cycle time must be less then 225 ms.

Appendix B

Case study: parallel mechanism robot

B.1 Case study model

In this project a case study parallel mechanism P&P robot is built. This P&P robot is built to prove feasibility of some design specifications from Appendix A. Integrating the shuttle and the alignment systems have not been taken into account. This case study model will be used to first test the feasibility of a parallel mechanism robot. Secondly, it is used for a feasibility study to use poly-amide selective laser sintering machine parts in dynamic systems. In the next section the case study robot is briefly explained. Followed by the discussion on some considerations of the properties.

B.2 Parallel mechanism pick-and-place robot

A way to reduce the moving mass of P&P robots, is the use of parallel mechanism robots. Commercial there is a P&P robot from ABB, which is realised by using 6 rods (IRB340) (see Fig. B.1). This robot [8] can accelerate up to 100 $m/s^2$with a payload of 1 kg and speeds up to 10 m/s. If this robot would be scaled down then a robot with low moving mass is

Figure B.1: *Flex Picker from ABB*

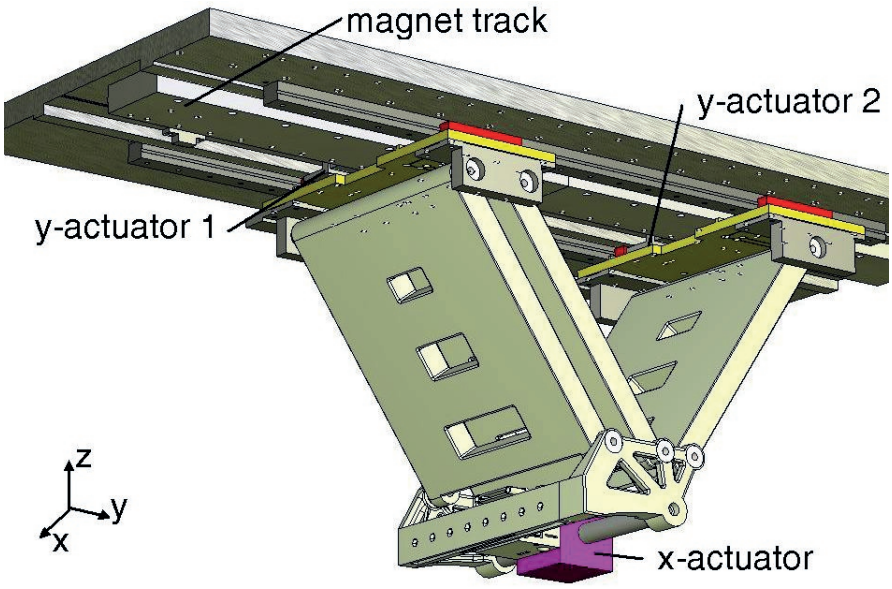

Figure B.2: *3 DOF parallel mechanism P&P robot*

created. But for the use in the shuttle concept P&P machine the dimensions do not fit. The x-stroke is to long and the y-stroke is not long enough.

2D-parallel mechanism P&P robot

To overcome the disadvantages, a robot must be designed that can work within the desired envelop of 80 mm×500 mm×50 mm(x×y×z).

Liu [72] shows two new concepts with less then 6 DOFs placing the motors vertical. Huang [50] proposes a combination of a linear slide with a rotational parallel mechanism. Miller [76] shows a new concept called linear Delta where three motors are placed in parallel. With the mechanism a 3 DOF system is built. This idea is adopted but because the width of the frame in x is restricted only one motor magnet track is placed on top. The robot is developed to realise a stroke in z-direction of 50 mm.

Figure B.2 shows a drawing of the case study P&P robot. If y-actuator 1 and y-actuator 2 are moving in the same direction, the end effector (attached to the x-actuator) will move in the y-direction. If the y-actuator 1 will move the opposite direction of actuator 2 the end effector will move in z-direction. A x-actuator is added to realise the x-movement. This design is able to accelerate in z-direction with specified accelerations. The main idea behind this robot is to keep as much mass as possible on the frame and try to minimise the moving mass. This robot has been built with poly-amide. The technique used to build this robot is Selective Laser Sintering (SLS). The benefit of this technique is the possibility to realise complex forms to

Figure B.3: *Case study: build functional model of parallel mechanism in poly-amide*

generate almost ideal parts in poly-amide.

The advantage of this robot is the low moving mass. When added a small ϕ-motor the total moving mass in y and z-direction is about 300g. The half of this mass is the mass of the x-actuator. The construction in poly-amide weighs also about 150g. Al magnet tracks of the linear motor used in the y-direction are placed on the frame so only the coils move. This way the mass can be kept low of the moving parts. The analysis of the construction shows an deformation of $\pm$ 36 μm while moving y-direction. The main reason for this deformation is the mass attached to the end of the poly-amide plates. The forces on the plates are to high because of this mass.

The disadvantage of this robot is the size of the construction. The height of the robot is about 200 mm. And also the control of a parallel mechanism is more complex. In a simple 1D-system, if an actuator is actuated the result is a movement in one direction. In a mechanism, the movement of one actuator results in a 2D-movement. Advanced multi axes controllers are available to control parallel mechanism robots.

B.2.1 Actual status

The robot is operational. The accelerations are in y-direction 25 m/s^2 and the speed in y-direction maximal of 1.25 m/s. The main reason that the accelerations are limited to 25 m/s^2 is a mechanical reason. During tests it has become clear that the mechanical connection between the poly-amide parts and the metal bearings is not optimal. The poly-amide deforms and the final effect is play in the connection between the poly-amide and bearings. Redesign of the inserts is necessary to solve this problem. The mounting of the x-encoder to measure the position is not stiff enough. The x-

actuator can only move very slow ($2\ m/s^2$, $0.05\ m/s$) otherwise the position information is lost.

B.2.2 Conclusion

A poly-amide parallel mechanism robot is designed and built. This case study robot has some mechanical problems that must be solved: encoder mounting of the x-direction and the connection between the bearings and poly-amide parts. To realise a better accuracy (less deformation) the mass of the x-actuator must be reduced.

Because the sizes of a parallel mechanism P&P robot, necessary to realise the working area, are rather big it is decided not to continue with this design. These sizes are opposite to the requirement to realise a shuttle and alignment system nearby the end-effector of the P&P robot.

Bibliography

[1] M. Arra, D. Geiger, D. Shangguan, and J. Sjöberg. A study of smt assembly processes for fine pitch csp packages. *Soldering & Surface Mount Technology*, 16(3):16–21, 2004.

[2] M. Ayob. *Optimimisation of Surface Mount Device Placement Machine in Printed Circuit Assembly*. PhD thesis, University of Nottingham, Nottingham, 2005.

[3] M. Ayob, P. Cowling, and G. Kendall. Optimisation for surface mount placment machines. *IEEE International Conference on Industrial Technology*, 1:498–503, 2002.

[4] M. Ayob and G. Kendall. A monte carlo hyper-heuristic to optimise component placement sequencing for multi head placement machine. *Proceedings of the international conference on intelligent technologies, InTech*, 3:132–141, 2003.

[5] M. Ayob and G. Kendall. Proceedings of the ieee international symposium on assembly and task planning, 2003. *Real-time scheduling for multi headed placement machine*, pages 128–133, July 2003.

[6] J.P. Baartman, A.E. Brennemann, S.J. Buckley, and M.C. Moed. Placing surface mount components using coarse/fine positioning and vision. *IEEE Transactions on Components, Hybrids, and Manufacturing Technology*, 13(3):559–564, 1990.

[7] C.B. Bose and I. Amir. Design of fiducials for accurate registration using machine vision. *IEEE Trans. Pattern Anal. Mach. Intell.*, 12(12):1196–1200, 1990.

[8] H. Brantmark and E. Hemmingson. Flexpicker with pickmaster revolutionizes picking operations. *Industrial Robot: An International Journal*, 28(5):414–419, 2001.

[9] J.B. Bryan. The abbé principle revisited: an updated interpretation. *Precision Engineering*, 3:129–132, 1979.

[10] R. Buckingham. Snake arm robots. *Industrial Robot: An International Journal*, 29(3):242–245, 2002.

[11] R Calvel. Delta, a fast robot with parallel geometry. *proceedings of the 18th International Symposium on Industrial Robot*, 18:91–100, 1988.

[12] H.J. Coelingh. *Design support for motion control systems*. PhD thesis, University Twente, Enschede, 2000.

[13] W.E. Coleman, D.J., and J.R. Bradbury-Bennett. Stencil design for mixed technology throughhole/smt placement and reflow. *Soldering & Surface Mount Technology*, 12(3):8–12, 2000.

[14] Y. Crama, O.E. Flippo, J. van de Klundert, and F.C.R. Spieksma. The assembly of printed circuit boards: A case with multiple machines and multiple board types. *European Journal of Operational Research*, 98(3):457–472, 1997.

[15] Y. Crama, J. van de Klundert, and F.C.R. Spieksma. Production planning problems in printed circuit board assembly. *Discrete Applied Mathematics*, 123(1-3):339–361, 2002.

[16] P. Csaszar, P.C. Nelson, R.Rajbhandari, and M. Tirpak. Optimization of automated high-speed modular placement machines using knowledge-based systems. *IEEE Transactions on Systems, Man, and Cybernetics, Part C: Applications and Reviews*, 30(4):408–417, 2000.

[17] P. Csaszar, T. Tirpak, and P.C. Nelson. Optimization of a high-speed placement machine using tabu search algorithms. *Annals of Operations Research*, 96:125–147, 2000.

[18] P. Csaszar, T.M. Tirpak, and P.C. Nelson. Object-oriented simulator design for an automated high-speed modular placement machine family. *Simulation*, 73(6):341–351, 1999.

[19] Dalsa. *Datasheet Dalsa IT-P1 image sensors*, 2005.

[20] A. Dikos, P.C. Nelson, T.M. Tirpak, and W. Wang. Optimization of high-mix printed circuit card assembly using genetic algorithms. *Annals of Operations Research*, 75(0):303–324, 1997.

[21] Bosch Rexroth Electric Drives and Controls AG B.V. *NYCe4000 Hardware manual*, 2008.

[22] A. Efrat and C. Gotsman. Subpixel image registration using circular fiducials. *International Journal of Computational Geometry & Applications*, 04(04):403–422, 1994.

[23] Electro schientific industries. *Datasheet CorrectCam*, 2002.

[24] A.T. Elfizy, G.M. Bone, and M.A. Elbestawi. Design and control of a dual-stage feed drive. *International Journal of Machine Tools & Manufacture*, 45:153–165, 2005.

[25] K.P. Ellis, J.E. Kobza, and F.J. Vittes. Development of a placement time estimator function for a turret style surface mount placement machine. *Robotics and Computer Integrated Manufacturing*, 18:241–254, 2002.

[26] K.P. Ellis, L.F. McGinnis, and J.C. Ammons. An approach for grouping circuit cards into families to minimize assembly time on a placement machine. *IEEE Transaction On Electronics Packaging Manufactoring*, 26(1):22–30, 2003.

[27] K.P. Ellis, F.J. Vittes, and J.E. Kobza. Optimizing the performance of a surface mount placement machine. *IEEE Transactions on Electronics Packaging Manufacturing*, 24(3):160–170, 2001.

[28] Eureca Messtechnik GmbH. *Datasheet LSO-2048SH1-8EPP*, 2005.

[29] T.A. Feo, J.F. Bard, and S.D. Holland. Facility-wide planning and scheduling of printed wiring board assembly. *Operations research : the journal of the Operations Research Society of America*, 43:219–230, 1995.

[30] B. Fowler, J. Balicki, D. How, S. Mims, J. Canfield, and M. Godfrey. An ultra low noise high speed cmos linescan sensor for scientific and industrial applications. *2003 IEEE workshop on Charge-Coupled Devices and Advanced Image Sensors*, 2003.

[31] J.J.M. van Gastel. A comparison of smd placement machine concepts. *SMT in FOCUS*, pages 1–8, 2002. www.smtinfocus.com.

[32] J.M.M van Gastel, P.A.H. Goede, P.P.H. Verstegen, and H.M.J. van Logten. Component placement apparatus. *Patent Register*, NL2005000415, 2008.

[33] S. van Gastel, M. Nikeschina, and R. Petit. *Fundamentals of SMD assembly*. RTFB Publishing Limited, Southhampton, 2004.

[34] J. Gausemeier, S. Moehinger, et al. New guideline vdi 2206- a flexibale procedure model for the design of mechatronic systems. *DS 31: Proceedings of ICED 03, the 14th International Conference on Engineering Design*, 2003.

[35] P. Gerits and A. Mandos. 0201 placement - only with the right team and tools. *SMTnet Library; http://www.smtnet.com/express/200209/0201placement.pdf*, pages 1–8, 2003.

[36] W.C.M. van Gerwen. Optimized motion control system for semiconductor machines. *IEEE Control Systems Magazine*, 25(2):18–19, 2005.

[37] T. Gilb. Advanced requirements specification: Quantifying the qualitative. *PSQT Conference*, 1999.

[38] T. Gilb and L. Brodie. *Competitive Engineering: A Handbook for Systems Engineering, Requirements Engineering, and Software Engineering Using Planguage*. Butterworth-Heinemann, 2005.

[39] MVTec Software GmbH. *halcon 7.1 - intelligent and powerful machine vision software*, 2005.

[40] P.A.H. Goede, P.P.H. Verstegen, and J.M.M. van Gastel. Design of a shuttle used in an innovative pick and place machine concept. *International symposium on Assembly and Manufacturing - Ann Arbor*, pages 135–140, 2007.

[41] M. Grunow, H-O Günther, M. Schleusener, and I.O. Yilmaz. Operations planning for collect-and-place machines in pcb assembly. *Computers & Industrial Engineering*, 47:409–429, 2004.

[42] H.F. van Heek. Illumination for machine vision. *Philips Production Means*, 4:21–25, 1989.

[43] W. Ho and P. Ji. A hybrid genetic algorithm for component sequencing and feeder arrangement. *Journal of Intelligent Manufacturing*, 15(3):307–315, 2004.

[44] W. Ho and P. Ji. A genetic algorithm to optimise the component placement process in pcb assembly. *The International Journal of Advanced Manufacturing Technology*, 26(11):1397–1401, 2005.

[45] W. Ho and P. Ji. A genetic algorithm approach to optimising component placement and retrieval sequence for chip shooter machines. *The International Journal of Advanced Manufacturing Technology*, 28(5):556–560, 2006.

[46] A. Hodac and R. Siegwart. End-point control of fast and precise macro/micro-manipulator. *Proceedings of the Fourth International Conference on Motion and Vibration Control*, MOVIC1998:883–888, 1998.

[47] A. Hodac and R. Siegwart. Decoupled macro/micro-manipulator for fast and precise assembly operations: design and experiments. *SPIE Conference on Microrobotics and Microassembly*, 3834:122–130, 1999.

[48] R. Hollis. A planar xy robotic fine positioning device. *Proceedings IEEE International Conference on Robotics and Automation*, 2:329–336, 1985.

[49] P. N. Houston, J. Bentley, B. J. Lewis, B. A. Smith, and D. F. Baldwin. Processing strategies for high speed 0201 implementation. *27th Annual IEEE/SEMI International Electronics Manufacturing Technology Symposium*, pages 166–172, 2002.

[50] T. Huang, Z. Li, M. Li, D.G. Chetwynd, and C.M. Gosselin. Conceptual design and dimensional synthesis of a novel 2-dof translational parallel robot for pick-and-place operations. *Journal of Mechanical Design*, 126(3):449–455, 2004.

[51] M. van Hulsen. Timing FCM. *Internal Report, Philips*, 4022590-0207, 1997.

[52] L.T. Hwang and J. Poarch. Placement repeatability study of two flip chip die attach machines: Leadscrew vs. linear motor. *Proceedings of the 1999 IEEE/ASME International Conference on Advanced Intelligent Mechatronics*, pages 478–483, 1999.

[53] IPC. Ipc-9850 surface mount placement equipment characterization. *IPC*, 2002.

[54] B. Janse, P. Schuur, and M.P. de Brito. A reverse logistics diagnostic tool: the case of the consumer electronics industry. *The International Journal of Advanced Manufacturing Technology*, 47(5):495–513, 2010.

[55] J.W. Jansen, E.A. Lomonova, A.J.A. Vandenput, J.C. Compter, and A.H. Verweij. Improvement of the dynamic performance of an ac linear permanent magnet machine. In *Electric Machines and Drives Conference, 2003. IEMDC'03. IEEE International*, volume 2, pages 785–790. IEEE, 2003.

[56] K. Jeevan, A. Parthiban, K.N. Seetharamu, I.A. Azid, and G.A. Quadir. Optimization of pcb component placement using genetic algorithms. *Journal of Electronics Manufacturing*, 11(01):69–79, 2002.

[57] F. de Jong. *Range Imaging and Visual Servoing for Industrial Applications*. PhD thesis, Delft University of Technology, Delft, 2008.

[58] D. Kalen. Part II: Placing 0201 components accurately. *SMT Magazine*, pages 1–3, 2002.

[59] J.H. Kim, S. Ahn, J.W. Jeon, and J.E. Byun. A high speed high resolution vision system for the inspection of tft lcd. *Proceedings ISIE 2001 IEEE International Symposium on Industrial Electronics*, 1:101–105, 2001.

[60] J.H. Kim and H.S. Cho. Neural network-based inspection of solder joints using a circular illumination. *Image and Vision Computing*, 13(6):479–490, 1995.

[61] C. Klomp, J. v.d. Klundert, F.C.R. Spieksma, and S. Voogt. The feeder rack assignment problem in pcb assembly: A case study. *International Journal of Production Economics*, 64(1-3):399–407, 2000.

[62] K.W. Ko, J.W. Kim, H.S. Cho, K.S. Jin, and K.I. Ko. Enhancement of placment accuracy for smd via development of a new illumination system. *Proceedings of SPIE*, 4190:51–61, 2001.

[63] L.J. Kozlowski, D. Standley, J. Luo, A. Tomasini, A. Gallagher, R. Mann, B.C. Hsieh, T. Liu, and W.E. Kleinhans. Theoretical basis and experimental confirmation: why a cmos imager is superior to a ccd. *SPIE Conference on Infrared Technology and Applications XXV*, 3698:388–396, 1999.

[64] D. Kundur and D. Hatzinakos. Blind image deconvolution. *IEEE Signal Processing Magazine*, 13(3):43–64, 1996.

[65] H. Kunzmann, T. Pfeifer, and J. Flügge. Scales vs. laser interferometers performance and comparison of two measuring systems. *Annals of the CIRP*, 42(2):753–767, 1993.

[66] S.J. Kwon, W.K. Chung, and Y. Youm. Robust and time-optimal control strategy for coarse/fine dual-stage manipulators. In *Proceedings 2000 ICRA. Millennium Conference. IEEE International Conference on Robotics and Automation. Symposia Proceedings (Cat. No.00CH37065)*, volume 4, pages 4051–4056 vol.4, 2000.

[67] S.J. Kwon, W.K. Chung, and Y. Youm. On the coarse/fine dual-stage manipulators with robust perturbation compensator. In *Robotics and Automation, 2001. Proceedings 2001 ICRA. IEEE International Conference on*, volume 1, pages 121–126 vol.1, 2001.

[68] T. Laakso, M. Johnsson, T. Johtela, J. Smed, and O. Nevalainen. Estimating the production times in pcb assembly. *Journal of Electronics Manufacturing*, 11(02):161–170, 2002.

[69] P. Lambrechts, M. Boerlage, and M. Steinbuch. Trajectory planning and feedforward design for high performance motion systems. *Feedback*, 14:4637–4642, 2004.

[70] D.Y. Lee and H. Cho. Precision force control via macro/micro actuator for surface mounting system. *Proceedings of the 2002 IEEE/RSJ International Conference on Intelligent Robots and Systems*, pages 2227–2232, 2002.

[71] D. Litwiller. Ccd vs. cmos. *Photonics spectra*, 1:1–4, 2001.

[72] X.J. Liu and J. Kim. Two novel parallel mechanisms with less than six dofs and the applications. *Proceedings of the Workshop on Fundamental Issues and Future Research for Parallel Mechanisms and Manipulators*, pages 172–177, 2002.

[73] X.J. Liu and J. Wang. Some new parallel mechanisms containing the planar four-bar parallelogram. *The International Journal of Robotics Research*, 22:717–732, 2003.

[74] S. Macfarlane and E.A. Croft. Jerk-bounded manipulator trajectory planning: design for real-time applications. *IEEE Transactions on Robotics and Automation*, 19(1):42–52, 2003.

[75] Melles Griot. Machine vision lens fundamentals. *http://www.mellesgriot.com/pdf/pg11-19.pdf*, 2005.

[76] K. Miller. Optimal design and modeling of spatial parallel manipulators. *The International Journal of Robotics Research*, 23(2):127–140, 2004.

[77] L.K. Moyer and S.M.Gupta. An efficient assembly sequencing heuristic for printed circuit board configurations. *Journal of Electronics Manufacturing*, 07(02):143–160, 1997.

[78] V. Nabat, M. de la O Rodriguez, O. Company, S. Krut, and F. Pierrot. Par4: very high speed parallel robot for pick-and-place. In *2005 IEEE/RSJ International Conference on Intelligent Robots and Systems*, pages 553–558, 2005.

[79] K. Ohtani and M. Baba. A fast edge location measurement with subpixel accuracy using a ccd image. *IEEE Transactioins on Information Theory*, 44(7):3156–3162, 1998.

[80] Opto-Engineering. Telecentric lenses: basic information and working principle. *http://www.opto-engineering.com/telecentric.php*, 2005.

[81] G. Otten, T.J.A. De Vries, J. Van Amerongen, A.M. Rankers, and E.W. Gaal. Linear motor motion control using a learning feedforward controller. *IEEE/ASME transactions on mechatronics*, 2(3):179–187, 1997.

[82] R. Petit. Axq accuracy budgets. *Internal Report Assembléon B.V.*, DC-000005873-2, 2004.

[83] U. Probst. *High Speed, High Accuracy Linear Direct Drive Pick and Place Manipulator*. PhD thesis, École Polytechnieque Fédérale de Lausanne, Lausanne, 2002.

[84] R. Ray. Automated inspection of solder bumps using visual signatures of specular image-highlights. *IEEE Computer Society Conference on Computer Vision and Pattern Recognition, Proceedings CVPR*, pages 588–596, 1989.

[85] R. Ray. Placement of surface mount components: Machine accuracy and performance modeling. *IEEE International Conference on Systems, Man and Cybernetics, 1995. Intelligent Systems for the 21st Century*, 2:1746–1752, 1995.

[86] Renishaw. *Datasheet RGE series interpolators*, 2005.

[87] Renishaw. *Datasheet RGH24 series readhead*, 2005.

[88] Renishaw. *Datasheet RGS20-S, RGS20-PC, RGS40-S, RGS40-PC scale*, 2005.

[89] Renishaw. *Datasheet REE series interpolators*, 2009.

[90] C. Röhrig and A. Jochheim. Motion control of linear permanent magnet motors with force ripple compensation. In *Proceedings of the Third International Symposium on Linear Drives for Industry Applications, Nagano, Japan*, volume 128, 2001.

[91] P. Rook. Controlling software projects. *IEEE Software Engineering Journal*, 1(1):7–16, 1986.

[92] T. Satoru and T. Kazuhide. Electronic component mounting machine. *Patent Register*, JP5037193, 1992.

[93] T. Satoru and T. Kazuhide. Mounting apparatus for electronic parts. *Patent Register*, DE69127154T, 1998.

[94] R.H. Munnig Schmidt, G. Schitter, A. Rankers, and J. van Eijk. *The design of high performance mechatronics: high-tech functionality by multidisciplinary system integration (2nd revised edition)*. IOS Press, 2014.

[95] A. Sharon, N. Hogan, and D.E. Hardt. The macro/micro manipulator: an improved architecture for robot control. *Robotics & Computer-Intergrated Manufacturing*, 10(3):209–222, 1993.

[96] C.-L. Shih and C.-W. Ruo. Auto-calibration of an smt machine by machine vision. *The International Journal of Advanced Manufacturing Technology*, 26(3):243–250, 2005.

[97] R. Solomon, P. A. Sandborn, and M. G. Pecht. Electronic part life cycle concepts and obsolescence forecasting. *IEEE Transactions on Components and Packaging Technologies*, 23(4):707–717, 2000.

[98] Sony. *Datasheet Digital Video Camera Module, Technical Manual, XCL-X700/V500*, 2004.

[99] R. De Souza and W. Lijun. Intelligent optimization of component onsertion in multi-head concurrent operation pcba machines. *Journal of Intelligent Manufacturing*, 6(4):235–243, 1995.

[100] Tecnotion. Leaflet uc-motors. *www.tecnotion.com*, 2006.

[101] M. Tichem and M.S. Cohen. Subμm registration of fiducial marks using machine vision. *IEEE Transactions on Pattern Analysis and Machine Intelligence*, 16(8):791–794, 1993.

[102] T.M. Tirpak. Design-to-manufacturing information management for electronics assembly. *International Journal of Flexible Manufacturing Systems*, 12(2-3):189–205, 2000.

[103] T.M. Tirpak, P.C. Nelson, and A.J. Aswani. Optimization of revolver head smt machines using adaptive simulated annealing (asa). *Twenty-Sixth IEEE/CPMT International Electronics Manufacturing Technology Symposium*, pages 214–220, 2000.

[104] Verein Deutscher Ingenieure. Vdi 2206: Design methodology for mechatronic systems. *Beuth Verlag*, 2004.

[105] C. Wang, L.S. Ho, and D.J. Cannon. Heuristics for assembly sequencing and relative magazine assignment for robotic assembly. *Computers and Industrial Engineering*, 34(2):423–431, 1998.

[106] M. Watanabe and S.K. Nayar. Telecentric optics for focus analysis. *IEEE Transactions on Pattern Analysis and Machine Intelligence*, 19(12):1360–1365, 1997.

[107] S. Wischoffer. Step 6: Component placement. *Surface Mount Technology*, 15(6):70–77, 2001.

[108] G. Woodhouse. Automatic optical pick and place calibration and capability analysis system for assembly of components onto printed circuit boards. *Patent Register*, US 5537204, 1996.

[109] J. Woolstenhulme and E. Lubosky. Machine vision placement considerations. *SMT Magazine*, 14(11):135–140, 2000.

[110] T. Yamada, K. Tanaka, and M. Yamakita. Winding and task control of snake like robot. *SICE 2003 Annual Conference*, 3:3059–3063, 2003.

Summary

The demand for electronic devices like telephones, tablets and computers is still growing and will grow further in the future. All these devices contain electronic components, which are placed on printed circuit boards (PCBs). The assembly of a PCB is performed by several machines in an assembly line. As the accurate placement of several hundreds of these components on a PCB is a complex task, specialised Pick and Place (P&P) machines are used in an assembly line to perform this task. The production time required to assemble a PCB is determined by the a number of components a P&P machine can place per hour. The "extremely high-volume production machine" AX-5 P&P machine (Assembléon B.V.) has a maximum of 20 P&P robots in parallel and is selected as the benchmark machine. Each robot is capable of placing 8,000 components per hour. To double the throughput from 8,000 to 16,000 components per hour per P&P robot a shuttle is added while maintaining the accuracy.

The performance of the shuttle concept P&P machine is determined using two performance indicators. The first performance indicator is the throughput expressed in the number of components placed per hour. The second performance indicator is repeatability, expressing the one sigma deviation of the placement position. The smallest components have a size of $0.254 \times 0.508\ mm$ requiring a placement repeatability of 15 μm (1σ).

The first step is the analysis of the processes that take place in a P&P cycle. The influence of these processes on throughput and repeatability is determined. An repeatability budget is generated using the repeatability contribution of each process and the values of the benchmark P&P machine.

The main objective of the shuttle concept is to reduce the distance between the position where a component is picked and the position where the component is placed onto the PCB. Generally, in P&P machines the P&P robot moves from the component feeders, positioned on the outside of the machine, to the placement position inside the machine. These robot movements can take up to 70% of the total P&P cycle time. The shuttle concept, however, contains a shuttle that brings the components close to the P&P robot, decreasing the distances between the component pick and the placement position on the PCB. Hence, the time required for the move step is decreased.

Components and PCBs are fed into the machine without the required position repeatability. Therefore, it is necessary to determine the PCB and component position using board and component alignment systems. An alignment system is a vision system containing a camera with sensor array, lens, illumination and image processing software. In this thesis the design and realisation of a new board and component alignment system is discussed. In contrast to other P&P machines, in this concept a single-camera, attached to the P&P robot, is used for both board and component alignment. Therefore, the shuttle, which moves nearby the P&P robot, is equipped with three mirrors. Consequently, the realisation of the alignment system includes the integration of the P&P robot and shuttle. In addition, the alignment of board or component may not contribute to the P&P cycle time. Therefore, the images of the components or PCB are acquired in less than 4 μs while the robot is moving. A special illumination system is designed to fulfill this requirement.

A full demonstrator was designed and built to specifically test the new single board and component alignment concept. The demonstrator was calibrated and tests were performed to determine the repeatability.

The repeatability of the alignment system of the demonstrator appeared to be not within specifications, but the tests have indicated where improvements must be realised to achieve repeatability within specifications.

The aim to realise 15 $\mu m\,(1\sigma)$ repeatability has resulted in the design of a new component and board alignment system. This board and component alignment system contains only a single-camera and three mirrors attached to the shuttle that moves close to the P&P robot. Hereby, the throughput can be guaranteed while the board and component alignment processes can be used to determine the actual position of the board or component. The concept's repeatability was determined using the realised demonstrator. The shuttle concept with a single-camera board and component alignment system, when taking the recommendations into account, seams a feasible concept. The shuttle concept was patented.

Samenvatting

De vraag naar elektronische apparatuur zoals telefoons, tablets en computers groeit nog steeds en zal in de toekomst alleen maar verder groeien. Deze apparaten bevatten allemaal een printplaat met elektronische componenten. Het assembleren van deze printplaten met honderden van deze componenten is complex. Voor het plaatsen van deze componenten worden speciale component plaatsingsmachines gebruikt. De benodigde tijd, productietijd, voor het plaatsen van deze componenten op een printplaat wordt bepaald door het aantal componenten dat de plaatsingsmachine kan plaatsen per uur. De modulaire AX-5 plaatsingsmachine (Assembléon B.V.) kan maximaal 20 parallelle plaatsingsrobots bevatten waardoor deze machine geschikt is om zeer veel printplaten per uur te assembleren. De eigenschappen van de AX-5 plaatsingsmachine zijn in dit onderzoek gebruikt als referentie waarden. Het uitgangspunt van dit onderzoek is om het aantal te plaatsen componenten per uur te verdubbelen naar 16,000 componenten per uur per plaatsingsrobot waarbij de nauwkeurigheid gelijk moet blijven. Om de plaatsingscapaciteit van 16,000 componenten per uur te realiseren is een concept geselecteerd waarbij een shuttle wordt toegevoegd aan de plaatsingsrobot.

Om de performance van plaatsingsrobots te kunnen vergelijken wordt gebruik gemaakt van twee performance indicatoren. De eerste performance indicator is de plaatsingscapaciteit uitgedrukt in het aantal componenten geplaatst per uur. De tweede indicator is nauwkeurigheid, welke uitgedrukt wordt in de één sigma afwijking van de plaatsingspositie. De afmetingen van de kleinste componenten die tijdens dit onderzoek geplaatst moeten worden bedragen 0.254 $mm \times 0.508$ mm en vereisen een plaatsingsnauwkeurigheid van 15 μm (1σ).

De eerste stap in de analyse van een plaatsingsmachine is het bepalen van de processtappen die plaatsvinden in een P&P cyclus. Hierna kan de invloed van deze processen op de plaatsingscapaciteit en de nauwkeurigheid van het concept bepaald worden. Een nauwkeurigheidsbudget voor de verschillende processen is opgesteld. Hierbij worden de parameters van de AX-5 plaatsingsmachine gebruikt als referentie.

De shuttle concept plaatsingsmachine is gebasseerd op het reduceren van de afstand tussen de positie waar een component gepakt wordt en de positie waar het component geplaatst moet worden. In het algemeen beweegt de

P&P robot van de component feeders buiten de machine naar de plaatsingspositie in de machine waarbij deze beweging van de robots 70% van de totale P&P cyclus tijd in beslag kan nemen. Het shuttle concept daarentegen bevat een shuttle die de componenten naar de P&P robot brengt. Hiermee worden de afstanden tussen de pakpositie en de plaatsingspositie gereduceerd. Dit resulteert in een kortere tijd benodigd voor de bewegingen.

De componenten en de printplaten worden onnauwkeurig in de machine gebracht. Het is daardoor noodzakelijk om zowel de positie van de printplaat als van de componenten te bepalen met behulp van een alignment systeem. Een alignment systeem bestaat uit een camera/sensor, een lens, belichting en image processing software.

Het ontwerp en de realisatie van een nieuw alignment systeem voor het het bepalen van de positie van zowel componenten als printplaten wordt in dit proefschrift besproken. De meeste bestaande plaatsingsmachines hebben twee separate alignment systemen, een voor bord alignment en een voor component alignment. In dit proefontwerp maken deze twee alignment systemen gebruik van één enkele camera die voor zowel het bepalen van de positie van componenten als voor de bepaling van de positie van de printplaat kan worden gebruikt. De camera is bevestigd aan de P&P robot en drie additonele spiegels zijn gemonteerd aan de shuttle.

De realisatie van dit systeem betekent dat naast het ontwerp van de shuttle en de P&P robot, ook de integratie van deze twee systemen gerealiseerd moet worden. Omdat het alignment systeem geen aditionele tijd mag toevoegen aan de P&P cyclus, is de keuze gemaakt om de beelden in te nemen terwijl de P&P robot beweegt. Om verstoringen in dit beeld te minimaliseren, moet het beeld ingenomen binnen 4 μs. Dit heeft geresulteerd in de ontwikkeling van een LED-fliser die kan voldoen aan deze eis.

Een opstelling is ontworpen en gebouwd. Deze opstelling is speciaal ontworpen en gebruikt om het nieuwe alignment systeem te testen. Nadat de opstelling gekalibreerd was, zijn nauwkeurigheidstesten uitgevoerd. De nauwkeurigheid van het alignment systeem van de opstelling voldoet niet aan de gestelde eisen maar met behulp van de testen zijn verbeterpunten bepaald.

Het doel om een plaatsingsnauwkeurigheid te realiseren van 15 $\mu m\,(1\sigma)$, heeft geleid tot het ontwerp van een nieuw alignment systeem geschikt voor het bepalen van de positie van componenten en printplaaten. Dit alignment systeem bevat slechts één enkele camera die bevestigd is aan de P&P robot en drie spiegels die aan de shuttle bevestigd zijn. Uiteindelijk is in dit ontwerp de plaatsingscapaciteit gegarandeerd terwijl het alignment systeem kan worden gebruikt om de positie van zowel de componenten als de printplaten te bepalen, zonder de P&P cyclus te beïnvloeden. Met behulp van de opstelling is de nauwkeurigheid bepaald. Het ontworpen shuttle concept, voorzien van een alignment systeem met slechts een camera, lijkt haalbaar mits de aanbevelingen in acht worden genomen. Dit concept is gepatenteerd.

Curriculum Vitae

Paul Verstegen was born on the 16th of may 1971, in Zeeland, the Netherlands. He obtained his HAVO diploma at the "Kruisheren Kollege" in Uden.

In 1988, he started his education at the "Hogeschool Eindhoven", in electrical engineering. In 1994 he received his bachelor degree on the subject "optimisation of a servo system", at the control laboratory at the "Hogeschool Eindhoven".

In 1994 he started working at the R&D of "Roto Electronics" as a hardware and software engineer. He realised several products such as: a weighing indicator, a control unit for refrigerators, a module to detect multiple papers in a paper feeder, a control unit for water mixing using fuzzy control and system modeling. In 1997 he was working at ASML as integrator.

In 1999 he started working at "Fluidwell B.V." in Veghel, with as main objective the development and approval of an intrinsic safe flow indicator.

In 2001 he founded the company M2Control: Measuring, Mechatronics and Control. The main objective was implementation of software, data analysis and control. Projects realised are: a measuring and control system for improving the performance of concrete stone production machines; implementation of an operator support system; design and implementation of a service machine measurement tool; implementation of several software systems to process, save and display data; the development of software for motion control systems.

In 2003 he started his PhD project at the mechatronics laboratories at "Fontys Hogeschool Eindhoven". This project was the design and realisation of a P&P machine with an output of 16,000 components per hour and an accuracy of 15 μm (1σ). This project was a cooperation between "Hogeschool Utrecht" and "Fontys Hogeschool Eindhoven" under supervision of prof.dr.ir. J. van Eijk and ir. J.W. Spronck of the Delft University of Technology. This thesis was finished under supervision of prof.dr.ir. J.L. Herder and ir. J.W. Spronck of the Delft University of Technology.

From 2007 to 2010 he worked at the "Fontys Hogeschool Eindhoven" as researcher. Starting in 2011 he became CTO at Focal Meditech B.V. and developed with the R&D team several arm support systems for impaired persons. Since august 2017 he is working at MI-partners as senior mechatronic system designer.

Publications

First Author

P.P.H. Verstegen, J.M.M. van Gastel and J.W. Spronck. Design of a novel single camera vision system for both component and board alignment in pick and place machines. *Proceedings of the 4th IFAC Symposium on Mechatronic Systems*, 706-712, 2006

P.P.H. Verstegen, P.A.H. Goede, J.W. Spronck, J.M.M. van Gastel and J. van Eijk. Realized positioning accuracy in pick and place machines with one single camera for board and component alignment. *Proceedings of the Euspen International Conference - Zurich*, 338-342, 2008.

Co-Author

P.A.H. Goede, P.P.H. Verstegen and J.M.M. van Gastel. Design of a shuttle used in an innovative pick and place machine concept. *International symposium on Assembly and Manufacturing - Ann Arbor*, 135-140, 2007.

Patents

J.M.M van Gastel, P.A.H. Goede, P.P.H. Verstegen and H.M.J. van Logten. Component Placement Apparatus. *Patent Register*, NL2005000415, 2008.

Dankwoord

Het laatste hoofdstuk wil ik gebruiken om iedereen die meegeholpen heeft aan dit project te danken en een aantal mensen in het bijzonder.

Als eerste de mensen van het Fontys lectoraat Mechatronica: Henk van Logten, Huub Lonij, Paul Janssen, Jan Bernards, Jan van Lierop, Enno Veenstra, Ton Hülsman, Harrie Wagenmakers, Antoon Pepping, Ine Noukens. Dank jullie wel voor jullie hulp en gezelligheid. Dank aan de 23 studenten die allen meegewerkt hebben aan dit onderzoek.

Een aantal personen zijn zeer betrokken geweest bij dit project. Sjef van Gastel; met hem heb ik de nodige kilometers afgelegd op de Productronica om de laatste ontwikkelingen te bekijken. Jos Gunsing; hij heeft er mede voor gezorgd dat de opstelling ook gerealiseerd werd. Rene van der Slot; hij heeft me inzicht gegeven in positie meting. Naast jullie wil ik ook alle andere betrokken bedrijven danken voor de steun en discussies.

Ik heb dit onderzoek samen uitgevoerd met Paul Goede. Paul, ik heb prettig met je samengewerkt en veel van je geleerd. Samen hebben we hebben een mooie opstelling gerealiseerd.

Ondanks het feit dat ik in Eindhoven mijn werkplek had, heb ik heel wat bezoeken aan de universiteit in Delft gebracht om Jan en Jo en later Just te bezoeken. Jan, ik wil je danken voor de uren privé les die je me hebt gegeven. Ik heb van je uitleg over mechatronica genoten. Beste Jo, we hebben heel wat uren gesproken over techniek, het project en oude auto's. Daarnaast was jij het die me bleef motiveren. Dank je wel voor je optimisme en steun. Just, ik vond het heel bijzonder om samen met jou dit proefschrift te realiseren. Jan, Jo en Just, hopelijk houden we contact en wellicht werken we nog eens samen in een mooi project.

Een dankwoord aan al mijn vrienden. Fijn dat jullie interesse tonen in wat ik allemaal uithaal. Beste Maud, samen met jou heb ik een mooie tijd gehad. Dank je wel voor je goede zorgen voor Eefke!

Mieke en Willem, ik ben blij dat we zo'n hechte band hebben. Dank dat jullie er altijd voor mij zijn. En dan, zoals we in Brabant zeggen, ons-pap en ons-mam. Hadden jullie ooit kunnen denken dat ik een proefschrift zou schrijven? Door jullie ben ik zover gekomen.

Tot slot: lieve Eefke, fijn dat jij er bent! Dit is dus het boekje waar papa het altijd over had.

Paul Verstegen